UNIVERSITY *of the*
WESTERN CAPE

TREATMENT OF PERSISTENT ORGANIC POLLUTANTS IN WASTEWATER WITH COMBINED ADVANCED OXIDATION

By

Kassim Olasunkanmi Badmus (3481395)

Thesis in fulfillment of the requirement for the degree

DOCTOR OF PHILOSOPHY

In

CHEMISTRY

In the

FACULTY OF NATURAL SCIENCE

Supervisor: Professor L. F. Petrik

April 2019

DECLARATION

I declare that Treatment of Persistent Organic Pollutants in Wastewater with Combined Advanced Oxidation is (apart from the recognised assistance of my supervisor) my own research work which has not been submitted before for any degree or examination in any university and that all the sources I have quoted have been indicated and acknowledged as a complete references.

Full name: Kassim Olasunkanmi Badmus August 2018

Signed (Candidate) …….. on this ……day of ……..

Signed (Supervisor) …… on this ……day of ……....

DEDICATION

This PhD thesis is dedicated to my dear wife; Kehide Zikra Badmus, our children; Yusra Ololade Badmus and Faiza Eniola Badmus.

ACKNOWLEDGEMENT

Praise and adoration is due only to almighty Allah for his mercy on me and my family. I wish to express my since gratitude to my esteemed leader, Professor Leslie Petrik for the provision of the world class mentorship, supervision and motherly love. The four years of my doctorate degree at Environmental and Nano Science will remain memorable in my autobiography. I have been refined through a systematic grooming and exceptional leadership provided by Professor Leslie Petrik. I would like to thank all my colleagues that have motivated me in one way or another. The ENS is such a big family and I regret that the space provided for the acknowledgement is definitely too small for me to make a list of all my exceptional colleagues and motivators.

However, I will seize the opportunity to show appreciation to very few special people who have made significant contributions in the current achievement. My coming to university of the Western Cape was facilitated by my brother; Dr Badmus Jelili. On alighting at Cape Town international airport, I was warmly welcomed by Dr Jimoh Tijani who gave me the first orientation. In the course of the PhD research, I have had special privilege to work closely with exceptional researchers such as Dr Olanrewaju Fatoba, Dr Olushola Adeniyi, Dr Paul Eze, Dr Chionyedua Theresa Onwordi, Dr Chris Bode-aluko, Dr Omoniyi Pereao, Emile massima, Emmanuel Ameh, Ninette Irakonze, Lokuboga Kombese and Natacha Kakama. I also appreciate the contributions by Mrs Ilse Wells, Mrs Venessa Kellerman, Mr Timothy Lesch and Mr Rallston Richards.

The support of University of the Western Cape staffs such as Professor Lorna Holtman, Hilda Wilson and Sedicka Cassiem is highly acknowledged.

Finally, I congratulate my good parents and our entire family on the successful “production” of another doctor (PhD) through their uncommon discipline and God’s favor.

I will continue to trust almighty Allah and hope for the greater tomorrow.

PUBLICATIONS AND PRESENTATIONS

The results emanating from this study have been either published or submitted to peer-review Journals for publication or presented in the national and international conferences indicated below.

Peer-reviewed Publications

- Badmus, K.O., Coetsee-Hugo, E., Swart, H. and Petrik, L., 2018. Synthesis and characterisation of stable and efficient nano zero valent iron. *Environmental Science and Pollution Research*, pp.1-18.

- Badmus, K.O., Tijani, J.O., Massima, E. and Petrik, L., 2018. Treatment of persistent organic pollutants in wastewater using hydrodynamic cavitation in synergy with advanced oxidation process. *Environmental Science and Pollution Research*, pp.1-16.

- Badmus, K.O., Tijani, J., Eze, C.P., Fatoba, O. and Petrik, L., 2016. Quantification of radicals generated in a sonicator. *Analytical and Bioanalytical Chemistry Research*, *3*(1), pp.139-147.

- Badmus, K.O., Irakoze N., Petrik, L., 2018. Treatment of Azo-dye in textile wastewater with Hydrodynamic cavitation catalysed by the Novel Nano zero valent iron (Submitted in Journal of Environmental Chemistry and Chemical Engineering, JECE-D-18-00244).

Conference Presentation

- Badmus, K.O., Irakoze N., Petrik, L., 2017. Treatment of Textile wastewater in a combined Hydrodynamic cavitation, Fenton process and Nano zero valent iron (gnZVI) system**,** sciforum-009779**.** The 6th World Sustainability Forum, Environmental Management, Social Development and Economic Development *(*Oral presentation).

- Badmus, K.O. *and* Petrik, L. 2017. 'Challenges in the Synthesis and Characterization of Stable and Efficient Nano Zero Valent Iron' has been accepted as an oral. International Symposium on symposium on water, wastewater and environment (iwa-ppfw2017). 2nd iwa regional international *(*Oral presentation).

- Badmus, K.O**.** Tijani, J., Fatoba, O. and Petrik, L. **2015.** Synthesis and Characterization of Green Nano Zero Valent Iron (gnZVI) from the Extract of *Harpephyllum caffrum. Royal society of chemistry/ Pan African chemistry network (PACN) congress, University of Nairobi, Kenya, 17-19 November (*Oral presentation).

ABSTRACT

Persistent organic pollutants (POPs) are very tenacious wastewater contaminants with negative impact on the ecosystem. The two major sources of POPs are wastewater from textile industries and pharmaceutical industries. They are known for their recalcitrance and circumvention of nearly all the known wastewater treatment procedures. However, the wastewater treatment methods which applied advanced oxidation processes (AOPs) are documented for their successful remediation of POPs. AOPs are a group of water treatment technologies which is centered on the generation of OH radicals for the purpose of oxidizing recalcitrant organic contaminants content of wastewater to their inert end products. Circumvention of the reported demerits of AOPs such as low degradation efficiency, generation of toxic intermediates, massive sludge production, high energy expenditure and operational cost can be done through the application of the combined AOPs in the wastewater treatment procedure. The resultant mineralisation of the POPs content of wastewater is due to the synergistic effect of the OH radicals produced in the combined AOPs.

Hydrodynamic cavitation is the application of the pressure variation in a liquid flowing through the venturi or orifice plates. This results in generation, growth, implosion and subsequent production of OH radicals in the liquid matrix. The generated OH radical in the jet loop hydrodynamic cavitation was applied as a form of advanced oxidation process in combination with hydrogen peroxide, iron (II) oxides or the synthesized green nano zero valent iron (gnZVI) for the treatment of simulated textile and pharmaceutical wastewater.

Firstly, a stable and efficient green nano zero valent iron (gnZVI) was synthesized for its application during the treatment of POPs in the jet loop hydrodynamic cavitation system. The synthesis of gnZVI was through the simultaneous addition of an optimum amount of the $NaBH_4$ and *H. caffrum* extract to $FeCl_3$ in an inert environment (nitrogen). The solution was stirred for thirty minutes, washed with ethanol (99%) and separated using a vacuum filtration with a 0.22 µm pore size cellulose acetate filter paper. The gnZVI was characterised using TGA, TEM, SEM, XRD, FT-IR and XPS. A stable, crystalline, reactive, well dispersed and predominantly 50

nm diameter sized gnZVI was synthesized. Furthermore, the synthesised gnZVI was applied in the treatment of simulated textile or pharmaceutical wastewater in the jet loop hydrodynamic cavitation system.

The preliminary optimisation of the jet loop conditions gave 4 mm orifice holes size, 400 kPa initial pressure and pH 2 as the optimum conditions for the treatment of POPs in the jet loop hydrodynamic cavitation system. Application of terephthalic acid dosimeter and monitoring of produced hydroxyl-terephthalic acid using fluorescence spectrophotometer revealed that 11.29 mg/ L OH radicals was generated during the 60 minutes operation time in the jet loop hydrodynamic cavitation system.

A simulated textile wastewater was prepared by using orange II sodium salt (OR2). The OR2 was subjected to decoloration in the jet-loop hydrodynamic cavitation system in hybrid combination with hydrogen peroxide and iron (II) sulfate or gnZVI was investigated. The 70% decoloration of OR2 which was achieved in jet-loop hydrodynamic cavitation system by itself (400 kPa inlet pressure, 10 L of 10 mg/ L OR2, 4 mm orifice hole sizes, pH 2, n = 3) was further enhanced when hydrogen peroxide and gnZVI was applied leading to the 98% and 74% decoloration and mineralisation of OR2 respectively. Besides, generation of high nitrate as well as evolution of relatively small amount of sulfate salt during the 60 minutes treatment of OR2 in the jet-loop hydrodynamic cavitation system at the optimum treatment condition (400 kPa, pH 2, 10 L of 10 mg/ L OR2, 10 mg/L gnZVI, 1 mg/L H_2O_2, 60 minutes). This result represent a novel advancement in the treatment of azo dye content of wastewater using a low energy option as provided by the jet loop hydrodynamic cavitation system.

Furthermore, gnZVI was investigated as an alternative Fenton catalyst in the mineralisation of acetaminophen (ACE) solution in the jet loop hydrodynamic system aided by hydrogen peroxide. The effect of parameters such as reaction time, concentration of hydrogen peroxide, pH, iron (II) sulfate and gnZVI loading on the extent of transformation of ACE were investigated. The demonstrated low transformation of ACE solution at pH 2 in jet loop hydrodynamic cavitation was enhanced by the separate applications of iron (II) sulfate (10 mg/ L), gnZVI (10 mg/ L) or hydrogen peroxide (5 mg/ L). The amount of intermediates produced during the application of 10

mg/ L iron (II) sulfate was higher (59.1%) than that which was obtained when the gnZVI (23.5%) was applied. Increased amount of iron (II) sulfate (20 or 40 mg/ L) led to the scavenging of the hydroxyl radical and a reduction in the extent of intermediates production while the increased in the amount of applied gnZVI gave a corresponding increased in the formation of intermediates. Therefore, the gnZVI does not scavenge the hydroxyl radical as generated in the jet loop hydrodynamic cavitation system. Besides, more than 41% removal of residual iron was achieved with the aid of bar magnet when gnZVI was applied during the treatment of ACE in the jet loop hydrodynamic cavitation. Consequently, a magnet bar can be used to remove the residual or leached iron from the jet loop hydrodynamic cavitation system. This is the first report of the recovery of iron and a significant reduction in the quantity of elemental iron to be applied as a Fenton catalyst.

The effective degradation of ACE was achieved after 30 minutes treatment time using 5 mg/ L hydrogen peroxide in the jet loop hydrodynamic cavitation system. The hydrogen peroxide aided treatment of ACE led to the 49.3% degradation. However, simultaneous application of hydrogen peroxide (5 mg/ L) and iron (II) sulfate (10 mg/ L) or gnZVI (10 mg/ L) led to 57.8% or 57.6% degradation respectively. Likewise, the % reduction in total organic carbon was 52.7% or 48.1% when iron (II) sulfate (10 mg/ L) or gnZVI (10 mg/ L) was applied to the jet loop hydrodynamic cavitation system for the treatment of ACE solution (400 kPa, pH 2, 10 L of 10 mg/ L ACE, 5 mg/L H_2O_2, 60 minutes). Invariably, the combination of hydrogen peroxide and gnZVI at their optimum amount in the jet loop hydrodynamic cavitation was able to convert acetaminophen into its mineral forms. Based on the achieved results, it can be reported that the jet loop hydrodynamic cavitation system in combination with optimum amount of hydrogen peroxide and gnZVI is suitabe as a treatment method for treatment of ACE in wastewater.

Finally, a complex textile wastewater effluent was treated using alum coagulation or Fenton oxidation as a primary treatment, followed up with secondary treatment in the jet loop hydrodynamic cavitation system. A 92 % reduction in Chemical Oxygen Demand (COD) was achieved when alum coagulation was used in the treatment of real textile wastewater effluent while Fenton oxidation gave 95 % COD reduction. Consequently, the sludge quantity in the alum coagulated treated textile wastewater was 37% of the wastewater effluent with microbial count

of 2800 ± 06 cfu while Fenton oxidation treated textile wastewater effluent was 22% of the wastewater effluent with microbial count of 1410 ± 04 cfu. It was also discovered that the alum coagulation treatment method could only increase the BOD/ COD ratio marginally from 0.083 to 0.14. Therefore, alum coagulation treated wastewater effluent is very toxic and cannot be further treated using biological method. Meanwhile, the Fenton oxidation treated textile wastewater gave a BOD/ COD of 0.43, which indicates a high value for biodegradability and non toxic nature of the treated wastewater effluent. Further treatment of the two primarily treated wastewater effluent; alum coagulation or Fenton oxidation in the jet loop hydrodynamic cavitation system gave BOD/ COD values of 0.32 or 0.34 respectively. The secondary treatment using jet loop hydrodynamic cavitation system at its optimum condition is very efficient and has capability for enhancing biodegradability of the treated wastewater effluent.

TABLE OF CONTENTS

LIST OF FIGURES

LIST OF TABLE

LIST OF EQUATION

LIST OF ABBREVIATION

AOP:	Advanced oxidation process
BET:	Brunauer Emmett-Teller
BOD	Biochemical Oxygen Demand
COD	Chemical Oxygen Demand
CEC:	Chemicals of emerging concern
UNESCO	United Nation Educational Scientific and Cultural Organisation
WHO	World Health Organisation
UV:	Ultra-violet
TGA	Thermo gravimetric analysis
EDC:	Endocrine disrupting compounds
EDS:	Energy dispersive spectroscopy
FTIR:	Fourier-transform infrared spectroscopy
HRSEM:	High Resolution Scanning Electron Microscopy
HRTEM:	High Resolution Transmission Electron Microscopy
HPLC:	High Performance Liquid Chromatography
TOC:	Total organic carbon
UNEP:	United Nations Environmental Program
LC-MS:	Liquid Chromatography-Mass Spectrometry
XPS	X-ray Photo-electron Microscopy
nZVI:	nano Zero Valent Iron
gnZVI	green nano Zero Valent Iron
SAED:	Selected Area Electron Diffraction (SAED)
TGA:	Thermogravimetric analysis

CHAPTER 1

INTRODUCTION

1.1 Overview

The quality of water is being threatened due to the exponential increase in anthropogenic activities which have contributed to the growing accumulation of organic pollutants in the environment and the consequential increased incidence of chronic diseases (UNEP/AMAP, 2011). The impacts of water pollution on all living creatures are enormous and have been widely recognised and documented in the literatures (Counts, 2013; UN-Habitate, 2006). The application of chemical oxidation for the removal of environmental toxicants has witnessed strong opposition due to its formation of toxic, non-biodegradable and complex products. Besides, the partially metabolised compounds are often more toxic than the parent compounds and as such resistant to further chemical and biological decomposition. The conversion of these intermediate products into harmless inorganic compounds requires more energy, long reaction times and use of expensive chemical oxidants. The current study is an investigation into an efficient treatment method for persistent organic pollutants in wastewater effluent.

1.2 Background

The world population is ever increasing with a possibility of growth from 6.8 to 9.1 billion between the year 2009 to 2050 (ONU, 2009). Approximately 70% of the current population are living in urban settlements with increasing rural-urban migration rates (UN-Habitate, 2006). The upsurge in anthropogenic activities such as the increased commercial and agricultural activities, industrialisation, energy generation, advancement in medicine and globalisation are stressors to water resources. A recent report has revealed that about 1.1 billion of people all over the world have no access to clean water and there are also several million people who spend the entire day seeking for scarce water resources (Counts, 2013). The water shortage due to climate change will have dire consequence on global populations especially in countries of Asia and Africa that depend on rain fall and other natural means for their water sources (Molden, 2007). Water scarcity can be seen as a consequence of factors such as poor water management, drought,

pollution, distance and conflict. The devastating effects of water scarcity include poverty, poor sanitation, illiteracy and disease (Marshall, 2011). Therefore, investment in potable water production will yield tremendous benefits ranging from meeting the Sustainable Development Agenda (SDA) to assisting in overcoming poverty and diseases. The green Economic Initiative reported that every dollar invested in safe water and sanitation has a pay back of between $3 to $34 depending on the technology and region (UNW-DPC, 2012). A good education in water management such as water conservation, reclamation, improved sewerage systems and effective treatment would assist to alleviate the global water challenge.

1.3 Wastewater

Wastewater can be defined as the aqueous effluents from one or more of industrial, domestic, agricultural, institutional and commercial sources. The importance of wastewater management in the actualisation of Sustainable Development Agenda (SDA) of accessibility to potable drinking water and sanitation cannot be overemphasised (United Nation Water Analytical, 2009). The major components of wastewater such as organic pollutants, toxic metals, micro-pollutants, plant nutrients, organic dyes and pathogenic micro-organisms can cause serious health and environmental problems when released untreated. There is a rapid growth of deoxygenated dead zones across the oceans and seas because only 10% of the produced wastewater can be adequately treated (Corcoran et al., 2010). The consequences of this on living organisms and the environment can be grievously costly. Evolution of gases such as methane and nitrous oxide which cause ozone layer depletion, chemical contamination and microbial pollution are all responsible for the recent upsurge in poor global economic activity and ill health (UNESCO, 2012). The majority of the mega cities are on the coast with little or no means of safely disposing sewerage from toilets, kitchens and baths except by discharge into the ocean (Corcoran et al., 2010). Domestic wastewater; either black water (excreta, urine and fecal sludge) or grey water (kitchen and bathing wastewater) has a significantly high concentration of pathogens especially in high epidemic regions. These pathogenic organisms are responsible for the death of about 1.45 million people annually (Pandey et al., 2014). The wastewater management system must therefore be efficient for disease prevention and control among many other benefits. Besides, diffuse and end of the pipe pollutants are mostly originating from agricultural and industrial

wastewater. The wastewater from agricultural sources is difficult to quantify because of its diffused nature. However, it has globally been recognised as the largest contributor of pollutants (Frenken and Gillet, 2012; OECD, 2011). Conversely, industrial wastewater contains a very significant number of persistent organic pollutants, toxic chemicals, toxic metals and micro pollutants. It has been reported that 90% of industrial wastewater is intentionally dumped untreated in developing countries (Corcoran et al., 2010).

1.4 Persistent Organic Pollutants

Persistent organic pollutants (POPs) are a group of bio-accumulating chemicals with a propensity for long distance transportation and long retention time in environmental media without degrading into less toxic forms. They are termed contaminants of emerging concern (CEC) because of the recent increase in the awareness of their negative biological and economic impacts. Especially worrying is the negative health impact and endocrine disrupting role of a number of them (Clara et al., 2005; Kiparissis et al., 2003). The diverse sources and volumes of POPs are increasing while fresh water is consequently depreciating in both quality and quantity (Hossain et al., 2012). The sources of POPs include domestic, agricultural and industrial effluents. Pharmaceuticals, personal care products, hormones, industrial chemicals, organic dyes and pesticides are known examples of POPs. These chemicals are responsible for disruption of immune system, cause cancer, disrupt the central nervous system and cause reproductive disorders (WHO, 2008). Contamination of water by POPs constitutes a great environmental liability for the current generation due to their resistance to photolytic, chemical and biological degradation and their harmful impact on abiotic and biotic species. POPs are capable of bioaccumulation and bio-magnification as well as circumvention of the available treatment facilities (Chiron and Minero, 2007). The characteristic semi-volatility and lipophilicity of POPs encourages its widespread environmental transportation and bioaccumulation. A number of these compounds are chemically made up of carbon-halogen bonds which are very strong covalent bonds in the form of an aromatic-chlorine or aromatic-fluorine (Svetla, 2006). As a result of this, the compounds cannot be easily hydrolysed and therefore persist in the environment. Furthermore, their lipophilicity ensures passage through the lipid bilayer of the cell membrane and they get locked up in the fatty tissue, where they may reach toxic concentrations (Tartu et al.,

2017). Examples are organo-halogens which can be in the form of a fluorinated compound, hexachloro benzene, chlordane, dioxins, polychlorinated biphenyl (PCBs), mirex, furans, toxaphene, dichloro diphenyl trichloroethane (DDT) and heptachlor. POPs are generated by both anthropogenic and non-anthropogenic sources with a significant proportion from the former (Miniero and L'lamiceli, 2008). The route of these chemicals depends on their use, the media of transportation as well as their physical and chemical properties. Primarily, POPs exposure is through water and consumption of contaminated food, especially sea food such as fish. Efficient treatment facilities must therefore be installed to properly remove the POPs in wastewater and ensure their absence in potable water.

1.5 Rational and Motivation

Advance oxidation process is known for its diverse production of highly reactive hydroxyl radicals with capability for rapid oxidation of organic pollutants in wastewater, leading to their mineralisation (Bethi et al., 2016). The different form of AOPs system have been tested in electrical discharge (ED), Fenton oxidation, photoctalysis, ozonation and hydrodynamic cavitation (Chong et al., 2012). They have demonstrated efficiencies in both single and combined processes. Application of AOP depends on the treatment objectives and the properties of the wastewater stream. In the recent evaluation of the AOPs systems by Shah et al., (2013), the application of peroxide base system was reported to be the most efficient of the investigated system (O_3, O_3/H_2O_2 and UV/H_2O_2). The preference for hydrogen peroxide over ozone based oxidation may be as a result of the poor efficiency of ozone system in highly turbid wastewater, its toxicity and high maintenance (Reis et al., 2012). Consequently, hydrogen peroxide catalysed by Fe^{2+} in Fenton oxidation and Fenton-like processes has been highlighted to be successful in production of reactive hydroxyl radicals for the purpose of wastewater purification. Conversely, difficulties in the conveyance and high cost of hydrogen peroxide have been the greatest limitation in its application as a Fenton reagent. Besides, the concentration of hydrogen peroxide must be optimised in order to prevent its scavenging of OH radicals at an excessive amount. Since wastewater contains many chemical scavengers, a continuous flow of oxidants must therefore be ensured to achieve complete mineralisation of the contaminants. Efficient and low cost of treatment in AOPs can be achieved through the combined application of several AOPs in

a single system with low chemical and energy inputs (Mahdad et al., 2015). This ensures synergistic effects, with the combined efficiency greater than the sum of individual efficiencies that could be achieved with a separate treatment (Badmus et al., 2018b; Barik and Gogate, 2018).

1.6 Problem statement

Textile and pharmaceutical productions make use of large amounts of clean water during the batch productions which start from washing of raw materials to the finished products. Consequently, large volumes of effluents that contain high chemical oxygen demand (COD), biochemical oxygen demand (BOD), total organic carbon (TOC) and turbidity (Pang and Abdullah, 2013). One of the major environmental concerns is the mineralisation of industrial wastewater effluent before discharge into the environment (Multani et al., 2014). The application of chemical oxidation for the removal of environmental toxicants is considered very expensive as well as resulting in the formation of un-identified intermediate products. Aside from this, the toxicity level of the partially metabolised compounds remains an issue, as it has been observed that the intermediate products are often more toxic than the parent compounds and as such resistant to chemical decomposition. The conversion of these intermediate products into harmless inorganic compounds requires high energy, long reaction times and the use of expensive chemical oxidants. The combination of various advanced water treatment methods such as activated carbon adsorption and ozonation (Kasprzyk-Hordern et al., 2009) or advanced oxidation and membrane filtration has been confirmed to be effective in the removal of POPs from wastewater (Suárez et al., 2008). Although, oxidation methods such as ozonation generate low quantities of effluent, the formation of toxic or unidentified intermediates are their common disadvantages. Currently, the two most important assessment parameters for wastewater treatment technology are their technical and economical feasibilities (Mahamuni and Adewuyi, 2010). The options for low energy and cost effectiveness in the treatment of highly persistent chemical compounds must be exploited. The current challenges may be resolved through the deployment of hydrodynamic cavitation technology and a novel green nano zero valent iron (gnZVI) in the treatment of wastewater which is the focus of this thesis.

1.7 Aim and Objectives of the Study

1.7.1 Aim of the study

The general aim of this research is to devise an efficient combined advanced oxidation process for the treatment of persistent organic pollutants in wastewater. This aim can be achieved through the outlined objectives.

1.7.2 Research objective

The specific objectives of this study are:

- to synthesis and characterise green nano zero valent iron (gnZVI) as a stable and efficient alternative to the conventional nano zero valent iron (nZVI) for use as a catalyst in the treatment of POPs in wastewater.
- to determine the optimum conditions for degradation of POPs using orange II sodium salt solution in jet loop hydrodynamic cavitation system.
- to investigating the influence of the synthesised green nano zero valent iron as a Fenton catalyst for the degradation of POPs using orange II sodium salt in the jet-loop hydrodynamic cavitation system.
- to determine the optimum conditions for degradation of POPs using acetaminophen solution in jet loop hydrodynamic cavitation system.
- to investigating the influence of applying the synthesised green nano zero valent iron as a Fenton catalyst for the degradation of POPs using acetaminophen solution in the jet-loop hydrodynamic cavitation system.
- to determine the optimum amount of Fenton agent (iron II sulfate and hydrogen peroxide) required for the primary treatment of real textile wastewater effluent.
- to determine the optimum amount of aluminium sulfate required for the primary treatment of real textile wastewater effluent.
- to investigate the synergistic effect of a combination of Fenton oxidation and jet-loop hydrodynamic cavitation for the secondary treatment of real textile wastewater effluent.

1.8 Research question

The following questions shall be answered at the end of this study:

- How can a stable and efficient nano zero valent iron be synthesised using aqueous extract of *H. caffrum*?
- What are the optimum conditions for decolouration of orange II sodium salt in jet loop hydrodynamic cavitation equipment?
- What is the optimum amount of hydrogen peroxide that was needed for the degradation of orange II sodium salt in jet loop hydrodynamic cavitation equipment?
- Does applying the synthesised green nano zero valent iron/ hydrogen peroxide in jet-loop hydrodynamic cavitation offer a greater efficiency compared to the iron (II) sulfate/ hydrogen peroxide combination during the decolouration of OR2 solution?
- What is the optimum pH for the transformation of acetaminophen solution in jet loop hydrodynamic cavitation equipment?
- Does applying hydrogen peroxide during the degradation of acetaminophen solution influence the extent of degradation in jet-loop hydrodynamic cavitation?
- Does the application gnZVI as a substitute to iron (II) sulfate lead to the reduction of the elemental iron in the acetaminophen solution during their treatment in the jet loop hydrodynamic cavitation?
- What are the optimum conditions for the primary treatment of raw real textile wastewater effluent using aluminum sulfate that is needed?
- What is the optimum amount of Fenton reagent (iron sulfate and hydrogen peroxide) that is needed for the primary treatment of real textile wastewater effluent?
- Can jet loop hydrodynamic cavitation be used in a secondary treatment of real textile wastewater effluent?

1.9 Scope and delimitation of the study

The current study focuses on the treatment of POPs in wastewater emanating from textile and pharmaceutical manufacturing industries. The two industries are well known for their consumption of large volume of water and the generation of diverse POPs in their effluents. The treatment of Orange II sodium salt, paracetamol and real textile wastewater effluent using Fenton oxidation in the jet loop hydrodynamic cavitation system were investigated. The combinations of Fenton oxidation and jet loop hydrodynamic cavitation were also investigated to determine the efficiency of the combined process. Nano zero valent iron was tested as an alternative Fenton catalyst in the mineralisation of the POPs. This study did not investigate the effect of heterogeneous catalyst or photo catalyst as alternative to the Fenton catalyst.

1.10 Thesis Outline

The research work presented in this thesis is as summarised in eight chapters:

Chapter 1

A brief introduction includes research overview and backgrounds of the studies were provided in this chapter. The rationale, motivations, problem statements, research questions, scope and delimitation of the study were also stated.

Chapter 2

The chapter is an overview of the current status of jet-loop hydrodynamic cavitation in combination with other advanced oxidation for efficient degradation of persistent organic pollutants in wastewater. This includes a general introduction to the concept of wastewater as a potential source for the recycle and reuse of water. The ineffectiveness of conventional treatment systems in the removal of persistent organic pollutants in wastewater was discussed. The treatment of persistent organic pollutants in textile and pharmaceutical wastewater by advanced oxidation processes and the limitations of the systems were provided. This chapter also has a summary highlighting the knowledge gap in the state of the art that informed the study focus.

Chapter 3

This chapter provides a brief description of methods that were used in the synthesis of the green nano zero valent iron (gnZVI), include the optimisation for activity and stability of gnZVI using leaves extract of wild plum (*H. caffrum*). It also highlighted the various characterisation and analytical techniques as well as a list of chemical used.

Chapter 4

This chapter provides the information on the synthesis and characterisation of stable and efficient nano zero valent iron using aqueous extract of *H. caffrum*. The synthesised green nano zero valent iron (gnZVI) were applied in the Fenton oxidation of the orange II sodium salt to determine their activities.

Chapter 5

This chapter covers the degradation of orange II sodium salt solution in jet loop hydrodynamic cavitation system using the synthesised green nano zero valent iron as a form of Fenton catalyst. The orange II sodium salt solution was used to simulate the persistent organic pollutant in textile wastewater. The optimum conditions for degradation of orange II sodium salt solution in jet loop hydrodynamic cavitation system were determined and the synergistic effect of applying the synthesised green nano zero valent iron as a Fenton catalyst for the degradation of orange II sodium salt in the jet-loop hydrodynamic cavitation system was estimated. The mechanism of the degradation of orange II sodium salt was studied using ion chromatography and liquid chromatography-mass spectra to capture the intermediate and the final products.

Chapter 6

This chapter covers the degradation of acetaminophen solution in jet loop hydrodynamic cavitation system using the synthesised green nano zero valent iron as a form of Fenton catalyst. The acetaminophen solution was used to simulate the persistent pharmaceutical pollutant in wastewater. The optimum conditions for degradation of acetaminophen solution in jet loop hydrodynamic cavitation system was determined and the synergistic effect of applying the synthesised green nano zero valent iron as a Fenton catalyst for the degradation of acetaminophen solution in the jet-loop hydrodynamic cavitation system was estimated.

The Mechanism of the degradation of acetaminophen was studied using ion chromatography and liquid chromatography-mass spectra to capture the intermediate and the final products.

Chapter 7

This chapter presents the treatment of real textile wastewater effluent using alum coagulation and Fenton reagent in the primary stage with main goal of removing insoluble solid particle and reducing the chemical oxygen demand. Jet-loop hydrodynamic cavitation was used in the secondary treatment to further reduce COD, and remove total dissolvable solid (TDS) and biological oxygen demand (BOD). The optimum amount of Fenton agent (iron II sulfate and hydrogen peroxide) required for the primary treatment of real textile wastewater effluent was determined. The optimum amount of aluminum sulfate required for the primary treatment of real textile wastewater effluent was also determined. The synergistic effect of a combination of Fenton oxidation and jet-loop hydrodynamic cavitation for the secondary treatment of real textile wastewater effluent was investigated and the efficiency of alum coagulation method and Fenton oxidation was compared in term of quantity and microbial content of sludge.

Chapter 8

This includes the general conclusion of the thesis and scope for future research work.

CHAPTER 2

LITERATURE REVIEW

2.1 Overview

Persistent Organic Pollutants (POPs) are very tenacious wastewater contaminants. The consequences of their existence have been acknowledged for negatively affecting the ecosystem with specific impact upon endocrine disruption and hormonal diseases in humans. Their recalcitrance and circumvention of nearly all the known wastewater treatment procedures are also well documented. The reported successes of POPs treatment using various advanced technologies are not without setbacks such as low degradation efficiency, generation of toxic intermediates, massive sludge production, high energy expenditure and operational cost. However, advanced oxidation processes (AOPs) have recently recorded successes in the treatment of POPs in wastewater. AOPs are technologies which involve the generation of OH radicals for the purpose of oxidising recalcitrant organic contaminants to their inert end products. This review provides information on the existence of POPs and their effects on humans. Besides, the merits and demerits of various advanced treatment technologies as well as the synergistic efficiency of combined advanced oxidation processes (AOPs) in the treatment of wastewater containing POPs was reported. A concise review of recently published studies on successful treatment of POPs in wastewater using hydrodynamic cavitation technology in combination with other advanced oxidation processes is presented with the highlight of direction for future research focus.

2.2 Introduction

The combinations of effluents from one or more of industrial, domestic, agricultural, institutional and commercial practices constitute wastewater. The concept is very important in water resource management because it allows economically feasible reuse or controlled discharge of toxic waste into the environment. Efficient wastewater management, availability of potable water and good sanitation is an important ingredient in the actualisation of Millennium Development Goals (MDG) (UNESCO, 2012). The major components of wastewater such as organic pollutants, toxic metals, micro-pollutants, plant nutrients and pathogenic micro-organisms can cause serious

health and environmental problems when released untreated (Corcoran et al., 2010). Meanwhile, only a small volume of the produced wastewater can be adequately treated with conventional treatment facilities (Frenken and Gillet, 2012). The consequence of this is the rapid growth of deoxygenated dead zones across the oceans, seas and lakes with grievous impact on living organisms and their environment. Evolution of gases (from the dead zone) such as methane and nitrous oxide which cause ozone layer depletion as well as chemical contamination and microbial pollution may partially be responsible for the recent upsurge in poor global health (UNESCO, 2012). Besides, the majority of the mega cities are adversely affected because of their high population status and location which is generally on the coastal line with little or no means of adequately disposing effluents from toilets, kitchens and baths (Corcoran et al., 2010)

Apparently, wastewater can originate from a discrete and identifiable point source or from a diffuse and difficult to control non-point source. Domestic and industrial wastewaters are very common point sources while agricultural wastewater predominate the non point sources of contamination. Domestic wastewater, either black water (excreta, urine and fecal sludge) or grey water (kitchen and bathing wastewater) has a significant concentration of excreted pathogens, especially in high epidemic regions. These pathogenic organisms are responsible for the preventable death of about 1.45 million people annually (Pandey et al., 2014). The wastewater management system must therefore be efficient for disease prevention and control among many other functions. Besides, diffused and end of pipe pollutants are mostly sourced from agricultural wastewater. Agricultural practices account for the highest percentage of global water use. Wastewater from agricultural sources is difficult to quantify because of its diffused nature. However, it has been recognised as a major global contributor of pollutants (OECD, 2011). Industrial wastewater contains a significant number of persistent organic pollutants, toxic chemicals, heavy metals and micro pollutants. 90% of industrial wastewater is intentionally dumped untreated in developing countries (Corcoran et al., 2010). The success stories in some countries are based on clear allocation of responsibilities for wastewater managers and strict adherence to the principles of urban wastewater treatment directives (DEFRA, 2012). Permits or consents can also be issued based on the quantity and quality of waste to be discharged and some substances (arsenic, mercury, cadmium, selected pesticides, cyanides and a number of complex organic compounds) are banned completely. The huge amount of wastewater generated in manufacturing companies and the household must be treated to ensure effective

reclamation and reuse of the scarce water resources for profitability and efficient management. In view of this, investment in low energy, environmentally friendly and cost effective wastewater treatment technology can no longer be delayed. The major focus of contaminant removal is based on organic matter which is primarily measured by oxygen demand. Chemical oxygen demand (COD) is the amount of dissolved oxygen required by a chemical oxidizing agent for the oxidation of organic content of the treated water. Meanwhile, biochemical oxygen demand (BOD) measures the dissolved oxygen used in the oxidation of organic matter by micro-organisms. COD is higher in magnitude than BOD because there are many organic chemicals that cannot be oxidized by micro-organisms but can be easily oxidised by chemicals. The oxygen used in the incineration (physical oxidation) of organic matter in the treated water is measured by total oxygen demand (TOD) while the amount of organic carbon remaining after incineration of the treated water is termed total organic carbon (TOC). This paper examines the existence of POPs contamination in wastewater, its effect on humans, the success and failure of conventional wastewater treatment to degrade the POPs in wastewater. Furthermore, the attempt made through the development of various forms of advanced treatment options in removing these POPs and the opportunities offered by the use of heterogeneous Fenton processes in hybrid combinations with hydrodynamic cavitation are also reviewed.

2.3 Persistent Organic Pollutants (POPs)

Persistent organic pollutants (POPs) are a group of bioaccumulative chemicals with the propensity for long distance transportation and long retention time in the environmental media without degrading into less toxic forms. They are contaminants of emerging concern (CEC) due the recent increase in the awareness of their biological and economic importance. Especially worrying is the negative health impact and endocrine disrupting role of a number of these compounds (Clara et al., 2005; Kiparissis et al., 2003). The diverse sources and volumes of persistent organic pollutants (POPs) are increasing while fresh water is consequently depreciating in both quality and quantity (Hossain et al., 2012). The sources of POPs include, domestic, agricultural and industrial. Pharmaceuticals, personal care products, hormones, industrial chemicals, organic dyes and pesticides are known examples of POPs. These chemicals are responsible for disruption of the immune system, cause cancer, central nervous system and

reproductive disorders (WHO, 2008). Initially, 12 chemicals were already recognised at Stockholm convention for their responsibility for causing adverse effects on human and ecosystem (Table 1). Contamination of water by POPs constitutes a great environmental liability for the current generation due to their resistance to photolytic, chemical and biological degradation and their harmful impact on abiotic and biotic species (Chiron and Minero, 2007). The characteristic semi-volatility and lipophilicity of POPs encourages their widespread, environmental transportation and bioaccumulation respectively. A number of these compounds are chemically made up of carbon-halogen bonds which are very strong covalent bonds in form of an aromatic-chlorine or aromatic-fluorine (Svetla, 2006). As a consequence of this, the compounds cannot be easily hydrolyzed and therefore persist in the environment. Furthermore, their lipophilicity ensures passage through the lipid bilayer of the cell membrane and causes them to be locked up in the fatty tissue, where they may reach toxic concentrations (Tartu et al., 2017). Examples are organo-halogens which can be in the form of fluorinated compounds, hexachloro benzene, chlordane, dioxins, polychlorinated biphenyl (PCBs), mirex, furans, toxaphene, dichloro diphenyl trichloroethane (DDT) and heptachlor. POPs are generated by both anthropogenic and non-anthropogenic activities with a significant proportion from the latter (Miniero and L'lamiceli, 2008). The route of these chemicals depends on human uses, the media of transportation, physical and chemical properties. Primarily, POPs exposure is through water and consumption of contaminated food, especially sea food such as fish. Efficient treatment facilities must however be installed to properly remove the POPs in wastewater and ensure their absence in potable water.

Table 2.1:Recognised POPs in the Stockholm convention

Name	Use	Mode of persistence	Effect	References
Endrin	Insecticide and pesticide	Long half-life and persist in soil for more than 12 years.	Toxic to fish and result in early hatchery of eggs and death of fingerlings. Can damage the central nervous system	(World Health Organization, 2004)
Polychlorinated dibenzofurans (PCDF)	Produced during the manufacturing of PCBs and dioxins	Enter the environment through waste incineration and automobile exhaust.	Carcinogenic chemical, causes toxicity to infants and hormonal compromised organisms	(Colt et al., 2009; Dianyi, 2016; Liu and Lewis, 2014)
Heptachlor	Insecticide and pesticide	Highly persistent and bio accumulative in the environment. Detected in blood of cattle and processed food.	Carcinogenic and high toxicity and low concentration.	(Pokethitiyook and Poolpak, 2012)
Polychlorinated dibenzo-p-dioxins (PCDF)	Produced during the manufacture of pesticides and other chlorinated compounds	Seven out of the indentified dioxins are of concern. They are emitted during the combustion of hazardous waste and automobile emission. They can persist in soil for more than 10 years after emission.	Causes birth defect and labeled as carcinogenic. They are also toxic to aquatic animals	(Toft et al., 2004)
Hexachloroben zene (HCB)	Fungicide, Exist as impurity in the manufacturing of certain pesticides.	Highly persistent and bio accumulative, detected in breast milk and blood of animals.	Lethal substance, causing reproductive problem, Birth defects, metabolic disorder (porphyria turcica)	(Silverstone et al., 2012; Toft et al., 2004)
Toxaphene	Insecticide and pesticide	Highly persistent and bio accumulative. The half-live is amount 12 years.	Carcinogenic, high toxicity for fish and aquatic organisms. Causes	

			reduction in weight and reduced egg viability.	
Polychlorinated biphenyl (PCBs)	Used as heat exchange fluid, electrical transformer, additive in paints and in capacitor	The persistency depends on the degree of chlorination with half-life from 1- 10 years	High toxicity to fish and other aquatic animals. Listed as human carcinogen and immune suppressant.	(Côté et al., 2006)
DDT	Insecticides	Half-life between 10-15 years. Bioaccumulative, detected in breast milk	Chronic health effect on adults and infants. Carcinogenic chemical	(Thuy, 2015)
Aldrin	Pesticide	High toxicity, bio-accumulative, biomagnifications. Causes food contamination	Death of animals along the food chains	(Chhillar et al., 2013)
Chlordane	Broad spectrum insecticide	Bioaccumlative, it can be air bourn with half-life not less than 1 year	Carcinogenic, can damage human immune system and causes death of marine animals	(Multigner et al., 2016)
Dieldrine	Insecticide	Conversion of Aldrin to dieldrine causes more dieldine than the labeled in the environment.	Causes spinal deformation in frogs' embryos	(Kataoka et al., 2010)
Mirex	Insecticide	Found in animals including human, air, water and soil. The half-life is between 1-5 years Very stable and persistent. The half-live is about 10 years. It has been detected in food such as meat and fish	Human carcinogen and high toxicity to fish and other aquatic animals	(Charlier et al., 2002)

2.4 Treatment Options

Contaminated water contains hazardous chemicals and toxins which cause diseases and organ disruption. Water for human and animal use must be treated to ensure good health. Besides, transformation of contaminants into harmless end products and complying with legal approval for discharge is very important. Wastewater treatment methods ensure removal of the undesirable components from water and its conversion into a potable form which is free of waterborne pathogens and other hazardous compounds. Water treatment methods can be categorised into physical, chemical and biological treatment. Efficiency in wastewater treatment can most likely be achieved with the prudent combinations of two or more of these methods. Conventional treatment is the term that covers some of the successful water treatment techniques deployed in the service and provision of industrial or municipal potable water. Any of the physical, chemical or biological routes can be combined at the different stages of a particular conventional treatment technology. The stages in conventional wastewater treatment are generally referred to as preliminary, primary, secondary and tertiary, in increasing order of treatment level with the final pH adjustment as necessary. The appropriate conventional method must be able to meet the recommended microbiological and chemical standards set by the regulatory authority at an inexpensive operational and maintenance cost (Pescod, 2004). However, POPs are resistant to conventional treatment methods such as flocculation, coagulation, filtration and oxidant chemical treatment with chemicals like chlorine (Swartz et al., 2016). They are not likely to adsorb on organic matter despite their documented lipophilicity and application of treatment chemicals often leads to the formation of unwanted intermediates (Benitez et al., 2001). However, various advanced wastewater treatment technologies such as activated carbon adsorption, membrane bio reactor (MBR) and AOP have been applied in the treatment of POPs (Kasprzyk-Hordern et al., 2009; Suárez et al., 2008).

2.5 Activated Carbon Adsorption

Activated carbon is an extremely porous material with large surface area that allows the adsorption of a number of substances in their gaseous or liquid phases. Activated carbon can be used in commercial industries such as pharmaceuticals and foods for decolourisation, deodorisation and purification. It is capable of removing a large amount of dissolved compounds

from wastewater because of its large surface area to volume ratio. The mechanism of removal is usually adsorption which occurs when the attractive forces on the carbon surface outweigh the attractive forces of the liquid. The large surface area of activated carbon accumulates large numbers of contaminant molecules. It is generally recommended in the tertiary stages of wastewater treatment for removal of chemical substances, colourants and reduction of chemical oxygen demand (COD). The activated carbon powder can be a form of granular activated carbon (GAC) or powdered activated carbon (PAC). The formation of toxic sludge, high maintenance cost and fouling of adsorbent material is their greatest limitation. Researching the use of low cost materials and surface functionalising has improved the use of activated carbon in water treatment (Dağdelen et al., 2014). Synthesis of activated carbon can be achieved through the use of waste carbonaceous substances or biomass. Üner, et al. (2016) reported a significant removal of methylene blue (MB) dyes from aqueous solution using activated carbon synthesised from the activation of *Citrullus lanatus* (Melon) rind by zinc chloride. Altmann et al. (2014) in their direct comparison of activated carbon and ozonation for POPs treatment in wastewater, reported the successful removal of carbamazepine and diclofenac by both treatment options. A greater efficiency was reported for activated carbon in the removal of bezafibrate, benzotriazole and iomeprol compared to ozone, while sulfamethoxazole was more efficiently removed by ozonation. However, each option has its own specificity, depending on the treatment objective. The use of activated carbon is very efficient and it may remove more than 90% of the POPs, especially those that contain benzene and/or amine functionalities which enhance their sorption activity (Snyder et al., 2003). One of the advantages of GAC is the possibility of thermally reactivating and reusing of the carbon content. The powdered activated carbon (PAC) is usually added as dry powder or aqueous solution simultaneously with the flocculation step. PAC's economical advantages include reduction of cost due to aeration tanks and secondary settlement basins as well as its flexibility in term of dosing. Wong et al. 2016, reported the capability of triethoxyphenylsilane (TEPS)-functionalized magnetic palm-based powdered activated carbon (MPPACTEPS) for the low cost and effective degradation of POPs. Demerits are large volume of toxic sludge and the mere transfer of contaminants from aqueous phase to solid phase.

2.6 Membrane Bioreactor (MBR)

Membrane bioreactor (MBR) is an integration of a biological process (such as a suspended growth reactor) with a perm-selective membrane. The solid material which is developed by biological process is preferentially rejected by a membrane to create a clarified and disinfected product. It is usually an active sludge with membrane filtration equipment based on ultra filtration or micro filtration. MBR systems can be a gravity-driven or pressure-driven type. The gravity-driven systems involve the use of hollow fibers or flat sheet membranes in either the bioreactor or in a subsequent membrane tank while a pressure-driven system uses in-pipe cartridges located externally to the reactor. Generally, the process is initiated by a microbial degradation of the pollutants, followed by continuous filtration and air scouring in a series of working membrane units. The type of membrane is generally dependent on the size of the contaminant. It incorporates a series of filters such as nano-filters; used for contaminant sizes in the range 1 to 5 nm, ultra-filters; used for contaminant sizes in the range 5 to 100 nm and microfiltration which is used for contaminants of size ranges between 100 to 1000 nm. MBR is considered efficient, simple, cost effective and reliable for the treatment of both organic and inorganic pollutants (Trzcinski and Stuckey, 2016). It generates a high quality effluent. However, fouling of membranes which leads to the increase in trans-membrane pressure (TMP), processing time and cost of maintenance are the greatest hindrances in the application of MBR for wastewater treatment (Snyder et al., 2003). Likewise, generation of solid phase effluents which are very difficult to dispose is also a serious demerit associated with MBR. More research is desirable in order reduce the fouling effect and improve the integration of MBR in hybrid with treatment technologies for the increase exploitation of its many benefits (Mahamuni and Adewuyi, 2010). Currently, the MBR do not always produce the expected result in the treatment of POPs and show poor removal of non-biodegradable aliphatic and aromatic hydrocarbon compounds, halogenated organic compounds, organic dyes, pesticides, phenols and their derivatives. The two most important assessment parameters for satisfaction of the objective in wastewater treatment technology are the process technicalities and economical feasibilities (Ozonek and Lenik, 2011). An efficient, safe, low energy and cost effective option must be exploited for effective treatment of highly persistent chemical compounds. Consequently, other important modern techniques currently undergoing intensive investigations must be exploited.

2.7 Advanced Oxidation Processes (AOPs)

Advanced oxidation processes (AOPs) are aqueous phase oxidation systems that generate highly reactive hydroxyl (OH) radicals as the predominant species with high capabilities for destruction of persistent organic pollutants. The OH radicals ensure the effective degradation of soluble organic contaminants into simple and biodegradable forms. Factors such as water turbidity, solution pH, time of reaction, amount/ volume of the organic compound susceptible to degradation and the presence of OH radical scavengers or stimulator substances can significantly affect the degradation activity of the OH radical (Bethi et al., 2016). The AOPs can be in the form of an electrical discharge (ED) oxidation or a cavitation system, both of which are recently acknowledged as wastewater treatment technologies (Chong et al., 2012). The uniqueness of these processes is their diverse production of highly reactive OH radicals, which react non-specifically and rapidly oxidise organic pollutants in wastewater. AOPs can be applied as a single process or in combination with other AOPs or with conventional methods depending on the treatment objectives and the properties of the wastewater stream. The most commonly applied chemical in AOPs is ozone, or its combinations such as O_3/H_2O_2, O_3/UV or O_3/Fe_2O_3 (Shah et al., 2013). Shah et al., (2013) evaluated the degradation of acetaldehyde and amine in O_3, O_3/H_2O_2 or UV/H_2O_2 AOPs systems. He reported that OH radical based AOPs were more efficient than ozone in the destruction of acetaldehyde. Meanwhile, ozonation is considered to be a preferable treatment because it is more efficient for the destruction of amines and there is no need for the injection of hydrogen peroxide for optimum performance of the system (Giri and Ozaki, 2010). The studies have also confirmed the capability of ozone based techniques for simultaneous removal of POPs when mineralising simulated wastewater containing sixteen commonly used pharmaceuticals by using several combination AOP techniques. Despite the opportunities offered by ozone treatment of POPs, its toxicity, high cost of treatment and costly maintenance are big disadvantages. Besides, ozone performance is very poor in wastewater with high soluble solids (SS) content, high chemical oxygen demand (COD), high biological oxygen demand (BOD) or high total organic carbon (TOC) levels (Reis et al., 2012). Hydrogen peroxide with ferrous ion as a catalyst in Fenton oxidation and Fenton-like processes has been highlighted to be successful in production of reactive hydroxyl radicals for the purpose of wastewater purification. The iron needed for catalytic oxidation in Fenton reactions is often available in

industrial wastewater. Fenton oxidation can be applied in both primary and secondary stages of treatment. In this regards, the hydrogen peroxide with ferrous ion as a catalyst can disinfect the water by killing the micro-organisms while the OH radicals degrade the persistent organic pollutants and the generated Fe^{3+} complex acts as an excellent coagulant (Hamamoto and Kishimoto, 2017). Difficulties in it the conveyance and cost of hydrogen peroxide have been the greatest limitation in the application of Fenton oxidation. However, electro-Fenton systems with capabilities for in situ generation of OH radicals have been very successful in wastewater treatments in AOPs (Asghar et al., 2015). Factors such as initial concentration of the effluent stream, pH, temperature, operating parameters (inlet pressure) and reactor design play vital roles in the determination of the process efficiency (Badmus et al., 2016). All these factors are very important and must be applied at the specific optimum conditions. The free radical generation process is pH sensitive and a good understanding of its manipulation is required for the successful degradation of POPs (Bagal and Gogate, 2014a). Slow degradation can occur due to a low production rate of OH radicals in an acidic solution (pH < 2.0). This can be caused by stabilisation of hydrogen peroxide due to the formation of oxonium ions at low pH, or the formation of a slow reacting aqueous iron complex or the scavenging effect of hydrogen peroxide by the excess protons (Gore et al., 2014). Besides, Fe II complexes may be produced at pH > 4, this also reduces the production rate of the OH radical and consequently slows the degradation of POPs (Muruganandham et al., 2014; UNESCO, 2012). The concentration of hydrogen peroxide must be optimised in order to prevent its excessive scavenging of OH radicals (Dimitrakopoulou et al., 2012; Gore et al., 2014). These highlighted challenges can be redressed with the deployment of novel cavitation technology and nano zero valent iron (nZVI) in the treatment of wastewater. The insitu generation of OH radical/ hydrogen peroxide in cavitation technology and nZVI system has been recently reviewed (Lester et al., 2011). Either energy intensive UV or chemical intensive hydrogen peroxide can also be used to complement ozone or together in an AOP system to give efficient treatment of POPs. Dimitrakopoulou et al., (2012) investigated UV-A/TiO_2 photocatalytic degradation of amoxicillin (AMX) in aqueous suspension (Dimitrakopoulou et al., 2012). This system successfully degraded AMX in simulated wastewater, under the control of irradiation time, solution pH, water matrix, photocatalyst types and loading. The degradation of the AMX was however very slow resulting in the formation of unknown intermediate products. A single AOP system can accomplish partial degradation of

recalcitrant organic pollutants, but rarely achieves complete mineralisation except in combination with other forms of AOPs or treatment procedures (Cai et al., 2015; Hou et al., 2016; Zhang et al., 2013). Other challenges are the formation of unknown secondary by-products, costly chemical reagents (peroxide) and high energy requirement (UV and ultrasound). Since wastewater contains many chemical scavengers, a continuous flow of oxidants must therefore be ensured to achieve complete degradation or mineralisation of the contaminants. Efficient and low cost of treatment in AOPs can be achieved through the combined application of AOPs in a single system with potentially no or low chemical and energy inputs (Mahdad et al., 2015). This ensures synergistic effects, with the combined efficiency greater than the sum of individual efficiencies that could be achieved with a separate treatment.

Table 2.1: Characteristics of advanced oxidation processes

Process	Important Reaction	Advantages	Disadvantages
Fenton Oxidation	$Fe^{2+} + H_2O_2 \rightarrow OH^{\bullet} + OH^{-} + Fe^{3+}$	Effective AOP for organic pollutant, colour and COD removal, no energy is needed (Thakur and Chauhan, 2016)	Effectiveness is within narrow pH, formation of large volume of iron sludge, H_2O_2 is expensive (Chong et al., 2012)
Photo-Fenton	$Fe^{2+} + H_2O_2 + UV \rightarrow OH^{\bullet} + OH^{-} + Fe^{3+}$	Effective AOPs for organic pollutant. UV light enhances the efficiency of the Fenton process.	High cost of treatment due to UV source. Energy intensive procedure (Mahdad et al., 2015)
Ozone /UV	$O_3 + hv + H_2O \rightarrow 2OH^{\bullet} + 0_2$	Very efficient method for highly polluted effluent. Mechanism is the photolysis of ozone in presence of water	High cost of treatment due to the cost of energy and chemicals. Removal is pH dependent (Chin and Bérubé, 2005)
Ozone /H_2O_2	$2O_3 + H_2O_2 \rightarrow 2OH^{\bullet} + 0_2$	Very efficient method for highly polluted effluent. Degradation is facilitated by both ozone and hydrogen peroxide	The method is costly and chemical intensive (Jelonek and Neczaj, 2012)
UV /H_2O_2	$H_2O_2 + hv \rightarrow 2OH^{\bullet}$	Photolysis of hydrogen peroxide generates radical. The amount of radical generated depends on the intensity of UV (Chin and	Not applicable to all contaminant, high cost of treatment

		Bérubé, 2005). Sunlight can also be used with optimised quantity of hydrogen peroxide.	
O_3/UV /H_2O_2	$H_2O_2 + O_3 + H_2O\ (hv) \rightarrow 4OH^{\bullet} + O_2$	Very effective and low cost of treatment. The combined AOPs result in synergistic effect on pollutants.	The method is chemical intensive (Lester et al., 2011)
Ultrasonicator	$2H_2O + US \rightarrow 2OH^{\bullet} + 2H^{\bullet}$	Green AOPs, no or little secondary product is generated, it requires no or little chemical	Difficult to upscale, cost of treatment is high (Zhang et al., 2013)
Hydrodynamic Cavitation	$2H_2O\ (in\ jetloop) \rightarrow 2OH^{\bullet} + 2H^{\bullet}$	Green AOP, little or no secondary product is generated, requires little or no chemicals, capability to treat large volumes of wastewater, low cost of treatment (Tinne et al., 2014).	In the developmental stage
Nano zero valent Iron	$Fe^0 + H_2O + O_2 \rightarrow Fe^{2+} + 2OH^{\bullet}$	Reduced iron sludge, more effective than the Fenton, can be combined with another metal for heterogeneous catalysis. reduced treatment cost	Safety of nano particle is in doubt (Yaacob et al., 2012)

2.8 Cavitation

This is the formation, growth and collapse of bubbles (cavity) within a liquid as a consequence of local pressure pulsations. The liquid which contains vaporous bubbles experiences a consistent pressure reduction which results in the increase in size (growth) of bubbles and eventual collapse (implode) at a critical magnitude of pressure (Šarc et al., 2017). At this state, the critical pressure is lower or very close to the liquid specific saturated vapour pressure. The implosion of the bubble is accompanied with local destruction of chemical bonds, hydraulic shock, high temperature and pressure of about 5000 Kelvin and 60,000 kPa respectively for a short period in the trapped vapour (Gong and Hart, 1998). Until recently, cavitation was only known for causing the erosion of metallic surfaces and research attention was on its prevention. Surface destruction and material displacement caused by cavitation have been huge challenges for mechanical equipment users and producer (Ozonek and Lenik, 2011). This extreme condition is adequate for rupture of biological or organic structures and dissociation of water molecules into OH and H radicals. The generated OH radical is an excellent initiator of chain reactions and

one of the most powerful oxidants with the capability for spontaneous, non-specific degradation of unsaturated hydrocarbons. Since the unsaturated hydrocarbon bond is a basic chemical structure of organic contaminants, the generated OH radical can therefore be applied for the treatment of persistent organic pollutants (POPs) in wastewater and sewage. Degradation of pollutants depends on their functional group content because only a small amount of radicals reach the bulk liquid bulk. Apparently, the OH radical is responsible for the degradation of organic pollutant during cavitation in three locations; inside the bubble, at the gas-liquid interface and in the bulk liquid phase (Mehrvar et al., 2001). The cavitation can be initiated by a local power supply as in optical (strong laser beam) and molecular cavitation (elementary particle) or by stretching forces, as in acoustic and hydrodynamic cavitation. The sizes of bubbles and their position can be controlled in both optical and molecular cavitation. Their commercial application is limited due to the high operational cost (Santos et al., 2008). The acoustic cavitations and hydrodynamic are the two most used types of cavitation technology with capability for large scale application in wastewater treatment plants. Acoustic cavitation is caused by the acoustic waves in liquid while hydrodynamic cavitation is caused by hydrodynamic phenomena in liquid. Other existing cavitations are optical cavitation and molecular cavitation caused by strong laser beam and elementary particles (proton) respectively (Ozonek, 2012).

Acoustic cavitation using ultrasound is a physical phenomenon which is caused by sound waves in alternating compression and rarefaction. The performance of ultrasonic cavitation depends upon the frequency, intensity of the sound waves, as well as temperature, the nature of solvent and the external pressure (Santos et al., 2008). The formation of bubbles in an ultrasonicator may be favored at low frequencies (20 kHz) because the higher the frequency the lower the cycle of compression and decompression. Therefore, the void needed for achievement of cavitation is absent at higher frequencies (Šarc et al., 2017). Conversely, an increase in sonochemical intensity can be caused by an increase in the amplitude of vibration. This is due to the proportional relationship between the amplitude and intensity. The intensity must be at the optimum value for achieving a positive sonochemical effect because too high an intensity may be detrimental to sonochemical degradation, leading to the deterioration of the transducer. Furthermore, optimum application of temperature must be ensured during ultrasonic cavitation.

Too high temperatures can lead to disruption of the solute-matrix interaction, promote microbial integration and enhance the diffusion rate. The consequence of this is the reduction in sonication effect because increased evaporation leads to reduced bubble formation and successful bubble collision (Santos et al., 2008). Besides, cavitation is not easily achieved in a liquid of high natural cohesion i.e. high magnitude of viscosity and surface tension (Webb et al., 2011). Atmospheric pressure is very adequate for ultrasonic cavitation. The pressure can be generated either through an ultrasonic bath or probe by manipulating parameter such as the amplitude or frequency. These pressure pulse parameters are easy to control and reproduce. Consequently, acoustic cavitation is the best way to demonstrate the phenomenon of cavitation in the laboratory (Louisnard and González-garcía, 2011). It can be applied directly using an ultrasonic probe or indirectly through the wall of the container using a sonication bath or sonoreactor. The unifying factor is the production of oxidative species, like hydroxyl radicals which invariably react with contaminants. According to hot-spot theory, reaction with free radicals can occur in the surrounding liquid, within the collapsing bubble and at its interface (Mahamuni and Adewuyi, 2010). Ultrasonic applications are currently limited to laboratory scale and developing stage. However, they are increasingly gaining acceptance in the treatment of POPs in wastewater because of their environmental friendliness and cost effectiveness. The different types of probe can be immersed in a liquid directly for the purpose of sonication. Contamination and loss of volatile sample content are usually experienced as a consequence of direct contact of the probe with the liquid. The indirect application of sonication (glass probe) can take care of the contamination defect associated with the direct use of a probe (Santos et al., 2008; Santos and Capelo, 2007). Ultrasonicator can be applied in wastewater decontamination, electrocoagulation, disinfection and membrane filtration (Sillanpää et al., 2011). The beneficial removal of several POPs by ultrasonication has been demonstrated in many studies (Chu et al., 2011). Adewuyi and Khan (2012) provided a framework model for robust and rigorous development of sonochemical systems and reactors (Adewuyi and Khan, 2012). Effective mineralisation of POPs however, depends on the combination of ultrasonicator with other AOPs (de Vidales et al., 2015).

The cavity in hydrodynamic cavitation is generated as a consequence of constrictions in liquid flow. The smooth convergence/divergence of a venturi design ensures that the greatest degree of degradation could be obtained (venturi) compared to an orifice designed with similar levels of

operating pressure (Mishra and Gogate, 2010). The possibility of multiple holes within the same cross sectional area and simple fabrication are the comparative advantages of using an orifice plate. The efficiency of hydrodynamic cavitation depends on the cumulative effect of factors such as device parameters, properties of the investigated velocity at the expense of pressure in a reactor. For hydrodynamic cavitation, orifice or venturi designs are capable of generating cavitation in a flowing liquid system and technology process parameter (Ozonek, 2012). Device parameters such as the size or shape of the cavitation inducer and flow chamber defines the structural characteristics of the reactor while properties of the investigated system such as viscosity, density, dissolved gas and surface tension are the parameters characterising the properties of the medium. The technology process parameters are the liquid flow rate, temperature and inlet pressure. The lower the cavitation number, the higher the magnitude of velocities existing in a reactor and consequently the number of passes through the cavitating zone for the same time of operation will be higher (Dular et al., 2016). Therefore, higher degradation of pollutants is as a result of the high number of passes through the cavitating device which ensures that the liquid experiences cavitating conditions more frequently. The operating pressure in hydrodynamic cavitation is due to the high variation in liquid or fluid acceleration/deceleration inside a closed pipe. The inflexible experimental procedures of hydrodynamic cavitation create difficulties in its optimisation (Benito et al., 2005). Meanwhile, the operating cost is relatively low and the possibility of treating large volume of wastewater with inexpensive component parts such as tank, venturi tube and pipes is feasible.

Cavitation is usually applied after the treatment with biological processes or in combination with other advanced oxidation processes. The combination of cavitation with other AOP methods during wastewater treatment is to compensate for the challenges of each of the methods with regard to the mineralisation of POPs. In such cases, cavitation methods are very effective if carefully applied. Braeutigam and coworkers (2012) reported 63% transformation of carbamazepine (5 µg/ L) in a combined hydrodynamic cavitation and ultrasonic cavitation processes within 15 minutes. Zupanc et al., (2013) studied the removal of clofibric acid, ibuprofen, naproxen, ketoprofen, carbamazepine and diclofenac by hydrodynamic cavitation. They obtained between 30-70% degradation when their system was combined with UV/H_2O_2 at optimum conditions. The two methods of cavitation (acoustic and hydrodynamic) are very

efficient, green and cost effective for the treatment in wastewater, especially in the tertiary application to remove or mineralise POPs. Worth noting is the advantageous edge of hydrodynamic (jet-loop) over acoustic (ultrasonicator) in terms of simplicity, energy efficiency (except multiple frequency flow cell), cost and large scale application (Bother, 1993).

2.9 Application of hydrodynamic cavitation in hybrid AOP systems

Hydrodynamic cavitation at optimum operational conditions establishes the continuous generation of free radicals and allows the maximum contact between the generated radicals and the pollutants in the shortest possible time. Apparently, energy efficiency of hydrodynamic cavitation is highly dependent on experimental conditions and pollutant characteristics. Its various advantages such as low operational cost, no chemical addition, low energy utilisation and treatment of large volume of pollutants makes it a very efficient procedure for the mineralisation of POPs in partially treated water (Dular et al., 2016). The combination of hydrodynamic cavitation with other advanced oxidation processes ensure efficient mineralisation of micro pollutants with better synergistic effects compared to stand-alone advanced oxidation processes (Gore et al., 2014). Sunita et al (2016) reported effective degradation of methomyl using hydrodynamic cavitation and enhanced the treatment by combining it with other AOPs such as H_2O_2, Fenton reagent and ozone (Raut-jadhav et al., 2016). In their studies, hydrodynamic cavitation- ozone combination gives the highest mineralisation and energy efficiency among all the tested hybrid methods. Therefore, one or more of the popular AOPs such as ozone oxidation, Fenton process, photocatalytical oxidation, UV oxidation and recently zero valent iron application can be combined in hybrid AOPs for better treatment and elimination of associated disadvantages of a single treatment method.

2.9.1 Photocatalysts and hydrodynamic cavitation

Semiconductor photocatalysts such as TiO_2, SeO_2 and ZnO can absorb a substantial quantity of (UV) radiation from a light source (greater than its band gap) and generate an electron/ hole pair. The generated negative electrons are capable of using the available excess energy to gain promotion (excitation) from the valence band (VB) to the conduction band (CB) and therefore

leave behind positive holes (Figure 1). The holes break down water molecules into hydrogen and hydroxyl radicals as the electrons react with oxygen to produce the super oxide anion (O^{-}_{2}). Both radicals and superoxides are capable of reacting with persistent organic pollutants (POPs) to generate more biodegradable end-products (Khan et al., 2015). The mechanism of POPs degradation may be through absorption of light by the photocatalyst and charge transfer reaction to create radical species for decomposition of adsorbed pollutants. Photocatalysts can either be homogenous or heterogeneous. The common challenges associated with photocatalysts are their high band gabs, agglomeration, small surface areas, instability and difficult recovery after treatment (Rehman et al., 2009). Techniques such as modification by organic materials, semi-conductor coupling and metal doping have been deployed by researchers to reduce the band gap and ensure the utilization of lower energy (sourced from sunlight) by these photo active semi-conductors (Rehman et al., 2009). The capability for utilisation of natural resources such as sunlight, activity at room temperature and pressure, chemical stability and low cost of titania as well as it total mineralization of a variety of organic pollutants are advantages of photocatalytic degradation using Titanium (IV) Oxide (Zhu, 2006). However, the degradation of pollutants depend on physicochemical properties of the metal oxide, the amount of pollutants, the nature of the pollutant, its volume, the surface area of photocatalysts and the solution pH (Kaur and Singh, 2007). Fouling of the photocatalysts and the presence of many radical scavengers will lower the rate of degradation and render the process ineffective in wastewater treatment, except when applied in combination with other AOPs. The simultaneous application of cavitation and photo catalytic oxidation has been reported to be a very effective method of contaminant degradation in wastewater treatment (Kavitha and Palanisamy, 2011). The combination of hydrodynamic cavitation with UV/TiO_2 has been successfully applied in the laboratory scale degradation of diclofenac sodium, resulting in enhanced rates of degradation under optimised condition compared to the stand alone single treatment options using the two processes separately (Bagal and Gogate, 2014b). Likewise, degradation (sonophotocatalytic oxidation) of reactive blue 19 (RB 19) dye was successfully carried out using sulfur-doped TiO_2 (S-TiO_2) nanoparticles, sonolysis and sunlight. Khan et al., (2015) demonstrated the possibility of reducing the band gap in TiO_2 for the utilisation of visible light. However, the degradation rate depended on factors such as the initial concentration of blue 19 (RB 19) dye, the catalyst dosage, the ultrasonic power and the amount of sulfur doping. In spite of the reported successful cases of modification of TiO_2

for its utilisation in visible light, commercial photocatalyst composites remain an illusion. It is therefore imperative that poor environmental and thermal stability of the photocatalyst must be resolved along with the formation of an excellent composite for photo degradation (Zangeneh et al., 2015).

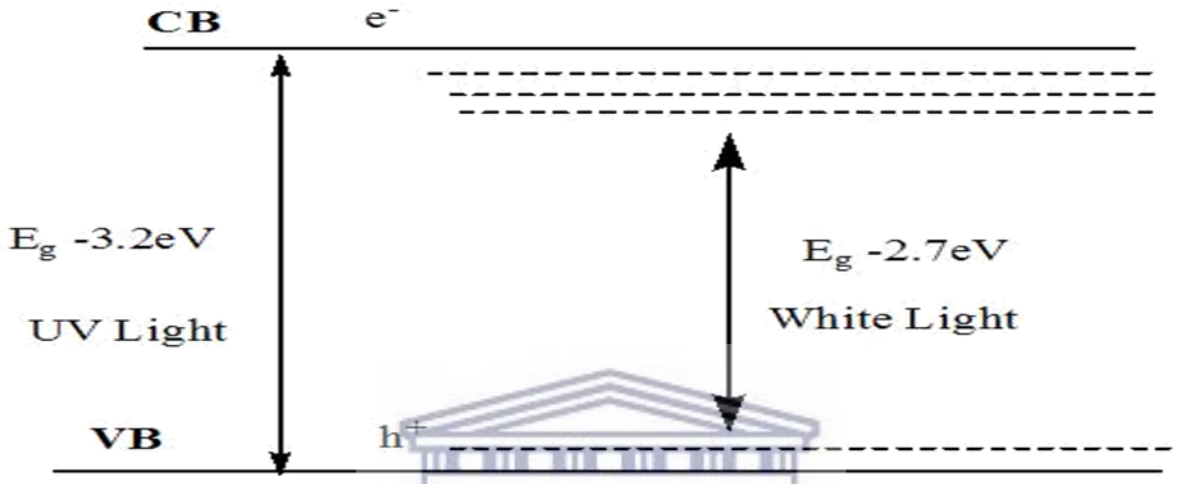

Figure 2.1: Excitation of photocatalyst in UV and white light (CB represent the conduction band while VB represent the valence band)

2.9.2 Ozone and hydrodynamic cavitation

Ozone oxidation is reputed for its success in removal of odour, colour, with disinfection and wastewater decontamination over a wide pH range. Advantages include high oxidation power (E^O= +2.07 V), non-selectivity, environmental friendliness and ability to simultaneously react with unsaturated species in the polluted water (U.S. EPA., 1999). Ozone can achieve the splitting of large organic molecules into smaller, biodegradable materials without the addition of disinfection chemicals. The reaction with POPs can be via a direct pathway, which involves the direct reaction between ozone and the dissolved pollutant at pH < 4 or the indirect pathway, which is the generation of the OH radical through the decomposition of ozone in water and the subsequent reaction of the generated radical with the pollutant (Grande, 2015). As a result of its capability to combine a selective process via direct ozone oxidation and an unselective process via radical oxidation, ozonation can effectively degrade several POPs compared to other type of

AOPs (Wang et al., 2016). The resulting biodegradable waste can be dealt with in the biological secondary/ tertiary treatment stage. The kinetic of POPs degradation in ozone is typically second order, i.e. first order for the ozone and first order for the POPs. The achievement of effective non-linear degradation in ozone oxidation is due to the combined selective and non-selective reactivity of ozone gas and hydroxyl radical respectively. The accelerated mineralisation in the ozone-combination AOPs compared with other combined AOPs may be due the productions of the two oxidants (ozone and hydroxyl radical) instead of hydroxyl radical only.

Consequently, ozonation can participate in the polymerisation of meta stable organic substances leading to their enmeshment, direct precipitation, bridging, or adsorption and subsequent removal (Santos et al., 2013). Ozone is best generated in-situ using energy sources such as the electrolytic process or cheminuclear, high voltage corona discharge or UV light (at a wavelength less than 200 nm). Corona discharge is the most efficient of all the in-situ ozone generation techniques (Carocci et al., 2014). It involves the generation of ozone by passing air or oxygen across a narrowly spaced pair of high voltage electrodes (Carocci et al., 2014). It is advantageous to apply molecular oxygen rather than air in the corona discharge gap (Malik et al., 2015). The ozone is produced as a result of dissociation of oxygen into its radical form and subsequent recombination in a closed chamber. The in-situ generation of ozone is possible through the electrical discharges (EDs). This type of equipment has gained particular attention in pollution control and environmental remediation. Electric discharge is the channel of charged particles through a conductive material such as wire electrodes (Panorel, 2013). This often results in the formation of an electrically neutral ionized gas referred to as plasma and known as the fourth state of matter. The term thermal plasma corresponds to high temperature and atmospheric pressure while non-thermal plasma (NTP) is referred to when the generation of free radicals is achieved at low temperature and atmospheric pressure. The generated energized electrons may cause a series of internal reactions and consequently the formation of free radicals. The formation of these oxidants in air or in aqueous systems follows consecutive mechanistic reaction chains that represent an in-situ generated oxidative chemical mixture used for pollution control such as air cleaning (Xiao et al., 2014) or in surface sterilisation of polymers (Pankaj et al., 2014) or for the removal of contaminants in water and wastewater (Barkhudarov et al., 2013).

Ozone can also be used in hybrid combination with other AOPs for a better treatment option. Ozone assisted hydrodynamic cavitation hybrid system may enhance pollutants' oxidation significantly with reduction in the amount of ozone used, lowering the cost of treatment and energy demand (Ozonek, 2012). The hybrid combination of hydrodynamic cavitation and ozone oxidation can synergistically eliminate the disadvantages associated with "stand alone" processes and significantly improve the degradation output (Patil et al., 2014). Parag et al., (2015) reported that hydrodynamic cavitation-ozone hybrid is vesy efficient for the degradation of triazophos achieving 100% degradation and TOC removal of 96% in 90 minutes (Gogate and Patil, 2015). It has also been reported that the combined cavitation-ozonation oxidation process can change the molecular structures of organic matter and transform the non-biodegradable organics to more biodegradable forms (Korniluk and Ozonek, 2013). Despite the significant degradation achievement of ozone hybrid processes in the treatment of persistent organic pollutants (Koutahzadeh et al., 2016), complications caused by the formation of toxic byproduct and difficulty in up-scaling remain the subject of continue investigation (Grande, 2015).

2.9.3 Fenton oxidation and hydrodynamic cavitation

Over a century ago, Fenton reported the oxidation of tartaric acid in the presence of a small quantity of ferrous salt (Haber, F. and Weiss, 1934). The produced solution from his reaction gave a violet colour on the addition of alkali. Apparently, this reaction which is popularly used today in water treatment was proposed by Fenton as an identification test for tartaric acid. The use of Fenton reagent in the degradation of organic pollutants has been widely reported (Babuponnusami and Muthukumar, 2014; Sharma et al., 2011; Sychev and Isak, 1995). It involves catalytical oxidation of hydrogen peroxide in the presence of Fe^{2+} to produce hydroxyl radical and other radicals that are responsible for degradation of POPs **(2.i) to (2.iii).**

$$\mathbf{Fe^{2+} + H_2O_2 \rightarrow Fe^{3+} + HO^- + HO^{\bullet}} \quad \textbf{(2.i)}$$

$$\mathbf{Fe^{3+} + H_2O_2 \rightarrow Fe-OOH^{2+} + H^+} \quad \textbf{(2.ii)}$$

$$\mathbf{Fe-OOH^{2+} \rightarrow Fe^{2+} + HOO^{\bullet}\ (slow)} \quad \textbf{(2.iii)}$$

The produced Fe^{3+} undergoes further reactions with hydrogen peroxide to regenerate Fe^{2+} and thereby established the catalytic role of the ferrous ion. The attractiveness of the Fenton process in the generation of OH radicals for treatment of persistent organic pollutants can be attributed to its cost effectiveness, the abundance and nontoxic nature of the resulting iron oxides as well as environmental friendliness of hydrogen peroxide (Sharma et al., 2011). Conversely, the narrow useful pH (2- 3.5) range, consumption of large amounts of iron compounds, cost of peroxide and resultant formation of large amounts of iron sludge which are difficult to remove are the disadvantages of the Fenton process (Cui et al., 2014; Thakur and Chauhan, 2016). Besides, the produced stable Fe^{3+}-complexes may reduce the efficacy of the treatment method (Natalija et al., 2006). Overcoming these drawbacks is essential in the achievement of efficient treatment of POPs with Fenton oxidation.

2.9.4 Hydrodynamic cavitation and nano zero valent iron

The generation of in situ ferric iron and the chain of reactions due to the corrosion of metallic iron in an acidic condition is the term advanced Fenton process (AFP). Application of heterogeneous iron catalysts in the AFP offers a possibility of wider pH ranges (pH 2- 9) and lower amount of Fe sludge (Kwan and Voelker, 2003). Unfortunately, Fe^{2+}/ Fe^{3+} rate of reaction in AFP is very low, causing a slow rate of reaction in the entire process (Wu et al., 2013). Developing efficient, reusable and durable heterogeneous Fenton catalysts that are active over a wide pH range is the subject of ongoing research (Araujo et al., 2011; Hou et al., 2016). The application of zero valent iron nano particle (nZVI) as a heterogeneous catalyst in an AFP has recently been reported (Zhang et al., 2013). nZVI is very versatile and eliminates nearly all demerits associated with Fenton oxidation (Wang, 2013). In the nano form, the inherent desirable properties of a catalytic substance such as reactivity, photo-activity and selectivity can be enhanced. Environmental applications of nano iron materials include elimination of pollutants in wastewater treatment plants as well as site remediation. The application of nano iron particles has been highlighted in environmental remediation. The advantages include improved performance, lower energy consumption and reduction in residual waste (Ali et al., 2008). Nano zero valent iron (nZVI) is an effective nano material for the mineralisation of a host of pollutants

in contaminated water (Cao et al., 2011; Jewell and Wilson, 2011; Yaacob et al., 2012). It is an ideal adsorbent with strong reducing capacity for contaminants such as organic dyes, persistent pollutant, halogens and heavy metals in wastewater treatment plants (Lopez-Telleza et al., 2011). A good number of publication have reported the degradation of persistent pollutants using nZVI in the treatment of contaminated water as a "stand alone" wastewater treatment method (K. M. Sirk et al., 2009) or in combination with cavitation technology for the treatment of hydrocarbons in oil (Cui et al., 2014). Cavitation is capable of improving the performance of the heterogeneous catalyst in AFP by breaking down the stable Fe^{3+}-complex and making the Fe^{3+} available for the regeneration of ferric ion. Cavitation combined with nZVI was found to significantly enhance the performance of AFP for mineralization of organisms in wastewater in an hybrid combined AOP treatment (Chakinala et al., 2009). The excellent resultant mineralisation associated with this procedure and its successful application in real wastewater that containing varieties of OH radical scavengers is widely reported (Liang et al., 2007; Ma, 2012). Cavitation-nZVI is a prospective hybrid process with significant capability for fast and efficient degradation of persistent organic pollutants. nZVI is a good source of heterogeneous iron catalyst for AFP. The Fenton-like chemistry reaction with hydrogen peroxide yielding a substantial amount of OH radical at a high reaction kinetic rate is shown in equation **(2.iv) to (2.ix).**

$$\mathbf{Fe-OOH^{2+}} + \text{))) } \rightarrow \mathbf{Fe^{2+}} + \mathbf{HOO^{\bullet}}\ \mathbf{(fast)} \quad \textbf{(2.iv)}$$

$$\mathbf{Fe^{2+}} + \mathbf{H_2O_2} + \text{))) } \rightarrow \mathbf{Fe^{3+}} + \mathbf{HO^{-}} + \mathbf{HO^{\bullet}} \quad \textbf{(2.v)}$$

$$\mathbf{Fe^{3+}} + \mathbf{H_2O} + \text{))) } \rightarrow \mathbf{Fe^{2+}} + \mathbf{H^{+}} + \mathbf{HO^{\bullet}} \quad \textbf{(2.vi)}$$

$$\mathbf{Fe^{0}} + \mathbf{2H_2O} + \text{))) } \rightarrow \mathbf{Fe^{2+}} + \mathbf{H_2} + \mathbf{2HO^{\bullet}} \quad \textbf{(2.vii)}$$

$$\mathbf{2Fe^{0}} + \mathbf{O_2} + \mathbf{2H_2O} + \text{))) } \rightarrow \mathbf{Fe^{2+}} + \mathbf{H_2} + \mathbf{2HO^{\bullet}} \quad \textbf{(2.viii)}$$

$$\mathbf{HO^{\bullet}} + \mathbf{POPs} \rightarrow \mathbf{CO_2} + \mathbf{H_2O}\ \mathbf{(mineralization)} \quad \textbf{(2.ix)}$$

This process integrates fast degradation of POPs by nZVI with the role of generated Fe^{2+} / Fe^{3+} in Fenton oxidation to achieve the desired output in the degradation of POPs. The initial reaction involves the oxidation of nZVI to yield Fe^{2+}/Fe^{3+} which acts as catalyst in the Fenton production of OH radicals from the generated hydrogen peroxide. Both consumption of chemical reagents and production of large sludge can be significantly reduced in AFP using nZVI as the heterogeneous Fenton catalyst (Li et al., 2015). Although, the research into wastewater treatment with hydrodynamic cavitation is still at the infant level, it offers a simple reactor design, inexpensive and less cumbersome operation procedures in comparison with acoustic cavitation (Gogate and Patil, 2015). Besides, the associated disadvantages in the stand alone AOPs such as production of large quantity of iron sludge and narrow effective pH range (2-3.5) in the Fenton process (Cui et al., 2014) as well as lower mineralisation rate in hydrodynamic cavitation are completely eradicated in this hybrid combination of the two (Gogate and Patil, 2015). Chakinala and co-workers in 2008 proved that the combination of hydrodynamic cavitation and the Fenton process is capable of achieving about 80% reduction in TOC after an hour of treatment time (Chakinala et al., 2009). The efficacy of p-nitrophenol degradation in the hydrodynamic cavitation-Fenton hybrid system was found to be strongly dependent on the operating pH and it is at optimum at a pH of 3.75 (Pradhan and Gogate, 2010). Amey et al. (2010), reported that the degradation efficiency for p-nitophenol degradation was dependent on the initial concentration of the pollutant (Pradhan and Gogate, 2010). With 63.2% degradation for 5 g/L p-nitrophenol concentrated solution and 56.2% for 10 g/L, it can be argued that high initial concentrations give low percentage degradation rate while low initial concentrations result in high percentage degradation. Apparently, there is equivalence between the molecules of generated radicals and molecules of pollutants.

2.10 Future perspective of cavitation process for POPs remediation

The evidence supporting the contamination of wastewater by POPs and its negative consequences on humans and their immediate environment is overwhelming. It is a well known fact that the conventional water treatment facilities have failed to effectively degrade persistent contaminants from wastewater into their mineral form. However, established and advanced water treatment options such as activated carbons, membrane bioreactors and advanced oxidation

processes are well documented for their capital intensive treatment of these recalcitrant pollutants. Efficiency of the treatment technology is very important to the successful removal of POPs from wastewater. Hydrodynamic cavitation and Fenton oxidation as a form of combined advanced oxidation process has been demonstrated for possession of a great capability and synergistic effect for degradation of POPs. The merits of this method include its efficiency, simplicity, energy conservation and commercial applicability. Notably, formation of large quantities of iron in the generated sludge and associated narrow pH range of activity will be investigated in the combined AOPs technology. Following the current review, the future research would be focused on the treatment of POPs in wastewater using optimized hydrodynamic cavitation system in presence of an efficient form of nano zero valent iron. This will be done to ensure the reduction of iron concentration in the sludge and efficient treatment of POPs in the wastewater.

CHAPTER 3

METHODOLOGY

3.1 INTRODUCTION

This chapter provides descriptions about the materials, methods and characterisation techniques used in obtaining the outlined aims and objectives of the present study.

3.2 MATERIAL AND METHODS

The flow chart describing the content of the current study is as displayed in Figure 3.1

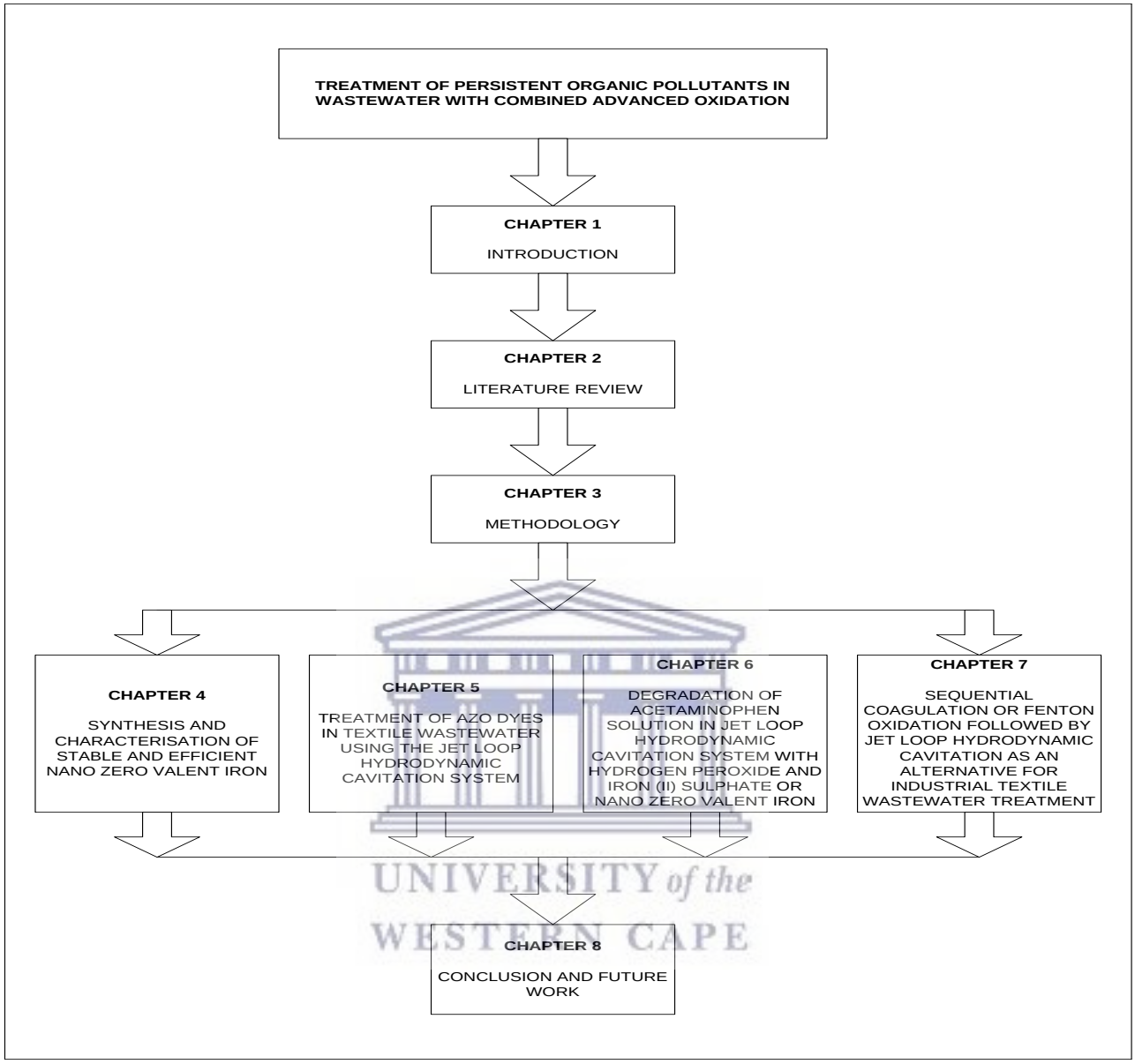

Figure 3.1: Flow chart describing the thesis content

3.3 Chemicals Used

The name, molecular formula, supplier, grade/purity of the chemicals, solvents and acids used in this study are presented in Table 3.1. All the chemicals are graded and were used as received without further purification and the preparation of solutions.

Table 3.1: List of the chemical used

Chemical	Molecular formula	Supplier	Grade/ Purity
Orange II sodium salt	$C_{16}H_{11}N_2NaO_4S$	Sigma Aldrich	99%
Acetaminophen	$C_8H_9NO_2$	Sigma Aldrich	99%
Terephthalic acid (TA)	$C_8H_6O_4$	Sigma Aldrich	29%
2-hydroxyterephthalic acid	$C_8H_6O_5$	Sigma Aldrich	97%
Sodium hydroxide solution	NaOH	Merck	98%
Iron (III) chloride. Hexahydrate	$FeCl_3.6H_2O$	Sigma Aldrich	99%
Sodium borohydride	$NaBH_4$	Merck	99%
Sodium chloride	NaCl	Sigma Aldrich	99%
Hydrochloric acid	HCL	Merck	99%
Disodium hydrogen Orthophosphate	Na_2HPO_4	Sigma Aldrich	98.5%
Ethanol	C_2H_5OH	Merck	99%
Methanol	CH_3OH	Sigma Aldrich	99%
Ascorbic acid	$C_6H_8O_6$	Sigma Aldrich	99%

3.4 Methods

3.4.1 Preparation of simulated wastewater solutions and reagents

(i) 1000 mg/ L orange (II) sodium salt

Textile wastewater was simulated using a solution of orange II sodium salt (OR2), 4-[(2-Hydroxy-1-naphthalenyl) azo] benzenesulfonic Acid Monosodium salt [molecular weight; 350.32, molecular formula; $C_{16}H_{11}N_2NaNO_4S$, λ_{max}; 483nm]**.** The choice of this particular azo dye was motivated by its popularity as an industrial dye and structural semblance to some common persistent organic pollutants (Figure 3.2).

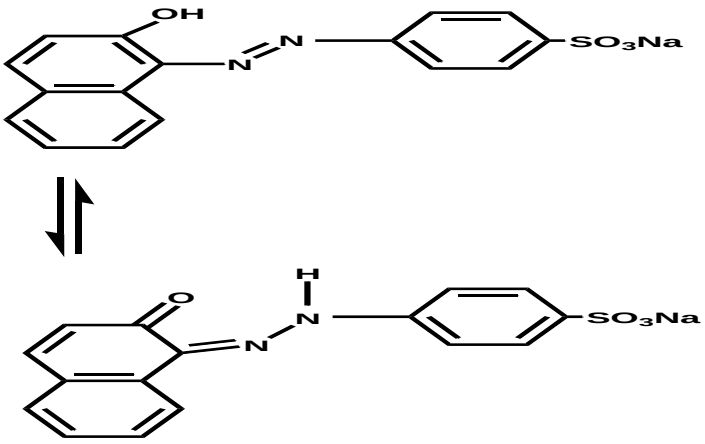

Figure 3.2: Tautomerisation of orange II sodium salt

OR2 was used as received from the supplier without any further purification or treatment. Exactly, 1 g of OR2 was accurately weighed into a 1 L volumetric flask containing deionised water obtained from a Millipore system. The mixture was shaken until the orange II sodium salt dissolved completely and thereafter made up to the 1 L mark with more deionised water. The working standards (10 mg/ L) were prepared from the stock solution (1000 ppm) by serial dilution using the dilution formula as presented in equation **(3.i)**.

$$\boldsymbol{C_1V_1 = C_2V_2} \quad \textbf{(3.i)}$$

Where

$C_1 = Concentration\ of\ stock$

$V_1 = Volume\ of\ stock$

$C_2 = Concentration\ of\ working\ standard$

$V_2 = volume\ of\ working\ standard$

(ii) 1000 mg/ L acetaminophen solution

Pharmaceutical wastewater was simulated using acetaminophen (ACE) solution. ACE was chosen as a representative pharmaceutical because it has the basic structure of common pharmaceutical compounds (Figure 3.2) and it is also a commonly prescribe over the counter

(OTC) pharmaceutical which is widely reported to be present in drinking water. A standard solution of ACE was prepared by accurately weighing it powder form equal to 1 g into a 1L volumetric flask containing deionised water from Millipore system. The mixture was shaken until all the acetaminophen dissolved completely and thereafter the solution was made up to the 1 L mark with more deionised water. The working standards (10 ppm) were prepared from the stock solution (1000 ppm) by serial dilution using the dilution formula presented in **(3.i)**.

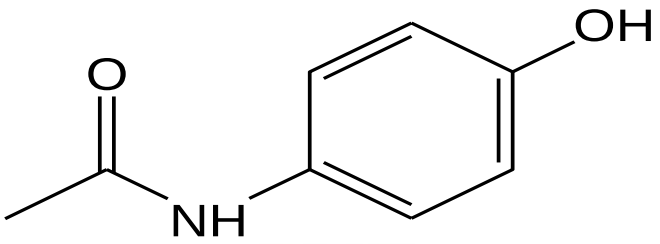

Figure 3.3: Chemical structure of acetaminophen

3.5 Preparation of Plant extract

The collection of the leaf of *H. caffrum* was done at Kirstenbosch National Biodiversity Garden, Rhodes Drive, Newlands 7700, Cape Town, South Africa on 17th June, 2015. Authentication was performed by Anthony Hitchcock; the nursery living collections and threatened species manager. The polyphenolic compounds were extracted using the method of Sharma and Lall (2014) with little modifications. Shade-dried leaves of *H. caffrum* (40 g) were grinded into powdered form using a Platinum 1.5L Jug Blender. The powdered leaves of *H. caffrum* were soaked in 100 mL of aqueous ethanol (25%) and stirred using magnetic stirrer (Heidolph™ MR series Magnetic Stirrer Hotplate) at 500 rpm for 2 hours to make an extract. The extract (liquid) was poured into a beaker and a fresh 100 mL aqueous ethanol (25%) was added to repeat the extraction process. The extraction process was repeated for five times and the retained solvent became clear. The extracted solvent was evaporated under reduced pressure and the resulting solution was freeze dried to give a brown amorphous powder which was stored in an air tight bottle at 20 ^{0}C to be used in the synthesis of nano zero valent iron.

3.6 Jet loop hydrodynamic cavitation design

The jet loop hydrodynamic cavitation equipment used for the treatment of POPs in simulated wastewater is as presented in figure 3.4. It has a holding tank of 80 L volume, a positive displacement pump of power rating 1.1 kW, control valves (V1, V2, V3 and V4), and a pressure gauge. The suction side of the pump was connected to the bottom of the tank and the discharge from the pump branched into two lines; the main line and a bypass line. The main line housed the cavitating device (venturi). V2 and V3 were provided to control the direction of the liquid flow. When the main line (venturi) was opened, the control valve V2 was closed to make sure that there was no flow in the bypass line. The main line terminated inside the tank while the bypass line joined the main line before returning to the tank. Both the mainline and bypass line terminated inside the tank below the liquid level to avoid any introduction of air into the liquid due to the plunging liquid jet. The whole set up was such that there was the generation of cavities within the hydrodynamic cavitation jet-loop device to ensure the collision of the impinging jets to one another in the slit circular venturi.

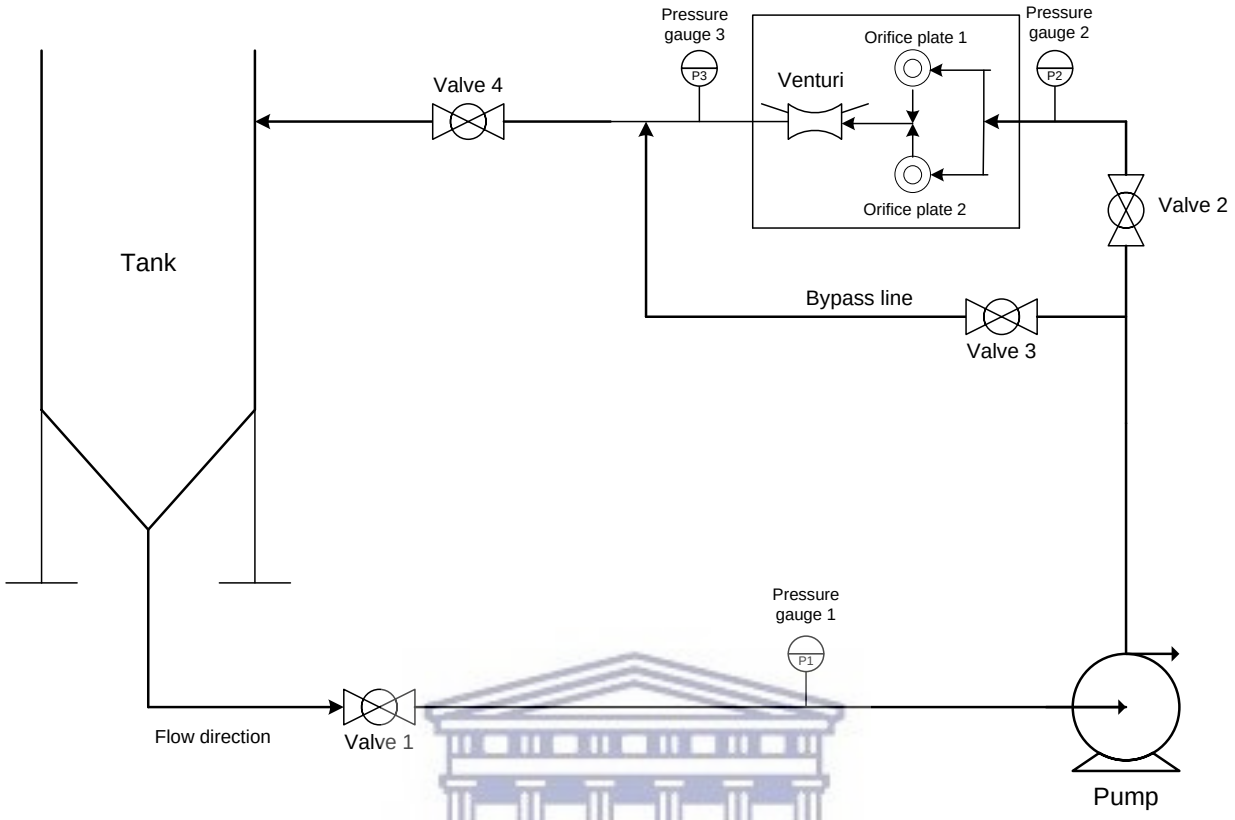

Figure 3.4: Design of jet loop hydrodynamic cavitation system

The cavitation in hydrodynamic equipment can be generated by using venturi (Figure 3.5) and orifice (Figure 3.6). A venturi has smooth convergent and divergent sections that can be used in the generation of high velocity at the throat. The pressure drop created as a consequence of high throat velocity can lead to lower cavitation number and subsequent production of cavitation event. The orifice can also have a number of holes in a given cross sectional area of the pipe. In the current studies both Venturi and single hole orifice (4 mm) were incorporated in a hydrodynamic cavitation jet loop. The venturi slit was so designed (Figure 3.5) to create narrower throat angle (23.5^0 to 5.5^0). The anticipated effect is the production of higher cavitation and comparative advantage over previous design.

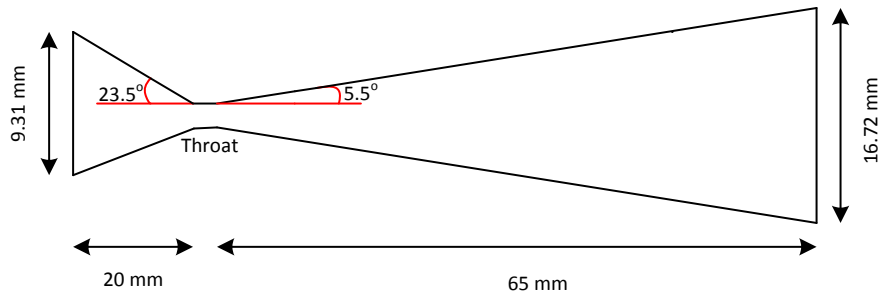

Dimensions of the throat:
Width = 6 mm; Height = 1.9 mm; Length = 1.9 mm

Figure 3.5: Detailed Geometry of Slit Circular Venturi used in jet loop hydrodynamic cavitation equipment

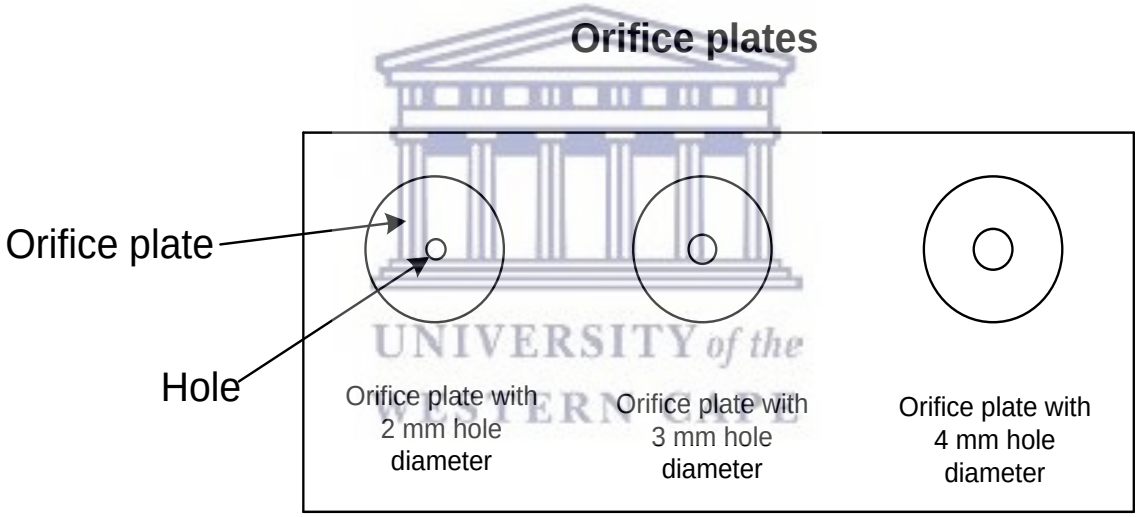

Figure 3.6: Single-hole orifice plate used in jet loop hydrodynamic cavitation equipment

3.7 Characterisation techniques

In this study, several analytical techniques were used to characterise the prepared *H. caffrum* plant extracts, synthesised nano zero valent iron as well as for the quantitative and qualitative identification of the intermediates and final products during the degradation of persistent organic pollutants in pharmaceutical and textile wastewater. The techniques included; X-ray Diffraction (XRD), High Resolution Scanning Electron Microscopy (HRSEM), High Resolution Transmission Electron Microscopy (HRTEM), Ultraviolet-visible spectrophotometry (UV-Vis),

Thermal Gravimetric analysis (TGA), Fourier Transform Infrared Spectroscopy (FTIR), Inductive Coupled Plasma, Liquid chromatography-mass spectroscopy (LC-MS), Gas chromatography-mass spectroscopy (GC-MS) and Ion chromatography (IC). Brief outlines of the analytical techniques are provided in the subsequent subsections.

3.7.1 X-ray Diffraction (XRD)

X-ray diffraction (XRD) is a non-destructive technique used for the finger print identification of new formed mineral phases of products. It can be used for monitoring the extent to which starting materials have reacted or to qualify the degree of amorphicity of the final products (Rosas-Casarez and Arredondo-Rea, 2014). It gives accurate quantification as well as the crystallographic structural of a metallic substance. It works by bombarding a single crystal or powder sample with X-rays photons to produce a diffraction pattern. The produced diffraction patterns can be recorded, analysed and compared to the well known diffraction pattern of a substance. A Bruker AXS (Germany) with D8 advanced, XRD was used for the analysis of powder samples of the synthesised nano zero valent (nZVI) in the current study. The nZVI were placed and clipped into a rectangular aluminum sample holder. The phase identification was subsequently done by operating the diffractometer at 40 kV and 35 mA using Cu Kα radiation (λ= 1.5406 Å) in 2 θ with collection range 6^0 - 90^0. The data was subsequently evaluated by using EVA software from BRUKER.

3.7.2 High resolution transmission electron microscopy

High resolution transmission electron microscope (HRTEM) is a non-destructive characterisation technique used for determination of the properties of a crystalline material. It gives accurate information on the surface morphology as well as the distribution pattern of particle size in a material (Rosas-Casarez and Arredondo-Rea, 2014). The nZVI samples were prepared by drop-coating one drop of specimen solution onto a holey carbon coated copper grid. This was then dried under a Xenon lamp for about 10 minutes and subsequently collected using FEI Tecnai G2 20 field-emission gun (FEG) operated in bright field mode at an accelerating voltage of 200 kV. Energy dispersive x-ray spectra were collected using an EDAX liquid nitrogen cooled Lithium doped Silicon detector.

3.7.3 High resolution scan electron microscope (HRSEM)

HRSEM is a characterisation tool with capability for production of high-resolution images of a solid sample surface. It uses a focused beam of high-energy electrons to generate a variety of signals at the surface of solid specimens. This gives rises to different multiple signals such as back scattered electrons and X-rays secondary electrons among others. The signals revealed sample specific information such as its external morphology, chemical composition, crystalline structure and orientation of materials making it up (Asahina et al., 2011). Data is collected over a selected area of the surface of the sample, and a two dimensional image is generated that displays spatial variations in these properties. The area ranging from 1 mm to 5 nm in width can be imaged in a scanning mode using conventional SEM techniques. The morphology and microstructure of the nZVI was analysed using Zeiss Auriga HRSEM. The HRSEM was equipped with EDS for further determination of the elemental composition of the synthesised nZVI. A 0.05 mg of the nZVI was sprinkled on a sample holder covered with carbon adhesive tape and sputter coated with Au-Pd using Quorum T15OT for 5 minutes prior to analysis. The microscope was operated with electron high tension (EHT) of 5 kV for imaging.

3.7.4 X-ray photoelectron spectroscopy

X-ray photoelectron spectroscopy (XPS) is one of the most sensitive analytical techniques for measurement of band alignment, band offset, as well as the band bending (Zhang et al., 2017). In the current study, a PHI 5000 Scanning ESCA Microprobe was used for measurement of surface properties such as oxidation state, electronic state and the chemical environment of the nZVI. The PHI Versa Probe was driven by a patented high flux X-ray source providing a focused monochromatic X-ray beam that can be scanned upon the sample surface. The X-ray source utilised a focused electron beam scanned upon an Al anode for X-ray generation and a quartz crystal monochromator that focused and scaned the generated X-ray beam upon the sample surface. The monochromator was based on a 200 mm Rowland circle with quartz (100) crystals on an ellipsoidal substrate to generate micro focused X-ray beam. The X-ray energy dispersion eliminates the Kα3,4, Kα5,6, and Kβ X-ray lines and the Al Bremsstrahlung radiation background and narrow the Al Kα1,2 line to approximately 0.26 eV FWHM. This narrowed line allowed core and valence band spectra to be acquired with high energy resolution of the photoemission peaks and without X-ray satellite-induced photoemission peak overlaps. The

removal of X-ray and Bremsstrahlung satellite radiation coupled with a narrow principle excitation line width results in significantly higher signal-to-background ratio data. The narrower X-ray line width also allows an electron energy analyzer to be observed with higher transmission, thereby reducing the observed damaged rate in monochromator-excited XPS spectra of X-ray sensitive sample. With the proper geometry configuration of X-ray source, crystal substrate and analysis target, the reflection beam yields a highly focused, monochromatic source of X-rays. In the current studies, a 100 μm diameter monochromatic Al Kα x-ray beam (hν = 1486.6 eV) generated by a 25 W, 15 kV electron beam was used to analyse the different binding energy peaks of the prepared nZVI. The pass energy was set to 11 eV to give an analyzer resolution ≤ 0.5 eV. Multipack version 9 software was utilised to analyse the spectra and identify the chemical compounds and their electronic states using Gaussian–Lorentz fits. A low energy Ar+ ion gun and low energy neutraliser electron gun was used to minimise charging on the surface.

3.7.5 Ultraviolet-visible absorption spectroscopy

Ultraviolet-visible absorption spectroscopy is a common analytical equipment used to obtain the wavelength of maximum absorbance for solution of known concentration of a compound. The calibration curve is generated for a specific compound from which the unknown concentration can be determined. During the current study, the wavelength of maximum absorbance and concentration of orange II sodium dye, acetaminophen as well as their intermediate products were monitored. The wavelength of maximum absorbance for orange II and acetaminophen are 483 nm and 243 nm respectively. The % degradation and adsorption capacity can be calculated using the information obtained from the UV spectrophotometer. The C_0 and C_t are the initial concentration and concentration at a particular time (t) respectively.

C_t = Absorbance/ slope of the calibration (straight line)…… **(3.ii)**

$$\%\,\boldsymbol{degradation} = \mathbf{100} * \left(\frac{\mathbf{C_0 - C_t}}{\mathbf{C_0}}\right) \text{... ...} \qquad \textbf{(3.iii)}$$

C_0 and C_t are initial and final concentration in mg/ L of the textile dye (orange (II) sodium salt) or pharmaceutical (acetaminophen) in the simulated wastewater respectively.

3.7.6 Fourier Transform Infrared Spectroscopy (FT-IR)

FT-IR provides information about the chemical bonding, molecular structure and functional groups present in a substance that is capable of absorbing the infrared light. The distinctive FT-IR spectrum of a substance is caused by the differences in the arrangement of atoms that make up the structure. It is therefore expected that a pure sample would give clear spectra with few functional groups while complex mixtures produce complex spectra with several absorption bands. Perkin Elmer PE1600 FT-IR Spectrometer model "Spectrum Two" was used for the analysis the *H. caffrum* as well as the synthesised nZVI. The scan wavenumber was between 4000-400 cm^{-1} measuring against % Transmittance. The FT-IR plate was first cleaned with methanol and the baseline was run to guard against interference. Taking into cognisance the aforementioned instrumental conditions, a 0.005 g sample was placed directly under the probe. This was followed by scanning and spectra corresponding to each individual sample were collected with appropriate peaks adjustment (smoothened).

3.7.7 Thermogravimetric analysis

Thermogravimetric analysis (TGA) is an analytical technique based on the measurement of residual weight change with respect to increased temperature or isothermally as a function of time, in an atmosphere of nitrogen, helium, air, other gas, or in vacuum. The loss in weight or mass (as the temperature increases) may be due to thermal decomposition, water loss or adsorption of oxygen. The thermal (TGA) studies were carried out in a Perkin Elma STA 4000, at a temperature ranging between 30 to 900 ^{o}C in a nitrogen atmosphere with a flow rate of 20 mL/ minute and a heating rate of 10 ^{o}C/ minute.

3.7.8 Total organic carbon (TOC)

Total organic carbon (TOC) can be defined as all the carbons that are covalently bonded in organic molecules and not purgable by acidification and gas stripping. The TOC method is suitable for freshwater and wastewater samples and is adapted to seawater by making use of calibration standards and quality control solutions made up in artificial seawater.

In the current study, the sample digestion was done by using the multi N/C 3100 at thermocatalytic (platinum) high-temperature oxidation. The sample was acidified outside of the analyzer with 2N HCl (pH 2) and the resulting CO_2 was purged to remove all the inorganic carbon present in sample. Afterwards the remaining carbon from the sample prepared in this manner was determined via combustion. For both standards and samples (15 Ml) were transferred into sample vial, using an A grade pipette for analysis. 15ml unfiltered sample was pipette into sample vial and analysed using a nondispersive infrared sensor (NDIR) detection.

3.7.9 Liquid Chromatography-Mass Spectrometry

Liquid Chromatography-Mass Spectrometry (LC-MS) is a routine analytical technique which is applicable to a wide range of biological and chemical molecules. The combinations of liquid chromatography with mass spectrometry enabled the economical and robust range of molecules to be analysed in a short time period (Pitt, 2009). LC-MS comprises of both the physical separation potential of liquid chromatography (LC) and the mass scrutiny ability of the mass spectrometry (MS). The technique was chosen because of its high specificity and the ability to handle complex mixtures with less clean-up. The column is often referred to as the stationary phase while separation of the charged particles or constituent occurs in the mobile phase. In short, LC-MS provides information on the mass-to-charge ratio (m/z) of charged particles in the sample, elemental composition and perhaps elucidation of molecular structures of the compounds. The liquid sample loaded onto the MS instrument goes through a vapourisation step followed by electrospray ionisation by beams of electron to produce charged particles, which are separated by the column in a mass analyser based on their mass-to-charge ratio. The mass analysers are of different categories, namely; single or triple quadruple, ion trap, time of flight (TOF), and quadruple-time of flight (Q-TOF). Samples for LC-MS analysis were freeze dried using Telstar LyoQuest Laboratory Freeze Dryer, HT 40 at -50 ^{o}C. They were subsequently dissolved in methanol (99.99%) and analysed at the temperature regime of the LC–MS oven using a column maintained at a profile temperature of 40 ^{o}C (holding time 3 min). This was followed by a temperature increase at a rate of 20^{o}C/minute, until 150 ^{o}C (holding time 1.5 min) and another temperature increase at a rate of 30^{o}C/minute, until 280 ^{o}C (holding time 5 min).

3.7.10 Ion chromatography (IC)

Ion chromatography (IC) is an analytical technique separate out various ions based on their charges. This technique is especially helpful for measuring the concentration of a particular ion in a water sample. A small volume of the sample (mobile phase) is pumped through a column of packed particles (stationary phase) and the time it takes for the ion to pass through is recorded as the retention time. The retention time of the ion depends on how it interacts with the column both physically and chemically. Known standard concentrations are used to estimate sample concentrations. In the current study the IC is made to analyze the concentration of anions such as sulfate and nitrate in the treated wastewater. A stock solution was prepared by dissolving 1.6485 g NaCl in 1000 mL deionised and degassed water to make a chloride solution equivalent to 1000 ppm. The calibration standards were also made (1 ppm to 10 ppm). A single standard was prepared for SO_4-S and NO_3-N as well as the triples calibration standards. All samples were filtered through a 0.45 um filter before running through the IC and the vials and caps rinsed thoroughly with deionised water. The eluent bottle was filled with fresh deionised, degassed water and sure to keep the tube submerged as the fresh water poured into the bottle. The machine and monitor were powered and eluent set to full level. The machine was warmed up for a half hour and the pump was allowed to run until all the bubbles were gone. The pump was turned off, the valve tightened, and the pump was turned on again. Once the conductance display is below 0.5 the run was started. Dilutions are highly recommended if a sample's predicted concentration is larger than the highest standard concentration. The IC uses the calibration curves to extrapolate the unknown concentration of the sample, which may or may not be accurate.

3.7.11 Inductive coupled plasma-Optical emission spectroscopy

Inductive Coupled Plasma-Optical Emission Spectroscopy (ICP-OES) is one of the most reliable analytical techniques used in the determination of trace metals. It works by emitting photons from excited atoms or ions in a radio frequency discharge. It is important to add water and ensures digestion of the solid sample while the liquid and gas can be directly injected. The injected solution will be converted to an aerosol and vapourised at the central compartment of the argon plasma at approximately 10, 000 K. At this condition, gaseous analyte elements change to free atoms which collides further with atoms within the argon plasma zone and get promoted to the excited state using a certain amount of energy. The exited atom/ ion must relax to the

ground state to enjoy stability. The transition from the exited to ground state leads to the emission of photons which possess unique amount of energy with specific wavelength. Therefore, the deduction of this element can be possible through the wavelength of the respective photon. The concentration of the elements in that particular sample is also related to the number of photons from each element.

3.7.12 Chemical oxygen demand (COD)

Chemical oxygen demand (COD) is the universal test for the estimation of the amount of wastewater material that can be subjected to strong oxidation by chemical oxidant such as dichromate. The COD reactor block was initially preheated to 150 ^{0}C and 2 ml quantities of each samples including blank were added into separate vials of COD digestion reagent. The vials were turned (up and down) for thorough mixing, inverted and placed in the preheated sample reactor block to incubate for 2 hours. The vials were subsequently placed in the rack to cool and the samples were tested for COD using colorimetric determinant for COD ranging 0-15 000 mg/L.

3.7.13 Biochemical oxygen demand (BOD)

Biochemical oxygen demand (BOD) can be described as a bioassay procedures for measuring the oxygen consumption of bacteria from the decomposition of organic matter. During this procedure, the BOD bottles were carefully filled with sample water to prevent formation of air bubbles. 2ml of manganese sulfate were added to BOD bottle by inserting the pipette below the water surface. 2 ml of alkali-iodide-azide reagent were also added. The appearance of brownish cloud in the solution was an indication of the presence of biochemical oxygen. The brown precipitates were allowed to settle down to the bottom and 2ml of concentrated (20 %) H_2SO_4 was added carefully. The bottles were tightly close, mixed thoroughly and left to incubate for 5 days. The 50 ml of samples were then titrated with 0.025N Sodium thiosulphate. The pale yellow color which were turn to blue on addition 2ml starch solution were observed as an indication of positive test. The titrations were continued until sample become clear. The amount of titrant used in correspondence to the concentration of dissolved oxygen in the sample.

3.7.14 Dilution Plate Counting Method

This is the method of measuring the live bacterial in a quantity of suspension. It involves the dilution of the samples with sterile saline until the quantity of bacteria can be accurately counted (i.e. 25-250). It is assumed that each viable bacterial cell is separated from all the others and can develop into a simple colony. Thus, the incubated bacterial are quantified and expressed in mL of the original suspension. In the current study, a 10^{-2} dilution of wastewater sample was made by transferring 1 ml of the raw sample into 99 ml sterile saline bottle. The bottle was caped and mixed thoroughly. Serial dilutions (10^{-4}, 10^{-6} and 10^{-8}) were made from the prepared wastewater stock solution using aseptic technique. Serial dilution of samples of treated wastewater and sludge were also prepared using the same procedure and all the samples were labeled. Starting from the highest (10^{-8}), 0.1 mL of each of the diluted samples was added into labeled petri dish containing nutrient agar. The samples were carefully spread on agar asepetically using glass rod. The pour plates were inverted and incubated at 37 ^{o}C for between 24 and 48 hours. The petri dishes with 25 to 250 colonies were selected and colonies quantified. The numbers of bacteria were calculated by dividing the number of colonies with the dilution factor.

3.7.15 Biodegradability of the treated wastewater

Biochemical oxygen demand (BOD) and Chemical oxygen demand (COD) are the analytical procedures used to quantify the composition of wastewater. BOD is a measure of the dissolved oxygen consumed by aerobic bacteria in 5 days at 20^{o} C while COD measures the amount of oxygen needed to convert the organic content of wastewater to inorganic salts and gases. The choice between BOD and COD for the wastewater analysis depends on factors such as reproducibility, cost and nature of wastewater. The two tests can also be applied together under specific conditions to produce a relationship which described the degradability of the treated wastewater effluent by micro organisms (biodegradability). The ratio of BOD and COD of a wastewater can be used to speculate its biodegradability as well as its toxicity. The knowledge of this ratio can also be used for the quick determination of BOD provided the COD is known.

When the BOD/COD of the treated wastewater is greater than 0.6, such wastewater can be sent for biological treatment at the final phase of water treatment or discharged. However, when the BOD/COD of the treated wastewater is between 0.3 and 0.6, the wastewater is said to be only fairly biodegradable because it would need to pass through a jump starting phase of (seeding) the

biological treatment. The acclimitisation of microorganisms is very important in the efficient biodegradation of the wastewater. Conversely, a wastewater with BOD/COD less than 0.3 is not biodegradable and therefore cannot be treated biologically as the wastewater possesses severe toxicity on microorganism and inhibits their metabolic activity.

3.7.16 Determination of weight of raw textile wastewater effluent

An ABK bench scale industrial balance was used for the determination of weight of the raw textile wastewater, treated wastewater as well as the sludge. The oversized LCD provides high visibility on production floors or in shipping/receiving operations. Dynamic weighing effectively captures readings of items that move during weighing, such as liquid ingredients during batching in a commercial bakery, at a chemical plant, or during concrete production.

3.7.17 Gas Chromatography-Mass Spectrometry

The Gass Chromatography-Mass Spectrometry (GC-MS) technique was chosen because of its high specificity and the ability to handle complex mixtures with less clean-up. The column is often referred to as the stationary phase while separation of the charged particles or constituent occurs in the mobile phase. In short, GC-MS provides information on the mass-to-charge ratio (m/z) of charged particles in the sample, elemental composition and perhaps elucidation of molecular structures of the compounds. GC-MS analyses were performed using a gas chromatograph (Trace Ultra) coupled to a mass spectrometer (PolarisQ Ion Trap) (ThermoElectron, San Jose, CA), with RTX-5MS column (5 % diphenyl, 95 % dimethyl polysiloxane) 30 m x 0.25 mm i.d. (Restec, Ireland) and the splitless mode. The temperature program was as follow: 80 °C for 1 min, 7 °C min^{-1} up to 150 °C, hold time of 5 min, 7 °C min^{-1} up to 200 °C, hold time of 5 min. The injector, transfer line and detector temperatures were kept at 250, 275 and 200 ºC, respectively. The MS detector was operated in the EI mode at 70 eV with a scan range of m/z 50-650.

3.8 Characterisation of plant extract

3.8.1 Antioxidant Assay

The radical scavenging activity of the extracts was determined by comparing against the stable free radical 2,2-diphenyl-1-picrylhydrazyl (DPPH). The assay involved reaction of DPPH with hydrogen donating antioxidant compounds in a reduction process that can be monitored by spectrophotometer at 517 nm as the DPPH colour changes from deep –violet to light yellow (Brand-Williams et al., 1995). 200 mg/L stock solutions of the *H. caffrum* extracts were prepared by dissolving 10 mg of the dry extract in 50 mL of methanol. Further dilutions were made from the stock to get lower concentrations of the *H. caffrum* extracts (100 mg/L to 0.4 mg/L). A 200 mg/ L solution of ascorbic acid (standard reference) were also made and serially diluted to lower concentrations (100 mg/ L to 0.4 mg/ L). Blank solutions were prepared (without the DPPH) from 100 µL of serially diluted *H. caffrum* solution and 50 µL methanol while the negative control was 100 µl DPPH and 50 µl methanol. 50 µL each of 150 mg/ L DPPH in methanol were added to 100 µL solution of *H. caffrum* extract in a micro plate which was kept in the dark for 30 minutes. The absorbance of the serially diluted extracts, ascorbic acid, blanks and controls were detected using a Biotek Power-wave XS multi well reader (Analytical and Diagnostic Products, Johannesburg, South Africa). The experiments were run in triplicate and the values were converted into the percentage inhibition using the formula as given in the equation **(3.iii)** below. The 50% inhibitory concentration (IC_{50}) values were then calculated by linear regression of the plots using Graph Pad Prism version 5.

$$\%\ \boldsymbol{Inhibition} = \frac{(\boldsymbol{Abs.\ Blank} - \boldsymbol{Abs.\ Sample})\ \boldsymbol{X}\ \mathbf{100}}{\boldsymbol{Abs.\ Blank}} \quad \textbf{(3.iv)}$$

3.8.2 Ferric Reducing Antioxidant Power (FRAP) Assay

FRAP activity was measured according to the method developed by Benzie and Strain (1996) with little modifications. Briefly, acetate buffer (300 mM, pH 3.6), 10 Mm TPTZ (2,4,6-tripyridyl-s-triazine) in 0.1M HCl and $FeCl_3 \cdot 6H_2O$ (20 mM) were mixed in the ratio of 10 : 1 : 1 to obtain the working FRAP reagent. 2 mg/ L each of ascorbic acid (standard) and leaf extract of *H. caffrum* were carefully prepared and subjected to agitation for 5 minutes with a vortex mixer (Dragon LAB MX-S), followed by centrifugation (Eppendorf centrifuge 5810R) at 1000 rpm for

another 5 minutes to allow for formation of clear solutions of the test samples. 100 mL of standard and leaf extract of *H. caffrum* solutions were separately mixed with 300 mL of the prepared FRAP reagent. The samples' absorbance was measured at 593 nm with the aid of 'Multiskan' spectrum (Thermo Electro Corporation). Methanol solutions of $FeSO_4 \cdot 7H_2O$ ranging from 100 to 2000 μM were prepared and used for creating the calibration curve of known Fe^{2+} concentration. The parameter equivalent concentration was defined as the concentration of antioxidant having a Ferric-TPTZ reducing ability equivalent to that of 1 Mm $FeSO_4 \cdot 7H_2O$.

3.8.3 Kinetic of degradation in the jet loop hydrodynamic cavitation system

The kinetic of degradation in the jet loop hydrodynamic cavitation can be determined using the integrated initial rate method. Estimation of variation in the initial concentration of a particular chemical substance can be done using natural logarithm on a specific rate equation. Recently, it **.**was reported that the treatment of POPs in a jet loop hydrodynamic cavitation systems were governed by a first order rate law Barik and Gogate (2016). Tentatively, the change in the initial concentration of POPs in the jet loop hydrodynamic cavitation system in the current study will be determined by first order rate law. Therefore, the initial rate can be verified according to equation **(3.iv)**

$$\ln\left(C_0/C_t\right) = Kt \quad \textbf{(3.v)}$$

Where Ct, C0, K and t are concentration at a specific time (t), C0 is the initial concentration, K is the degradation rate constant and t is the specific degradation time. The first order can be confirmed for a degradation reaction if plot of; $\ln\left(C_0/C_t\right)$ is a linear function of the reaction time while degradation constant K can be derived from the plotted slope.

3.8.4 Turbidity and pH meter

Turbidity is the measurement of the cloudiness of a wastewater sample. It is dependent on the ability of the solid particles in the tested sample to scatter or absorb light. The high quantity of slit, clay, particles or microbes will give a corresponding high turbidity in a treated water sample. The common units are Nephelometric Turbidity Units (NTU) or mg/ L. In the current study, a

Hanna instrument HI9829 waterproof multi-sensor probe was used. The instrument allow for the measurement of key parameters including turbidity and pH. It can transmit readings digitally with option to log data while disconnecting from the meter.

3.9 Quantification of hydroxyl radical (OH•) in the jet loop hydrodynamic cavitation

The hydroxyl radical (OH•) is a powerful oxidant that is produced as a consequence of fluctuation in the water velocity during its constriction in a jet loop hydrodynamic cavitation with a specifically designed orifice hole or venturi. The OH• is capable of reacting nonspecifically with an unsaturated substances or an electron rich centre and consequently get converted into its simpler form. For this reason, the OH• can influence the breaking down of POPs in wastewater into a mineral form. The reactions of OH• with POPs is presented in equation 2.ix (Chapter 2). The terephthalic acid (TA) dosimetry is well known for its efficient quantification of hydroxyl radical (Figure 3.7).

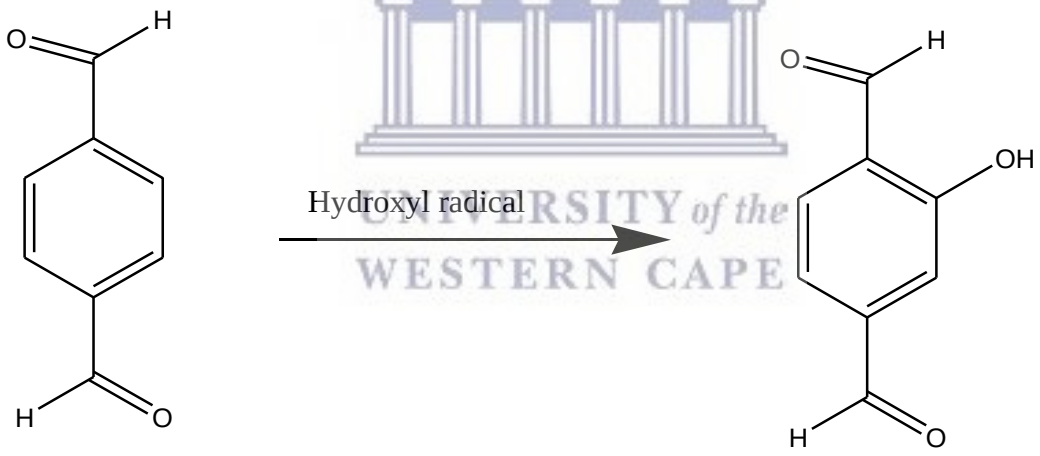

Terephthalic acid

2-hydroxyl terephthalic acid

Figure 3.7: Formation of 2-hydroxyl terephthalic acid from the reaction of hydroxyl radical and terephthalic acid

The generated OH• reacted with TA to form the 2-hydroxyl terephthalic acid (HTA), which can be quantified by using an optical fibre spectrometer.

3.9.1 Optical fibre spectrometer (NanoLog® i-HR 320, USA)

The optical fibre spectrometer (NanoLog® i-HR 320, USA) was used in the current investigation. The analytical instrument has a double-grating monochromator in the excitation position which offers a better sensitivity, resolution and stray-light rejection compare to the single-grating ones. Four ports generally are available in the NanoLog® iHR, two entrance ports ("lateral", i.e., on the side, and "axial", i.e., on the back) and two exit ports (lateral and axial). Usually the lateral entrance port is attached to the sample compartment. FluorEssence™-controlled flip mirror is available to choose between entrance ports and exit ports. Three gratings can be mounted on the rotatable grating turret. The standard sample compartment is a T-box, which provides efficient throughput with a choice of standard right-angle emission collection or optional front-face emission collection. The sample-compartment module comes equipped with a silicon photodiode reference detector to monitor and compensate for variations in the xenon lamp output. The standard detector offered on the NanoLog® is the Symphony® InGaAs array, which provides rapid and robust spectral characterization in the near-IR. The liquid-nitrogen cooling gives a lower background noise than room-temperature detection

3.9.2 Chemical Dosimetry

A quantity of 10 L dosimetry solution (TA) equal to 2 M was prepared and poured into a tank which was connected into the jet loop hydrodynamic cavitation equipment according to the standard protocol (Badmus et al., 2016b). The jet loop hydrodynamic cavitation (400 kPa, phosphate buffer 7.4) was powered for an hour period while 2 mL samples were collected at 10 minutes interval. The intensity of the collected solution was measured in an optical fibre spectrometer (Nanolog, i-HR 320, USA) set at excitation of 310 nm and emission wavelength of 425 nm. The experiment was performed in triplicate and the 2-hydroxyl terephthalic acid (HTA) which was formed as a consequence of the reaction between the OH• radical and TA has peak intensity at wavelength 425 nm. The amount of OH radical generated per unit time was calculated from the linearity obtained in the calibration curve prepared from the standard concentration of HTA.

CHAPTER 4

Synthesis and Characterization of Stable and Efficient Nano Zero Valent Iron

4.1 Overview

Nano Zero Valent Iron (nZVI) is an excellent adsorbent/ reductant with wide applicability in remediation of persistent contaminants in soil, water and groundwater aquifers. There are concerns about its environmental fate, agglomeration, toxicity and stability in the air. Several modification methods have applied including chistosan, green tea, carboxyl methyl cellulose and other coating substances to ensure production of nZVI with excellent air stability and effectiveness. The synthesis of a novel green nZVI (gnZVI) with *Harpephyllum caffrum* leaf extracts was successfully executed in the current study. Production of gnZVI involved the simultaneous addition of an optimum amount of the $NaBH_4$ and *H. caffrum* extract to $FeCl_3$ in an inert environment (Nitrogen). The solution was stirred for thirty minutes, washed with ethanol (99%) through a vacuum filtration with a doubled 0.22 µm pore size cellulose acetate filter paper. This procedure offered the best option for the synthesis of gnZVI in terms of nontoxic and inexpensive choice of stabilizer/ reductant. Systematic characterisations using TGA, TEM, SEM, XRD, FT-IR and XPS confirmed the synthesis of crystalline, stable, reactive, well dispersed and predominantly 50 nm diameter sized gnZVI compared to the conventionally synthesized nZVI which is 65 nm. The activity testing using Orange II sodium salt (OR2) confirmed the effectiveness of the synthesized gnZVI as an excellent Fenton catalyst with 65% degradation of 20 mg/ L OR2 dye in 1 hour reaction time.

4.2 INTRODUCTION

One of the consequences of the current global increase in human population is massive pollution which leads to devastating infectious diseases and other problems. Contributions of human anthropogenic activities to environmental degradation and climate change are very obvious (He et al., 2016). Since the environment is heavily burdened by ever increasing anthropogenic

activities, its protection and remediation should be prioritised. The most adversely contaminated sectors of the environment are air, soil and water, which are all an essential part of living systems and their importance to human survival is undeniable. Consequently, there is a need for the development of antipollution technology with significant capability for optimum performance. Nanotechnology has received considerable attention for various applications due to its capability for manipulation of inherent desirable properties of materials such as reactivity, catalysis, strength, photo-activity and selectivity at the nano size (Cayuela et al., 2016; Sun et al., 2017). Environmental applications of nano materials include detection and elimination of pollutants in wastewater treatment plants as well as on-site remediation. The application of nano particles in the environment offers advantages such as improved performance, lower energy consumption and reduction in residual waste (Ali et al., 2008). Nano zero valent iron (nZVI) is one of the most researched and efficient nano materials for the mineralisation of a host of pollutants in contaminated water, soil and aquifers (Cao et al., 2005; Jewell and Wilson, 2011; Yaacob et al., 2012; Bae et al., 2016; Lopez-Telleza et al., 2011; Pullin et al., 2017). The material nZVI, is predominantly 10-80 nm sized form of iron particles with exceptional application due to their properties such as small size, large surface area, magnetism and oxidation state (Meral and Simsek, 2017). Generally, iron based materials are widely used in wastewater treatment, pharmaceuticals, medicine, food production and other manufacturing processes because of their low toxicity, biodegradability and cost effectiveness (Adeleye et al., 2016). There are possibilities of better and deeper delivery as well as higher reactivity in nano sized substances rather than micro or macro scale particles (Xiu et al., 2010). Conversely, iron at an oxidation state of zero (Fe^{0}) is usually unstable and readily returns to its natural state of electro-potential stability of Fe^{+2} or Fe^{+3} (Greenlee et al., 2012). The reactivity of nZVI depends on factors such as the source and nature of the iron material, manufacturing method, morphologies, nature of crystals, age of the nZVI and the presence of impurities (Pullin et al., 2017). The efficacy of nZVI against various types of microorganisms is well established (Xiu et al., 2010) and likewise its role in environmental remediation, and its use in the treatment of contamination in soil and water are also well known (Kharisov et al., 2012). The integration of the unique properties nZVI in the development of sensors and diagnostic tools as well as biomedical applications are the subject of intense investigations (Giersig, 2008). In spite of its numerous applications and current commercial status, the universal acceptability of nZVI is hindered by its instability in moist

environments. Apparently, the achievement of stability without compromising the reactivity of the nZVI and cost of production is a big challenge (Dong et al., 2016; Hannah G. Bulovsky, 2016; Suponik et al., 2016).

4.3 Production of nZVI

Synthesis of nZVI can be achieved through the physical, physico-chemical or chemical reduction/ modification of a higher oxidation state of iron. The physical method which is a bottom up approach includes nucleation from homogeneous solution, annealing at elevated temperature and separation of phases (Li et al., 2009). Meanwhile, physico-chemical methods such as reduction of goethite (α-FeOOH) or hematite (α-Fe_2O_3H) at an elevated temperature or the use of an ultrasonicator may also be involved in synthesis of nZVI (Jamei and Khosravi, 2013). The products of these methods usually have a very high surface energy and consequently, high agglomeration tendency (Mukherjee et al., 2016). Consequently, chemical synthesis is gaining popularity (Bae et al., 2016). It is a simple method which includes the reduction of higher oxidation states of iron with active reducing agents such as sodium borohydride (Yuvakkumar et al., 2011). Usually, the produced nano iron has the propensity for high activity as a result of its larger surface area and intrinsic magnetic interaction. However, it is very unstable and rapidly reacts in air and moisture to give a non homogeneous nano iron (Pullin et al., 2017). The high cost of chemical reducing agents, the additional process of separation and generation of large quantities of effluents are the limitations associated with industrial application of chemical synthesis. The ultimate method of synthesis must be cost effective, environmentally friendly and result in the production of stable nZVI with extensive applications (Fazlzadeh et al., 2016; Wang et al., 2017). Various methods are already developed to ensure the synthesis of stable and effective nZVI for the purpose of environmental remediation and wastewater treatment (Table 4.1).

Table 4. 1: Methods of nano zero valent synthesis

Process	Principle	Benefits	Demerits
Precision milling	Physical synthesis	Effective, easy to control, use no chemical, no toxic effluent, possibility of large scale production, uniform size and high specific surface area.	Irregular shaped nZVI, agglomeration, energy intensive and need specific equipment (Li et al., 2009)
Carbothermal reduction	High temperature (>500 ^{o}C) endothermic reaction in presence of gaseous reducing agent	Inexpensive raw materials, waste material can be used for low cost environmental friendly production.	Cost of energy is high, Irregular shaped nZVI, agglomeration, likely generation of toxic gas (carbon monoxide) (Daniel, 2010)
Ultrasound	Physico-chemical synthesis	Small, uniform and equal-axes grains of iron are produces	Low yield due to simultaneous oxidation of iron (Jamei et al., 2014)
Electrochemical	Fe^{2+}/ Fe^{3+} salt electrodes and electrical current are used	Less expensive, simple and fast	Agglomeration is common (Yoo et al., 2007)
Green synthesis	Plant containing polyphenolic group are used. Decomposition of organo-metallic molecule containing iron i.e. $Fe(CO)_5$.	Need no expensive chemical, pressure and additional energy. Extremely small nZVI and excellent homogeneity	Destruction of plants and plant parts, incomplete synthesis and large iron impurity (Kozma et al., 2016)
Thermal decomposition			The process is energy intensive, $Fe(CO)_5$ is very toxic, unstable and difficult to handle. Generation of carbon monoxide (Hai-Jiao et al., 2016)
Chemical reduction	Fe^{2+}/ Fe^{3+} salt reduction with sodium borohydride	The most common method. Good for laboratory experiment. Production of homogenous and relatively small size nZVI.	Quick corrosion and agglomeration of nZVI. Iron III chloride is hydroscopic and acid. Production of excess sludge (Stefaniuk et al., 2016).

4.4 Characteristics of common modifiers

4.4.1 Surfactants

These are amphiphilic organic compounds which prevent agglomeration by steric or electrostatic repulsion, and are used for surface modification to improve solubilisation, desorption, transportation and reduction of agglomeration in an unstable nano particle (Gomes et al., 2014). The common examples are cationic surfactants such as cetylpyridinium chloride (CPC) and hexadecyl trimethyl ammonium (HDTMA) bromide or anionic surfactants such as sodium dodecyl sulfate (SDS) and sodium dodecyl benzene sulfonate (SDBS) as well as non-ionic surfactants such as polyoxyethylene alcohol ether, polyethylene, Saponin, Tween 80 and glycol octylphenol ether (Triton X-100). The use of this type of modifiers is limited because of their high cost of production and the fact that they cause inhibition of the activity of nZVI.

4.4.2 Polymers

Surface modification with negatively charged organic polymers is possible due to the large molecular weight and high density of their charged functional groups. These compounds can enhance the dispersal of nZVI, increase its stability as well as reduce its particle size. This type of modifier also has low or no environmental toxicity He et al., (2007). The common examples are polyacrylamide (PAM), carboxymethyl cellulose (CMC), polyacrylic acid (PAA), polyethylene glycol (PEG), polyvinyl pyrrolidone (PVP) and poly styrene sulfonate (PSS). They are also expensive, cause reduction in the mobility of nZVI and consequently loss of efficiency.

4.4.3 Biopolymer

Like conventional polymers, naturally occurring, large molecular weight and high density substances can be used for surface modification of nZVI. The surface adsorption of biopolymers results in steric repulsion and increased viscosity of the suspension, and slow aggregation. Common examples are starch, guar gum (GG) and xanthan gum (XG). They are neutral, nontoxic, hydrophilic, stable, cost-effective and biodegradable. The concentration of biopolymer must be determined before application as an excessive concentration may hinder the function of nZVI in the subsurface environment (He and Zhao, 2005). Recently, there is a significant achievement in the use of hydrophilic biopolymers (Wang et al., 2010), carboxymethyl cellulose

(He et al., 2007) chitosan (Geng et al., 2009); polyelectrolytes (Singh and Misra, 2015); amphiphilic substances (Bishop et al., 2010) and various oil-based micro-emulsions (Berger et al., 2006).

4.4.4 Natural product

Green synthesis remains the most outstanding method for the production of stable nZVI (Huang et al., 2014; Pattanayak and Nayak, 2013). It involves the use of polyphenolic compounds from green plants (green tea, lemon, grape, balm, bran, sorghum etc.) for chemical or physical synthesis of nZVI (Zaleska-Medynska et al., 2016). The advantages of polyphenolic containing green plants in the production of stable nZVI may due to their achievement of greater stability and effectiveness compared to the other methods (Mahmoud et al., 2016; Markova et al., 2014; Yew et al., 2016). However, the interaction between high oxidation state iron and polyphenolic plant extract cannot be clearly explained by a simple reduction reaction (Huang et al., 2014; Oakes, 2013; Pattanayak and Nayak, 2013; Yew et al., 2016). Besides, there are a lot of misconceptions about green chemistry and the nature of the association of polyphenolic constituents of green plants in the reduction of iron metal. The ideal capping agent for the efficient use of nZVI in environmental applications must be biodegradable to prevent further site contamination. It must not inhibit diffusion or adsorption of the substrate to the active surface site. It must also be effective, stable and cost effective. The stated properties of an ideal capping agent can also be found in some specific polyphenolic plant extracts which have been demonstrated to be capable of performing dual the roles of reducing agent and capping agent in the production of nZVI (Mystrioti et al., 2014; Shahwan et al., 2011). A number of plant extracts from green tea, lemon balm, sorghum bran and weeds are widely reported to be rich sources of polyphenols (Oakes, 2013). The choice of a polyphenolic plant candidate should be based on it abundance, biodegradability, solubility at room temperature and low market value of such plants. In this chapter extract from the dried leaves of *Harpephyllum caffrum*, a common Southern Africa garden tree was investigated for its ability to serve as reducing and capping agent in the synthesis of green nano zero valent iron.

4.5 Wild Plum (Harpephyllum caffrum)

The wild plum tree belongs to the family of Anacardiaceae (mango tree family). It is the fourth largest tree family in Southern Africa where it grows naturally in gardens. The tree is locally known as Umgwenya (Xhosa, Zulu); Mothekele (Northern Sotho), Wilde pruim (Afrikaans) or Wild Plum (English). The generic name, Harpephyllum which means sickle-like was coined from the shape of the leaves. The edible fruit is commonly used for making jams and jellies while the bark and leaves have found use in traditional medicine (Olivier, 2012). These are used for treatment of acne, eczema, skin rashes as well as blood purification among many other local uses. Alcoholic extracts of the leaves of *H. caffrum* contain a high proportion of polyphenols which are documented to possess free radical quenching (Proestos et al., 2008), hepato-protection (Tian et al., 2012), anti-inflammatory and antimicrobial properties (Fratianni et al., 2014). The presence of polyphenolic compounds in the *H. caffrum* plant extract could hasten the reduction of Fe^{2+}/Fe^{3+} into the desired zero oxidation form of nano iron as well as promote its stabilisation through the formation of a polyphenol Fe-complex (Oakes, 2013). Such complexes have been thoroughly investigated and confirmed to have no ecotoxicological impact on living organisms (Markova et al., 2014; Rajan, 2011). A number of polyphenolic compounds are already identified in the *H. caffrum* leaf extract (Nawwar et al., 2011). Meanwhile, identification of reducing capability and confirmation of the polyphenolic constituent in *H. caffrum* leaf extract is necessary for the purpose of the current studies.

4.6 EXPERIMENTAL METHODS

4.6.1 Green synthesis of nano zero valent iron (gnZVI)

In the current studies, the preparation of various form of nZVI is briefly described in the Table 4.2.

Table 4. 2: Methods of nano zero valent synthesis

sample code	Fixed parameter	Varied parameter
C	2.7 g $FeCl_3.6H_20$ in 50 mL 25% ethanol	50 mL solution of $NaBH_4$ (0.6M)
N	2.7 g $FeCl_3.6H_20$ in 50 mL 25% ethanol	50 mL solution of $NaBH_4$ (0.1M) + 200 mg dried leaf extract of *H. caffrum*
4GN	2.7 g $FeCl_3.6H_20$ in 50 mL 25% ethanol	50 mL solution of $NaBH_4$ (0.1M) + 400 mg dried leaf extract of *H. caffrum*
6GN	2.7 g $FeCl_3.6H_20$ in 50 mL 25% ethanol	50 mL solution of $NaBH_4$ (0.1M) + 600 mg dried leaf extract of *H. caffrum*
G	2.7 g $FeCl_3.6H_2O$ in 50 mL 25% ethanol	1 g dried leaf extract of *H. caffrum*

0.33 M $FeCl_3.6H_20$ was prepared by dissolving 2.7 g of the hydrated iron III chloride hexahydrate ($FeCl_3.6H_2O$) in 50 mL 25% ethanol. The solution was purged with nitrogen gas for 2 minutes in a three-neck round-bottom flask to reduce the amount of dissolved oxygen. A 50 mL solution of $NaBH_4$ (0.6M) was prepared and put into a burette connected to a three necked flask. The ferric solution was subsequently titrated with the $NaBH_4$ solution at 20 ^{0}C. The reaction mixture was stirred for 30 minutes and harvested carefully by pouring through a vacuum filtration with a doubled 0.22 µm pore size cellulose acetate filter paper. The iron particles were subsequently washed several times with deionised (DI) water and ethanol mixture in an increasing amount of ethanol (100%) and later stored in a desiccator. The synthesised nano zero valent iron was labelled **C**. Meanwhile, in another instance, 200 mg, 400 mg and 600 mg of dried leaf extract of *H. caffrum* were separately added to the mixture of 2.7 g hydrated iron III chloride hexahydrate ($FeCl_3.6H_2O$) in 50 mL 25% ethanol and 50 mL solution of $NaBH_4$ (0.1M) (as described above) to synthesise nano zero valent iron, labelled **N**, **4GN** and **6GN** respectively. A third nano zero valent iron labelled **G,** was also synthesised by addition of 1 g *H. Caffrum* leaf

extract to 2.7 g hydrated iron III chloride hexahydrate ($FeCl_3.6H_2O$) in 50 mL 25% ethanol and stirred for 12 hours. The formed iron nano particles were separateed carefully by pouring through a vacuum filtration flask with a doubled 0.22 µm pore size cellulose acetate filter paper. They were subsequently washed several times with deionised water and ethanol mixture in an increasing amount of ethanol (100%) and later stored in a desiccator.

4.7 Results and Discussion

4.7.1 Antioxidant activity

Following the extraction from the dried leafs of *H. caffrum*, the antioxidant activity was measured using the ferric reducing ability of plasma (FRAP) assay as described in section 3.8.2. The Ferric reduction to ferrous ion by polyphenolic substances at low pH causes the production of a colored ferrous-tripyridyltriazine complex. The absorbance change at 593 nm for the tested reaction mixtures and those of ferrous ions per dry weight of the tested sample were compare to obtain the FRAP values as presented in Table 4.3.

Table 4. 3: Antioxidant power of differently extracted powder from the dried leaf extract of H. caffrum as determined by the Ferrous Reduction Anti-oxidant Power (FRAP) Assay

H. caffrum sample	FRAP Power per dry weight of the sample (µmole/g)	Coefficient of variation (triplicate measurement)
Ethanolic extract	856.84	2.78
Ethanolic-aqueous extract (50 %)	863.30	2.89
Aqueous Extract	1205.42	1.87

The FRAP of the extracts were 856.84, 863.30 and 1205.42 µmole/g for the ethanolic, (50%) aqueous-ethanolic and aqueous extract respectively. The results show that the aqueous extract has the highest power for the reduction of free radicals i.e. changing the higher oxidation state of iron to a lower one. Consequently, a smaller amount of the aqueous extract will be needed for the reduction of a higher oxidation state iron to a lower one compared to the ethanolic and (50%) aqueous-ethanolic extracts. The FRAP test cannot indicate the specific polyphenolic compound

that is responsible for the reduction of elemental iron and neither does it able to show the identity of polyphenolic compounds in both aqueous and ethanolic extracts. Diem et al., (2013) reported that the mixture of organic and inorganic solvent is essential for the total extraction of a polyphenolic constituent in a powdered substance. Therefore, it is safer to use at least 20% ethanol as the solvent to ensure near total extraction of the polyphenols in the *H. caffrum* leafs. The current FRAP result supports the previous finding by Oakes (2013) which states that the *H. caffrum* leaf extracts contain a high amount of polyphenolic compounds with capability to act as a reducing agent by donating electrons for the reduction of Fe^{3+}. It is expected that compounds that donate electrons to reduce Fe^{3+} to Fe^{2+}can equally donate electrons to quench free radicals. Further investigation was done by the determination of the radical scavenging activity of the extracts against the stable free radical 2, 2-diphenyl-1-picrylhydrazyl (DPPH) as described in section 3.8.1. The antioxidant activity of aqueous-ethanolic (4:1) leaf extracts of *H. caffrum* is as presented in Table 4.4.

Table 4. 4: Antioxidant power of differently extracted powder from the dried leafs extract of H. caffrum as recorded with the Ferrous Reduction Anti-oxidant Power (FRAP) Assay

Antioxidant concentration (mg/ L)	Log Antioxidant concentration	% Ascorbic acid Inhibition	% *H. caffrum* Inhibition
0.00	0.00	0.00	0.00
0.40	-0.40	11.01 ± 9.74	4.05 ± 3.69
0.79	-0.10	13. 88 ± 6.53	5.81 ± 3.6
1.57	0.20	16.82 ± 4.73	10.64 ± 0.31
3.13	0.50	25.3 ± 2.73	17.44 ± 4.18
6.25	0.80	41.83 ± 5.24	21.57 ± 3.48
12.5	1.10	66.84 ± 6.00	26.44 ± 2.1
25	1.40	96.52 ± 0.82	40.32 ± 2.15
50	1.70	96.97 ± 0.19	58.04 ± 1.14
100	2.00	97.01 ± 0.07	81.13 ± 0.86

*Mean ± standard deviation for the triplicate experiment.

H. caffrum showed a high percentage inhibition (more than 80%) for DPPH at 100 mg/L. However, the used reference standard reductant i.e. ascorbic acid has a significantly higher percentage inhibition (more than 97%) as shown in Table 4.4. Consequently, *H. caffrum* can significantly react in a biological matrix and inhibit oxidative processes (Nawwar et al., 2011). Meanwhile, the concentration of the ascorbic acid and *H. caffrum* needed for the half maximum oxidation of DPPH (IC_{50}) were (antilog 0.91) 8.13 mg/ L and (antilog 1.58) 38.02 mg/ L respectively as calculated from the plot of % inhibition versus the log of antioxidant concentration (Figure 4.1).

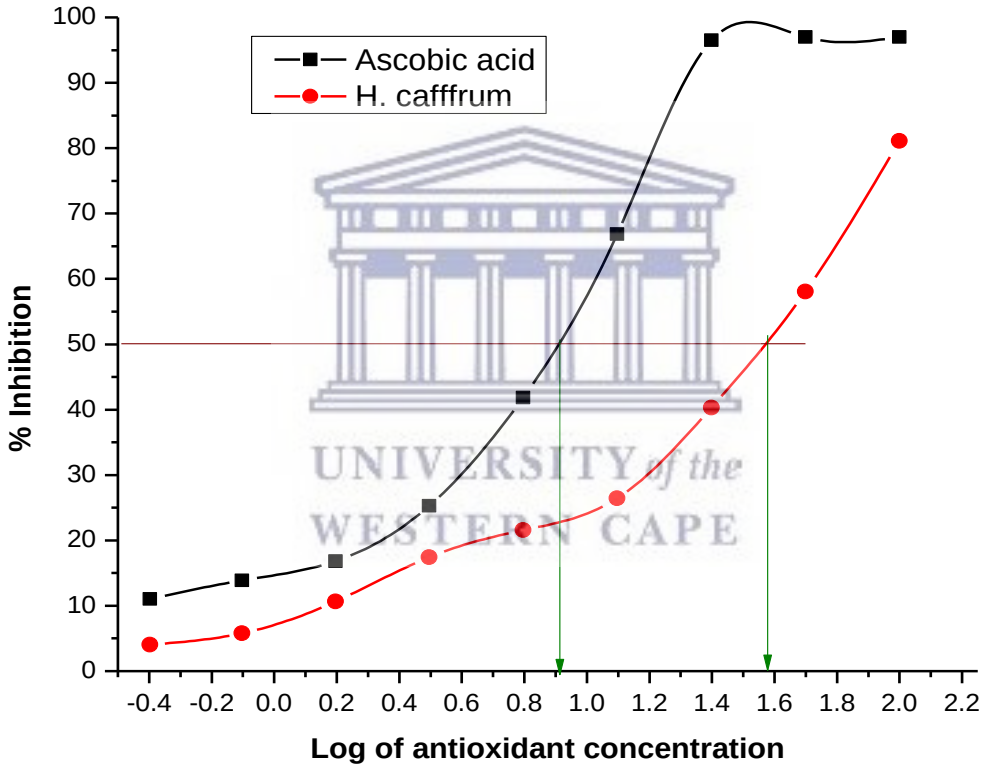

Figure 4.1: Correlation graph of % inhibition and log of antioxidant concentration

Although *H. caffrum* leaf extracts showed a high antioxidant capability, it was comparatively lower than that of the standard reference (ascorbic acid). According to the current findings, 4.70 multiple of *H. caffrum* (IC_{50} = 8.13 mg/ L) can effectively inhibit the oxidative process just like a unit of ascorbic acid (IC_{50} = 38.02 mg/ L). The disparity in the IC_{50} of *H. caffrum* leaf extract and

that of the standard (ascorbic acid) is apparently due to the high quantity of non reactive contents in *H. caffrum.* Therefore, it is necessary to detect the constituent organic compounds in *H. caffrum* leaf extract for possible isolation and direct application.

4.7.2 Identification of polyphenolic compounds in the leaf extracts of H. caffrum

The reported antioxidant activities of leaf extracts of *H. caffrum* may be due to its polyphenolic content. This was confirmed by the FT-IR analysis of the aqueous-ethanolic extract (1:4) using Perkin Elmer PE1600 as described in section 3.8.6. The FT-IR results were able to confirm the presence of polyphenolic compounds in *H. caffrum* (Figure 4.2).

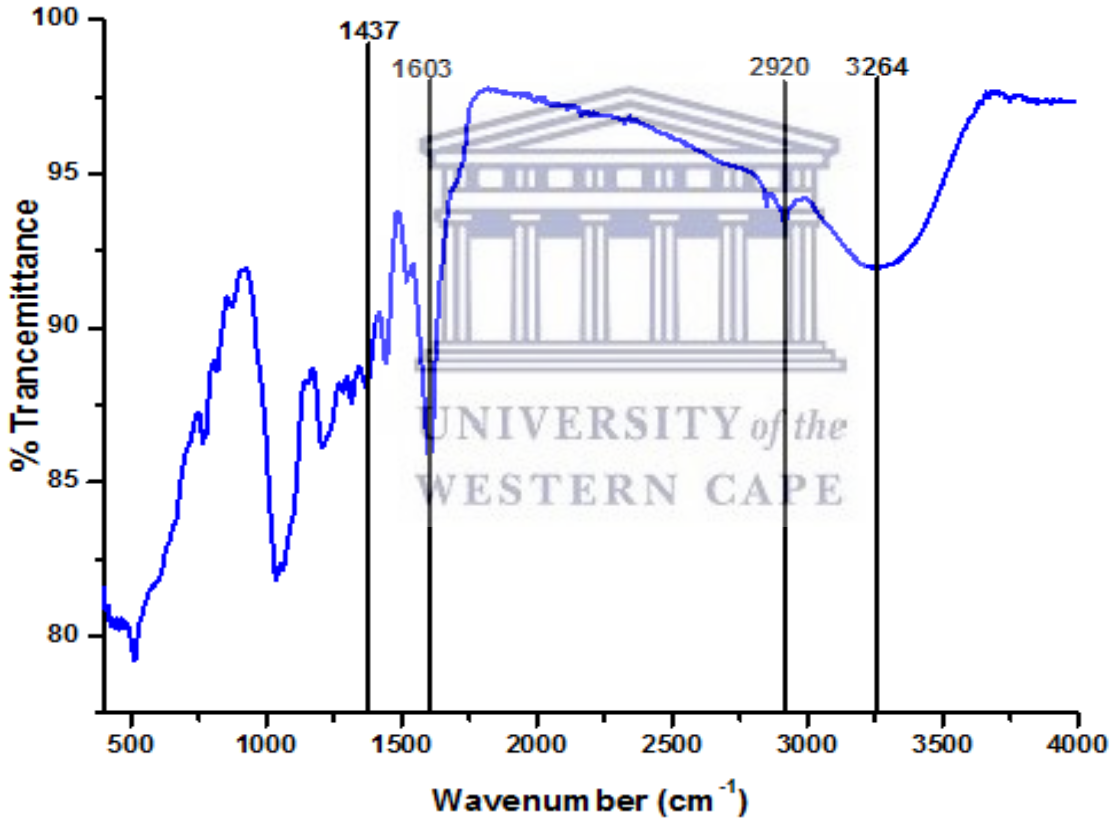

Figure 4.2: FT-IR Spectroscopy of aqueous-ethanolic extract (4:1) of H. caffrum

Peaks around 1437 and 1603 cm^{-1} are ascribed to aromatic skeletal vibration and carboxylic groups respectively (typical of phenolic compounds) while the bands at 2920 and 3264 cm^{-1} are assigned to C-H stretching and O-H stretching. Further analysis using the Liquid

chromatography-Mass spectroscopy (LC-MS) was done as described in Section 3.7.9. The LC-MS spectra confirmed the specific polyphenolic compounds in the studied *H. caffrum leaf* extracts (Figure 4.3 and 4.4).

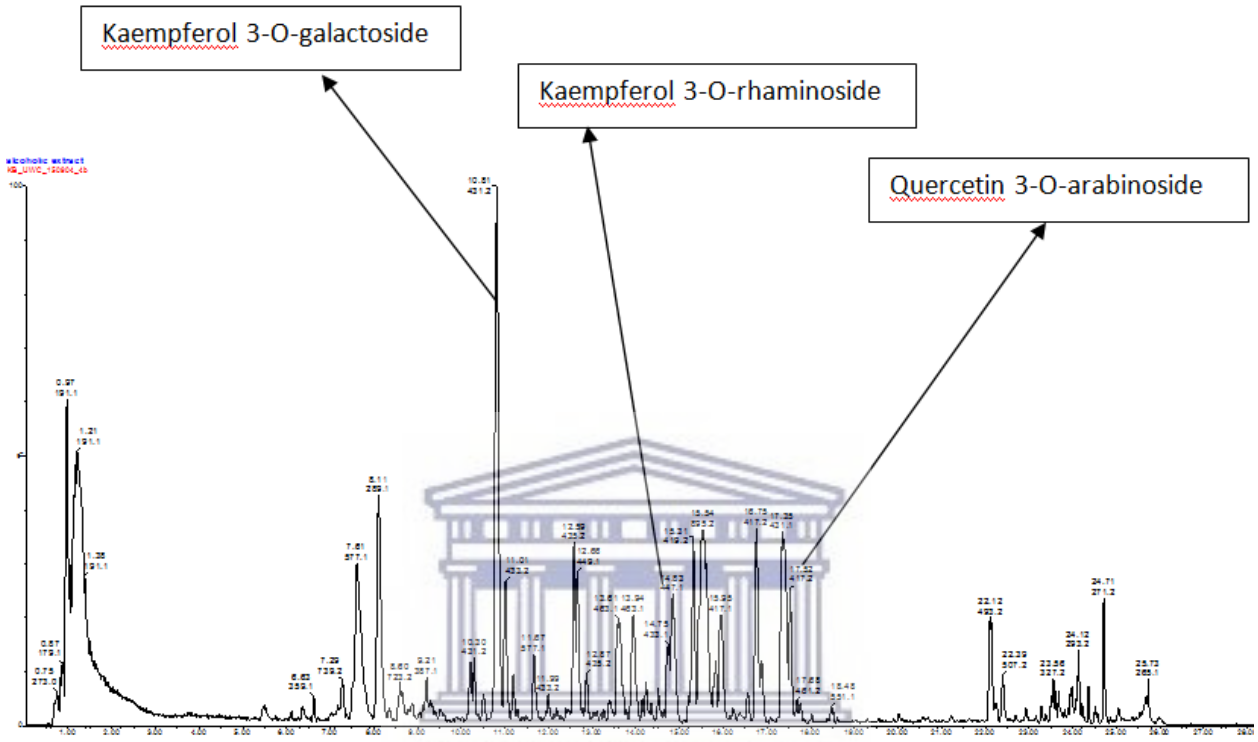

Figure 4.3: LC-MS Analysis of ethanolic extract of H. caffrum identifying Kaempferol 3-O-galactoside, Kaempferol 3-O-rhaminoside and Quercetin-3-O-arabinoside at 431.2, 447.1 and 417.1 respectively

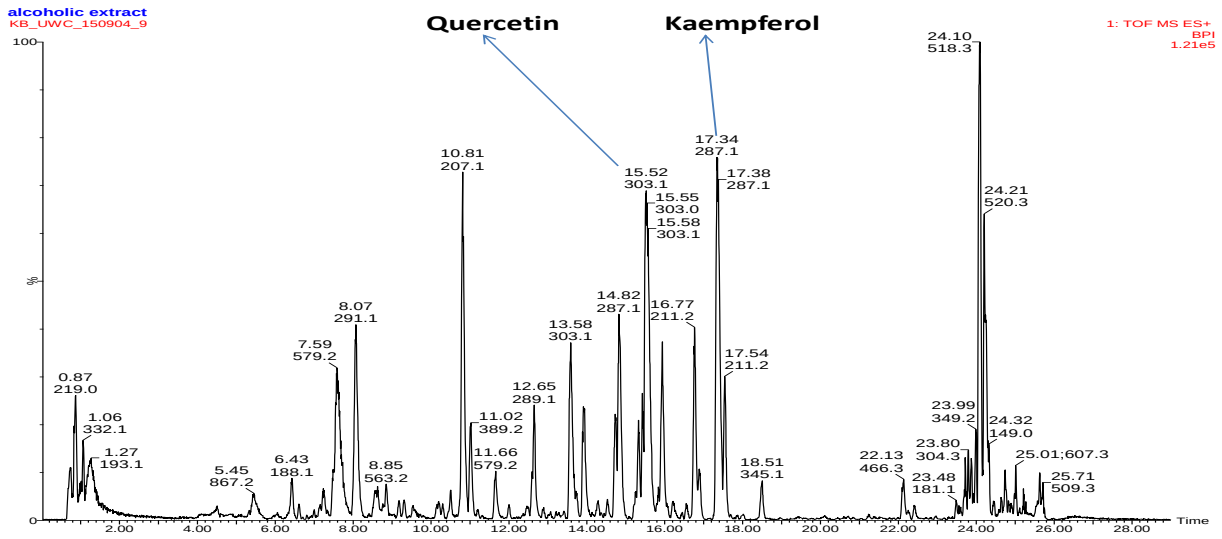

Figure 4.4: LC-MS Analysis of aqueous ethanolic extract of H. caffrum identifying Quercetin and Kaempferol at 303.1 and 287.1 respectively

Five of the previously isolated polyphenolic compounds (Nawwar et al., 2011) were confirmed in the aqueous-ethanolic extract of *H. caffrum* during the current studies using LC-MS as previously presented (Figure 4.3 and 4.4). These compounds are Quercetin, Kaempferol, Kaempferol 3-O-galactoside, Kaempferol 3-O-rhaminoside and Quercetin-3-O-arabinoside. Quercetin and kaempferol are flavonols while the others are their sugar based derivates. Each of these compounds have high antioxidant activity in the biological cells (Sharma and Lall, 2014). The compounds are polyphenols with the typical characteristic (catechol and gallol) functionalities and metal chelating. They bind with iron to form an octahedral geometry (mostly in the ratio 3:1). The binding involves several equilibrium constants with the resultant high overall complex's stability constant (Perron and Brumaghim, 2009). The deprotonated polyphenolic compound generates "hard-ligands" which possess an oxygen centre with a high charge density. This hard-ligand is a form of strong Lewis base which forms a stable complex with a Lewis acid such as Fe^{3+} (Texas, 2016). The reaction is specific for certain types of metal and depends on oxidation state and medium pH (Wang et al., 2017). The contribution of sugar based derivatives of the polyphenolic compounds in this synthesis cannot be overlooked. This is well documented by Demir et al., (2013) in the synthesis and capping of super paramagnetic

$FeSO_4$ nano particles through the reduction process by maltose and its glucose derivatives. Likewise, glucose has been used as a reducing agent in the green and facile synthesis of super paramagnetic Fe_3O_4 nanoparticle while gluconic acid stabilises and disperses the produced nano iron (Lu et al., 2010).

It is very clear that polyphenolic compounds easily give up their hydrogen in contact with a higher oxidation state metal and subsequently form a metal-polyphenol complex (Mystrioti et al., 2014; Yew et al., 2016). Consequently, polyphenolic constituents of green plants can be responsible for reducing, dispersing and capping of the iron-polyphenol nanoparticles through complexation processes (Wang et al., 2017). Iron-polyphenol complex nano particle structure has been proposed due to partial reduction of $Fe^{(3+)}$ and subsequent auto-oxidation (Saif et al., 2016; Stefaniuk et al., 2016). These processes may involve oxidation-reduction reactions followed by oligomerisation. The stable and surface modified nZVI as described in these studies (Figure 4.5) may be easily agglomerated and consequently become less active as an iron-nanoparticle. Apparently, the iron-polyphenolic complex is too stable to be reactive and since the target of this study is to synthesis a stable but reactive nZVI, it is therefore necessary to optimise the amount of polyphenolic compound that can be used in the synthesis of nZVI for good stability and reactivity.

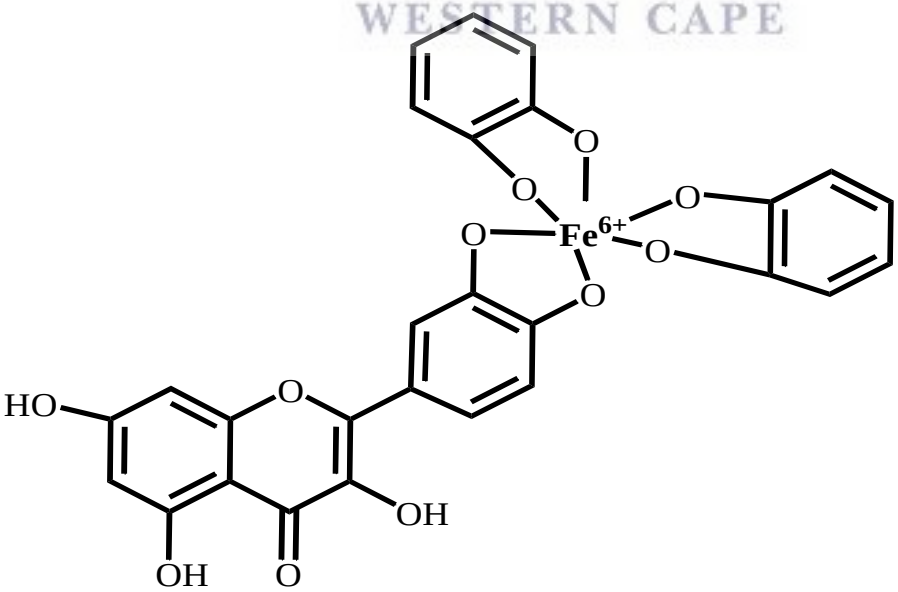

Figure 4.5: Theoretical structure of quercetin- Zero-valent Iron complex

4.7.3 Optimisation of Polyphenolic Compounds Load

nZVI sample N was synthesised by adding 200 mg of the dried leaf extract of *H. Caffrum* (20 mL) to $FeCl_3$ during its reduction with a small amount of sodium borohydride (200 mg) while sample 4GN and 6GN were synthesised by separate addition of 400 mg and 600 mg of the dried leaf extract of *H. Caffrum* to $FeCl_3$ sodium borohydride (200 mg) as presented in Table 4.2. The determination of thermal stability of the particles as well as the compositions of the polymeric blends of plant extract was done using Thermo gravimetric analysis (TGA) of the differently synthesised nZVI (Perkin Elma STA 4000) as described in Section 3.8.7. The TGA analysis was done to determine the nZVI with the suitable amount of the dried leaf extract of *H. Caffrum*, among the sample N, 4GN and 6GN and use it for the subsequent analysis and application.

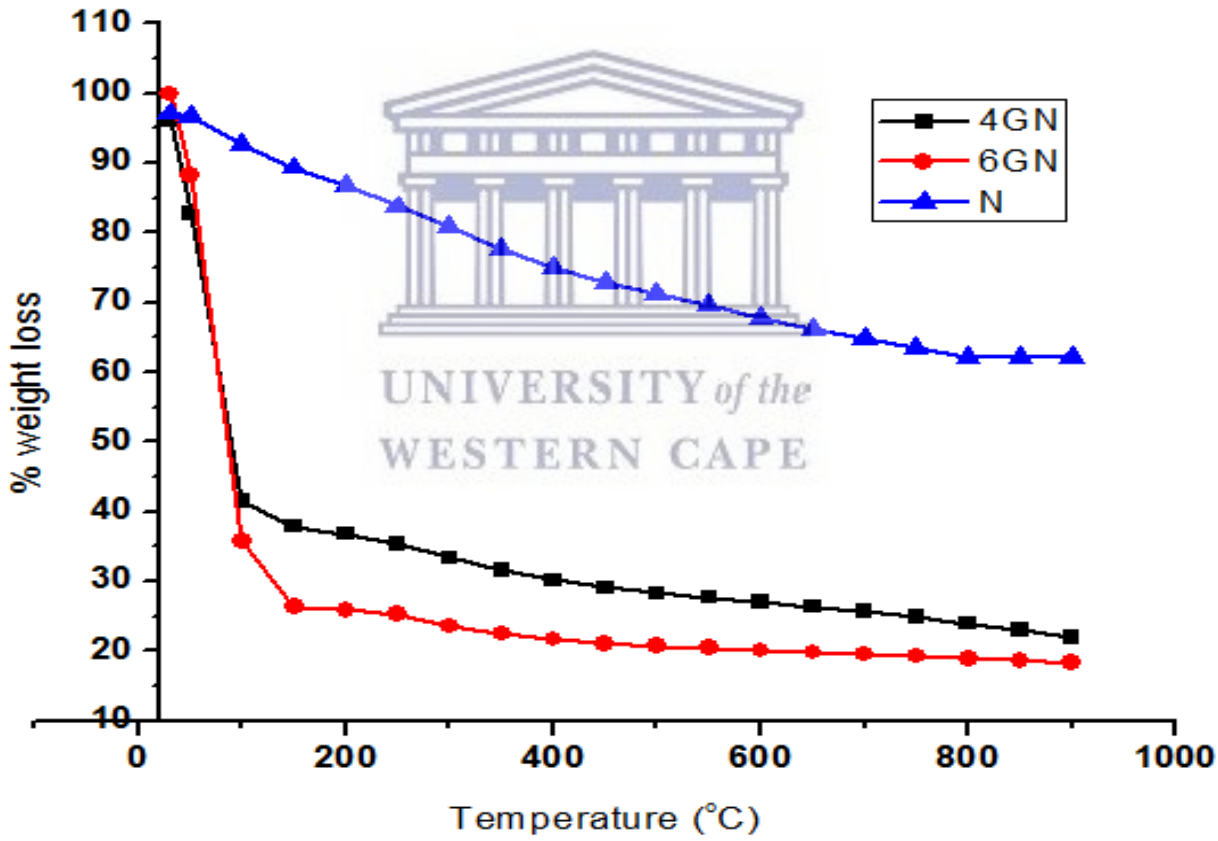

Figure 4.6: TGA of synthesized iron nano particles showing how the variation in the mass of *H. Caffrum* plant extract affect the stability of the nZVI at 10 °C/ minute heating rate and 20 ml/ minute argon flow rate (N; 200 mg *H. Caffrum was applied to nZVI, 4G*N; 400 mg *H. Caffrum was applied to nZVI, 6GN;* 600 mg *H. Caffrum was applied to nZVI*)

In the TGA analysis, N went through a slow mass loss and retained about 65 % metal its residue while 4GN and 6GN went through a rapid mass loss and retained 30 % and 20 % metal residues respectively. The implication of these results is that N is the most stable of the three samples with good amount of residual nZVI and weight loss was less than 30% at 500 ^{0}C. Apparently, 200 mg *H. Caffrum* is appropriate as reductant/ surface modifier in the preparation of nZVI with impressive thermal stability.

4.7.4 Characterisation of the synthesised nano zero valent iron

It is very important to compare the characteristic of nZVI, such as sample **G**; synthesised using only *H. Caffrum* leaf extract (1 g), the nZVI, sample **N**; synthesised with both sodium borohydride (500 mg) and *H. Caffrum* leaf extract (200 mg) and conventional nZVI, sample **C**; synthesised using sodium borohydride (1 g) by using common analytical equipment such as XRD, TEM, SEM, FT-IR, XPS and TGA. Finger print identification of the synthesised nZVI was analysed by using the X-ray Diffraction spectra (XRD) as described in section 3.8.1.

The result of the XRD analysis for **C**, **N** and **G** is presented in Figure 4.7.

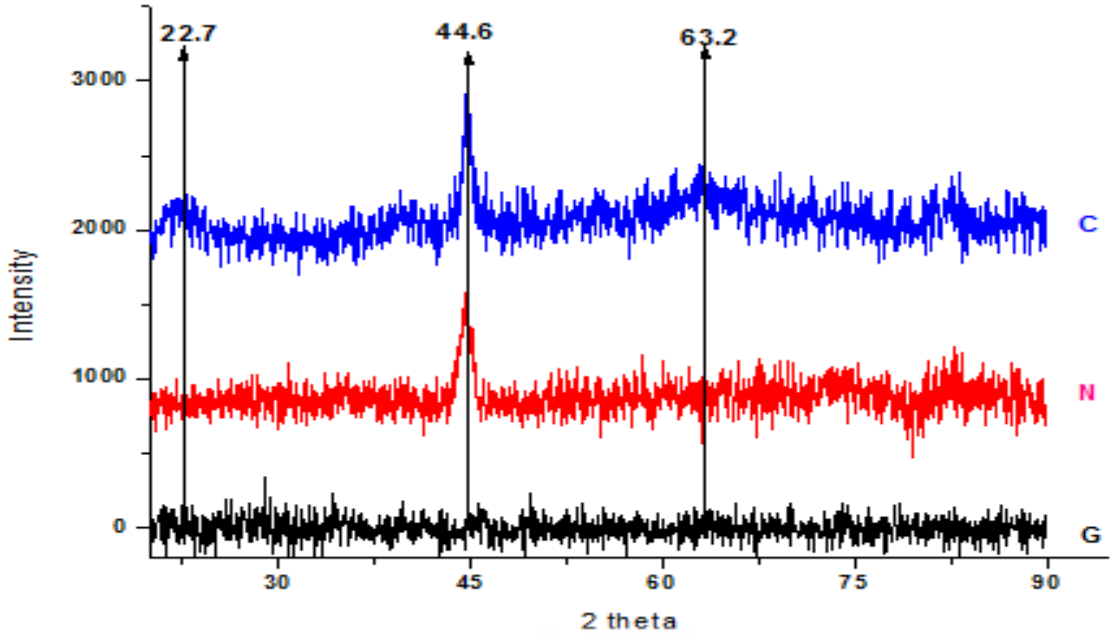

Figure 4.7: X-ray Diffraction pattern of nZVI C, N and G (G; synthesised using only *H. Caffrum* leaf extract (1 g), N; **synthesised with both sodium borohydride (500 mg) and *H. Caffrum* leaf extract (200 mg) and** C; **synthesised using sodium borohydride (1 g) only)**

A broad peak at 44.6^{o} 2θ presented in this study is a confirmation of the presence of nano zero valent iron in its crystalline form as described by Taha and Ibrahim (2014). This pattern is in accordance with diffraction pattern of body-centered cubic α-Fe (JCPDS No. 06-0696). Both the conventionally synthesised nano zero valent iron, **C** and the nano zero valent iron modified by simultaneous addition of *H. caffrum* extract, **N** have identical XRD spectra patterns with peaks as described above. However, the appearance of small peaks around 22.7^{o} and 63.2^{o} on close inspection of the XRD spectrum of **C** is a confirmation of the presence of ϒ-FeOOH (Lepidrocite) phase (JCPDS No. 17-0536). This is a consequence of the oxidation of nZVI in moist air due to its instability and absence of the capping agent or surface protecting substances. Therefore, **C** is an "iron-zero" core surrounded by higher oxidation state iron oxides (Fe^{2+}/ Fe^{3+}). The result is in agreement with previous publications on nano zero valent iron (Hoag et al., 2009; Kozma et al., 2016; Liu and Zhang, 2014). Besides, the XRD spectra of nano zero valent synthesised with only the leaf extract from *H. caffrum* (**G**) lack the typical well defined iron peaks. It is possible for the *H. caffrum* to bind with iron metal and form a metal chelating amorphous compound with a decreased XRD intensity (Su et al., 2018). Consequently, nano-

sized crystal substances formed has capacity for scattering the X-rays in many directions leading to a broader XRD main peak. Both the capping and surface oxidation of nZVI can alter its surface functionalities and increases its size. The determination of the surface functionality and size of nZVI can be better done with TEM (section 3.8.2) and SEM (section 3.8.3) analysis.

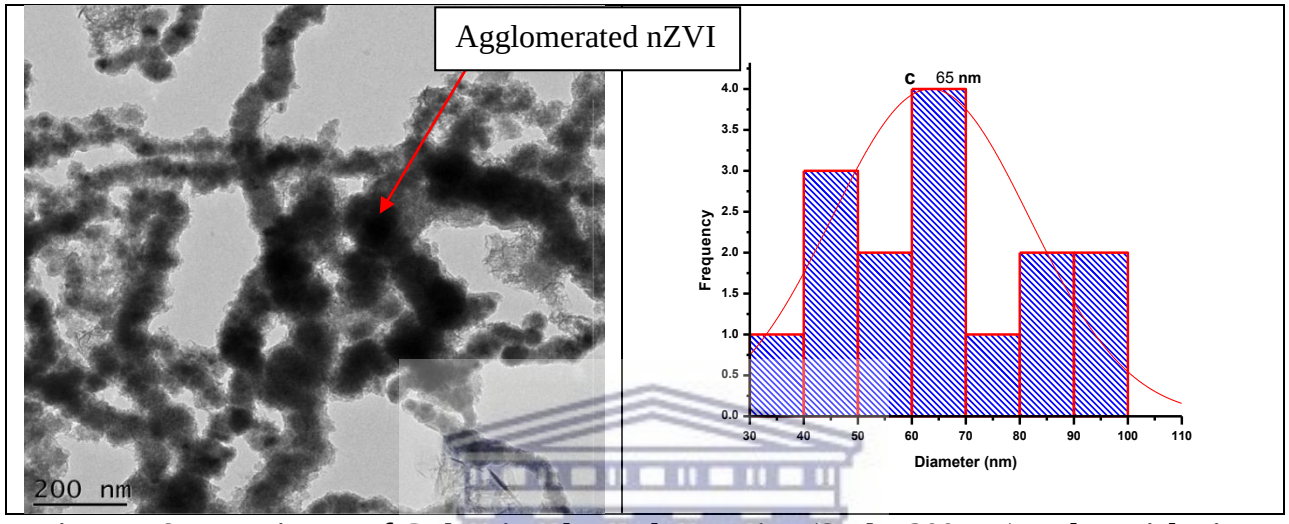

Figure 4.8: TEM image of C showing the agglomeration (Scale: 200 nm) and particle size distribution (30 nm to 100 nm) with the particle size bar chart (low frequency bar)

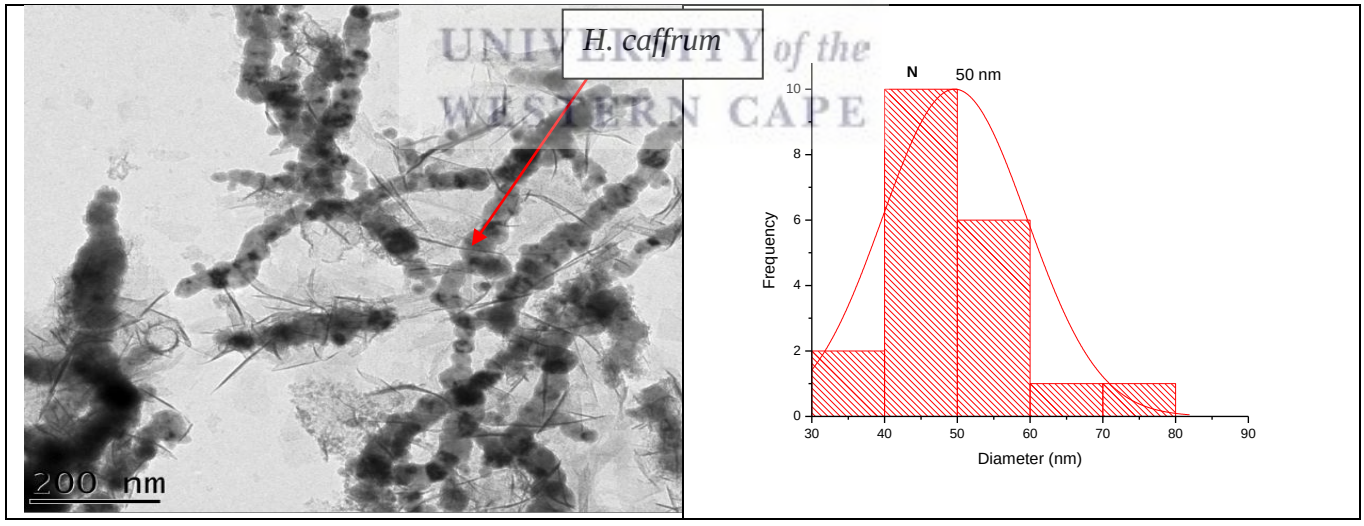

Figure 4.9: TEM image of N (Scale: 200 nm) particle identifying the *H. caffrum* location and size distribution with the particle size bar chart

High Resolution Transmission Electron Microscopy (HRTEM) images of nZVI samples (**C** and **N**) are as presented in Figure 4.8 and Figure 4.9 respectively. It was observed through the TEM images that the nZVI, sample **C** had a crystalline form of zero valent iron (Fe^0) with a number of agglomerated particles while nZVI, sample **N** is composed of relatively well dispersed crystals of zero valent iron. The sizes of nZVI, sample **C** is 65 nm at average but widely distributed between 30 nm and 100 nm while the sizes of nZVI, sample **N** is 50 nm at average with a narrow distribution, giving it a more uniform sizes compared with nZVI, sample **C**. Sizes of the synthesised nano particles during the current investigation are in concordance with the previously published reports on the nZVI (Markova et al., 2014; Thomé et al., 2015; Yaacob et al., 2012). The surface morphology of the synthesised nano iron particles were also analysed by the SEM as described in the section 3.7.3.

Conventionally synthesised nZVI, sample C, as revealed by SEM analysis shows the chain-like agglomeration of particles in which several layers of small particles clump together to form bigger agglomerates while SEM analysis of **N** shows better dispersed spherical shaped nano particles (Figure 4.10).

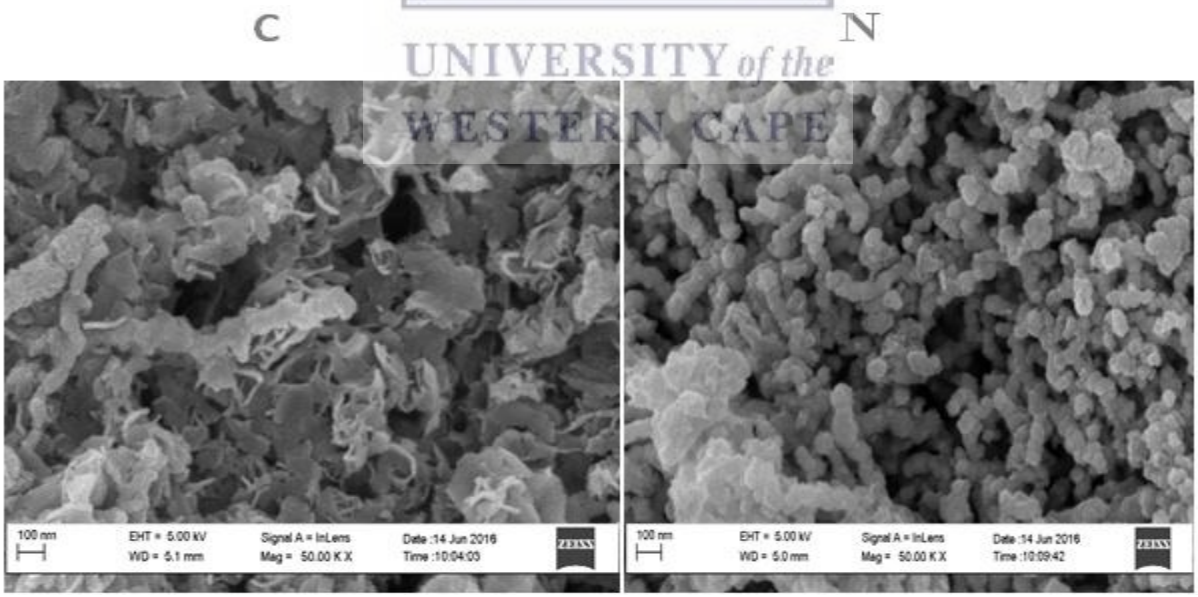

Figure 4.10: SEM of nano zero valent iron "C" and nano zero valent iron "N"

The differences in the capping agent's structural bonds and intermolecular forces are responsible for surface morphological differences exhibited in the synthesised nano zero valent irons as visible in the observed TEM and SEM images. Unlike the nZVI samples **C** and **N**, both the TEM and SEM methods cannot be use to characterise nZVI, sample **G**. The structural bonds and intermolecular forces of the dried leaf extract of *H. caffrum* (HF) as well as the nZVI, samples **C**, **N** and **G** were investigated by the FT-IR analysis described in section 3.8.6. The result of FT-IR analysis is presented in Figure 4.11.

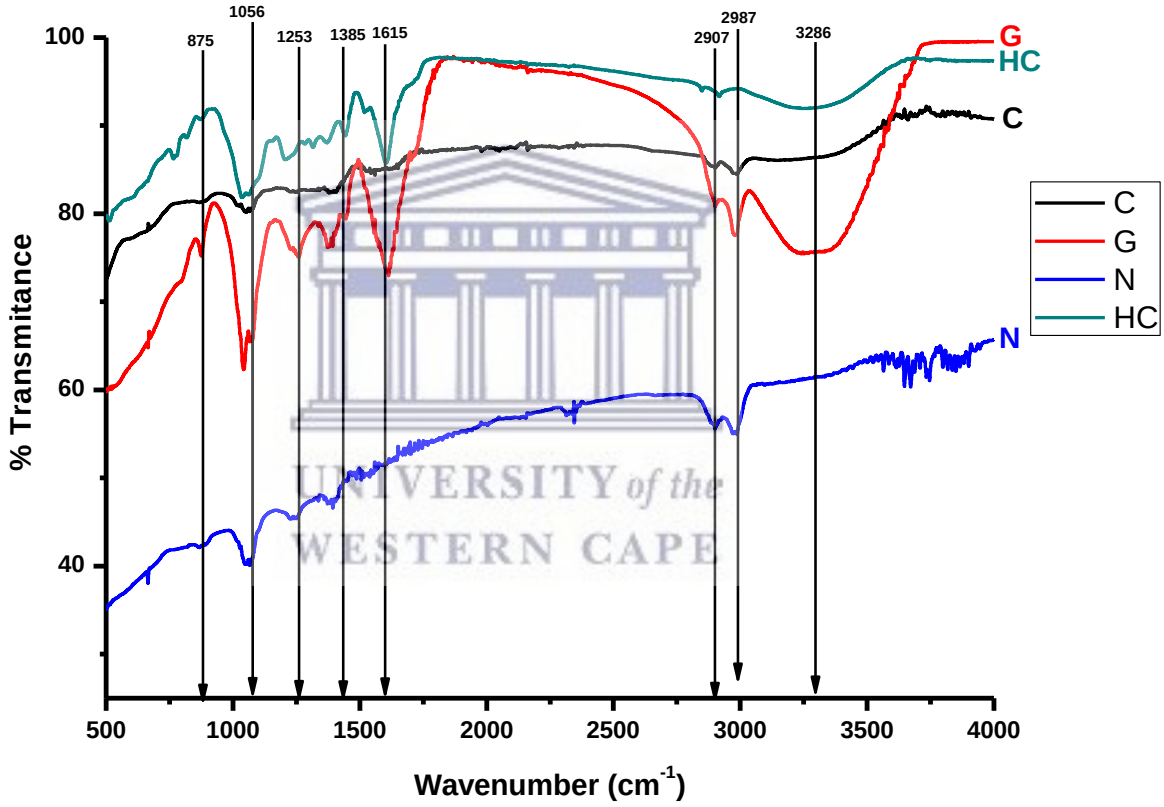

Figure 4.11: FT-IR spectra of *H. caffrum* (HF) plant extract and synthesised nano zero valent irons G, N and C

There are broad OH stretching vibration of around 3286 cm^{-1} on the FT-IR spectra of **C, G** and **HF.** The OH spectrum in the FT-IR of **C** is due to the sorbed water which resulted in formation

of (ϒ-FeOOH) Lepidrocite on the surface of nZVI. Meanwhile, the metal oxide peaks at 875 cm^{-1} on the FT-IR spectrum of **C** and N was the resultant effect of continous oxidation at their outer layers. This result is a confirmation of the claim that the surface of the synthesised nZVI is predominantly iron at higher oxidation state (Ashokkumar and Ramaswamy, 2014; Liu and Zhang, 2014). Besides, the spectra of **G** and **HF** also show intense broad OH stretching vibrations due to the contribution of benzylic OH from the polyphenolic plant extract. The intense aromatic skeletal vibration peaks around 1615 cm^{-1} in the FT-IR spectra of **HC** and **G** suggest the binding of the polyphenolic groups to the active surfaces of the synthesised nano iron particles. These peaks suggest the presence of aromatic groups in the compounds while their high intensity in **G** is a confirmation of the existence of Fe-O complex as previously documented by Lu et al. (2010) and Wang (2013). Similarly, symmetric and asymmetric carbonyl peaks at 1253 and 1385 cm^{-1} as well as the observed C-O stretching peak at 1042 cm^{-1} are present on the spectra of **HC**, **G** and **N.** There are specific distinctions between *H. caffrum* (polyphenol) containing nano iron (**G** and **N**) and the one synthesised with only $NaBH_4$ (**C**). The carbonyl containing sugar base in *H. caffrum* serves as surface modifier in the novel nanoparticle **G** and **N**, hence it prevents agglomeration and enhances the activity in nZVI (**N**). This is possible through the polymer entanglement and hydrogen bonding of the sugar moiety of the polyphenolic plant extract (Lu et al., 2010; Thekkae et al., 2017). However, the amount of *H. caffrum* needed for the stability of nZVI must be optimised to prevent possible loss of its activity.

4.7.5 Stability of the Synthesised Nano Zero Valent Iron

Thermogravimetric analysis can be used to measure the amount and rate of change in weight of nZVI material as a function of temperature in a controlled atmosphere. In these studies, the thermal stabilities of synthesised nZVI as revealed by TGA (Figure 4.12) were used to estimate the amount of nano iron or capping agent present in a unit of nZVI as well as speculating on their stability in the environment.

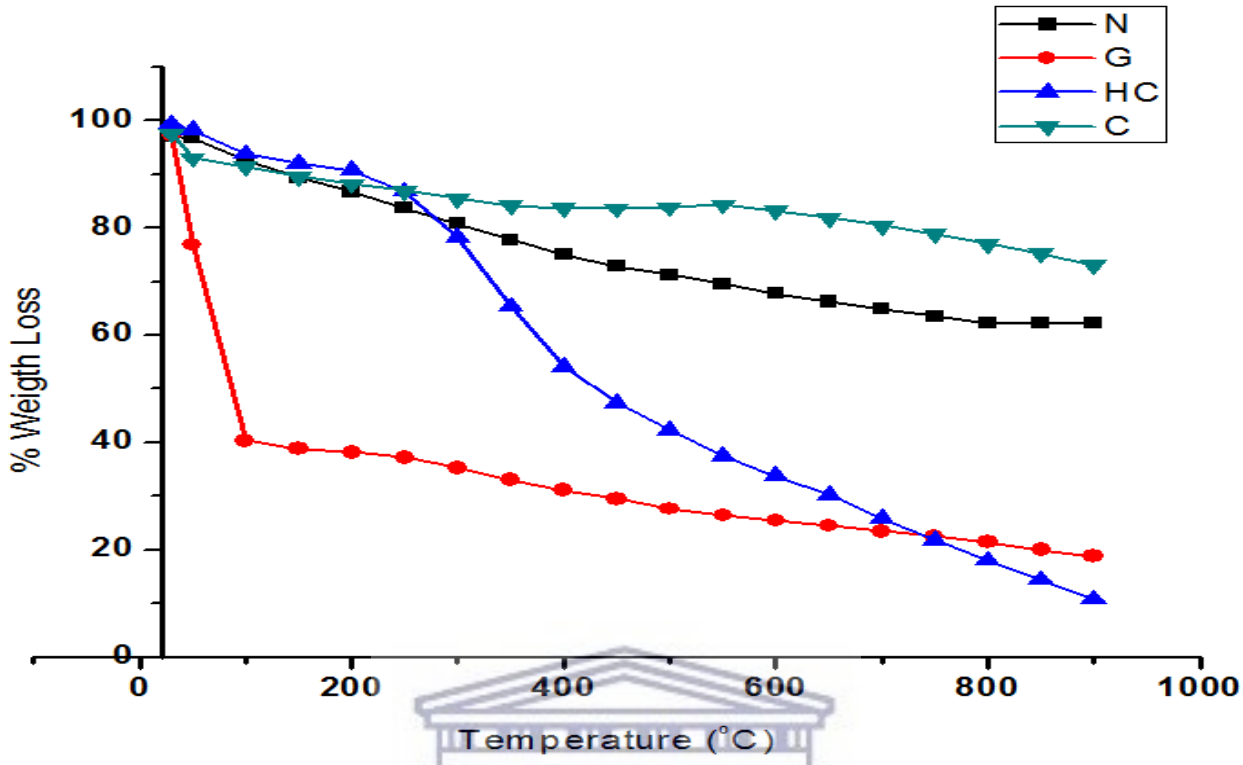

Figure 4.12: TGA graph of the *H. caffrum* (HF) plant extract and synthesised nano zero valent irons G, N and C (10 ^{o}C/ minute heating rate and 20 ml/ minute argon flow rate)

Thermal profiles of the synthesised nZVI shows that the TGA analysis of the conventional nano zero valent iron "C" (synthesised using sodium borohydride) has a low percentage weight loss against the operating temperature. Consequently, C has a high residual iron base (more than 80 %) because of the fact that no plant extract was used in its synthesis. Similarly, nano zero valent iron "N" which contains optimised amount of *H. Caffrum* also has high residual iron base (more than 70 %) and show uniform lost of volatilised polyphenolic compounds across the analysis temperature (0-900 ^{o}C). Meanwhile, nano zero valent iron "G" which was synthesised with only *H. Caffrum* extract has a low residual iron base (about 25 %). The low percentage iron residual in G may be caused by slow exchange of valent electrons between Fe and the polyphenolic constituent of *H. Caffrum* extract which results in formation of stable iron complexes. The 25 % constitution of Fe in nano zero valent iron G, is in support of the theoretical structure of Quercetin- Zero-valent iron complex that was speculated earlier (Figure 4.5). The amount of iron particles and its environmental stability is very important to its activity during the application.

However, nano iron stability and reactivity is highly dependent on the oxidation state of its surface.

4.7.6 Oxidation state of the synthesised nano zero valent iron

Optimisation of any material may not be possible without a good understanding of both the physical and chemical interactions at its surface or the interface of its layers. The chemical states of nZVI particles surface were investigated by high resolution X-ray photoelectron spectroscopy (XPS). Both elemental composition and empirical formula of a material can be measured using XPS. The spectra are obtained by irradiating a solid surface with a beam of X-ray while the kinetic energy and emitted electrons are simultaneously measured (Figure 4.13, 4.14 and 4.15).

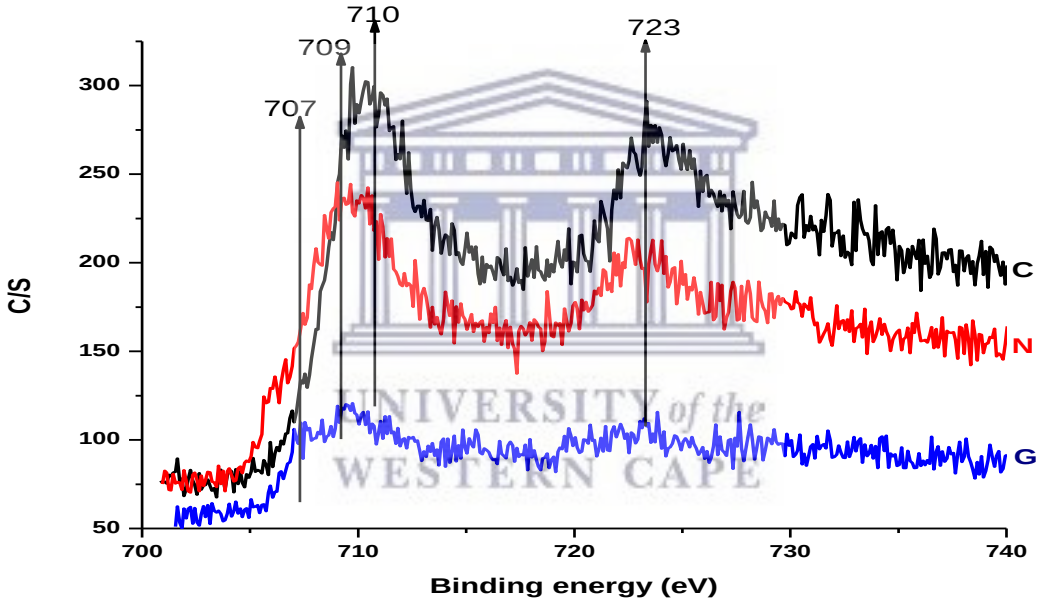

Figure 4.13: XPS spectra of nZVI samples indicating Fe 2p3/2 peaks of the nZVI synthesised with *H. caffrum* plant extract G, $NaBH_4$ plus *H. caffrum*, N and only $NaBH_4$, C

The presence of photoelectron peaks on the XPS spectra of C, N and G at ~ 707, ~ 709 and ~710 (Figure 4.13) represent the presence of iron in a zero valent state and its oxidized forms in the structure of the synthesised nZVI. The absence of $2p_{3/2}$ and $2p_{1/2}$ at ~723 ev BE in the spectrum of nZVI, **G** is an indication of its relatively stability in moist air. Meanwhile, the conventionally synthesised nZVI, **C** and the nZVI **N**; synthesised with both sodium borohydrid and *H. caffum*

plant extract shows the presence of core zero oxidation states iron nano particles surrounded by their oxidised forms. These findings were supported by Mu et al. (2017) among many other previously published articles on nZVI. Meanwhile, understanding the pattern of combination of polyphenolic plant extract in *H. caffrum* on the surface nZVI particles will enhances the differentiation of their distinguish nature. Figure 4.14 is the XPS carbon peaks of the synthesised nZVI.

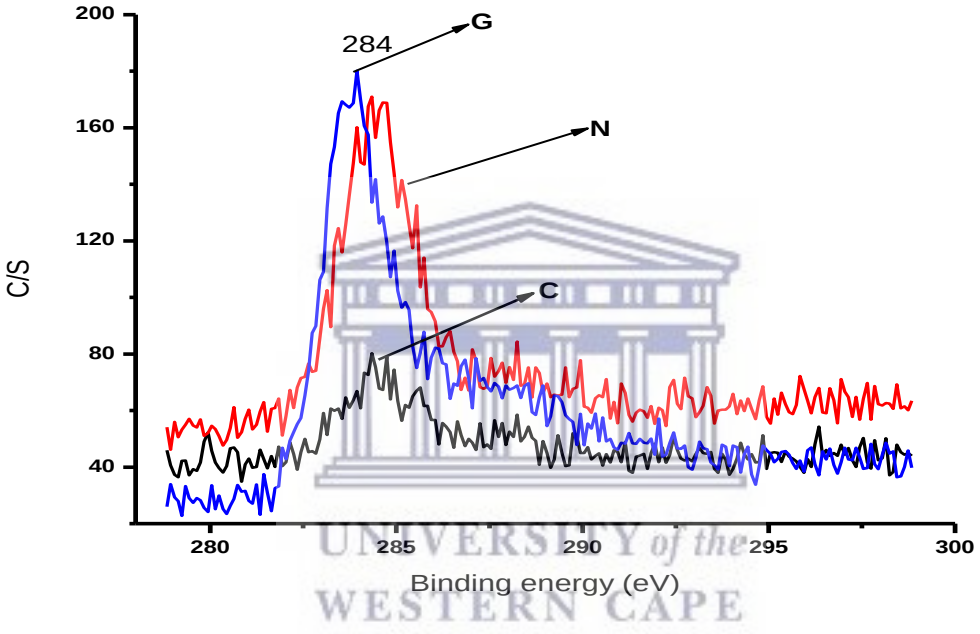

Figure 4.14: XPS spectra indicating carbon peaks in the nZVI synthesised with *H. caffrum* plant extract G, $NaBH_4$ plus *H. caffrum*, N and only $NaBH_4$, C

The presence of adventitious carbon was shown by the spectra of the synthesised nZVI, **C** at ~284 eV BE (Figure 4.14) meanwhile the peaks which were more intense (at ~284 eV BE) represent the carbon rich polyphenolic compounds on the surface of **N** and **G** as supported by Yan, (2011). This is a justification of the encapsulation of nZVI samples **N** and **G** with *H. caffrum* plant extract. Further analysis using the XPS also revealed the nature of oxygen combination on the surface of the synthesised nZVI samples (Figure 4.15)

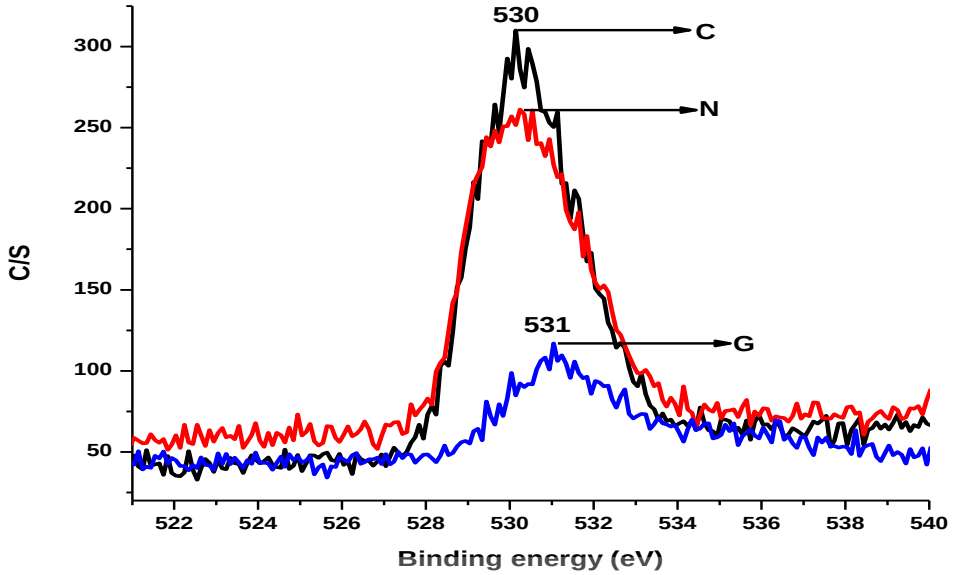

Figure 4.15: XPS Spectra of 1s oxygen peaks in the nZVI synthesised with *H. caffrum* plant extract G, $NaBH_4$ plus *H. caffrum*, N and only $NaBH_4$, C

Presented on the XPS spectra of the synthesised nZVI are the oxygen 1s peaks at ~530 and ~531 eV BE (Figure 4.15). The binding energy of 1s peaks for **G** was comparatively higher (~531 eV) because of the extensive conjugation between the iron and the polyphenolic group in the *H. caffrum.*

4.8 Chapter Summary

The synthesis of an efficient and stable novel green nano zero valent iron (gnZVI) was achieved through the simultaneous addition of the leaf extracts of *H. caffrum* (4 g/ L) and $NaBH_4$ (0.1 M) to the $FeCl_3.6H_2O$ (0.4 M). The high antioxidant activity and polyphenolic content of *H. caffrum* leaf extract enable capping, reducing and ensures the stability of the synthesised gnZVI in air and moisture. The synthesised gnZVI (**N**) possessed a significant higher surface area in comparison with the conventionally synthesised nZVI (**C**) obtained through $NaBH_4$ (0.1 M) solely reduction of $FeCl_3.6H_2O$ (0.4 M). The leaf extract of *H. caffrum* formed a metal-organic complex which protects the nano zero valent iron against oxidation in moist air and thereby enhances stability. The use of locally sourced environmentally benign and renewable material as described in this

study will enhance economic competiveness and sustainability in the production of nano zero valent iron.

CHAPTER 5

Treatment of azo dyes in textile wastewater using the jet loop hydrodynamic cavitation system

5.1 Overview

Azo dyes are complex organic dyes with opacity in liquid, poor bio-degradability and high chemical stability. Various expensive conventional treatment technologies were reportedly successful with azo dyes in textile wastewater but not without the generation of a large amount of toxic and unaccounted intermediate products and sludge. This chapter investigates the decolouration of Orange II sodium salt (OR2) using jet-loop hydrodynamic cavitation in hybrid combination with hydrogen peroxide and novel green nano zero valent iron. The degradation conditions such as initial pressure, pH of wastewater and initial concentration of dyes were investigated to establish the optimum conditions needed for the treatment of OR2. A 70% degradation of OR2 (10 mg/ L) was achieved per hour in the jet-loop hydrodynamic cavitation system by itself (inlet pressure = 400 kPa, pH=2, volume = 10 L). The enhancement of the degradation with hydrogen peroxide, iron sulfate or green nano zero valent iron led to the generation of high nitrate concentration as well as evolution of sulfate salt as evident by the TOC, IC, FT-IR and LC-MS analysis. The combination of hydrogen peroxide and iron sulfate in the jet loop hydrodynamic cavitation is not very effective because of the possible scavenging effect of the iron sulfate on the hydroxyl radical. Conversely, the combination of hydrogen peroxide and gnZVI during the degradation of OR2 in the jet loop hydrodynamic cavitation resulted in 99% degradation of the dye solution within an hour treatment. Furthermore, 74% mineralisation was also achieved as a function of TOC within an hour treatment of OR2 with the gnZVI combined with the jet-loop hydrodynamic cavitation at the optimum treatment conditions (400 kPa, pH 2, 1 mg/ L H_2O_2, 10 mg/L gnZVI, 1 hour). This result is a significant advancement in the treatment of azo dye containing of wastewater using a low energy option such as provided by the combined jet loop hydrodynamic cavitation system.

5.2 Introduction

The huge amount of wastewater generated by industries and households must be treated to ensure effective reclamation and reuse of scarce water resources. Wastewater generated by textile manufacturing industries is becoming one of the greatest environmental liabilities of the current era because of its large volume and the complex nature of the chemical content. The azo based dyes are central to the manufacturing of textiles. They are aromatic and heterocyclic chemical compounds with polarity and chromophoric functionalities. Modernisation has led to the increased utilisation and consequently the demand for different types of azo dyes. The global demand for azo dye pigments has increased from 1.9 million tons to 2.3 million tons between 2008 and 2013 with an annual growth rate of 3.5 (Pang and Abdullah, 2013). In this context, the annual discharge of more than 280,000 tons of azo dye pigments from textile manufacturing industries is well acknowledged (Ali, 2010). The complex organic dye effluent is opaque with poor bio-degradability, high chemical load and resultant persistence in the environment. The discharge of opaque and coloured wastewater have severe impacts upon the aquatic ecosystem and negative effect on biota (Shah, 2014). Most of the complex organic dye stuffs have been implicated in hepatotoxicity, mutagenicity, genotoxicity and cytotoxicity with documented biological effects on living creatures (Akhtar et al., 2016). In view of this, investment in a low energy, environmentally friendly and cost effective wastewater treatment technology for textile effluent can no longer be delayed.

5.3 Orange II sodium salt

Orange II sodium salt exists as a keto tautomer in aqueous form. It is an azo dye which is generally well known for the presence of at least one azo group (-N=N- linked to two carbon atoms) in their structure. Azo-dyes represent more than 75% of the dyes used in industrial operations (Rawat et al., 2016). Azo dyes are suitable raw materials for industrial use because of their high degree of fastness, colour range and intensity compared to the closest alternatives (Saranraj 2013; Akhtar et al. 2016). Their advantages include the application at a significantly lower temperature (60 ^{0}C) compared to azo-free dyes which temperature requirements are up to 100 ^{0}C. However, wastewater containing azo dyes are very recalcitrant and resistant to chemical

treatment systems as well as biological treatment under aerobic conditions. This is caused primarily by the presence of an electron withdrawing azo group($-N=N-$) and electron-deficient xenobiotic radicals such as the sulfonic ($-SO_3-$) group which create a molecular shortage of electrons. Typically, anaerobic biological treatment can substantially break the azo linkage in these dyes to colourless substances that are in turn predominantly toxic and carcinogenic forms of aromatic amines (Cripps et al., 1990). Despite the toxicity of the azo dye contained in textile wastewater and the quantity of research activities on their remediation, the identification of a single, low cost and efficient procedure for the mineralisation of this perennial environmental liability remains elusive. Feasibility of the target technical and economical treatment option must involve the minimum chemical and energy utilisation. The capability for the generation of hydroxyl radicals in a hydrodynamic cavitation system (Badmus et al., 2016) and their subsequent application in the treatment of persistent pollutants in wastewater was already reported by Jelonek and Neczaj, (2012). On the other hand, the advanced Fenton process (AFP) using a nano zero valent iron (nZVI) which has the capability of homogeneous catalysis, is a recently reported method for high efficacy in the degradation of POPs (Lin et al., 2017). Based on these reports, the application of nZVI in the jet loop hydrodynamic cavitation system could be investigated for aiding complete mineralisation of POPs into nontoxic end products.

In this chapter, decolouration of an aqueous solution of OR2 in a jet loop hydrodynamic cavitation system (described in Section 3.6) was studied in the presence of a novel green nano zero valent iron (gnZVI). The optimum decolouration conditions were also studied with respect to the configuration of the jet loop hydrodynamic cavitation, the concentration of hydrogen peroxide, the pH, the gnZVI loading and the initial concentration of OR2. Upon the analysis of the OR2 using a UV spectrophotometer as well as TOC and LC-MS, the derived data were used to report the kinetics of OR2 decolouration and its mechanism.

5.4 Experimental setup

The quantification of the amount of hydroxyl radicals generated in the jet loop hydrodynamic cavitation system was done using terephthalic acid (TA) dosimetry as described in Section 3.9. Subsequently, the optimisation of the degradation conditions for an OR2 solution (10 L) using

hydrodynamic cavitation was done by varying parameters such as the orifice plate hole size (mm), pressure (kPa), pH, initial concentration of OR2 (mg/ L), concentration of hydrogen peroxide (mg/ L), concentration of iron sulfate (mg/ L) and the concentration of gnZVI (mg/ L) (Table 5.1).

Table 5.5.1: Experiment operational conditions during the treatment of RO2 in the jet loop hydrodynamic cavitation system

Code	*Orifice hole diameter (mm)*	*Inlet pressure (kPa)*	*pH*	*Concentration of OR2 (mg/ L)*	*Concentration of H_2O_2 (mg/ L)*	*Concentration of Fe^{2+} (mg/ L)*	*Concentration of gnZVI (mg/ L)*
PS	4	400	2	10	0	0	0
HS	**2-4**	**400**	**2**	**10**	**0**	**0**	**0**
HS2	2	400	2	10	0	0	0
HS3	3	400	2	10	0	0	0
HS4	4	400	2	10	0	0	0
IP	**4**	**200-500**	**2**	**10**	**0**	**0**	**0**
IP2	4	200	2	10	0	0	0
IP3	4	300	2	10	0	0	0
IP4	4	400	2	10	0	0	0
IP5	4	500	2	10	0	0	0
pH	**4**	**400**	**2-10**	**10**	**0**	**0**	**0**
Ph2	4	400	2	10	0	0	0
Ph4	4	400	4	10	0	0	0
Ph6	4	400	6	10	0	0	0
Ph8	4	400	8	10	0	0	0
Ph10	4	400	10	10	0	0	0
OR	**4**	**400**	**2**	**5-20**	**0**	**0**	**0**
OR5	4	400	2	5	0	0	0
OR10	4	400	2	10	0	0	0
OR20	4	400	2	20	0	0	0
HR	**4**	**400**	**2**	**10**	**0.5-10**	**0**	**0**
HPS	4	400	2	10	0	0	0
P5HR	4	400	2	10	0.5	0	0
HR1	4	400	2	10	1	0	0
HR2	4	400	2	10	2	0	0
HR5	4	400	2	10	5	0	0
HR10	4	400	2	10	10	0	0
FE	**4**	**400**	**2**	**10**	**0**	**5-20**	**0**
FE5	4	400	2	10	0	5	0

FE10	4	400	2	20	0	10	0
FE20	4	400	2	10	0	20	0
HPZ	4	400	2	10	0	0	0
HPS	4	400	2	10	1	0	0
GH10	4	400	2	10	1	0	10
FH10	4	400	2	10	1	10	0

5.5 Results and Discussion

The rate and extent of degradation of persistent organic pollutants in the jet loop hydrodynamic cavitation system can be governed by factors such as the configuration of the jet loop hydrodynamic equipment, inlet pressure, solution pH and physico-chemical properties of the compound, initial concentration of the compound, nature and the amount of catalyst as well as the addition of oxidant. Subsequently, results obtained using UV spectrophotomer analysis (as presented in Section 3.7.5) of the treated OR2 solution were used to calculate its concentration as specific parameters were varied. The intermediate and final products of degradation were identified by means of FT-IR, GC-MS and IC analysis.

5.5.1 Quantification of OH Radicals in the jet loop hydrodynamic cavitation system

The aim of this investigation was to determine the amount of hydroxyl radical that can be generated in the jet loop hydrodynamic cavitation equipment as currently designed (Section 3.6). The terephthalic acid (TA) reacted with OH radical to produce 2-hydroxyl terephthalic acid (HTA) solutions which was detected and quantified using the spectrofluorometer described in Section 3.9.1. The dosimetry of HTA was described in Section 3.9.2 and the calibration curve for known HTA concentration (Appendix 1) was used to determine the amount of OH radical generated based on the chemical equation presented in Figure 3.7. The amount of hydroxyl radical produced over an hour operation time in the orifice-venturi jet loop hydrodynamic cavitation system is presented in Figure 5.1.

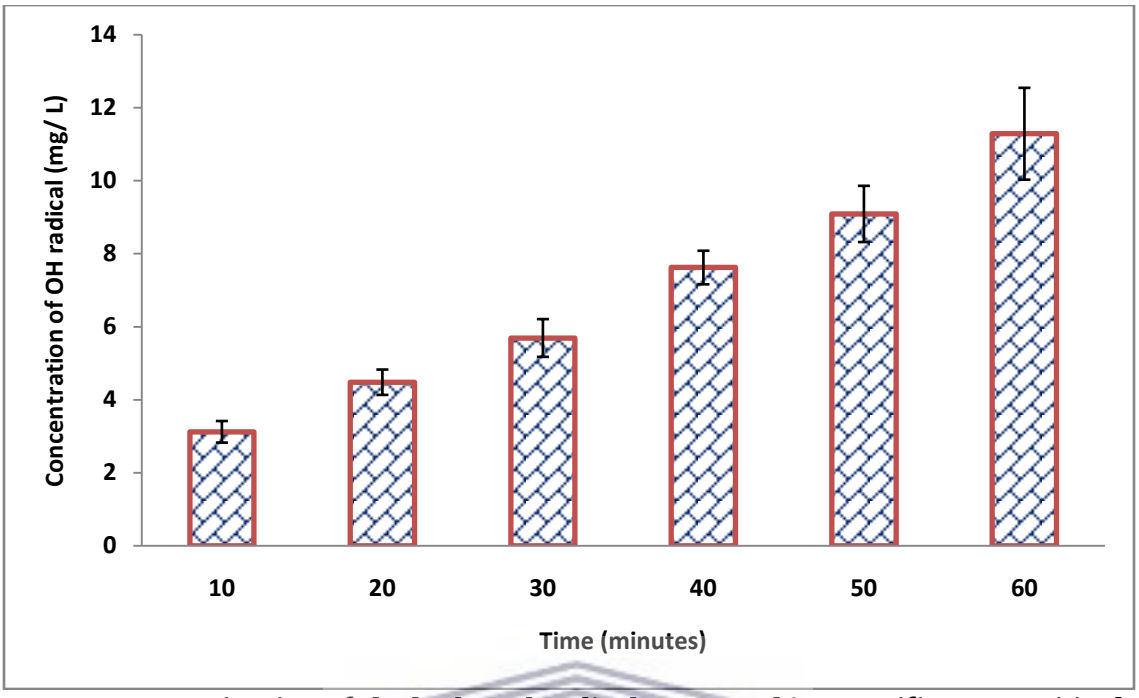

Figure 5.1: Determination of the hydroxyl radical generated in an orifice-venturi jet loop hydrodynamic cavitation system (4 mm orifice hole size, pH 7.4, 400 kPa, n = 3)

There was a uniform increase in fluorescence intensity with respect to the operating time of the jet loop hydrodynamic cavitation reactor. The generation of OH radicals in the jet loop hydrodynamic cavitation system increased with the operation time. The amount of OH radicals generated during an hour operation time in the jet loop hydrodynamic cavitation system was equal to 11.29 mg/ L. Therefore, the quantity of OH radical (per hour) in the current design of jet loop hydrodynamic cavitation is much higher than that of the sonicator system (0.465 mg/ L) which was reported by Badmus et al., (2016). Apparently, the jet loop hydrodynamic cavitation system is a promising AOP for the treatment of larger volume of wastewater with higher concentration of POPs (Tao et al., 2016). Factors such as the design and size of the orifice hole as well as venturi design may influence the generation of OH radical in the jet loop hydrodynamic cavitation system. Besides, the activity of the generated OH radical can also be influenced by the nature of the POPs, its concentration, pH, addition of other oxidants and catalyst.

5.5.2 Preliminary degradation of OR2 with Hydrodynamic cavitaton only

Firstly, a baseline experiment was setup using the optimum condition for cavitation as reported by Gore et al., (2014) with little modification. A solution of OR2 (10 mg/ L, 10 L, pH 2) was treated in the orifice-venturi bearing (orifice hole size = 4 mm) jet loop hydrodynamic cavitation system (Section 3.6) for an hour with a 10 minute sampling frequency. The % decolouration of OR2 solution in the jet loop hydrodynamic cavitation was derived after a triplicate experimentation through the "mathematical equation" that was described in Section 3.7.5. The applied experimental conditions were set out in Table 5.1 for PS runs. The decolouration pattern of OR2 solution across an hour treatment time at 10 minute sampling frequency in PS10, PS20, PS30, PS40, PS50 or PS60 for 10, 20, 30, 40, 50 or 60 minutes respectively is presented in Figure 5.2.

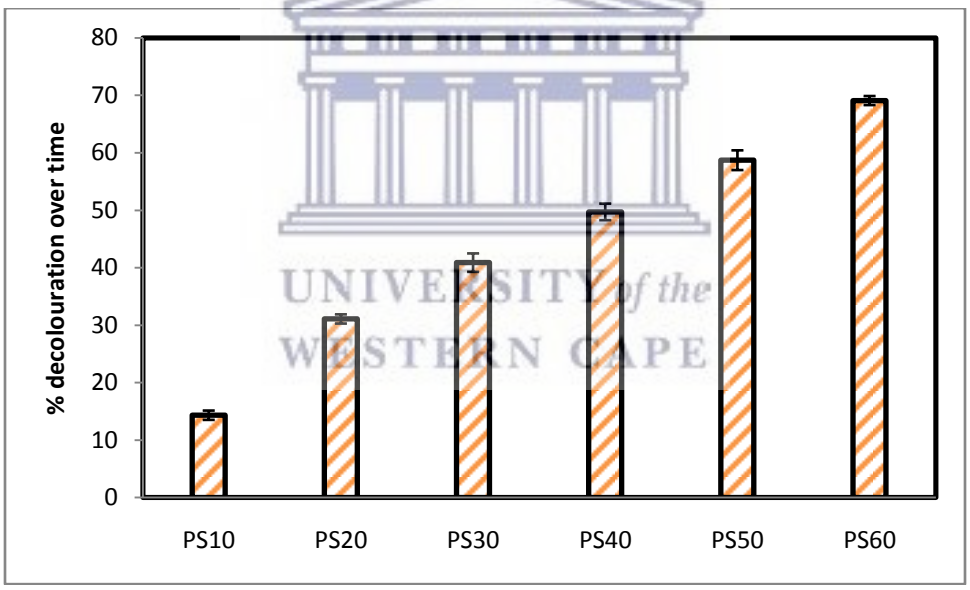

Figure 5.2: Percentage decolouration of OR2 by only jet loop hydrodynamic cavitation (10 mg/ L, 10 L, pH 2, orifice holes size 4 mm, 400 kPa, n = 3).

It was observed that the % decolouration of OR2 solution in the jet loop hydrodynamic cavitation system increased with the treatment time. The implication of this result is that approximately 69 ± 0.8% decolouration of OR2 solution (10 mg/ L, pH 2) was achieved after 1 hour treatment using only jet-loop hydrodynamic cavitation at 400 kPa. Understanding the law

governing the decolouration in the jet loop hydrodynamic cavitation is very crucial to this study because it will enable the prediction of the time required to achieve complete decolouration of OR2. A plot of natural logarithm of decolouration ratio [ln (C_0/ C_t)] against the reaction time is presented in Figure 5.3.

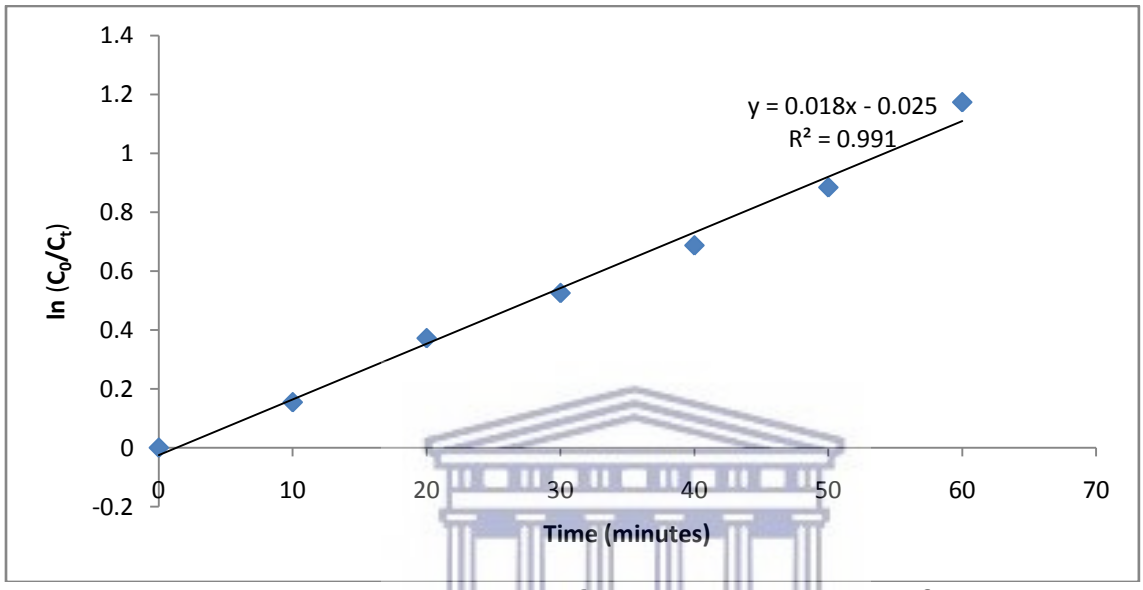

Figure 5.3: Pseudo First order graph for the decolouration of OR2 in the jet loop hydrodynamic cavitation (10 mg/ L OR2, 10 L OR2, pH 2, 4 mm orifice holes size, 400 kPa, triplicate, n = 3).

Production of a straight line graph during the plot of ln(C_0/ C_t) against the reaction time is an indication that the decolouration rate of OR2 in the jet loop hydrodynamic cavitation is governed by the first order law. On the basis of this, the slope of the plot (Figure 5.3) is equivalent to the first order rate constant (k) of OR2 decolouration. Likewise, the half-life of the decolouration ($t_{1/2}$ = 0.693/ k), which is the time taken for half the concentration (10 mg/ L) of OR2 (10 L) to be decoloured, can also be calculated as described in Section 3.8.3. The first order rate constant (k) and the half-life of decolouration ($t_{1/2}$) are 0.0189 minutes^{-1} and 36.67 minutes respectively. Alteration in the jet loop hydrodynamic cavitation design can have a corresponding influence on the fluid dynamics as well as the rate and extent of treatment in the jet loop hydrodynamic cavitation system (Barik and Gogate, 2018). It was therefore necessary to investigate whether the

change in the diameter of the hole in the pair of orifice plates can have an impact on the decolouration of OR2, using the jet loop hydrodynamic cavitation system as currently designed.

5.5.3 Influence of varied sizes of a pair of single hole orifice plates on the decolouration of OR2 in the jet loop hydrodynamic cavitation system

In the previous section, the first order kinetic was reported for decolouration of a 10 L solution of OR2 (10 mg/ L, pH 2) which was treated in the jet loop hydrodynamic cavitation system on its own for an hour with 10 minute sampling frequency. In this section, the diameter of a pair of single hole orifice plates was varied between 2, 3 or 4 mm as described in Section 3.6. The decolouration was measured using UV-Vis spectrophotometer as described in Section 3.7.5. The experimental conditions are set out in Table 5.1 for runs HS2, HS3 and HS4. The achieved % decolouration of OR2 solution in the jet loop hydrodynamic cavitation for triplicate measurement (n = 3) is presented in Figure 5.4.

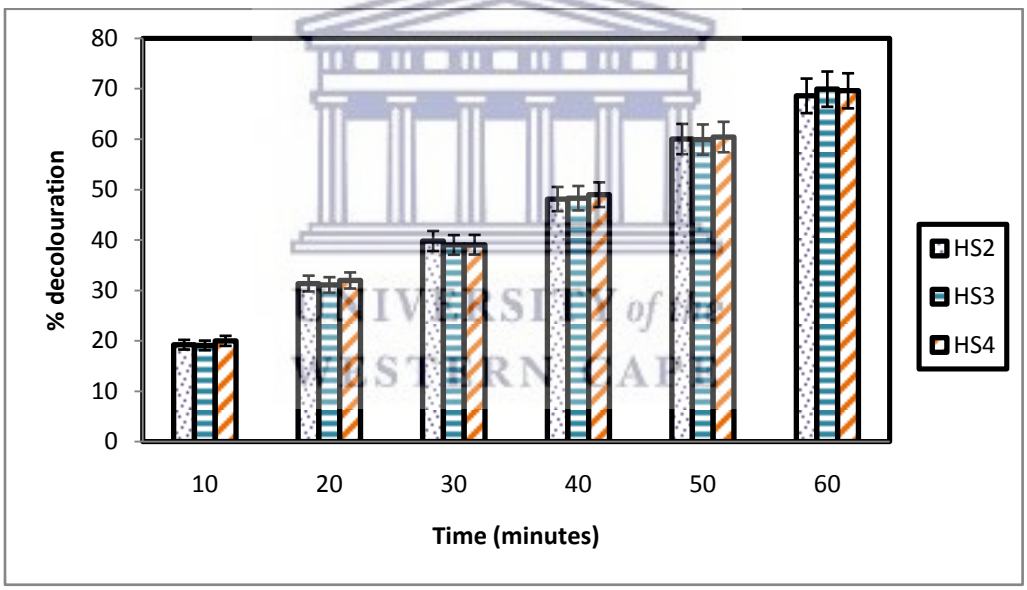

.

Figure 5.4: The effect of orifice plate hole size ([HS2] 2, [HS3] 3 or [HS4] 4 mm) on OR2 dye decolouration by jet loop hydrodynamic cavitation (400 kPa, 10 mg/ L OR2, 10 L OR2, pH 2, n = 3).

The lowest percentage decolouration (68.59 ± 1.2%) was achieved when the orifice plates hole sizes were 2 mm while the percentage decolouration for orifice plates hole sizes 3 mm and 4 mm were 69.92 ± 1.5% and 69.59 ± 0.7% respectively. Approximately, 70% decolouration was

achieved with all the different hole sizes of the orifice plates. Therefore, the extent of decolouration of OR2 solution in the jet loop hydrodynamic cavitation in the current design is not affected by the hole sizes (2, 3 or 4 mm) in the orifice plates. At this stage, the effect of the orifice plate hole and the single hole design on the velocity of the OR2 solution across the downstream end of the jet loop hydrodynamic cavitation system is not known. However, the decolouration half-life $t_{1/2}$, (as described in Section 5.5.2) for the 4 mm hole size orifice plate (HS4) was slightly lower in magnitude (36.47 minutes) and has best conformity with the first order kinetic (R^2 = 0.991) in comparison with the other orifice hole sizes (Table 5.2).

Table 5.2: Rate and extent of decolouration of OR2 treated the jet loop hydrodynamic cavitation system with varied orifice plate hole sizes (400 kPa, 10 mg/ L, 10 L, pH 2, n = 3).

Code	Orifice size (mm)	K	Decolouration half-life $t_{1/2}$, (0.693/ K) in minutes	% decolouration per hour $[1-(C_t/ C_0)]*100$	R^2
HS2	2	0.0184	37.66	68.59 ± 1.2	0.9875
HS3	3	0.0189	36.67	69.92 ± 2.7	0.9817
SH4	4	0.0190	36.47	69.59 ± 0.7	0.9910

Therefore, the orifice holes sizes of 4 mm were implemented consistently for subsequent experiments. According to Sharma et al. (2008), the downstream velocity in the jet loop hydrodynamic is dependent on either the size of the hole on the orifice plate or the inlet pressure. It was also reported that the cavitation inception in the jet loop hydrodynamic cavitation system depends on inlet pressure, the volumetric flow rate, liquid velocity and area of the throat (Gore et al., 2014). Therefore, it is important to investigate the effect of the inlet pressure on the decolouration of OR2 in the jet loop hydrodynamic cavitation.

5.5.4 Effect of inlet pressure on the decolouration of OR2 in the jet loop hydrodynamic cavitation system

The pressure drop across the venturi length is responsible for the cavitation in the jet loop hydrodynamic system and subsequent production of hydroxyl radicals. However, the pressure drop varies from one design of jet loop hydrodynamic equipment to another depending on the inlet pressure among other design specific factors (Gore et al., 2014). In the current study the extent of decolouration of OR2 solution (10 mg/ L) in the jet-loop hydrodynamic cavitation system alone (10 L) over an hour time period was determined by UV spectrophotometer at an

inlet pressure range between 200, 300, 400 or 500 kPa represented by IP2, 1P3, 1P4 or IP5 respectively (Table 5.1). The relationship between the inlet pressure (kPa) and the extent of decolouration of OR2 solution for the triplicate measurement in jet loop hydrodynamic cavitation is presented in Figure 5.5.

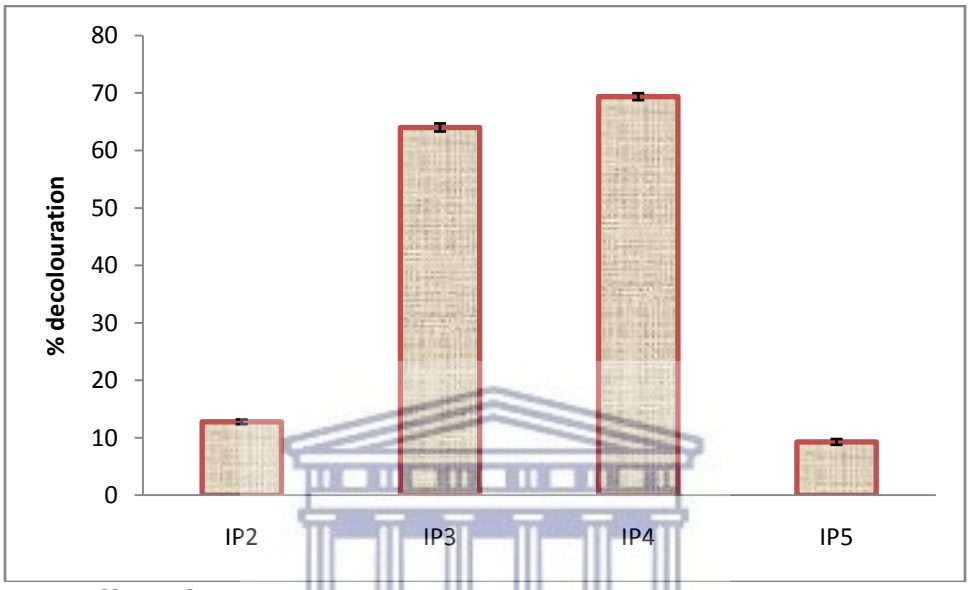

Figure 5.5: The effect of inlet pressure [200 (IP2), 300 (IP3), 400 (IP4) or 500 kPa (IP5)] on the extent of decolouration of OR2 in the jet loop hydrodynamic cavitation system (10 mg/ L OR2, 10 L OR2, pH 2, 4 mm orifice hole size, n = 3)

It was observed that the extent of decolouration of OR2 solution increased as the initial inlet pressure was increased from 200 kPa (IP2) and an optimum inlet pressure was observed at 400 kPa (IP4) where the extent of OR2 decolouration was 69.37 ± 0.6% within an hour.

The formation of cavities in a jet loop hydrodynamic cavitation system usually start when the inlet pressure is increased up to a certain critical quantity (Wu et al., 2013). The more the inlet pressure increases, the more the formation of cavity and subsequent formation of micro bubbles. The collisions of micro bubbles resulted in OH radical generation and the oxidation effect of the OH radical leads to the decolouration of OR2. The first order kinetic of decolouration of OR2 at the varied inlet pressure in a jet loop hydrodynamic cavitation is presented in Figure 5.6.

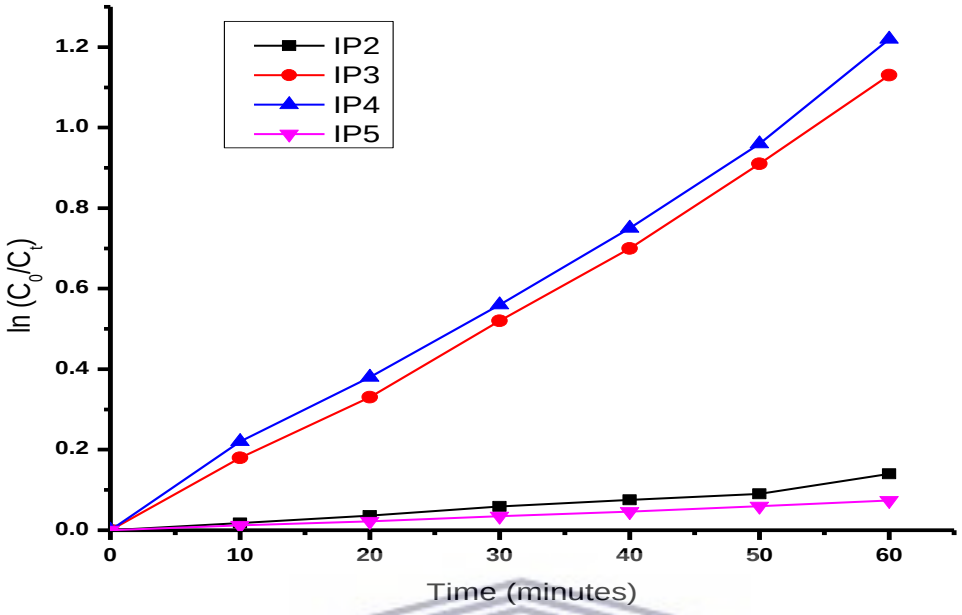

Figure 5.6: The effect of inlet pressure [200 (IP2), 300 (IP3), 400 (IP4) or 500 kPa (IP5)] on the rate of decolouration of OR2 (10 mg/ L) in the jet loop hydrodynamic cavitation system (10 mg/ L OR2, 10 L OR2, pH 2, 4 mm orifice hole size, n = 3)

It was observed that the rate of decolouration increased with the increase in the inlet pressure until the optimum pressure at 400 kPa. A further increase in the inlet pressure up till 500 kPa caused drastic reduction in decolouration rate. The varied rate of OR2 decolouration in the jet loop hydrodynamic cavitation system has significant effect on its treatment time. The estimation of treatment time can be presented based on the decolouration half-life, assuming the first order kinetic was obeyed. The decolouration half-life is the time taken for 50% of the applied OR2 (10 mg/ L) to be decoloured in the jet loop hydrodynamic cavitation system (Table 5.3).

Table 5.3: The effect of inlet pressure [200 (IP2), 300 (IP3), 400 (IP4) or 500 kPa (IP5)] on the decolouration kinetic of OR2 (10 mg/ L) in the jet loop hydrodynamic cavitation system (10 mg/ L OR2, 10 L OR2, pH 2, 4 mm orifice hole size, n = 3)

Code	Inlet pressure (kPa)	k ($minutes^{-1}$)	Decolouration half-life $t_{1/2}$, (0.693/ k) in minutes	% decolouration per hour $[1-(C_t/ C_0)]*100$	R^2
IP2	200	0.0022	315	12.8 ± 0.4	0.9644
IP3	300	0.0186	37.26	64.01 ± 0.7	0.9968
IP4	400	0.0197	35.18	69.37 ± 0.6	0.9955
IP5	500	0.0012	577.50	9.3 ± 0.5	0.9975

The decolouration half-life for IP2, IP3, IP4 and IP5 are 315, 37.26, 35.18 and 577.50 minutes respectively. The decolouration half-life of OR2 in the jet loop hydrodynamic cavitation was 315 minutes because a small quantity of micro bubbles was generated per minute when the inlet pressure was 200 kPa. As a result of this, minimal collision of bubbles generated only a small quantity of OH radicals. Besides, it was noticed that the coefficient of determination in IP2 is (0.9644) very much less than 1. This anomaly may be caused by error in the determination or the influence of increased temperature during the treatment. When the inlet pressure was 300 kPa, there was the formation of a substantial number of bubbles which went through successful collision to produce a corresponding high quantity of OH radical and consequently a shorter decolouration half-life. The optimum OR2 decolouration half-life was reached when the inlet pressure was 400 kPa. At a further increase in the inlet pressure (up to 500 kPa), the formed cavities started coalescing with each other and the decolouration half-life was increased to 557.5 minutes. The coalescing is caused by the large number and volumetric concentration of cavities from a vaporous cloud, which is termed choked cavitation. At this point, the OH radical come together to form hydrogen peroxide (5.i) and the hydrogen peroxide on the other hand acted as OH radical scavenger by reacting with it to form a less reactive hydroperoxyl radical (5.ii).

$$HO^{\bullet} + HO^{\bullet} \rightarrow H_2O_2 \quad \text{……} \quad \textbf{(5.i)}$$

$$HO^{\bullet} + H_2O_2 \rightarrow H_2O + HOO \quad \text{……} \quad \textbf{(5.ii)}$$

Prevention of coalescing of OH radical in jet loop hydrodynamic cavitation system can be achieved at a certain optimum pH of the solution (Kapalka, 2008). It is therefore important to determine the specific pH at which the OR2 would undergo maximum percentage degradation in the jet loop hydrodynamic cavitation system.

5.5.5 Effect of solution pH on the decolouration of OR2 in the jet loop hydrodynamic cavitation system

The effect of pH on the decolouration of OR2 solution in the jet-loop hydrodynamic cavitation system was investigated by using (1 M) sodium hydroxide or (1 M) sulfuric acid to adjust the pH between 2 and 10 as described in Section 3.4.1. The OR2 solution pH was varied between 2, 4, 6, 8 or 10 for Ph2, Ph4, Ph6, Ph8 or Ph10 respectively (Table 5.1). The inlet pressure and initial concentration of OR2 were maintained at 400 kPa and 10 mg/ L respectively. The absorbance and the concentration of OR2 across varied pH were determined using the UV spectrophotometer as described in Section 3.7.5. The percentage decolouration in an hour treatment of OR2 solution in a jet loop hydrodynamic cavitation system across the different pH is presented in Figure 5.7.

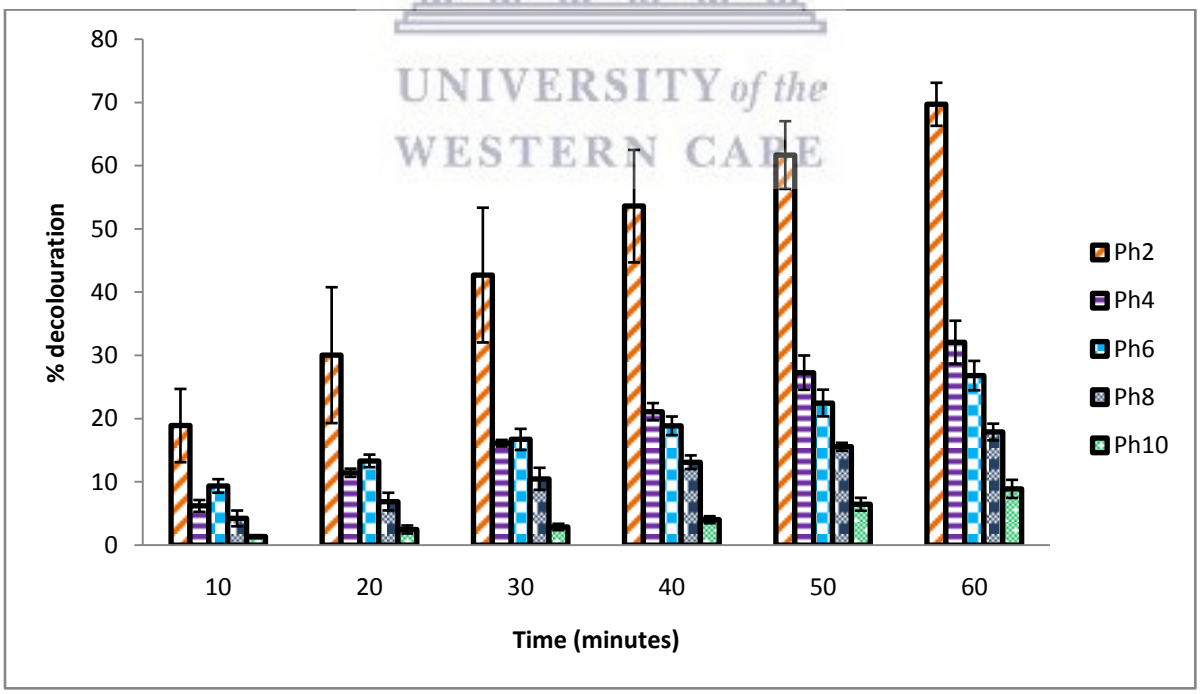

Figure 5.7: The effect of pH on the % decolouration of OR2 in a jet-loop hydrodynamic cavitation system (10 mg/ L of 10 L OR2, 4 mm orifice hole size, n = 3)

The % decolouration of OR2 solution decreased in the jet loop hydrodynamic cavitation as the pH of OR2 solution increased. The highest % decolouration of OR2 solution was achieved in the jet loop hydrodynamic cavitation system at pH 2. Furthermore, the first order kinetic which was adopted in Section 5.2.2 was applied to monitor the decolouration rate of OR2 in the jet loop hydrodynamic cavitation system. This resulted in the straight line graph for the pseudo first order decolouration kinetics as presented in Figure 5.8.

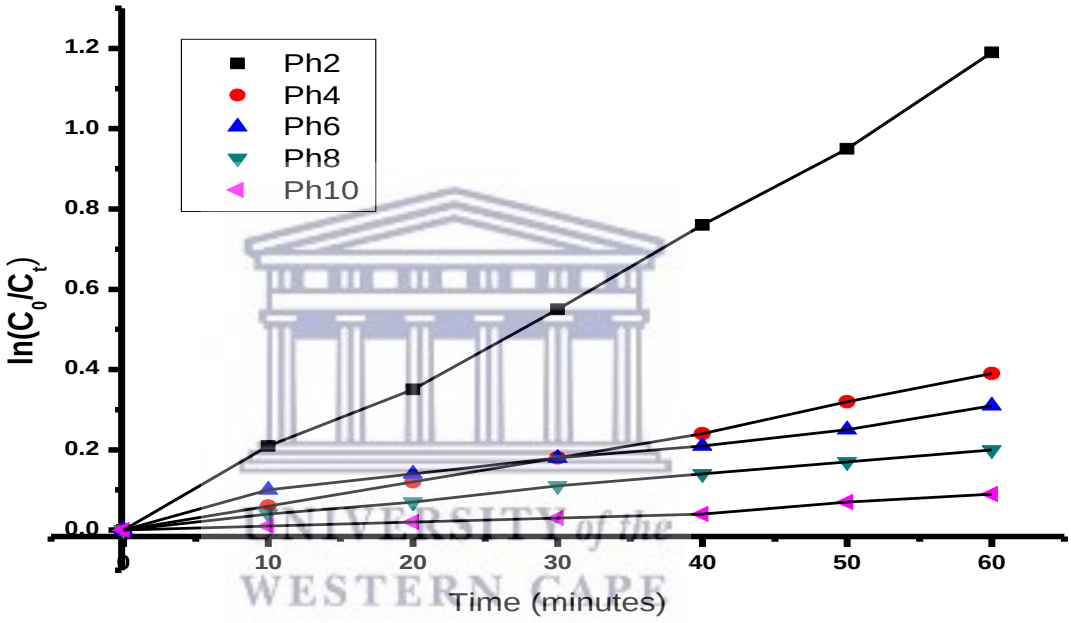

Figure 5.8: The effect of pH (2-10) on the decolouration of OR2 (10 mg/ L) in a jet-loop hydrodynamic cavitation system (10 mg/ L OR2, 10 L OR2, 4 mm orifice hole size, n = 3)

There is uniform and rapid decolouration of OR2 solution as the acidity increases in the jet loop hydrodynamic cavitation system. The percentage decolouration over an hour treatment time of the OR2 solution across the varied pH as well as the decolouration half-life assuming the first order kinetic was obeyed is presented in Table 5.4.

Table 5.4: Decolouration kinetic of OR2 solution in jet loop hydrodynamic cavitation system at the varied pH (10 mg/ L OR2, 10 L OR2, 4 mm orifice hole size, n = 3)

Code	pH	k (minutes^{-1})	Decolouration half-life $t_{1/2}$, (0.693/ k) in minutes	% decolouration per hour [1-(C_t/ C_0)]*100	R^2
Ph2	2	0.0195	35.54	69.70	0.9968
Ph4	4	0.0064	108.28	32.06	0.9962
Ph6	6	0.0047	147.45	26.81	0.968
Ph8	8	0.0033	210.00	17.89	0.995
Ph10	10	0.0014	495.00	8.90	0.9349

In the current study, the decolouration of OR2 in the jet loop hydrodynamic cavitation system was pH sensitive. The pH 2 gave maximum OR2 decolouration of 69.7% per hour at a half-life ($t_{1/2}$) of approximately 35.54 minutes while pH 10 gave the minimum decolouration of at 8.87% per hour at decolouration half-time ($t_{1/2}$) of 495 minutes. The production of OH radicals in the jet loop hydrodynamic cavitation system increased as the solution acidity increased. The increased production of OH radicals in a cavitation system as the solution become more acidic was previously documented (Badmus et al., 2016). Furthermore, the low tendency for the recombination of OH radicals generated in an acidic medium and their subsequent attack on the electron rich centres (azo linkage) of OR2 in the jet loop hydrodynamic cavitation have been noted to cause the enhanced degradation of the OR2 in an acidic initial pH (Goel et al. 2004). Similarly, Gore et al. (2014) reported that pH 2 was the optimum for the decolouration of OR2 solution using a circular venturi hydrodynamic cavitation system at higher concentration and pressure of 20 mg/L and 500 KPa respectively. However, an optimum pH of 3 was also reported by Li et al. (2015) using an adjustable orifice valve hydrodynamic cavitation system in combination with Cu nano particles as catalyst for the decolouration of 40 ppm methyl orange azo dye. Invariably, the optimum pH for the degradation of an azo dye is reported to be between 2 and 3. The current report is a confirmation of the pH sensitivity of the decolouration of POPs in the jet loop hydrodynamic cavitation system. The disparity in the reports may be due to the variations in some conditions such as the concentration and the type of applied catalyst among other factors.

5.5.6 *Effect of the concentration of OR2 on its decolouration in the Jet-loop Hydrodynamic cavitation*

Generally, the rate and extent of treatment of POPs in wastewater is expected to be higher when it is diluted than at a higher concentration. The decolouration of a 10 L quantity of OR2 was carried out at varied concentration of 5 mg/ L (OR5), 10 mg/ L (OR10) or 20 mg/ L (OR20) (Table 5.1) in the jet loop hydrodynamic cavitation system (pH 2, 400 kPa, 4 mm orifice hole size, 1 hour, n = 3) to establish how the dilution of a contaminated wastewater effluent affects its extent of treatment in the jet loop hydrodynamic cavitation system. The percentage decolouration of OR2 during an hour treatment in the jet loop hydrodynamic cavitation system at varied concentration is presented in Figure 5.9.

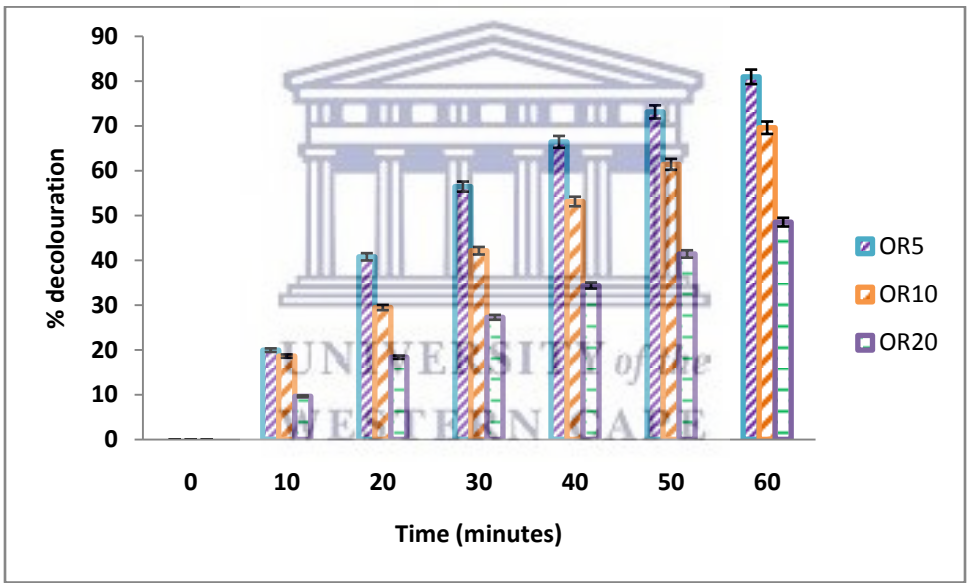

5.9: Percentage decolouration of different concentrations of OR2 in the jet loop hydrodynamics cavitation system at varied concentration (pH 2, 10 L OR2, 4 mm orifice hole size, 400 kPa, n = 3)

The extent of decolouration of OR2 in one hour treatment time was 80.92%, 69.56% and 48.50% for OR5 (5 mg/ L), OR10 (10 mg/ L) and OR20 (20 mg/ L) respectively. It was observed that the extent of decolouration of OR2 decreased as the initial OR2 concentration increased. Further investigation was done by using the first order kinetic to predict the rate of decolouration of OR2 as reported in Section 5.5.2. The pseudo first order kinetic linear graph for triplicate

measurement (n = 3) of the decolouration of OR2 solution (10 L) at varied concentration in the jet loop hydrodynamic system is presented in Figure 5.10.

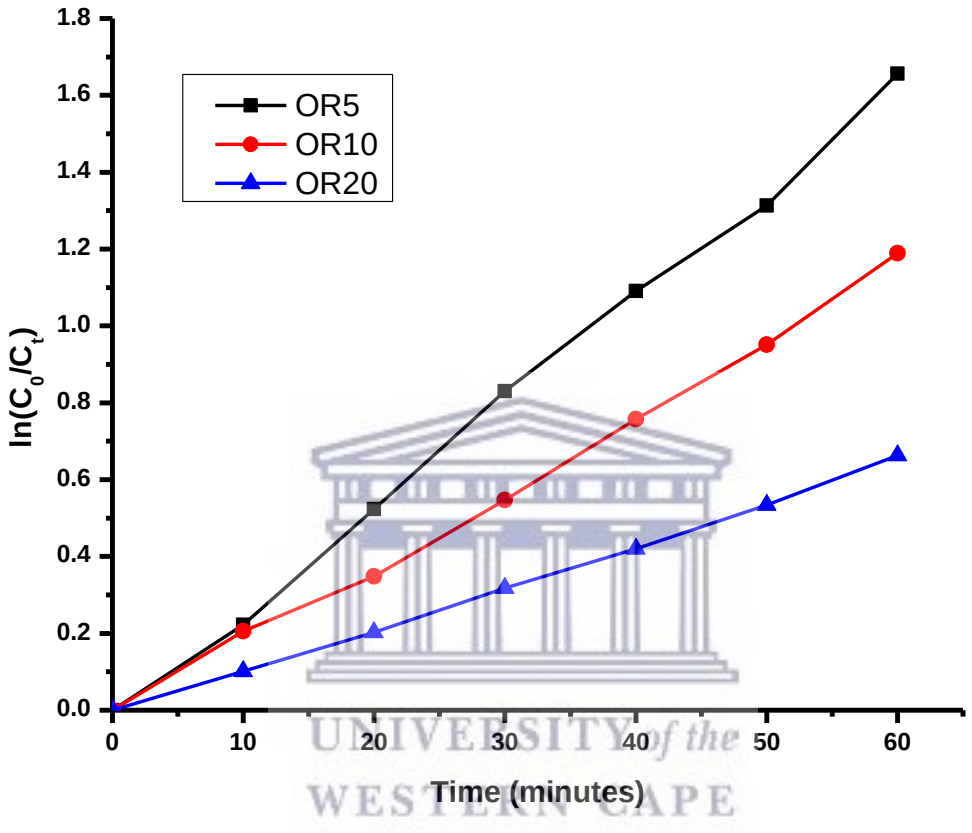

Figure 5.10: Pseudo-first order kinetic of decolouration of OR2 in the jet loop hydrodynamics cavitation system at varied OR2 concentration (pH 2, 10 L OR2, 4 mm orifice hole size, 400 kPa, n = 3)

According to the Figure 5.10, pseudo first order kinetic is applicable to the decolouration of varied concentration of OR2 solution in the jet loop hydrodynamic cavitation system (pH 2, orifice plate hole = 4 mm and inlet pressure = 400 kPa). The highest rate of decolouration was achieved when concentration of OR2 equal to 5 mg/ L (OR5) was treated, followed by the concentration of OR2 equal to 10 mg/ L (OR10) and the least decolouration rate was achieved when a concentration equal to 20 mg/L (OR20) was treated. The establishment of a pseudo first

other can be used to generate the decolouration time of OR2 in the jet loop hydrodynamic cavitation system as presented in Section 5.5.2. The kinetic information during the treatment of OR2 in the jet loop hydrodynamic cavitation at varied concentration is presented in Table 5.5.

Table 5.5: Decolouration kinetic of OR2 in the jet loop hydrodynamics cavitation system at varied concentration of OR2 (pH 2, orifice plate hole = 4 mm and in let pressure = 400 kPa, n = 3)

Code	Concentration (mg/ L)	k (minutes^{-1})	Decolouration half-life $t_{1/2}$, (0.693/ k) in minutes	% decolouration per hour $[1-(C_t/ C_0)]*100$	R^2
OR5	5	0.0276	25.11	80.92	0.9978
OR10	10	0.0195	35.54	69.56	0.9968
OR20	20	0.011	63.00	48.50	0.9986

Apparently, the more diluted the concentration of OR2 the shorter the treatment time in the jet loop hydrodynamic cavitation system. Therefore, the dilution of wastewater before treatment would thus ensure a higher rate and extent of treatment per unit time. However, the high energy cost of diluting concentrated wastewater effluent would make the process ineffective for large scale treatment (Gore & Chavan, 2013). Conversely, a suitable reagent (oxidant or catalyst) can be applied to increase the rate of degradation of OR2 without significant additional treatment cost.

5.5.7 The effect of hydrogen peroxide upon the degradation of OR2 in the jet loop hydrodynamic cavitation system

The introduction of a small quantity of hydrogen peroxide into the jet loop hydrodynamic cavitation system could have a positive effect on the OR2 decolouration rate. The hydrogen peroxide on its own has the capability of causing the oxidation of OR2 with a resultant decolouration effect. In the current study, the enhancing activity of hydrogen peroxide during the decolouration of OR2 in the jet loop hydrodynamic cavitation was investigated. Firstly, a control experiment (HPS) was set up by treating OR2 solution (10 mg/ L) in the jet loop hydrodynamic cavitation system without the addition of either hydrogen peroxide or iron sulfate (pH 2, 400 kPa, 10 L OR2, 4 mm orifice plate hole size). Subsequent experiments were performed by applying various quantities of hydrogen peroxide (30%) equal to 0.5 mg/ L, 1 mg/ L, 2 mg/ L, 5

mg/L or 10 mg/ L (and labeled P5HR, HR1, HR2, HR5 or HR10 respectively) while other parameters remained constant as presented in Table 5.1. The extent of OR2 decolouration was monitored by using the UV absorption spectrophotometer as described in Section 3.7.5, followed by the calculation of the percentage decolouration as described in Section 3.8.3. An increase in the % decolouration of OR2 solution (per hour) in the jet loop hydrodynamic cavitation system was noticed as the quantity of the hydrogen peroxide equal to 0.5 mg/ L was applied (Figure 5.11).

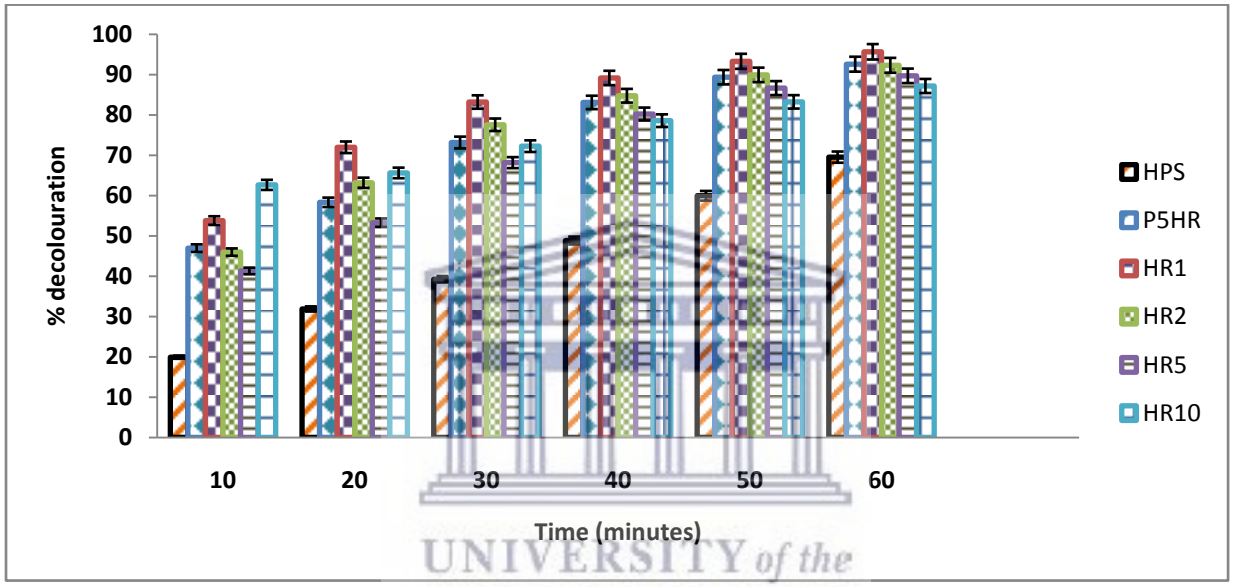

Figure 5.11: Effect of hydrogen peroxide (0.5 mg/ L [P5HR], 1 mg/ L [HR1], 2 mg/L [HR2], 5 mg/ L [HR5] and 10 mg/ L [HR10]) on the % decolouration of OR2 in the jet loop hydrodynamic cavitation system (pH 2, 10 mg/ L OR2, 400 kPa, 1 hour, 10 L OR2, 4 mm orifice plate hole size, n = 3)

The extent of decolouration of OR2 in the jet loop hydrodynamic cavitation system (pH 2, 400 kPa, volume of OR2 = 10 L, orifice plate hole = 4 mm) were 69.5%, 92.55%, 95.63%, 92.27%, 89.67% or 87.15% for HPS, P5HR, HR1, HR2, HR5 or HR10 respectively after an hour. It can be observed that an increase in the amount hydrogen peroxide (from 0.5 mg/ L to 10 mg/ L) resulted in a corresponding increase in the extent of decolouration of OR2 solution in the jet loop hydrodynamic cavitation system. It was noticed that the concentration of hydrogen peroxide

equal to 1 mg/ L gave the highest % decolouration (92.92%) of OR2 over an hour treatment time. Therefore, the optimum concentration of hydrogen peroxide found in this study was 1 mg/ L under the applied conditions (pH 2, 400 kPa, 10 mg/ L OR2, 10 L OR, orifice plate hole = 4 mm). Consequently, an increase in the concentration of hydrogen peroxide beyond 1 mg/ L (2 mg/ L, 5 mg/ L and 10 mg/ L) caused a reduction in the extent of decolouration of OR2 in an hour during its treatment in the jet loop hydrodynamic cavitation system. According to this data, hydrogen peroxide has the capability to enhance the degradation of OR2 solution in the jet loop hydrodynamic cavitation system up to its optimum concentration. This result is in agreement with the report of Zupanc et al (2013) where the authors demonstrated that cavitation time, initial pressure and the addition of H_2O_2 play important roles in the removal of pharmaceuticals in wastewater. Further addition of peroxide (beyond the optimum value) is detrimental to the treatment output in the jet loop hydrodynamic cavitation system as the hydrogen peroxide acted as hydroxyl radical scavenger and caused the reduction in the decolouration rate of OR2 solution. The first order kinetic was applied as described in Section 5.5.2, to investigate the relationship between the applied hydrogen peroxide and rate of decolouration of OR2 in the jet loop hydrodynamic cavitation (Figure 5.12).

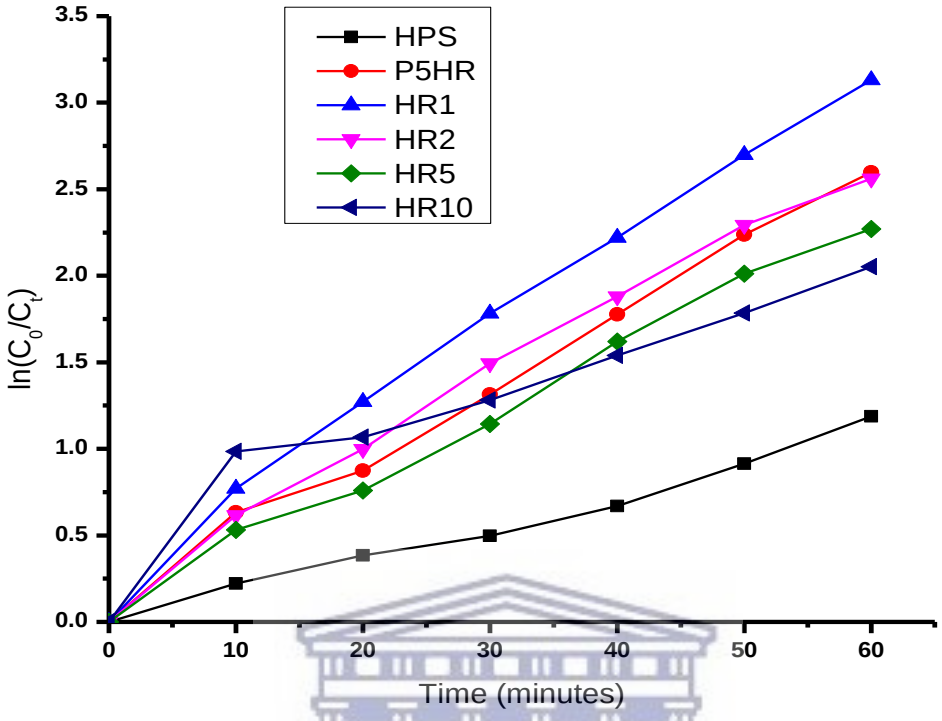

Figure 5.12: Pseudo first order decolouration kinetic of OR2 in the hydrogen peroxide aided (HPS= 0 mg/ L, P5HR= 0.5 mg/ L, HR1= 1 ,g/ L, HR2= 2mg/ L, HR5= 5 mg/ L, HR10= 10 mg/ L) jet loop hydrodynamic cavitation system (pH 2, 10 mg/ L, 400 kPa, 1 hour, volume of OR2 = 10 L, orifice plate hole = 4 mm)

The application of hydrogen peroxide led to an increased rate of decolouration of OR2 in the jet loop hydrodynamic cavitation system. However, reduction in the rate of decolouration of OR2 was noticed beyond the optimum dosage of hydrogen peroxide (1 mg/ L). The increased amount of hydrogen peroxide beyond the optimum led to its scavenging of the produced hydroxyl radical and subsequent reduction in the rate of decolouration. The rate of decolouration followed a pseudo first order decolouration kinetic in all cases except when 10 mg/ L (HR10) hydrogen peroxide was applied. The decolouration kinetic of OR2 in the hydrogen peroxide aided jet loop hydrodynamic cavitation system is presented in Table 5.6.

Table 5.6: Decolouration kinetic of OR2 in the jet loop hydrodynamics cavitation system at varied concentration (10 mg/ L OR2, 10 L OR2, pH 2, orifice plate hole = 4 mm and in let pressure = 400 kPa, n = 3)

Code	Concentration of H_2O_2 (mg/ L)	K	Decolouration half-life $t_{1/2}$, (0.693/ K) in minutes	% decolouration per hour $[1-(C_t/ C_0)]*100$	R^2
HPS	0	0.0180	38.50	69.50	0.9984
P5HR	0.5	0.0425	16.31	92.55	0.9942
HR	1	0.0507	13.67	95.63	0.9916
2HR	2	0.0426	16.27	92.27	0.9909
5HR	5	0.0380	18.24	89.67	0.9932
10HR	10	0.0294	23.57	87.15	0.9024

The reduced coefficient of determination (R^2 = 0.9024) was caused by the excessive scavenging when 10 mg/ L hydrogen peroxide was applied during the treatment of OR2 in the jet loop hydrodynamic cavitation. It was also observed that there is more than 100% reduction in the treatment time when a small dose of hydrogen peroxide (0.5 mg/ L) was applied ($t_{1/2}$ = 16.31 minutes) compared to when the OR2 was treated in the jet loop hydrodynamic cavitation system without the application of hydrogen peroxide ($t_{1/2}$ = 38.5 minutes). At the optimum application of hydrogen peroxide (1 mg/ L), the decolouration half-life was further reduced to 13.67 minutes. Application hydrogen peroxide (at its optimum) has been demonstrated for positive impact on the rate and extent of decolouration of OR2 in the jet loop hydrodynamic cavitation system. However, effort must be taking to prevent the excessive use of hydrogen peroxide during the wastewater treatment in the jet loop hydrodynamic cavitation system in order to prevent its scavenging effect. The alternative method of increasing the rate and extent of OR2 degradation in the jet loop hydrodynamic cavitation system is to apply a suitable catalyst. A typical catalyst used in the advanced oxidation process is the Fenton reagent (Babuponnusami and Muthukumar, 2014). Therefore, it is important to investigate the enhancing effect of the application of Fenton catalyst during the decolouration of OR2 in the jet loop hydrodynamic cavitation system.

5.5.8 *The effect of iron (11) sulfate as catalyst in the jet loop hydrodynamic dynamic cavitation system*

Catalytic technologies have gained increased attention in the treatment of POPs in wastewater due to their great potential in water purification. Catalysis is an efficient option for low energy treatment of contaminated water. Iron sulfate has been widely investigated as a source of homogeneous Fenton catalyst (Bahmani et al., 2013). In the current study, an OR2 solution was first treated by running it (OR2) through the jet loop hydrodynamic cavitation at the optimised conditions (pH 2, 400 kPa, 10 L OR2, 10 mg/ L OR2, orifice plate hole = 4 mm) without adding hydrogen peroxide or iron II sulfate (as presented in Table 5.1). Further treatments were done by applying a quantity of iron sulfate equal to 0.5 mg/ L, 1 mg/ L or 2 mg / L while the experiments were labeled FE5, FE10 or FE20 respectively (Table 5.1). The percentage decolouration which was calculated through UV absorbance in the triplicate experiment is presented in Figure 5.13.

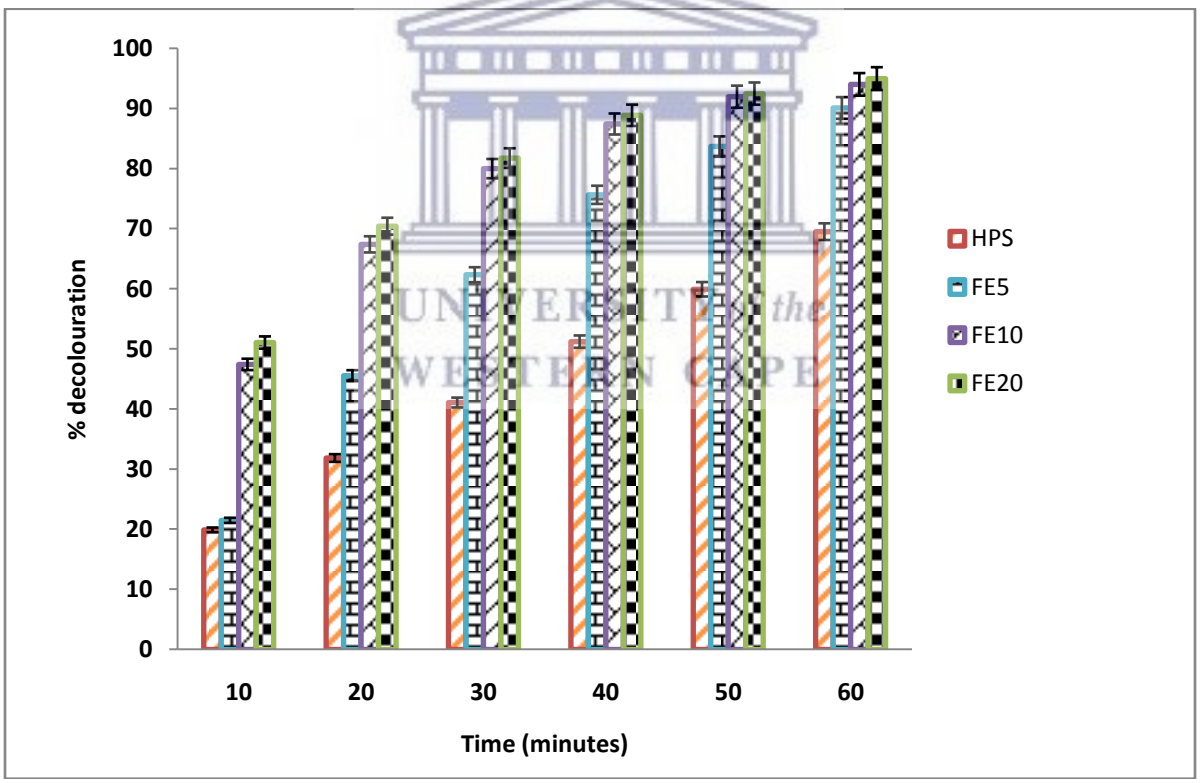

Figure 5.13: The effect of iron sulfate addition (HPS = 0 mg/ L; FE5 = 0.5 mg/ L; FE10 = 1 mg/ L; FE20 = 2 mg/ L) upon the degradation of OR2 in the jet loop hydrodynamic cavitation system (pH 2, 10 mg/ L OR2, 400 kPa, 10 L OR2, 4 mm orifice plate hole size, n = 3)

The extent of decolouration of OR2 in the jet loop hydrodynamic cavitation were 69.5%, 90.08%, 94.00% and 94.96% for HPS, FE5, FE10, FE20 respectively. It was observed that at the optimum condition (pH 2, 400 kPa, 10 mg/ L OR2, 10 L OR2, 4 mm orifice plate hole size), the jet loop hydrodynamic cavitation system on its own achieved 69.5% decolouration of OR2 solution. However, the addition of 0.5 mg/ L iron sulfate to the OR2 in the jet loop hydrodynamic cavitation under the applied conditions resulted in 90.08% decolouration. Meanwhile, increases in the amount of amount of Fe^{2+} by addition of 1 mg/ L or 2 mg/ L iron sulfate gave 94.00% and 94.96% OR2 decolouration respectively. Doubling the amount of iron sulfate from 0.5 mg/L to 1 mg/ L led to a significantly higher decolouration while further increases in the iron sulfate concentration from 1 mg/ L to 2 mg/ L did not have a significant impact upon the extent of decolouration. The results showed that it was necessary to limit the amount of the applied iron (II) sulfate to 1 mg/ L under the applied conditions in order prevent the application of an excessive amount of iron (II) sulfate with consequential OH radical scavenging (Babuponnusami and Muthukumar, 2014). Furthermore, first order kinetics were applied as described in Section 5.5.2, to investigate the catalytic effect of the applied iron sulfate on the rate of decolouration of OR2 in the jet loop hydrodynamic cavitation (Figure 5.14).

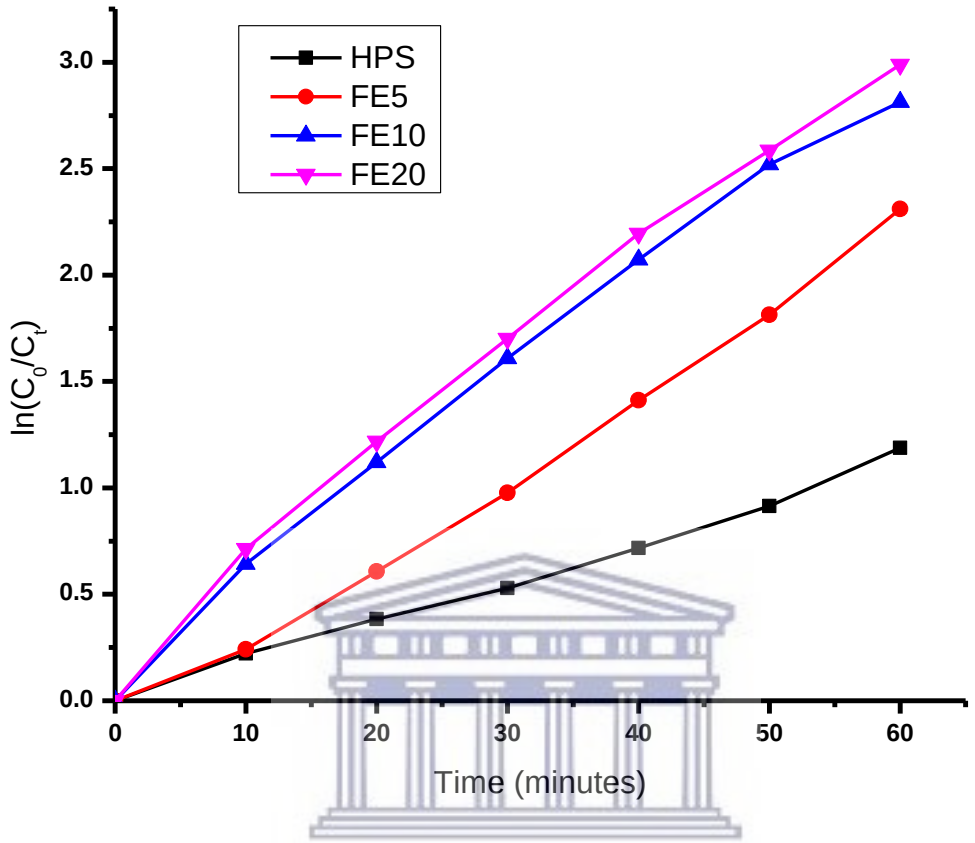

5.14: Pseudo first order decolouration kinetic of OR2 catalysed by iron sulfate (HPS= 0 mg/ L, FE5= 5 mg/ L, FE10 = 10 mg/ L, FE20= 20 mg/ L) in the jet loop hydrodynamic cavitation system (pH 2, 10 mg/ L OR2, 10 L OR2, 400 kPa, n = 3)

It can be observed that the first order kinetic can be used for monitoring the influence of iron sulfate (catalyst) decolouration rate of OR2 in the jet loop hydrodynamic cavitation system. The application of a 5 mg/ L iron sulfate during the decolouration of OR2 in the jet loop hydrodynamic cavitation system, resulted in an increased decolouration rate. A further increase in the concentration of iron sulfate to 10 mg/ L resulted in an increased decolouration rate. However, there is not much increase in the decolouration rate when a 20 mg/ L of iron sulfate was applied. These findings can be used to derive the treatment half-life as described in Section 3.8.3. The kinetic information for the iron sulfate catalysed decolouration of OR2 in the jet loop hydrodynamic cavitation is presented in Table 5.7.

Table 5.7: Kinetic information for the decolouration of OR2 catalyzed by iron sulfate (HPS= 0 mg/ L, FE5= 5 mg/ L, FE10 = 10 mg/ L, FE20= 20 mg/ L) in the jet loop hydrodynamic cavitation system (pH 2, 10 mg/ L OR2, 10 L OR2, 400 kPa, 1 hour, n = 3)

Code	Concentration of Iron sulfate (mg/ L)	K	Decolouration half-life $t_{1/2}$, (0.693/ K) in minutes	% decolouration per hour $[1-(C_t/ C_0)]*100$	R^2
HPS	0	0.0189	36.67	69.50	0.9922
FE5	0.5	0.0388	17.86	90.08	0.9924
FE10	1	0.0470	14.74	94.00	0.9919
FE20	2	0.0489	14.17	94.96	0.9912

The decolouration half-life for HPS, FE5, FE10 and FE20 are 36.67, 17.86, 14.74 and 14.17 minutes respectively. The application of iron sulfate can cause a substantial reduction in the treatment time during the decolouration of OR2 in the jet loop hydrodynamic cavitation system. Either hydrogen peroxide or iron sulfate thus demonstrated the capability to increase the rate and the extent of decolouration of OR2 in the jet loop hydrodynamic cavitation system. Addition of hydrogen peroxide has only a slight environmental implication and can be applied optimally without concern for its toxicity. However, the drawbacks of iron II sulfate application include generation of an excessive quantity of iron sludge as well as retained elemental iron in the treated effluent (Cai et al., 2015). formation of unquantifiable secondary complexes and ineffectiveness in mineralisation of POPs (Gadipelly et al., 2014). In view of this, the synthesised green nano zero valent iron (gnZVI) was evaluated for the improvement in efficiency of the system as recently reported by Badmus et al., (2018). Therefore, it is very important to investigate the decolouration of OR2 in the jet loop hydrodynamic cavitation in the presence of combined hydrogen peroxide and iron sulfate (H_2O_2/ Fe^{2}+) as well as combined hydrogen peroxide and gnZVI (H_2O_2/ nFe^0).

5.5.9 Influence of combined hydrogen peroxide-iron sulfate (H_2O_2/ Fe^{2}+) or combined hydrogen peroxide-green nano zero valent iron (H_2O_2/ nFe^0) on the decolouration of OR2 in the jet loop hydrodynamic cavitation system

In this set of experiments, the decolouration of OR2 solution in the jet-loop hydrodynamic cavitation system was evaluated to determine whether its rate and extent could be enhanced by combining hydrogen peroxide with iron sulfate or replacing iron sulfate with gnZVI in order to achieve the mineralisation of OR2. The decolouration of OR2 (10 mg/ L) was carried out at the

optimum condition in the jet loop hydrodynamic cavitation (pH 2, 400 kPa, 10 mg/ L OR2, 10 L OR2, orifice plate hole size = 4 mm, H_2O_2 = 1 mg/ L). The experiment was labeled HPZ, HRZ, FH10 or GH10 when the jet loop hydrodynamic cavitation degrade OR2 by itself (HPZ), when 1 mg/ L H_2O_2 was applied (HRZ), when 1 mg/ L H_2O_2 plus 10 mg/ L iron sulfate (FH10) was applied and when 1 mg/ L H_2O_2 plus 10 mg/ L gnZVI (GH10) was applied respectively (Table 5.1.). The decolouration in an hour was monitored by using UV spectrophotometry which was described in Section 3.7.5. The extent of decolouration achieved across an hour treatment time in the jet loop hydrodynamic cavitation system is presented in Figure 5.15.

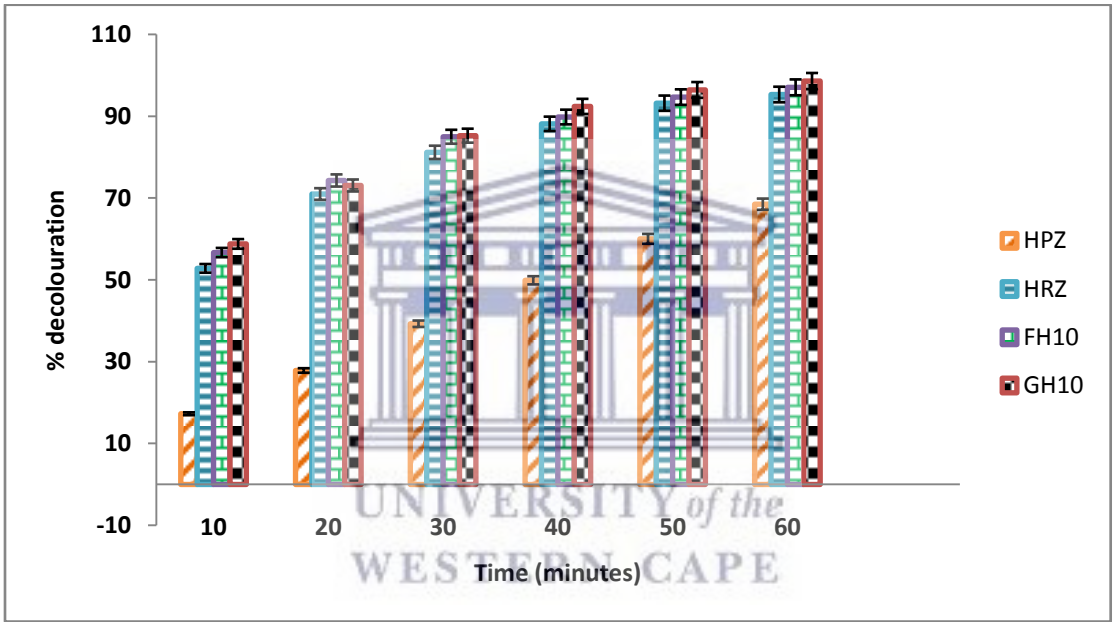

Figure 5.15: Comparison of the catalytic activity of iron sulfate + H_2O_2 (FH10) with gnZVI + H_2O_2 (GH10) in decolouration of OR2 in the jet-loop hydrodynamic cavitation system (400 kPa, pH 2, 4 mm orifice hole size)

The percentage decolouration of OR after an hour treatment in the jet loop hydrodynamic cavitation were 68.50%, 95.30%, 97.05% or 98.59% for HPZ, HRZ, FH10 or GH10 respectively. HPZ was the baseline for the decolouration of OR2 in the jet loop hydrodynamic system only (pH 2, 400 kPa, 10 mg/ L OR2, 10 L OR2, orifice plate hole size = 4 mm, H_2O_2 = 1 mg/ L). The addition of an optimum concentration of hydrogen peroxide (1 mg/ L, HRZ) gave 95.30%

decolouration during the one hour treatment of OR2 in the jet loop hydrodynamic cavitation system. Meanwhile, the combination of hydrogen peroxide and iron II sulfate (FH10) in the jet loop hydrodynamic cavitation system gave 97.05% decolouration after an hour treatment. Replacement of 10 mg/ L iron sulfate with 10 mg/ L gnZVI (GH10) in the combined hydrogen peroxide-jet loop hydrodynamic cavitation system gave 98.59% decolouration during the treatment of OR2 in the jet loop hydrodynamic cavitation system. The pseudo first order kinetic of decolouration of OR2 in the jet loop hydrodynamic cavitation in presence of combined hydrogen peroxide/ iron sulfate or hydrogen peroxide/ gnZVI.

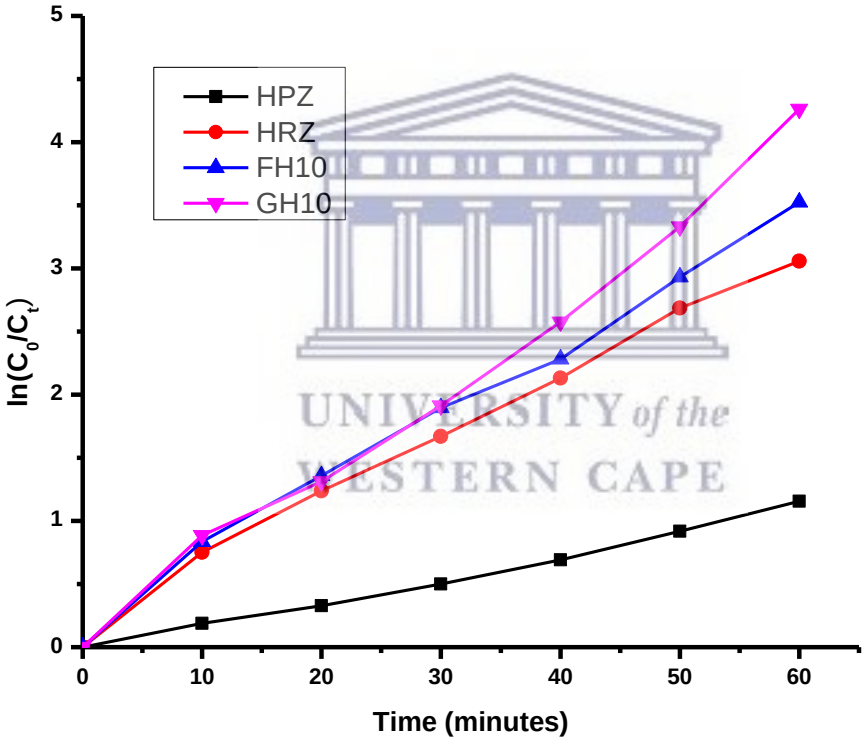

5.16: Pseudo first order rate for catalytic activity of iron sulfate and gnZVI duing the decolouration of OR2 in the jet-loop hydrodynamic cavitation system (400 kPa, pH 2, 4 mm orifice hole size)

The decolouration of OR2 in the jet loop hydrodynamic cavitation system consistently followed first order kinetic, either in the jet loop hydrodynamic cavitation system alone (HPZ), or when an optimum concentration of hydrogen peroxide was applied to the jet loop hydrodynamic

cavitation system (HRZ), or when the combination of optimum amount of hydrogen peroxide and iron (II) sulfate was applied to the jet loop hydrodynamic cavitation system (FH10), and when the combination of optimum amount of hydrogen peroxide and gnZVI was applied (GH10). The combined system has demonstrated the capacity for enhanced decolouration. The rate of decolouration was higher when the combination of hydrogen per oxide and iron (II) sulfate were applied to OR2 solution in the jet loop hydrodynamic cavitation system compared to when only (optimum) hydrogen peroxide was used. Likewise, subsequent replacement of iron (II) sulfate with gnZVI in the jet loop hydrodynamic cavitation system lead to improved decolouration of OR2. The application of a combination of optimum amount of hydrogen peroxide and gnZVI in the jet loop hydrodynamic cavitation system (GH10) gave the highest decolouration rate. The better catalytic effect offered of gnZVI compared to iron (II) sulfate can be explained through the understanding of the electron exchange in Fenton catalyst as presented in equation **(2.iv) to (2.ix)**. The iron at a zero oxidation state (gnZVI) has capacity to accommodate three units of electrons compare to the same amount of iron at an oxidation state of 2+ as in iton (II) sulfate which has the capacity to accommodate only a unity of an electron. Therefore, it is very important to further investigate the mineralisation potential of gnZVI as a catalyst during the treatment of OR2 solution in the jet loop hydrodynamic cavitation system.

5.5.10 Mineralisation of OR2 in the combined jet loop hydrodynamic cavitation system

The analysis of the decolouration of OR2 in the jet loop hydrodynamic cavitation which was determined with the UV spectrophotometer must be supported by the measurement of its Total Organic Carbon (TOC) as described in Section 3.7.8, in order to have a better understanding of the impact of combined hydrogen peroxide and gnZVI on the mineralisation of OR2 in the jet loop hydrodynamic cavitation system. Information on the extent of decolouration and mineralisation is presented in Table 5.8

Table 5.8: Comparison of decolouration and mineralisation of OR2 solution in jet loop hydrodynamic cavitation system (400 kPa, 20 mg/ L OR2, pH 2, 10 L OR2, 4 mm orifice hole size, n = 3)

Parameter	HPZ	HRZ	FH10	GH10
Decolouration rate constant (k) (minutes^{-1})	0.0189	0.0498	0.056	0.0676
Decolouration half-life ($t_{1/2}$) (minutes)	36.67	13.92	12.38	10.25
% decolouration	68.50	95.30	97.05	98.59
% mineralisation	40.60	67.50	65.70	74.30
R^2	0.9921	0.9927	0.9929	0.9908

The decolouration in an hour treatment of OR2 in the jet loop hydrodynamic cavitation system was 68.5 (HPZ), 95.3 (HRZ), 97.05 (FH10) or 98.59 (GH10) while the % mineralisation was 40.6 (HPZ), 67.50 (HRZ), 65.70 (FH10) or 74.30 (GH10). The extent of OR2 decolouration in the jet loop hydrodynamic cavitation increased when iron (II) sulfate was applied to the optimum concentration of hydrogen peroxide (FH10) and likewise when gnZVI was applied (GH10). However, the increment in decolouration of 95.30% with H_2O_2 (HPZ) to 97.05% with iron sulfate and H_2O_2 (FH10) does not lead to a corresponding increment in the mineralisation (67.5 to 65.7). The declined mineralisation in FH10 can be attributed to the scavenging of the produced hydroxyl radical through the formation of iron complex (Miller et al., 2016). The reaction between iron (Fe^{2+}) and hydrogen peroxide to form iron complex was outlined in (2.i) to (2.iii). Conversely, the extent of mineralisation was increased from 67.7% (HRZ) to 74.3% (GH10) along with the decolouration when the gnZVI was applied with hydrogen peroxide (1 mg/ L) in the jet loop hydrodynamic cavitation system (GH10). The enhanced mineralisation was due to the spontaneous exchange of electrons between the hydrogen peroxide and gnZVI, leading to the generation of hydroxyl radicals which subsequently oxidised the OR2. The current presentation of a novel mineralisation of OR2 using gnZVI aided jet loop hydrodynamic cavitation system was further supported by the analysis of anions formed during the treatment.

5.5.11 Quantification of the nitrate and sulfate produced during the mineralisation of OR2 in the jet loop hydrodynamic cavitation system

In addition to carbon (IV) oxide, the formation of inorganic salt in form of ion is an indication of mineralisation of an organic of the organic substances such as OR2. The produced inorganic anions during the mineralisation of OR2 in the jet loop hydrodynamic cavitation system can be monitored by using the ion chromatography (IC) as described in Section 3.7.10. The result of the IC analysis of treated OR2 in the jet loop hydrodynamic cavitation system (pH 2, 400 kPa, 10 mg/ L OR2, 10 L OR2, 4 mm orifice plate hole size, 10 mg/ L gnZVI, 1 mg/ L H_2O_2) is presented in Figure 5.17.

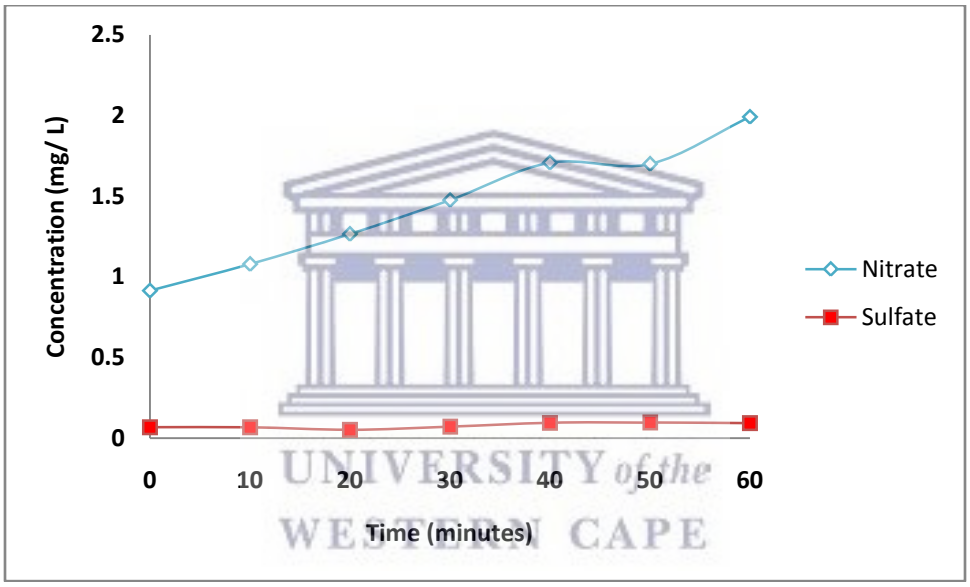

Figure 5.17: Quantification of nitrate and sulfate ions formed during mineralisation OR2 in the jet-loop hydrodynamic cavitation system (pH 2, 400 kPa, 10 mg/ L OR2, 10 L OR2, 4 mm orifice plate hole size, 10 mg/ L gnZVI, 1 mg/ L H_2O_2)

An increased concentration of the produced nitrate (1.9919 mg/ L) over time as determined by ion chromatography during the treatment of OR2 in the jet loop hydrodynamic cavitation was much higher than that of sulfate (0.0921 mg/ L). Besides, there was a slight increase in the liberation of nitrate (0.9138 mg /L to 1.9919 mg/ L) over one hour decolouration time while there was not much increase in the concentration of sulfate (0.0664 mg /L to 0.0921 mg /L). The influence of the air being mixed during the treatment under atmospheric conditions needs to be considered. Air, which is predominantly made up of N_2 gas cannot be unconnected with the

instantaneous generation of nitrate during the treatment of OR2 in the hydrodynamic cavitation as reported in the current investigation. Moreover, the inorganic nitrate produced during the mineralisation of OR2 in the jet loop hydrodynamic cavitation could be derived from the OR2 molecule. It can be confirmed from the results of the IC analysis that the likely end products of mineralised azo linkages and sulfonic acid (in Orange II sodium salt) are the nitrate and sulfate anions. Conversely, there is the possibility for the generation of a small quantity of organic compounds during the mineralisation of OR2 in the jet loop hydrodynamic cavitation system. Further analysis was done for the identification of the functional groups and the mass spectra of the generated organic compounds using the FT-IR which was described in Section 3.7.6 and the GC-MS which was described in Section 3.7.9.

5.5.12 Identification of the organic intermediate bye products generated during the mineralisation of OR2 in the jet loop hydrodynamic cavitation system

Based on the capability of the treated water samples to absorb infrared light, the FT-IR can provide information about the chemical bonds, molecular structure and functional groups present. The FT-IR was applied for the identification of the functional groups in the untreated and treated OR2 solution as described in Section 3.7.6. The FT-IR of the products formed after degradation in the jet-loop hydrodynamic cavitation system at the optimised conditions (pH 2, 400 kPa, 10 mg/ L OR2, 10 L OR2, 4 mm orifice plate hole size) using cavitation alone (HPZ), cavitation plus hydrogen peroxide plus iron sulfate (FH10) on cavitation plus hydrogen peroxide plus gnZVI (GH10) is presented in Figure 5.18.

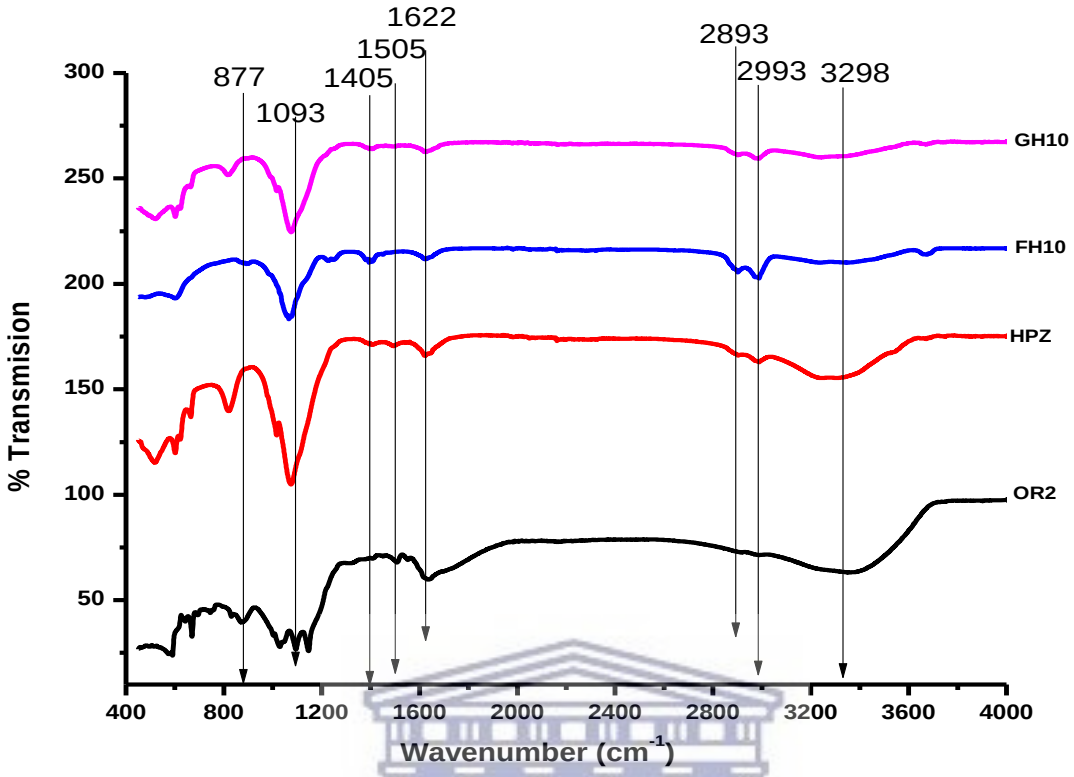

Figure 5.18: FT-IR spectrographs of OR2 before and after an hour degradation with either the addition of iron sulfate plus hydrogen peroxide (FH10) or gnZVI plus hydrogen peroxide (GH10) in the jet loop hydrodynamic cavitation system (pH 2, 400 kPa, 10 mg/ L OR2, 10 L OR2, 4 mm orifice plate hole size)

The untreated OR2 solution shows its aromatic nature through the broad OH peak around 3298 cm^{-1}, peaks at 1505 and 1622 cm^{-1} that show N=N azo linkages and aromatic C=C bonds respectively. The peak at 877 cm^{-1} is a finger print for a 1, 4-di-substituted (Para) benzene. The disappearance of some prominent peaks and appearance of new ones is evident after the OR2 was subjected to treatment in the jet loop hydrodynamic cavitation system. Specific peaks at 877 cm^{-1} for 1,4-disubstituted (Para) benzene and peaks at 1505 cm^{-1} for N=N azo linkage were no longer visible on the FT-IR spectra of OR2 solution that was subjected to treatment in the jet loop hydrodynamic cavitation system plus iron (II) sulfate catalyst (FH10) as well as on the FTIR spectra of the OR2 solution that was subjected to treatment in the jet loop hydrodynamic cavitation plus gnZVI catalyst (GH10). This is an indication of destruction of the benzene ring and the azo linkages in the OR2 solution during its treatment in the jet loop hydrodynamic

cavitation system. The appearance of the aliphatic CH peak around 2893 cm^{-1} was also noticed on the FT-IR spectra of HPZ, FH10 and GH10 while the aromatic ring at 1622 cm^{-1} was retained in all the analysed samples. Further analysis using GC-MS was thus necessary in order to identify the degradation intermediate products formed when OR2 is treated at the optimised conditions in the jet-loop hydrodynamic cavitation system.

5.5.13 The identification of intermediate products formed during the mineralisation of OR2 solution in the jet loop hydrodynamic cavitation by Liquid chromatography-Mass spectrometry

Identification of the intermediate by-products during the treatment of OR2 solution in the jet-loop hydrodynamic cavitation system (pH 2, 400 kPa, 10 mg/ L OR2, 10 L OR2, 4 mm orifice plate hole size, 10 mg/ L gnZVI, 1 mg/ L H_2O_2) was done using a hyphenated LC-MS instrument that was described in Section 3.7.9. The LC-MS spectra of the identified intermediate products during the mineralisation of OR2 solution in jet-loop hydrodynamic cavitation system are presented in Appendix 2. Based on the combination of the IC and FT-IR results as well as the mass spectrometer spectra of the pre and post degradation of OR2 in the jet loop hydrodynamic cavitation system, the proposed mechanism of the degradation is presented in Figure 5.19.

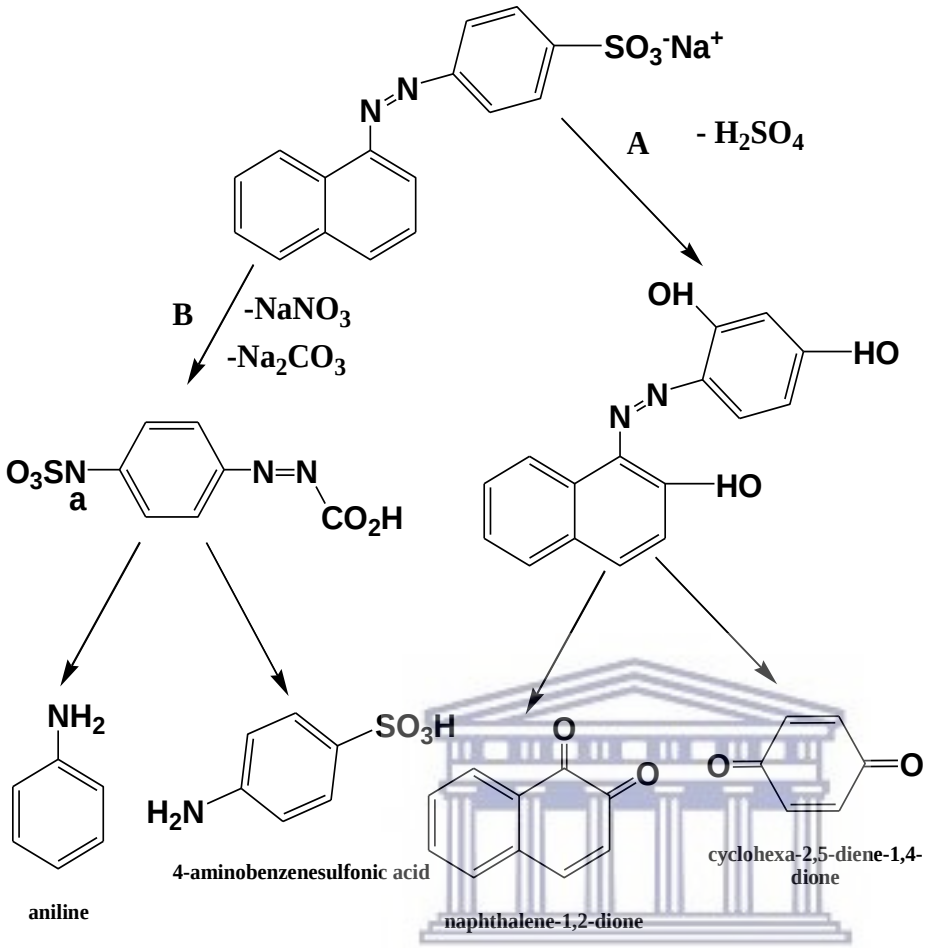

Figure 5.19: Proposed mechanism of degradation of OR2 solution (20 mg/ L) in the jet-loop hydrodynamic cavitation system (pH 2, 400 kPa, 10 mg/ L OR2, 10 L OR2, 4 mm orifice plate hole size, 10 mg/ L gnZVI, 1 mg/ L H_2O_2).

The mineralisation of OR2 solution in the jet loop hydrodynamic cavitation system at the optimised conditions (pH 2, 400 kPa, 10 mg/ L OR2, 10 L OR2, 4 mm orifice plate hole size, 10 mg/ L gnZVI, 1 mg/ L H_2O_2) led to the production of a trace amount of aniline, 4-aminobenzensulfonic acid, naphthalene-1,2-dione and cyclohexa-2,5-diene-1,4-dione, through the pathways A and B, as described in Figure 5.19. Pathway B is more favourable because nitrate ion was detected (IC analysis) in abundance during the treatment of OR2 in the jet loop hydrodynamic cavitation system as explained in Section 5.5.11. Thus, the major products of the mineralisation have been identified as the inorganic nitrates and sulfates in their ionic forms. Traces of the organic substances were identified as intermediate by-products during the FT-IR

and GC-MS analysis. None of the identified byproducts have been reported for causing toxicity in biological organisms or in the environment at low levels in the treated water.

5.6 Chapter summary

In this chapter, factors such as the initial pH of the solution, orifice hole size, inlet pressure, initial concentration of the pollutant, hydrogen peroxide, iron sulfate or gnZVI have been optimised to improve the rate of decolouration and mineralisation of OR2 in the jet loop hydrodynamic cavitation system. Out of all these factors, the orifice hole size had no significant contribution to the decolouration of OR2 in the jet loop hydrodynamic cavitation system as currently designed. The current treatment of OR2 solution in the jet loop hydrodynamic cavitation system with hydrogen peroxide and gnZVI resulted in 98% decolouration and 74% reduction in total organic carbon content and formation of mineralised end products that were predominantly inorganic nitrate anion within an hour treatment time. The achievement of a high degree of mineralisation of OR2 in the jet loop hydrodynamic cavitation by the addition of a small quantity of hydrogen peroxide with gnZVI was reported for the first time. Consequently, jet loop hydrodynamic cavitation is shown to be very suitable for the secondary or tertiary treatment of textile wastewater effluent. However, the choice of combination depends on the treatment objective and the nature of contaminants. The combination of hydrogen peroxide (1 mg/ L) and gnZVI (10 mg/ L) in a jet loop hydrodynamic cavitation system (pH 2, 400 kPa) was proved to be the best for the mineralisation of OR2 in simulated wastewater effluent. A novel mineralisation of OR2 solution was achieved through the catalytic enhancement of OR2 decolouration using gnZVI in combination with hydrogen peroxide in the jet loop hydrodynamic cavitation system. The mineralisation of persistent organic pollutants as represented by OR2, in the jet-loop hydrodynamic cavitation system thus offers a less chemical intensive form of advanced oxidation which may be used in the final stages POPs treatment in textile wastewater.

CHAPTER 6

Degradation of acetaminophen solution in jet loop hydrodynamic cavitation system with hydrogen peroxide and iron (II) sulfate or nano zero valent iron

6.1 Overview

Acetaminophen is a pharmaceutical product that is widely reported for its circumvention of advanced wastewater treatment facilities, causing environmental pollution. Recent mineralisation of acetaminophen by the application of combined advanced oxidation processes is not without side effects such as the formation of unwanted intermediate products (Torun et al., 2015), high energy consumption and high maintenance cost (Baloul et al., 2016). The treatment of acetaminophen solution (10 mg/L) in a jet loop hydrodynamic cavitation (10 L) system, aided by hydrogen peroxide and green nano zero valent (gnZVI) was investigated for the first time in this study. The effect of parameters such as reaction time, concentration of hydrogen peroxide, pH as well as iron (II) sulfate concentration or gnZVI dosage on the extent of degradation of acetaminophen was reported. This study has demonstrated the possibility for efficient degradation of acetaminophen solution (pH 2) in an advanced oxidation system using a jet loop hydrodynamic cavitation system in combination with hydrogen peroxide (5 mg/ L) and iron (II) sulfate (10 mg/ L) or gnZVI (10 mg/ L). The extent of mineralisation was 53% or 50% respectively in 60 minutes when iron (II) sulfate or gnZVI was used as catalyst during the treatment of acetaminophen solution in the jet loop hydrodynamic cavitation system. This demonstrates the suitability of the combined AOP system using hydrogen peroxide and gnZVI in the jet loop hydrodynamic cavitation system as a method for the treatment of POPs in pharmaceutical wastewater. The application of gnZVI led to 60% reduction in the applied iron and offers the possibility of removing the residual iron with a magnet at the end of the treatment.

6.2 Introduction

Pharmaceuticals are substances recognised by an official Pharmacopoeia and used in diagnosis, prevention, mitigation, cure or treatment of diseases and their symptoms. Chemical

characteristics of pharmaceuticals must be retained during passage through the body for optimum efficacy and therapeutic effectiveness. Generated metabolites and unchanged drugs must be eliminated from the body as quickly as possible to prevent toxicity and death of cells. The movement of pharmaceutical substances in and out of living cells is measured by their pharmacokinetic property. This is a very important property which is mostly dependent on the partition coefficient (Log P) and other parameters such as molecular weight, solubility and vapour pressure (Table 5.1). Log P is the ratio of compound concentration in a known volume of n-octanol compared to its concentration in a known volume of water at the n-octanol/water equilibrium. Compounds with a high partition coefficient value ($3 \leq \text{Log P} < 6$) may bio accumulate unless their molecular weight is high (Chiou et al., 1977). Essentially, pharmaceutical compounds must be lipophilic enough to be able to pass through the lipid bi-layer of the cell membrane and hydrophilic enough, to be easily eliminated from cells and by extension from the body. A very water soluble compound will most likely have a high elimination rate, short half-life ($t_{1/2}$) and difficult sorption (Kürschner et al., 1998). The pharmacokinetic study of most medicinal drugs measures how much of it is excreted via feces and urine. The possibility of finding a large number of pharmaceutical compounds and their metabolites in wastewater, groundwater or surface water is thus very high due to their pharmacokinetic properties (Andrade et al., 2011). Some bioactive and persistent pharmaceutical compounds can pass through sewage treatment plants and cause serious health impacts on non-target organisms (Ghosh et al., 2010). Besides, most of the pharmaceutical substances are non volatile, aromatic compounds with many amine functionalities or fluorine atoms, or hydroxyl side chains. Compounds with such functionalities may bio-accumulate and persist in the environment, due to their ability to remain unchanged and retain their physiological activity or through production of active, metabolites which function as the parent drug or revert to the parent drug.

6.3 Persistent pharmaceutical pollutants

The route of pharmaceutical pollutants entering the environment can be through a single identifiable point source such as a sewage treatment plant, from hospital and industrial effluent, or from a diffused source which may spread over a broad geographical area such as agricultural

runoff from animal waste (or manure), urban runoff from domestic waste, or the leakage from waste treatment plants. Pharmaceutical contaminants can originate from flushed, unused or expired medication, excreted unabsorbed medication or metabolites, used veterinary drugs, legally disposed pharmaceutical waste and improper disposal of expired drugs among others (Boxall et al., 2012). Ground water can be contaminated by infiltration of surface water containing pharmaceutical residues through leakages in landfill sites and sewer drains. Most of the pharmaceuticals are refractory in the environment because they are non biodegradable, inhibitory to activated sludge bacteria, circumvent the conventional treatment infrastructure and induce toxicity in potable water (Gome and Upadhyay, 2013; Radjenovic et al., 2007). The mobility of POPs from pharmaceutical wastewater through the various is as presented in Figure 6.1.

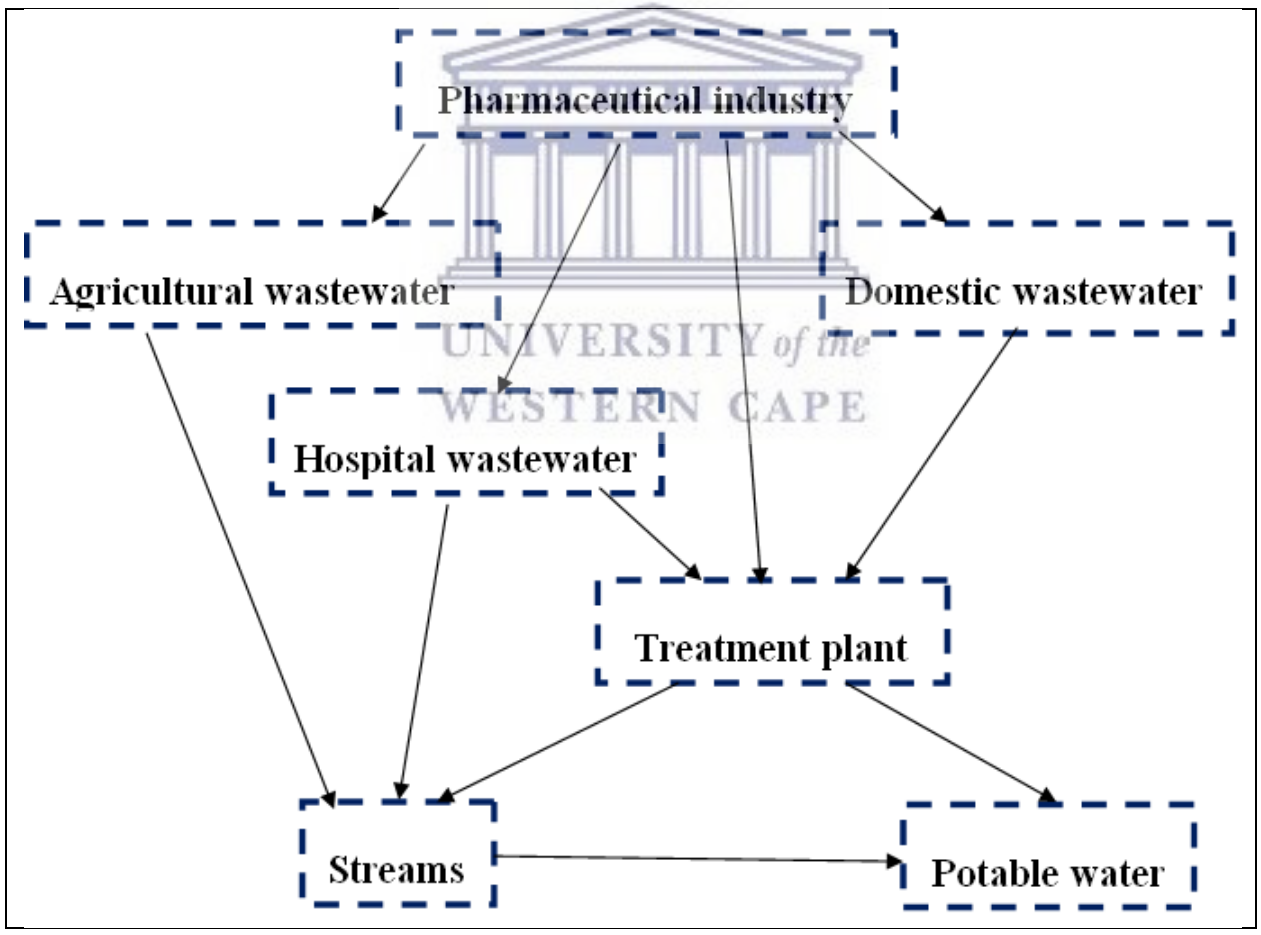

Figure 6.1: Environmental mobility of persistent pharmaceutical pollutants to potable water

The increased ability to quantify pharmaceuticals in ambient waste and drinking water can be attributed to the higher sensitivity of modern analytical techniques. Meanwhile, inefficient removal technology and dilapidated or inadequate wastewater infrastructure leads to the detection of high concentrations of pharmaceutical contaminants in the environment (EEA, 2011). As a result of this, there are serious concerns about ecotoxicological risks as well as the fate and impact of pharmaceutical contaminants in the environment. Several publications have linked abnormal behaviour in some aquatic animals to their exposure to estrogen-like compounds in the water (Wolff and Landrigan, 1994). There is strong evidence supporting the fact that abnormalities in sexual and morphological characteristics such as feminism and early maturity in animals, including humans, are a consequence of pharmaceutical contaminants in wastewater (Aksglaede et al., 2006; Ganiyat, 2008).

According to the anatomical therapeutic chemical (ATC) classification system, active pharmaceutical ingredients are classified according to their activity or therapeutic, chemical and pharmacological properties. Examples of this classification include analgesics (for reduction of pain), antibiotics (for treatment of bacterial infection), tranquilisers (for induction of tranquility), stimulants (for enhanced alertness, locomotion) antipyretics (fever reducing), statins (cholesterol lowering drug) and antiepileptic medicationd. Pain is a common feature of many disease conditions and its selective management requires the application of analgesics such as acetaminophen, diclofenac and ibuprofen. A very short representation of the physical properties of a wide network of compounds known as pharmaceuticals is presented in Table 6.1.

Table 6.1:Environmental mobility of persistent pharmaceutical pollutants to potable water (https://www.pharmacopoeia.com/)

Group	Pharmaceuticals	Log K_{ow}	Molecular weight (g/mol)	Water solubility (mg/L at 25 ^{0}C)
Analgesics	Acetaminophen	0.91	151.16	14,000
	Diclofenac	4.26	296.15	2.37
	Ibuprofen	3.84	206.28	21
Antibiotics	Cephalosporin	2.9	470.30	Poor
	Metronidazole	-0.02	171.16	9500
	Sulfamethoxazole	0.89	253.28	610
Tranquilisers	Meprobamate	0.93	218.25	4700
	Clonazepam	3.15	315.71	100
	Diazepam	3.08	284.74	50
Stimulant	Amphetamine	1.76	135.21	Slightly
	Methylphenidate	0.2	233.31	Insoluble
Antipyretics	Aspirin	1.19	180.16	4600
	Metamizole	-1.8	311.36	5800
Statins	Lovastatin	4.26	404.55	0.4
	Pravastatin	2.18	424.53	6.07
	Simvastatin	4.68	418.57	0.03
Antiepileptic	Carbamazepine	2.77	236.27	17.7

Acetaminophen (N-actyl-p, aminophenol, 4-acetamidophenol) is one of the most common analgesic and antipyretic pharmaceutical compounds usually sold over the counter. The prescription as well as production of acetaminophen (ACE) is comparatively higher that most other pharmaceuticals (Clark et al., 2012). Consequently, there are reports of ACE detection in the aquatic environment and in potable water (Fram and Belitz, 2011). ACE has been implicated in causing hepatic necrosis, nephrotoxicity and extra hepatic lesions (Clark et al., 2012). Recently, removal of ACE through various advanced oxidation processes (AOPs) has been reported (Polar, 2007). The generated hydroxyl radicals in AOPs can be applied for the mineralisation of persistent organic pollutants. The challenge with most of the AOPs include the formation of complex intermediate by-products which may be difficult to quantify or/and have greater toxicity than the parent compound, the costs of chemicals such as $FeSO_4$ or peroxide as well as the generation of iron sludge (in Fenton oxidation), high energy consumption and maintenance costs (UV systems). Besides, none of the AOPs, on their own can lead to complete

mineralisation of the persistent pharmaceutical pollutants. Therefore, the possibility of efficient mineralisation of ACE depends on the application of a combination of non/ less chemically intensive methods of advanced oxidation. In this chapter, degradation of an aqueous solution of ACE in a jet loop hydrodynamic cavitation system was studied in the presence of a novel green nano zero valent iron (gnZVI). The current investigation was based on the achieved optimum orifice holes size (Section 5.5.2) and the initial pressure (Section 5.5.3). In this section, investigation of the degradation of ACE in a cavitation system was done with respect to the pH, hydrogen peroxide concentration, iron sulfate or gnZVI dosage. Upon the analysis of the ACE using a UV spectrophotometer, TOC, GC-MS and LC-MS, the derived data were used to report the extent of ACE degradation and described the proposed reaction mechanism.

6.4 Experimental setup

The synthesis (Section 4.6.1) and characterisation (Section 4.7.4) of a novel green nano zero valent iron (gnZVI) was reported in this thesis. The design (Section 3.6) of the jet loop hydrodynamic cavitation system as well as the quantification of the hydroxyl radical (Section 5.5.1) was also reported. Based on those findings, a volume of 10 L standard solution of ACE (10 mg/ L) was prepared in deionised water and subjected to degradation in a jet loop hydrodynamic cavitation system for 60 minutes. The parameters such as initial pressure, concentration of hydrogen peroxide, amount of iron sulfate or gnZVI were optimised and the experiment were run in triplicate (n = 3) according to Table 6.3.

Table 6.2: Operational conditions during the treatment of 10 L of 10 mg/ L ACE solution in the jet loop hydrodynamic cavitation system (60 minutes, 400 kPa in let pressure, 4 mm orifice hole sizes)

Experimental Code	*pH*	*Concentration of iron sulfate (mg/ L) in 10 L solution*	*Concentration of gnZVI (mg/ L) in 10 L solution*	*Concentration of H_2O_2 (mg/ L) in 10 L solution*
pH (PH)	**2-4**	**-**	**-**	**-**
PH2	2	0	0	0
PH3	3	0	0	0
PH4	4	0	0	0
Iron (II) sulfate (F2)	**-**	**10-40**	**-**	**-**
1F2	2	10	0	0
2F2	2	20	0	0
4F2	2	40	0	0
gnZVI (N2)	**-**	**-**	**10-40**	**-**
1N2	2	0	10	0
2N2	2	0	20	0
4N2	2	0	40	0
H_2O_2 (P)	**-**	**-**	**-**	**0.5-10**
P5P	2	0	0	0.5
1P	2	0	0	1
2P	2	0	0	2
5P	2	0	0	5
10P	2	0	0	10
1PF	**2**	**10**	**0**	**5**
1PN	**2**	**0**	**10**	**5**

6.5 Results and Discussion

Treatment of wastewater in the jet loop hydrodynamic cavitation system depends on the specific properties of its chemical content. The collapsing bubbles during cavitation have the tendency to generate chemical species (free radicals), cause mechanical shear stress and/ or thermal (hot spot) properties. The combination of these processes produces hydroxyl radicals which degrade the POPs in wastewater. Quantification of the OH radicals produced in the current design of jet loop hydrodynamic cavitation was presented in Section 5.5.1.

Meanwhile, the characteristics of the cavitation bubbles and the hydroxyl radicals that were formed at the throat of the venturi tube or orifice plates in the jet loop hydrodynamic cavitation

system can be predicted based on the solution pH, initial pressure, nature of applied catalyst and the oxidants (Barati et al., 2007; Šarc et al., 2017).

6.5.1 Initial pH of the solution

The initial pH of a wastewater is very crucial to its effective degradation in a jet-loop hydrodynamic cavitation system. Firstly, the UV absorbance of ACE samples were obtained at 10 minutes interval during the 60 minutes treatment in the jet-loop hydrodynamic cavitation system by itself (400 kPa initial pressure, pH 2, 4 mm orifice hole size, 10 L of 10 mg/L ACE, n = 3). The PH20, PH21, PH23, PH24, PH25 and PH26 are the spectra obtained at 0, 10, 20, 30, 40, 50 and 60 minutes respectively during the ACE treatment as presented in Figure 6.2.

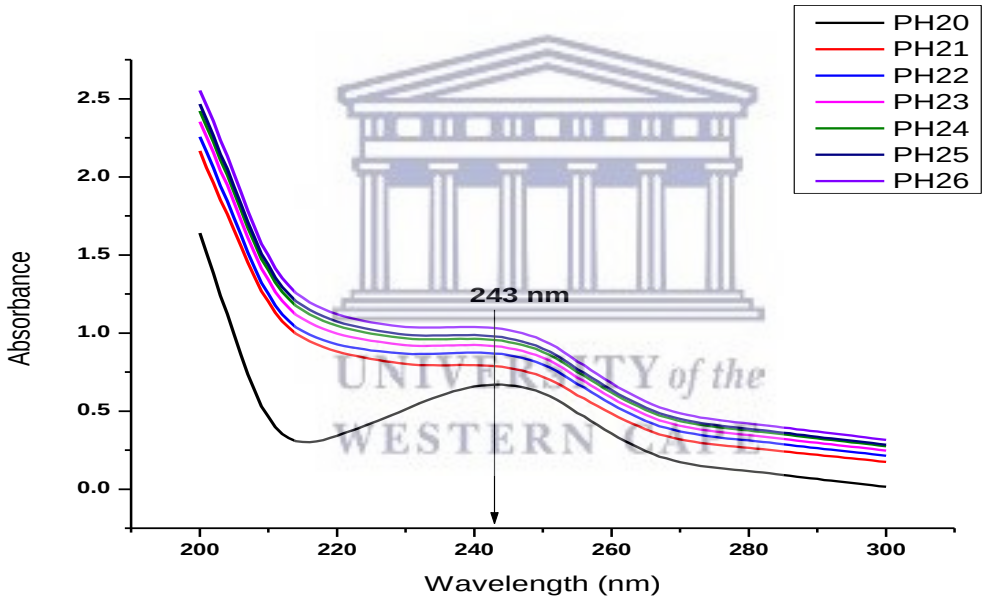

Figure 6.2: Effect of time on the UV absorbance spectra of samples taken at 10 minutes intervals during the 60 minutes degradation of ACE in the jet-loop hydrodynamic cavitation system (pH 2, 400 kPa initial pressure, 4 mm orifice hole size, 10 L of 10 mg/ L ACE, n = 3)

The UV absorption spectra presented in Figure 6.2 shows the absorption spectra of ACE solution with the characteristic maximum absorption peak (λ_{max}) at 243 nm. It can be observed that the λ_{max} increased as the reaction time increased. It was expected that the λ_{max} would be lowered and

by implication there would be degradation and reduction in ACE concentration. It can be confirmed from the UV spectrophotometer results that intermediates were formed when the hydroxyl radicals reacted with ACE in the jet loop hydrodynamic cavitation system (400 kPa initial pressure, pH 2, 4 mm orifice hole size, 10 L of 10 mg/L ACE, n = 3). Besides, the produced intermediates had the same λ_{max} as ACE but with higher intensity. The LC-MS analysis (Figure 6.3) also revealed the generation of a compound with molar mass of 168 g/ mol. Therefore, it can be confirmed that one of the intermediate products was N-(2, 4-dihydroxyphenyl)acetamide (Ashton et al., 1995). The transformation of ACE to N-(2, 4-dihydroxyphenyl) acetamide is presented in Figure 6.3.

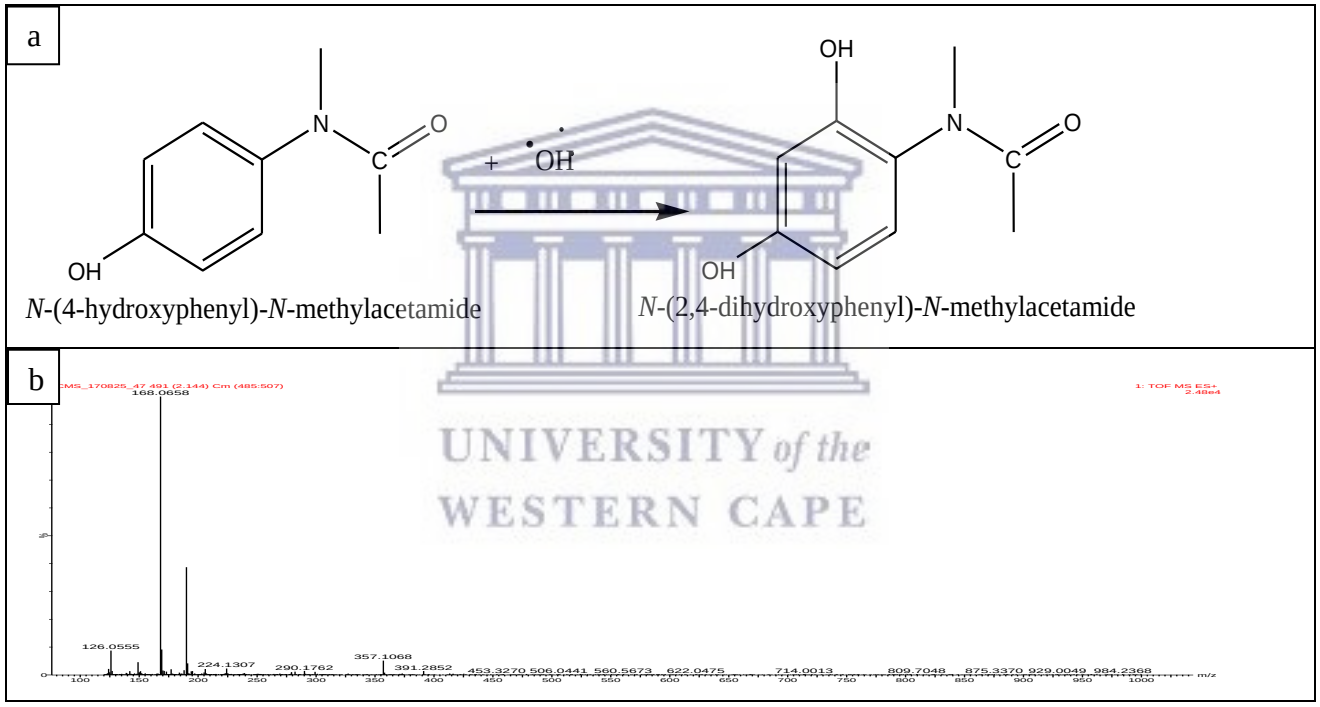

Figure 6.3: [a] Reaction showing transformation of N-(4-hydroxyphenyl)-N-methylacetamide to N-(2,4-dihydroxyphenyl)-N-methylacetamide during treatment of ACE in the jet loop hydrodynamic cavitation system and [b] LC-MS spectrum of N-(2,4-dihydroxyphenyl)-N-methylacetamide (400 kPa, 4 mm orifice plate hole size, 10 L of 10 mg/ L ACE, 60 minutes, n = 3)

The binding of the hydroxyl radical during the transformation of ACE to N-(2, 4-dihydroxyphenyl)acetamide can occur on either the ortho or meta position of the benzene ring. However, the two substituents that make up the ACE (hydroxyl and amine) are know to be ortho and para directors. Since the para position in the ACE is already occupied, the hydroxyl radical can only bind at the ortho positions to form N-(2, 4-dihydroxyphenyl)acetamide. A lot of insight about the transformation of aromatic compounds by the hydroxyl radical was provided in the work of Minakata et al., (2015). Meanwhile, traces of meta substituents and N-(2, 4, 6-trihydroxyphenyl)acetamide can also be produced as intermediate during the transformation of ACE. The identification and quantification of these intermediate products is very difficult using the UV spectrophotometer as described in Section 3.7.5. Meanwhile, confirmation of degradation was achieved in the later section by supporting the UV spectrophotometer data with FT-IR and GC-MS. An alteration in the treatment conditions may favour futher transformation and possible degradation of ACE in the jet loop hydrodynamic cavitation system.

Typically, pharmaceutical wastewater has a wide range of pH because of the complex nature of its chemical content. Previous reports have shown that for the optimum generation of hydroxyl radicals, the initial pH of the wastewater must be acidic (Badmus et al., 2016; Dular et al., 2016; Rajoriya et al., 2017). Therefore, during the current study, the initial pH was monitored from 2 to 4 while the operating inlet pressure was maintained at 400 kPa and 10 L of 10 mg/L ACE solution was degraded for 60 minutes in an orifice-curve venturi jet-loop hydrodynamic cavitation system described in Section 3.6. The control experiment was done by degradation ACE solution (pH 2) for 60 minutes in the jet loop hydrodynamic cavitation system (400 kPa initial pressure, 4 mm orifice hole size, 10 L of 10 mg/L ACE, n = 3) after the initial sampling at 0 minute. The PH20, PH2, PH3 and PH4 represent the recorded absorbance spectrogram of ACE solution during its transformation at pH 2 at 0 minute, at pH 2 in 60 minutes, at pH 3 in 60 minutes and pH 4 in 60 minutes respectively. The variation in the absorption spectra of ACE at varied pH of 2, 3 and 4 (400 kPa initial pressure, 4 mm orifice hole size, 10 L of 10 mg/L ACE, 60 minutes, n = 3) is presented in Figure 6.4.

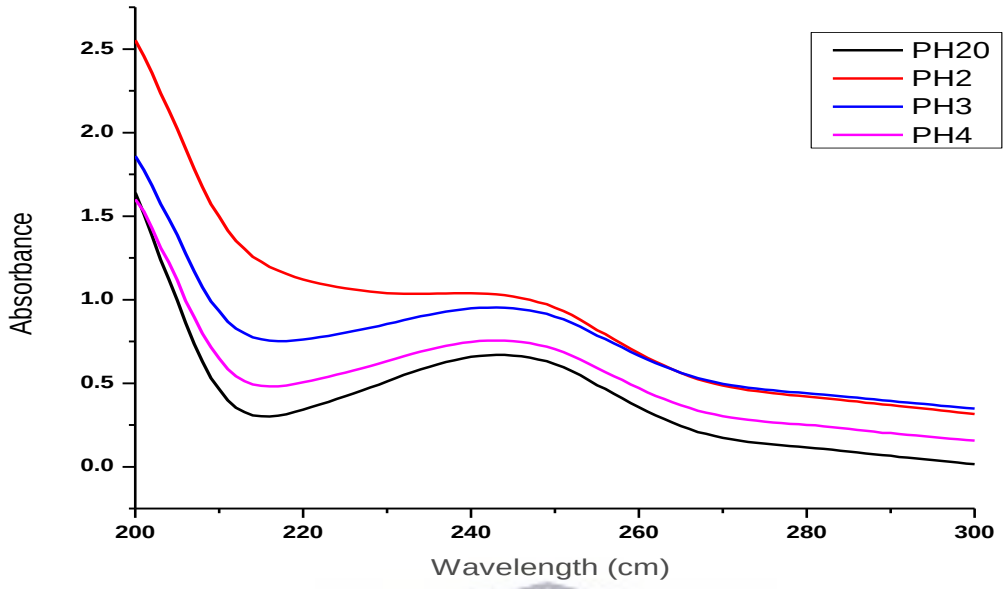

Figure 6.4: Effect of initial solution pH during the treatment of ACE in the jet-loop hydrodynamic cavitation system at PH20, PH2, PH3 and PH4 for solution pH 2 at 0 minutes, solution pH 2 at 60 minutes, solution pH 3 at 60 minutes and solution pH 4 at 60 minutes respectively (400 kPa initial pressure, 4 mm orifice hole size, 10 L of 10 mg/ L ACE, n = 3)

It was observed in Figure 6.4 that the UV absorbance intensity decreased as the initial pH was increased from 2 to 4. The highest absorbance intensity was observed when the ACE solution pH was 2. The solution pH 2 has been extablished as the optimum for the production of hydroxyl radical in the jet loop hydrodynamic cavitation system (Pradhan and Gogate, 2010; Samaei et al., 2015; Wu and Shi, 2010). Apparently, the increased in the UV absorbance intensity at a lower pH is an indication of the generation of more hydroxyl radical and therefore production of more intermediate in the jet loop hydrodynamic cavitation system. The % change in absorption can be used to estimate the formation of intermediate during the treatment of ACE in jet loop hydrodynamic cavitation as described in appendix 12. The transformation of ACE in jet loop hydrodynamic cavitation at varied pH during an hour treatment time is as represented in Figure 6.5.

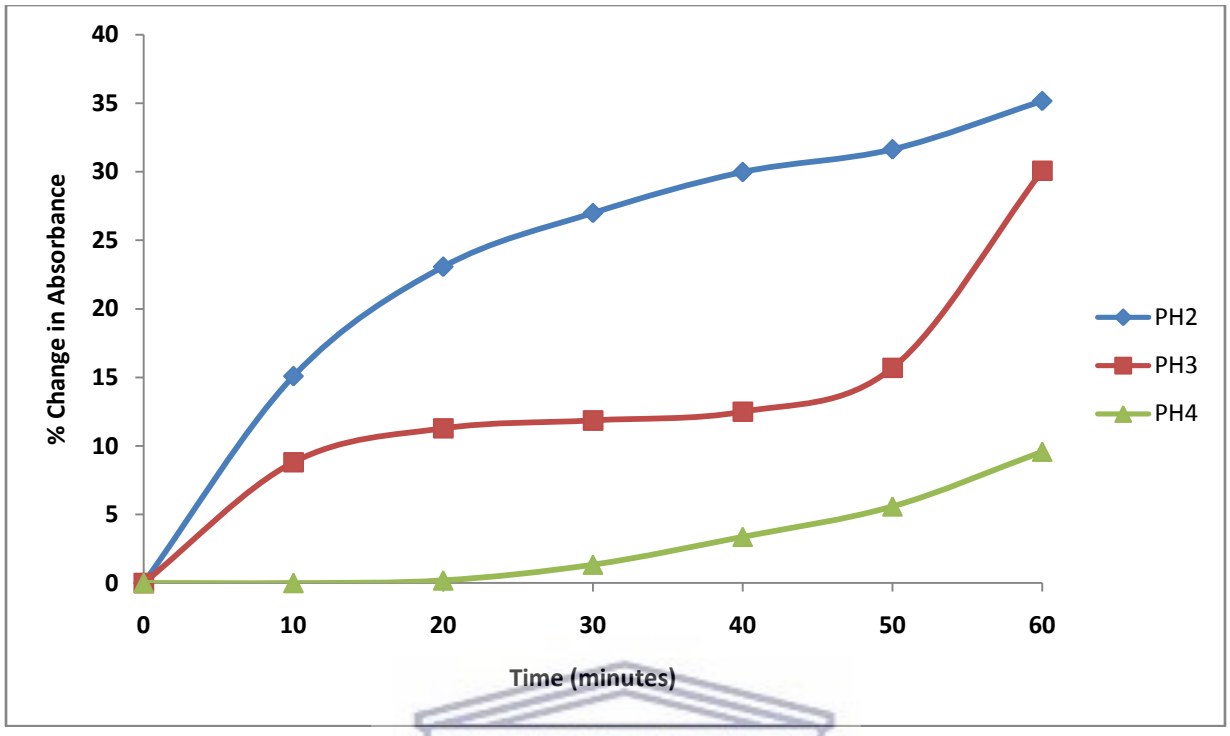

Figure 6.5: Effect of solution pH on the intermediates produced during the transformation of acetaminophen in the jet loop hydrodynamic cavitation system (400 kPa initial pressure, 4 mm orifice hole size, 10 L of 10 mg/ L ACE, 60 minutes, n = 3)

The % change in absorbance increased at the end of 60 minutes treatment of ACE in the jet loop hydrodynamic cavitation system for pH 2, pH 3 and pH 4. The highest % change in absorbance of maximum intensity for the treated ACE solution was achieved when the pH of the solution was 2. Therefore, ACE solution was sustained at pH 2 in the follow up investigations. The enhancement of the transformation of ACE solution at pH 2 can be done through the application of a catalyst (in the form of iron (II) sulfate or nano zero valent iron) or a source of oxygen such as hydrogen peroxide.

6.5.2 Influence of iron (II) sulfate or gnZVI on the transformation of acetaminophen using jet loop hydrodynamic cavitation system

Iron sulfate or the gnZVI as synthesised in Section 4.6.1., can participate in the degradation of acetaminophen solution in the jet loop hydrodynamic cavitation by acting as Fenton catalyst. It should be noted that the hydroxyl radical is generated in-situ in the jet loop hydrodynamic

cavitation system as was demonstrated in Section 3.9. The 11.29 mg/ L hydroxyl radicals which can be generated per hour in the jet loop hydrodynamic cavitation system (as described in Section 5.5.1) cab be enhanced by a catalyst (iron sulfate or gnZVI) or oxidant (hydrogen peroxide) in order to achieve efficient treatment of POPs. The capacities of iron sulfate or gnZVI to function as a Fenton catalyst in the jet loop hydrodynamic cavitation without additional hydrogen peroxide (pH 2, 400 kPa, 10 L of 10 mg/ L ACE, 4 mm orifice plate hole size, n = 3) was investigated by varying their respective dosage between 10 mg/ L to 40 mg/ L (Table 6.3). The PH2, 1F2, 2F2 or 4F2 represents the transformation of ACE solution in the jet loop hydrodynamic cavitation system (pH 2, 400 kPa, 10 mg/ L in 10 L ACE solution, 4 mm orifice plate hole size, n = 3) under the influence of 0 mg/ L iron (II) sulfate, 10 mg/ L iron (II) sulfate 20 mg/ L iron (II) sulfate or 40 mg/ L iron (II) sulfate respectively. The transformation of ACE solution (per hour) in the jet loop hydrodynamic cavitation at varied concentration of iron (II) sulfate was monitored by estimating the % change in absorbance of treated ACE solution across the 60 minutes treatment time as presented in Figure 6.6.

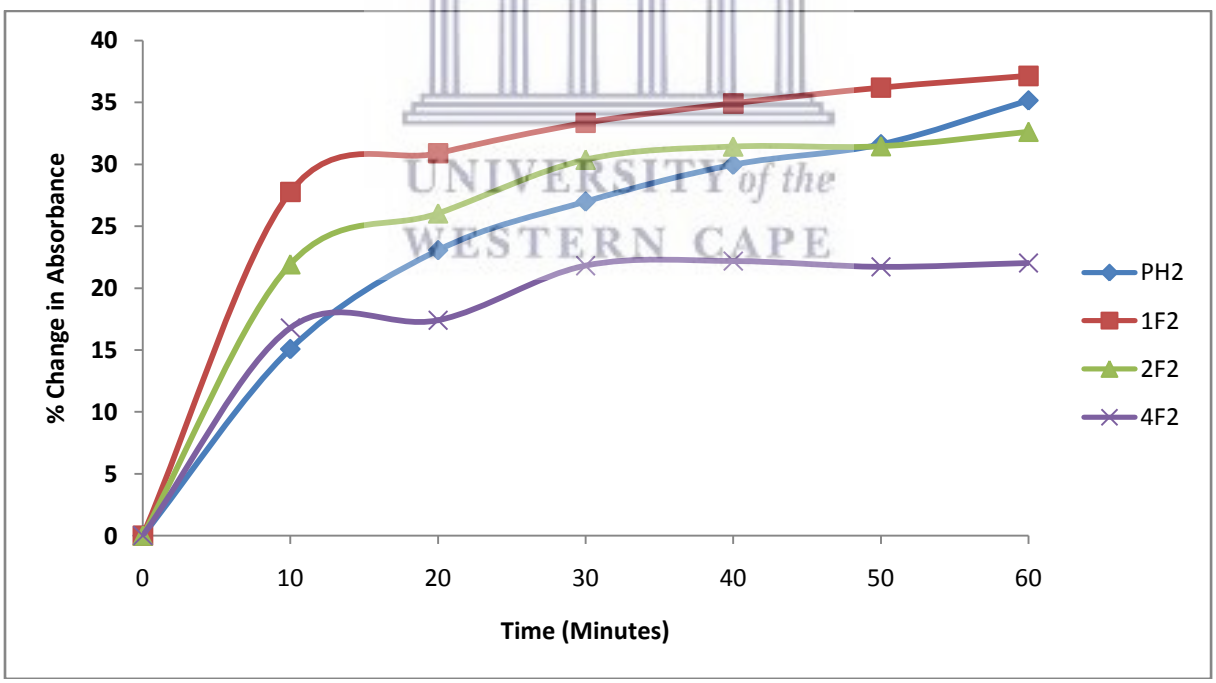

Figure 6.6: The effect of iron (II) sulfate concentration on the production of intermediates during the transformation of ACE in the jet loop hydrodynamic cavitation system (10 L of 10 mg/ L ACE solution, 400 kPa inlet pressure, pH 2, 60 minutes, n = 3)

The % change in absorbance of maximum intensity as represented by 1F2, 2F2 or 4F2 decreases as the amount of applied iron (II) increased. Consequently, the intermediate generated during the 60 minutes treatment time of ACE in the jet loop hydrodynamic cavitation system reduces as the concentration of iron (II) sulfate was increased. 1F2 gave the highest amount of intermediate product during the transformation of ACE in the jet loop hydrodynamic cavitation system. Therefore, application of 10 mg/ L iron (II) sulfate resulted in highest transformation of ACE in the jet loop hydrodynamic cavitation system (pH 2, 400 kPa, 10 L of 10 mg/ L ACE, 4 mm orifice plate hole size, 60 minutes, n = 3). When the concentration of iron (II) sulfate was increased beyond the 10 mg/ L (20 or 40 mg/ L), there was a reduction in the extent of intermediate production. Therefore, it can be reported that the addition of 20 mg/ L or 40 mg/ L iron sulfate resulted in a decreased production of the intermediate in the jet loop hydrodynamic cavitation system (pH 2, 400 kPa, 10 L of 10 mg/ L ACE, 4 mm orifice plate hole size, 60 minutes, n = 3). The decreased formation of intermediate products upon the application of an higher amount of iron II sulfate was caused by the increased degradation effect of ACE solution in the jet loop hydrodynamic cavitation system (López and Eunice, 2016). The scavenging effect of OH radical can also be attributed as the cause of a reduced intermediate product (Akbari et al., 2016; Giannakis et al., 2017).

The gnZVI which synthesis was described in Section 4.6.1., can be applied in place of iron (II) sulfate to prevent the scavenging effect of the ferric iron on the hydroxyl radical. The PH2, 1N2, 2N2 or 4N2 represents the transformation of ACE solution in the jet loop hydrodynamic cavitation system (pH 2, 400 kPa, 10 mg/ L ACE 10 L ACE, 4 mm orifice plate hole size, n = 3) under the influence of 0 mg/ L of gnZVI, 10 mg/ L of gnZVI, 20 mg/ L of gnZVI or 40 mg/ L of gnZVI respectively. The transformation of ACE solution (per hour) in the jet loop hydrodynamic cavitation at varied dosage of gnZVI was monitored by estimating the % change in absorbance of treated ACE solution across the 60 minutes treatment time as presented in Figure 6.7.

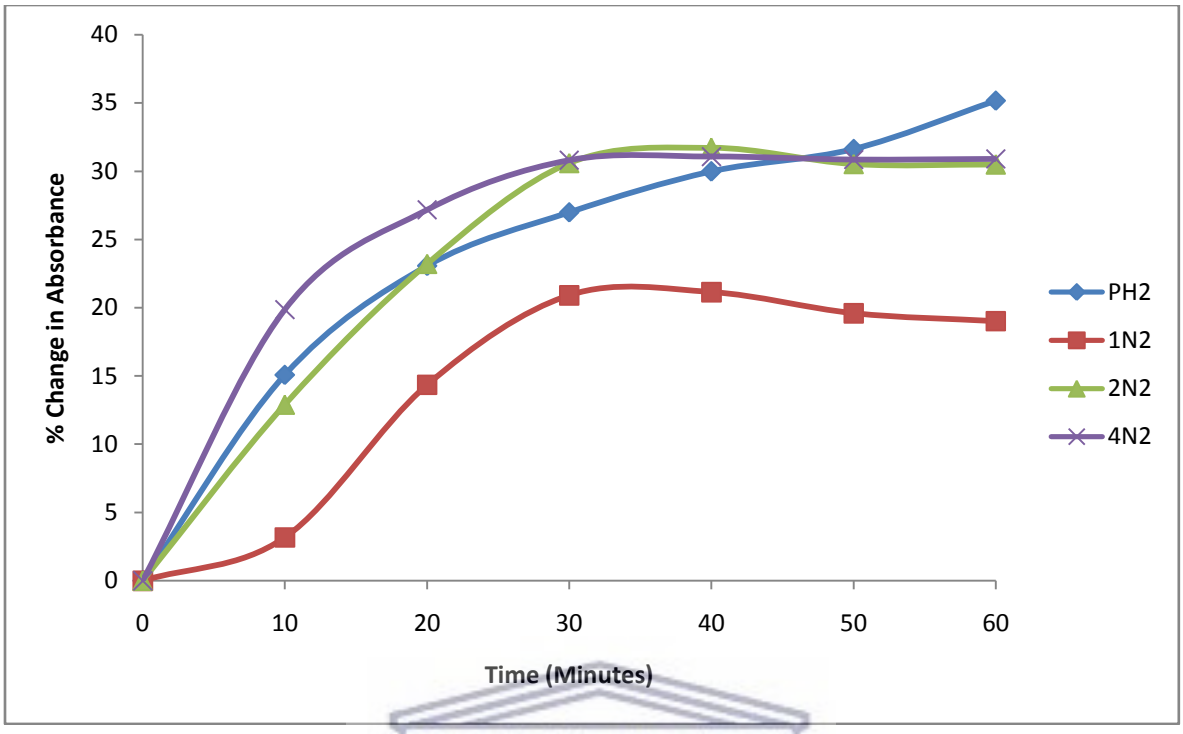

Figure 6.7: The effect of gnZVI dosage on the formation of intermediates during the transformation of ACE in the jet loop hydrodynamic cavitation system (10 L of 10 mg/ L ACE solution, 400 kPa, pH 2, 60 minutes, n = 3)

The % change in absorbance of maximum intensity as represented by 1N2, 2N2 or 4N2 increases as the concentration of applied gnZVI increased. It was observed that the increased concentration of gnZVI lead to the corresponding increased production of intermediates. It appears that the treatment of ACE solution in the jet loop hydrodynamic cavitation using gnZVI catalyst (pH 2, 400 kPa, 10 L of 10 mg/ L ACE solution, 4 mm orifice plate hole size, n = 3) lead to the production of a lower amount of the intermediates in comparison with when iron (II) sulfate was applied as Fenton catalyst. Apparently, no much intermediate was formed when gnZVI was applied as catalyst during the treatmen t of ACE in the jet loop hydrodynamic cavitation. Besides, the gnZVI does not scavenge the hydroxyl radical during its application in the jet loop hydrodynamic cavitation system. Therefore, it offers a more efficient alternative than iron (II) sulfate as a Fenton catalyst during the treatment of ACE solution using jet loop hydrodynamic cavitation system. The application of iron material such as iron (II) sulfate or nano iron during the wastewater treatment may contribute the quantity of elemental iron present in the sludge.

Excessive amount of iron in both the effluent and sludge has negative impact on the efficiency of the system (Wilén et al., 2008).

6.5.3 Iron sludge generation during the treatment in jet loop hydrodynamic cavitation system

Another important reason for the application of gnZVI as alternative catalyst was the possible reduction in the residual iron in both sludge and effluent. The high concentration of iron and its removal from both effluent and sludge is one of the disadvantages of the Fenton-like processes using iron (II) sulfate (Yoo et al., 2001). A novel gnZVI (10 mg/ L) that was synthesised in Section 4.6 was applied as an alternative to iron (II) sulfate try to reduce the amount of elemental iron in the effluent generated during the degradation of ACE solution using jet loop hydrodynamic cavitation system (pH 2, 400 kPa, 10 mg/ L of 10 L ACE solution, 4 mm orifice plate hole size, 60 minutes, n = 3).

In the current investigation a jet loop hydrodynamic cavitation system (J) was firstly operated with only deionised water (10 L) in order to determine the possibility and extent of iron leaching from the jet loop equipment during the (60 minutes) operating time. In a subsequent experiment, 10 L of a 10 mg/ L of ACE solution was degraded in the jet loop hydrodynamic cavitation system using either (10 mg/ L) gnZVI (JN) or iron II sulfate (JF). The samples were collected at 10 minutes intervals during the 60 minutes operation time. A parmanet magnetic bar (Science Wiz, 7/8" wide, 17/8" long and 3/8" thick) was used to remove the residual iron oxide from the ACE solution (JMN) while in the other gnZVI set (JN), the magnetic bar was not used. Thereafter, all the recovered effluent samples were filtered and their elemental iron concentration was determined using ICP-OES analysis that was described in Section 3.7.11. The concentration of elemental iron detected in each effluent sample was presented in Table 6.3.

Table 6.3: Concentration of elemental iron (mg/ L) detected in the effluent generated in the jet loop hydrodynamic cavitation system (pH 2, 400 kPa, 10 L, 4 mm orifice plate hole size, n = 3)

Code	J	JN	JMN	JF
Time (minutes)	Iron concentration ± SD (mg/ L)	Iron concentration ± SD (mg/ L)	Iron concentration ± SD (mg/ L)	Iron concentration ± SD (mg/ L)
0	00.01 ± 0.02	00.42 + 0.058	00.12 ± 0.06	01.04 ± 0.16
10	20.88 ± 1.11	21.36 + 2.03	11.57 ± 1.64	24.27 ± 3.88
20	30.49 ± 2.36	30.50 + 3.10	17.42 ± 2.57	33.50 ± 5.70
30	44.87 ± 3.88	46.34 ± 5.03	25.68 ± 4.13	45.13 ± 7.97
40	54.01 ± 4.42	58.95 ± 6.63	32.92 ± 5.90	57.86 ± 8.23
50	64.64 ± 6.13	73.68 ± 9.24	41.17 ± 7.54	64.62 ± 10.26
60	73.27 ± 8.69	85.6 0 ± 10.71	49.76 ± 10.26	73.81 ± 11.06

As presented in Table 6.3, the concentration of iron at 0 time when the jet loop hydrodynamic cavitation was operated with only deionised water (J) or when 10 mg/ L of gnZVI was applied (JN) or when bar magnet was used to recover unused gnZVI (JMN) or when 10 mg/ L iron (II) sulfate (JF) was applied; were 0.01 mg/ L or 0.42 mg/ L or 0.12 mg/L or 1.04 mg/ L respectively. On the bases of the amount of iron detected at zero time, it can be reported that there was 60% reduction in the applied iron during the treatment of ACE (10 L of 10 mg/ L), when iron (II) was replaced with gnZVI. Hence, a significant reduction in the quantity of elemental iron to be used as the iron catalyst in the Fenton based treatment of ACE solution using the jet loop hydrodynamic cavitation system can be achieved using gnZVI. Furthermore in run J, where only deionized water was used, 73.27 mg/L of iron was leached into the water after 60 minutes from corrosion of the jetloop equipment. The amount of leached iron was far greater than the dosed iron after even 10 minutes. It was also observed that 85.6 mg/ L of elemental iron was detected in the effluent when gnZVI was used as catalyst during the treatment ACE in the jet loop hydrodynamic cavitation system. However, the amount of iron in the run JN effluent was reduced to 49.76 mg/ L (more than 41% removal) when a bar magnet was used to remove the

residual iron from the solution. Consequently, a bar magnet can be used to remove the residual iron caused by corrosion from the effluent or sludge. The concentration of elemental iron as measured by ICP-OES in samples recovered after various treatment times is presented in Figure 6.16.

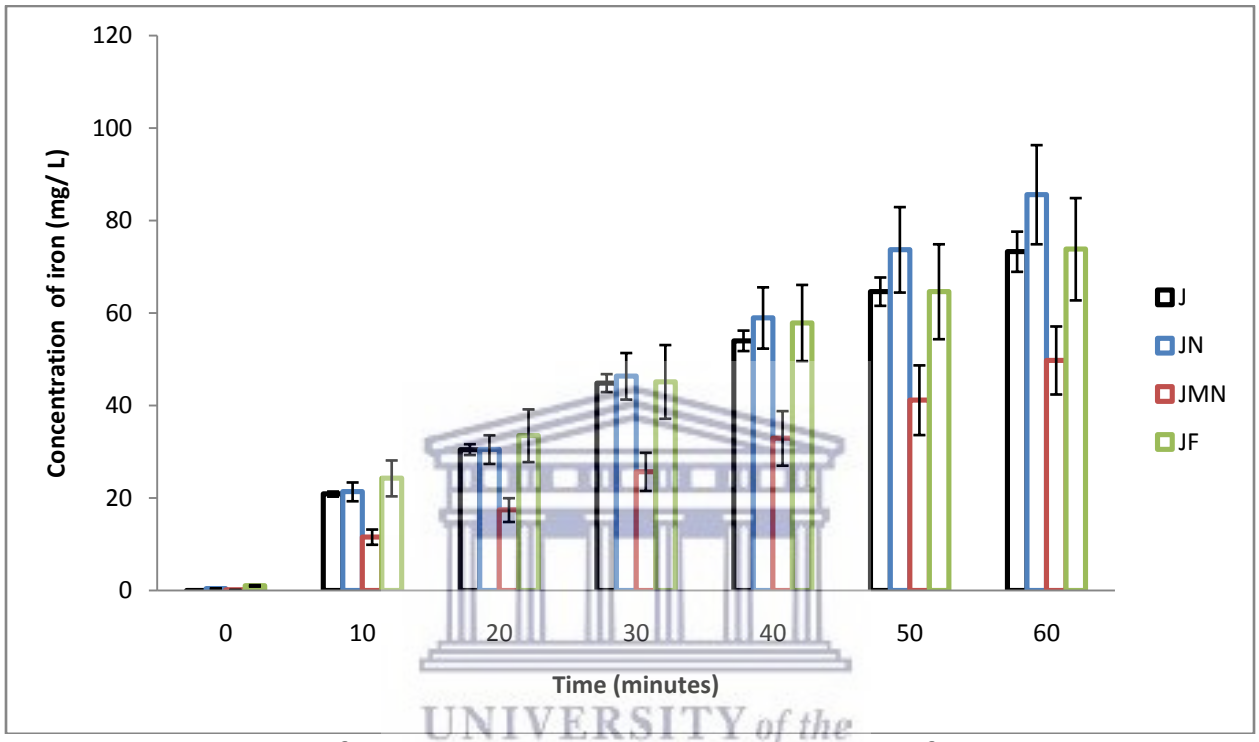

Figure 6.7: Leaching of elemental iron during the treatment of ACE in the jet loop hydrodynamic cavitation system (pH 2, 400 kPa, 10 L, 4 mm orifice plate hole size, n = 3)

Iron corrosion was thus a major nuisance factor in the jet loop hydrodynamic cavitation system used. It continuously increased in concentration over the 60 minutes treatment at zero application (J) of either iron (II) sulfate or gnZVI as observed in Table 6.3, which is a clear demonstration of its leaching due to corrosion in the oxidative environment created by the free radicals. At the same time, it was observed that the concentration of iron that was measured only slightly increased across the treatment time when 10 mg/ L of either iron (II) sulfate or gnZVI was applied. Meanwhile, a significant amount of iron oxide was recovered with the residual gnZVI when a bar magnet was used for the removal of magnetic iron from the treated water.

The increase in the iron (showing in Figure 6.16) across the treatment period in the current study can be traced to the leaching of iron from the jet loop hydrodynamic equipment. Apparently, the source of the corroded iron could be from the mildsteel material used in the manufacturing of the jet loop hydrodynamic equipment. Therefore, stainless steel or a heat and acid resistance non corrosive material is recommended for the future construction of the jet loop hydrodynamic equipment. It should be noted that iron (II) sulfate is dosed in its Fe^{2+} form whereas ngZVI is dosed in its Fe^{0} form, thus able to promote oxidation. On the contrary, the rust corroding from the mild steel equipment is in Fe^{3+} form and does not participate in the oxidation reactions taking place in the cavitation system, except to consume oxygen, and the extent to which the rust was produced during 60 minutes was fairly consistent from run to run, therefore the experiments were continued in the equipment despite the rust, since it was not possible to replace the system.

6.5.4 Influence of hydrogen peroxide

A limited amount of hydrogen peroxide is a source of supplementary oxidising agent which could cause a high rate of degradation of persistent organic pollutants (POPs) until a certain optimum concentration (Chakinala et al., 2009). An excessive quantity of hydrogen peroxide could also serve as hydroxyl radical scavenger, thus promoting the recombination of the hydroxyl radical and consequently leading to a reduced degradation rate (Chakinala et al., 2008). The formation of hydroxyl radicals from hydrogen peroxide and its scavenging effect in the presence of hydrogen peroxide is presented in *(6.i)* and *(6.ii)*.

$$H_2O_2 \rightarrow HO^{\bullet} + HO^{\bullet} \ldots\ldots\ldots\ldots\ldots \quad (6.i)$$

$$H_2O_2 + HO^{\bullet} \rightarrow H_2O + HOO \ldots\ldots\ldots\ldots\ldots \quad (6.ii)$$

The optimum amount of hydrogen peroxide needed for the degradation of a specific amount of acetaminophen in a jet loop hydrodynamic cavitation system must be determined to ensure the efficiency of the process. During the current studies, the concentration of hydrogen peroxide applied for the treatment of ACE solution in a jet loop hydrodynamic cavitation system was varied between 0.5 mg/ L and 10 mg/ L as described in Table 6.2.

PH20 was the untreated ACE solution while PH26, P5P6, 1P6, 2P6, 5P6 or 10P6 represents the application 0.0 mg/ L, 0.5 mg/ L, 1 mg/ L, 2 mg/ L, 5 mg/L or 10 mg/ L of hydrogen peroxide respectively in the jet loop hydrodynamic cavitation system system (pH 2, 400 kPa, 10 L of 10 mg/ L ACE, 4 mm orifice plate hole size, 60 minutes, n = 3). The UV spectra obtained after 60 minutes treatment of ACE solution in the jet loop hydrodynamic cavitation is presented in Figure 6.10.

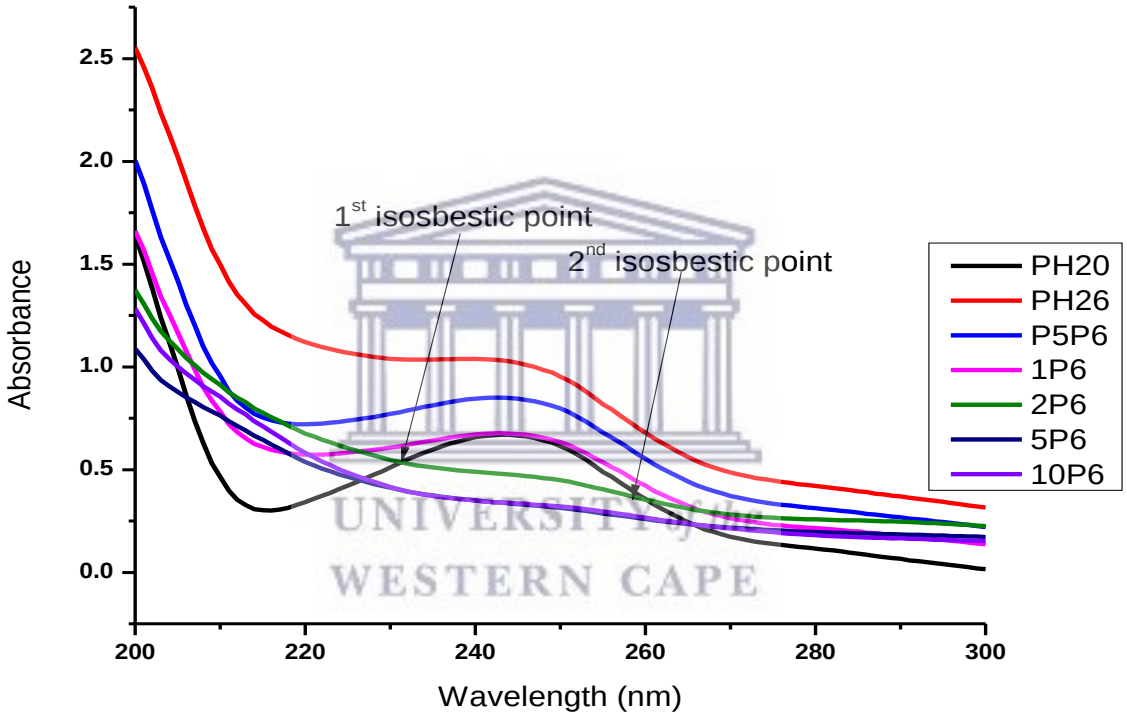

Figure 6.8: UV spectra showing the effect of hydrogen peroxide application during the transformation of acetaminophen in the jet-loop hydrodynamic cavitation and showing the first isosbestic point at the application of 2 mg/ L hydrogen peroxide (400 kPa, pH 2, 4 mm orifice plate hole size, 10 L of 10 mg/ L ACE, n = 3)

It was observed at the end of the treatment, that the UV absorbance spectra of the experiments (PH26, P5P6 and 1P6) which represent the addition of 0 mg/ L, 0.5 mg/ L and 1.0 mg/ L respectively of hydrogen peroxide to ACE solution in the jet loop hydrodynamic cavitation

system (pH 2, 400 kPa, 10 L of 10 mg/ L ACE, 4 mm orifice plate hole size, 60 minutes, n = 3) were more intense than the UV specrum of the untreated ACE (PH20). This implies that the added hydrogen peroxide was only able to produce intermediates with an intense absorbance spectrum during the treatment in the jet loop hydrodynamic cavitation system. Conversely, the UV spectra at 60 minutes treatment of ACE solution when 2.0, 5.0 or 10 mg/ L hydrogen peroxide (2P6, 5P6 or 10P6) was applied show intersections with the spectrum obtained for the untreated ACE (PH20). These points of intersections are known as isosbestic points. They mark the wavelength at which the absorption of light by a mixed solution remains constant as the equilibrium between the components of solution changes. The appearance of isosbestic point in the current investigation is a justification of the existence of the equilibrium mixture of degraded ACE solution and the residual ACE solution, making up the two major chemical components in the treated solution. It was observed from the obtained spectra of treated ACE that the maximum intermediate products were generated in the first 10 minutes of treatment and there after, its transformation started. The spectra obtained when 0, 0.5 or 1.0 mg/ L of hydrogen peroxide was applied during the treatment of ACE solution in the jet loop hydrodynamic cavitation system is presented in appendix 3.

The obtained spectra show that after 60 minutes treatment, the application 0.5 or 1.0 mg/ L hydrogen peroxide in the jet loop hydrodynamic cavitation system was not able lower the λ_{max} below that which was obtained for the untreated ACE solution. Conversely, the application of 2.0, 5.0 or 10 mg/ L hydrogen peroxide in the jet loop hydrodynamic cavitation system was able to lower the λ_{max} below that which was obtained for the untreated ACE solution after 30 minutes of treatment (Appendix 4).

Based on this account, it can be reported that the substantial transformation of ACE solution leading to its degradation was achieved after 30 minutes of treatment when 2 mg/ L, 5 mg/ L or 10 mg/ L hydrogen peroxide (2P6, 5P6 and 10P6) was applied in the jet loop hydrodynamic cavitation system (pH 2, 400 kPa, 10 L in 10 mg/ L ACE, 4 mm orifice plate hole size, 60 minutes, n = 3). Therefore, the % degradation of ACE was extimated using kinetic of degradation equation that was described in Section 3.8.3. The bar chart of % degradation during the treatment of ACE in the jet loop hydrodynamic cavitation system is presented in Figure 6.11.

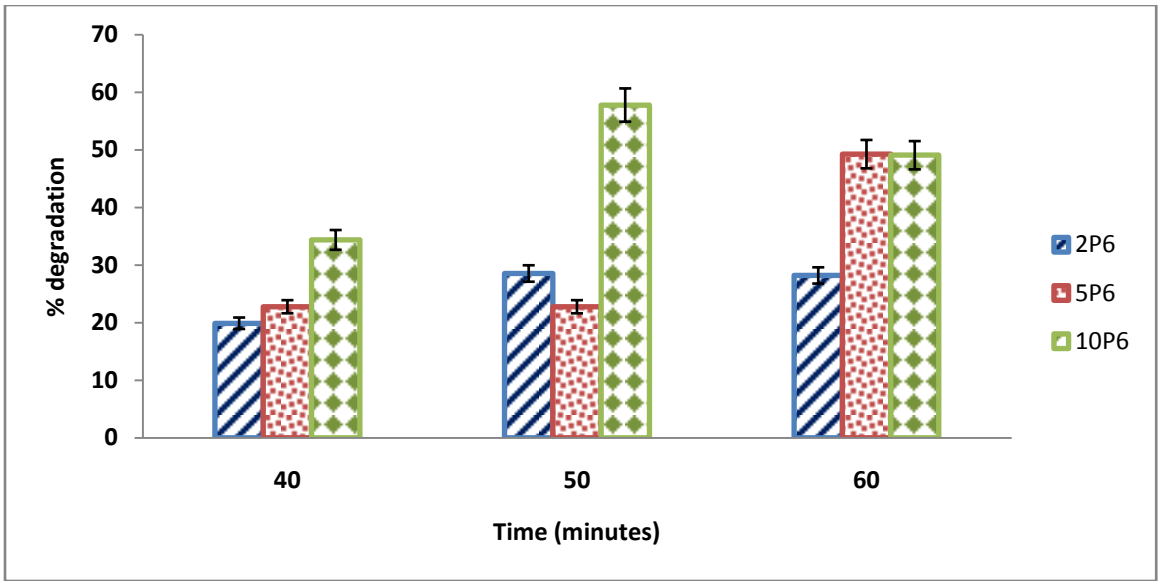

Figure 6.9: The effect of H_2O_2 concentration on % degradation during the treatment of ACE in the jet loop hydrodynamic cavitation system (pH 2, 400 kPa, 10 L of 10 mg/ L ACE, 4 mm orifice plate hole size, n = 3).

The degradation of ACE became effective after 30 minutes treatment time with the application of 2 mg/ L or 5 mg/ L hydrogen peroxide in the jet loop hydrodynamic cavitation system (pH 2, 400 kPa, 10 L of 10 mg/ L ACE, 4 mm orifice plate hole size, 60 minutes, n = 3). Meanwhile, when the higher amount of hydrogen peroxide (10 mg/ L) was applied the scavenging effect was noticed after 50 minutes treatment. On the basis of this, an optimum degradation of ACE solution was achieved when 5 mg/ L hydrogen peroxide was applied in the jet loop hydrodynamic cavitation system as currently designed. Addition of a higher concentration of hydrogen peroxide up to 10 mg/ L did not produce an improvement in the extent of degradation at the end of the (60 minutes) treatment time. The benefits of effective application of hydrogen peroxide during the degradation of ACE solution in the jet loop hydrodynamic cavitation system includes the reduction of the energy demand as well as decreased degradation time. The reduction in effectiveness on the addition of excessive hydrogen peroxide (more than 5 mg/ L) is primarily due to the scavenging effects of hydrogen peroxide on the hydroxyl radical or the recombination reaction of the hydroxyl radical (Stocking et al., 2011). In the next section, the combination of hydrogen peroxide with Fenton catalyst (Iron (II) sulfate or gnZVI) was

considered in order to ensure efficient degradation of ACE solution in jet loop hydrodynamic cavitation system.

6.5.5 Application of the optimum conditions during the degradation of acetaminophen in the jet loop hydrodynamic cavitation system

A combination of the previously achieved optimum conditions were applied to the degradation of ACE in the jet loop hydrodynamic cavitation system (pH 2, 400 kPa, 10 L of 10 mg/ L ACE, 4 mm orifice plate hole size, 5 mg/ L hydrogen peroxide, 60 minutes, n = 3) by the application of either iron (II) sulfate or gnZVI (10 mg/ L). During this investigation, it appeared that significantly high quantities of the intermediates were generated at 10 minutes treatement time. Thereafter, its degradation was followed up with the corresponding degradation of ACE until the appearance of isosbestic points (Appendix 5 and Appendix 6) at 40 minutes treatment time. The appearance of isosbestic points on the UV spectrograph of degraded ACE is an indication that mixtures of at least residual two compounds (ACE and intermediate) exist in the effluent solution. Therefore, the intermediate product (ACE-OH) and a small quantity of un-reacted ACE solution were apparently contributing to the UV absorptions. The bar chart representing the achieved % degradation of ACE solution in the jet loop hydrodynamic cavitation system is present in Figure 6.12.

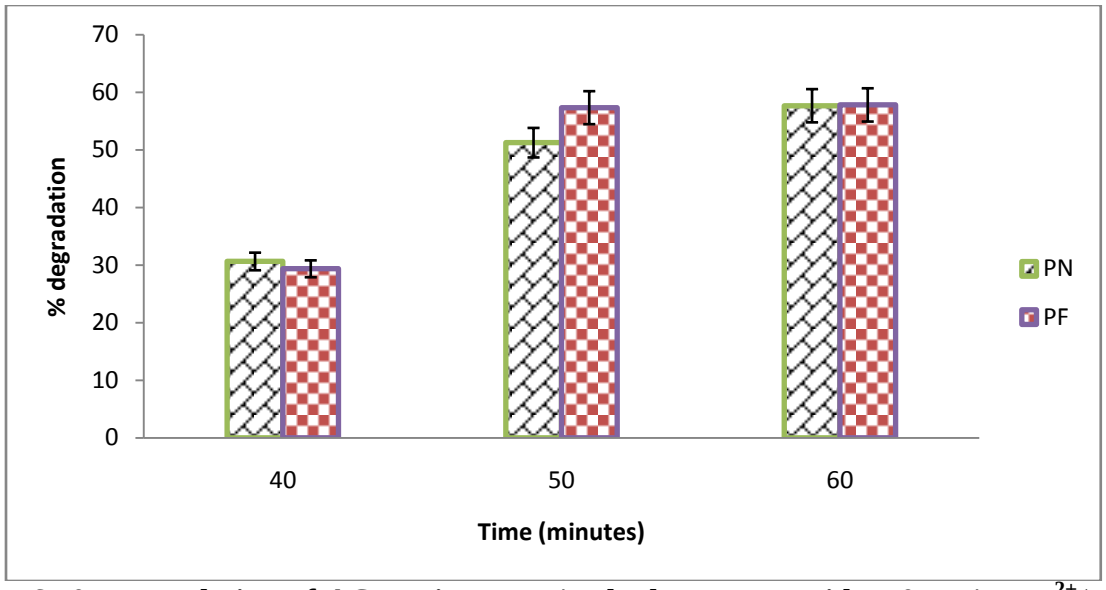

Figure 6.10: Degradation of ACE using 5 mg/ L hydrogen peroxide, 10 mg/ L Fe^{2+}(PF) or 10 mg/ L gnZVI (PN) in the jet loop hydrodynamic cavitation system (400 kPa, 4 mm orifice hole size, 10 L, 60 minutes, pH 2, n = 3)

Approximately, 57.79% or 57.65% degradation of ACE were respectively achieved when the jet loop hydrodynamic cavitation system (pH 2, 400 kPa, 10 L of 10 mg/ L ACE, 4 mm orifice plate hole size, 60 minutes, n = 3) was applied in their combination with 5 mg/ L hydrogen peroxide and either iron (II) sulfate (10 mg/ L) or gnZVI (10 mg/ L) to treat ACE in simulated wastewater. The synergistic effect of application of either the suitable Fenton reagents with H_2O_2 in combination in the jet loop hydrodynamic cavitation system at the optimum conditions can be predicted through the understanding of their reaction mechanism (Babuponnusami and Muthukumar, 2014; Gogate and Patil, 2015) which will be discussed in the Section 6.5.6.

6.5.6 Reaction mechanism and mineralisation study

The generated hydroxyl radicals initiated the degradation of acetaminophen by forming a bond at the electron rich ortho position part of benzene ring and/ or the lone pair electron on the amide side chain. Subsequently, ACE would be broken down to a simpler form through the cleavage in one or two of the unsaturated locations. The total organic carbon (TOC) was measured as described in Section 3.7.8, to determine the reduction in the organic carbon and the extent of mineralisation of the ACE solution during its treatment in the jet loop hydrodynamic cavitation

(Appendix 7). The calculated % TOC reduction which was measured when 5 mg/ L hydrogen peroxide, combined with either 10 mg/ L iron (II) sulfate or 10 mg/ L gnZVI was applied during the degradation of acetaminophen in the jet loop hydrodynamic cavitation (pH 2, 400 kPa, 10 L of 10 mg/ L ACE, 4 mm orifice plate hole size, 60 minutes, n = 3) is presented in Figure 6.14.

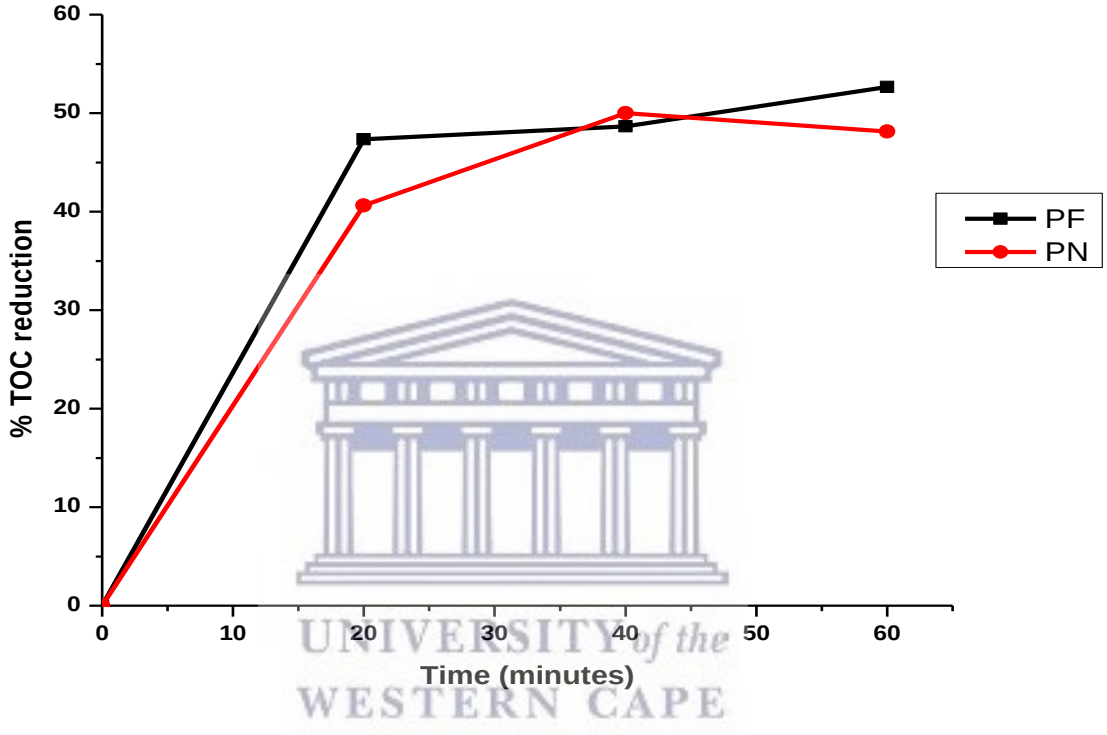

Figure 6.11: % Total Organic Carbon reduction during the treatment of acetaminophen solution with 5 mg/ L H_2O_2 in combination with 10 mg/ L Fe^{2+}(PF) or 10 mg/ L gnZVI (PN in the jet-loop hydrodynamic cavitation system (400 kPa, 4 mm orifice hole size, 10 L of 10 mg/ L ACE, 60 minutes, pH 2, n = 3)

It can be observed (Figure 6.14) that the TOC reduction after the first 20 minutes of ACE solution mineralisation was about 47% or 40% respectively when iron (II) sulfate or gnZVI was used as catalyst in the degradation of acetaminophen in the jet loop hydrodynamic cavitation system. Meanwhile, after 60 minutes of treatment in the same system, the %TOC reduction was approximatel 48% or 53% respectively for iron (II) sulfate or gnZVI application. The TOC

values are in agreement with the extent of degradation achieved when iron (II) sulfate (57.79%) or gnZVI 57.65%) was used as catalyst during the treatment of acetaminophen in the jet loop hydrodynamic cavitation system as obtained in Section 6.5.5. It can be deduced that the majority of the organic carbon containing compounds were converted to CO_2 leading to a rapid increased mineralisation of an ACE solution in the jet loop hydrodynamic cavitation system. On this note, it can be reported that the continuous generation of the hydroxyl radical for 60 minutes in the jet loop hydrodynamic cavitation system led to the mineralisation of ACE solution. During the formation of nitrate and other inorganic minerals the parent compound (ACE) must pass through a sequence of organic chemical intermediate products. The identification of the intermediate products and generation of a plausible mechanism of ACE mineralisation was done with FT-IR and LC-MS analytical instruments which were described in Section 3.7.6 and 3.7.8 respectively. The identified peaks of spectra during FT-IR analysis of ACE and intermediate products are presented in Table 6.4., while the FTIR spectra are presented in Appendix 8.

Table 6.4: The indentified peaks in FT-IR of acetaminophen and intermediate products formed during the treatment in the jet loop hydrodynamic cavitation system (400 kPa, 5 mg/ L H_2O_2, 4 mm orifice hole size, 10 L of 10 mg/ L ACE, 60 minutes, pH 2, 10 mg/ L Fe^{2+}(PF) or 10 mg/ L gnZVI (PN), n = 3)

Identified FT-IR peaks	C-N (stretch)	C=C (benzyl)	C=O (carbonyl)	C-H (Sp^3)	N-H (2^0 amide)	O-H (benzylic)
Acetaminophen (PF0 or PN0)	C-N at 1234 cm^{-1}	C=C at 1593 cm^{-1}	C=O at 1659 cm^{-1}	C-H at 3105 cm^{-1}	N-H at 3320 cm^{-1}	
PF6	C-N at 1234 cm^{-1}	C=C at 1593 cm^{-1}	-	-	N-H at 3320 cm^{-1}	O-H at 3325 cm^{-1}
PN6	-	C=C at 1593 cm^{-1}	-	-	N-H at 3320 cm^{-1}	O-H at 3325 cm^{-}

The FT-IR peaks of pure ACE are found at 1234 cm^{-1}, 1593 cm^{-1}, 1659 cm^{-1}, 3105 cm^{-1} and 3320 cm^{-1} for the, C-N stretch, benzylic ring, carbonyl, alkane and secondary amide respectively.

However, after 60 minutes degradation in the jet loop hydrodynamic cavitation system for run PF6 (pH 2, 400 kPa, 10 mg/ L ACE, 10 L ACE, 4 mm orifice plate hole size, 5 mg/ L hydrogen peroxide, 60 minutes, n = 3) enhance by iron (II) sulfate (10 mg/ L), there were disappearance of FT-IR peaks at 1659 cm^{-1} (C=O) and 3105 (C-H) while the intense OH peak was observed at 3325 cm^{-1} (Appendix 9). There is possible addition of OH radical to the benzene side chain as earlier reported in Section 6.5.1. Besides, there may be a cleavage at C-N side chain. Likewise, the enhancement in the jet loop hydrodynamic cavitation system for run PN6 (pH 2, 400 kPa, 10 L of 10 mg/ L ACE, 4 mm orifice plate hole size, 5 mg/ L hydrogen peroxide, 60 minutes, n = 3) by gnZVI (10 mg/ L) was more efficient because there were disappearance of peaks at three locations (1234 cm^{-1}, 1659 cm^{-1} and 3105 cm^{-1}) during the 60 minutes treatment, there was also appearance of broad OH peak (Appendix 10). At this point, it is very likely that the ACE was broken down to the mineral nitrate with very small remnants of organic compounds. Mineralisation of ACE solution in the jet loop hydrodynamic cavitation system can be described in 5 different steps (a-e) as presented in Section 6.15.

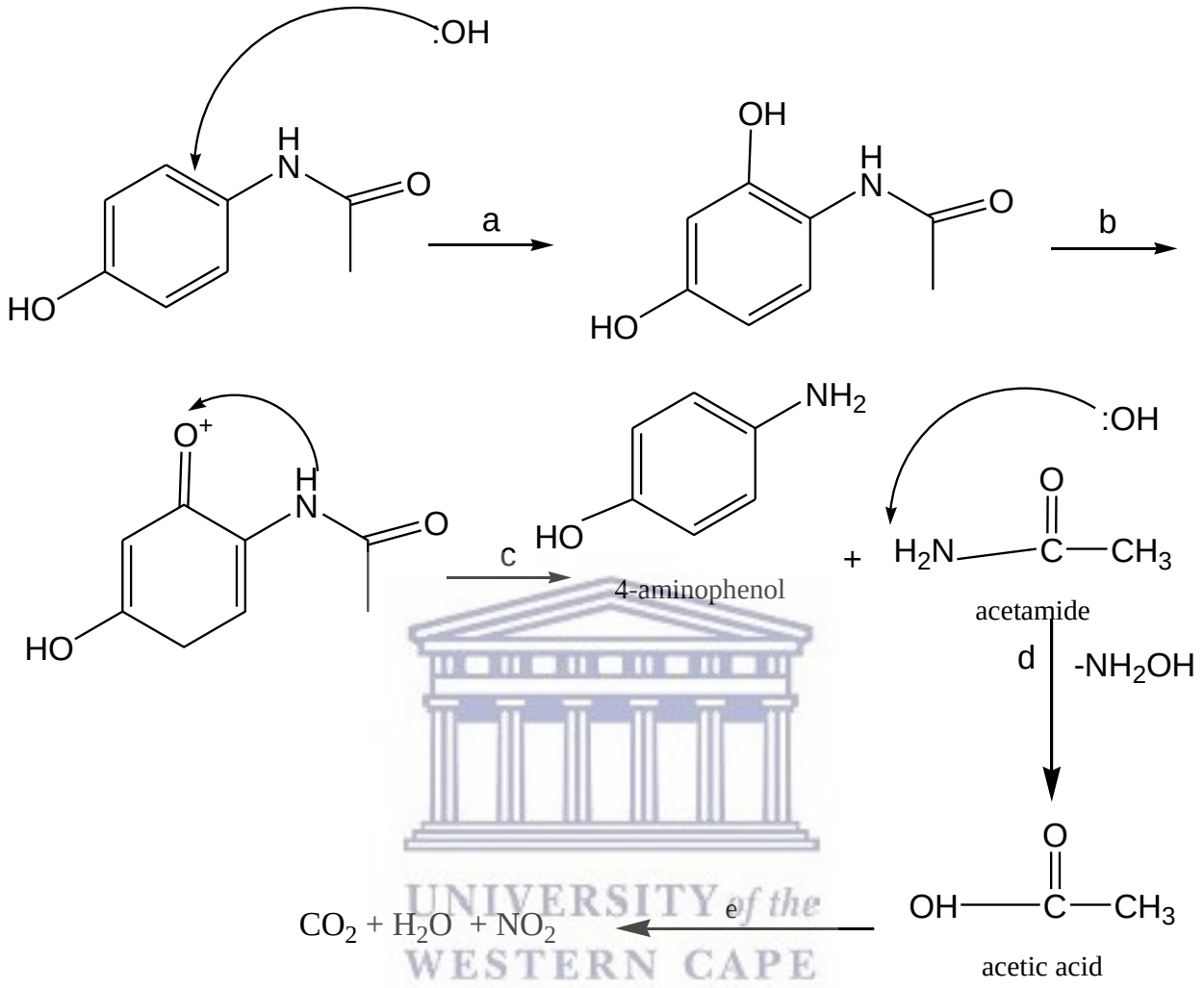

Figure 6.12: Reaction mechanism during the mineralisation of acetaminophen in jet loop hydrodynamic cavitation using the GC-MS data

The GC-MS analysis was carried out as described in Section 3.7.17. The dominant intermediates found from the attack on acetaminophen by hydroxyl radicals is N-(2,4-dihydroxylphenyl) acetamide (ACE-OH). This intermediate compound was formed when OH radical was attached to the ortho side position of benzene group in ACE (a). The protonation of the ACE causes instability in its structure. The phenolic proton immediately attacked the lone pair of electrons on NH of ACE (b). The products formed were (c) 4-aminophenol and acetamide. On one hand, an acetamide was oxidised to an acetic acid (d), which was further oxidised into carbon (iv) oxide

and water (e). The GC-MS spectrograph of ACE and the intermediate products detected after the degradation in the jet loop hydrodynamic cavitation system is presented in Appendix 11.

6.6 Chapter summary

Degradation of acetaminophen was carried out using the jet loop hydrodynamic cavitation system in combination with hydrogen peroxide and either iron sulfate or green nano zero valent iron. The application of only hydrogen peroxide (5 mg/ L) resulted in 49% degradation of acetaminophen solution (10 L of 10 mg/ L) in the jet loop hydrodynamic cavitation system at 60 minutes treatment. Meanwhile, the enhancement of the jet loop hydrodynamic cavitation system (pH 2, 400 kPa, 10 L of 10mg/ L ACE, 4 mm orifice plate hole size, 60 minutes, n = 3) with 5 mg/ L hydrogen peroxide combined with either iron (II) sulfate (10 mg/ L) or green nano zero valent iron (10 mg/ L) yielded 57.6% or 57.8% degradation respectively. Likewise 53% or 50% mineralisation was achieved when iron (II) sulfate (10 mg/ L) or green nano zero valent were respectively applied for the treatment acetaminophen in the combined system of jet loop hydrodynamic system, hydrogen peroxide. The degradation was achieved when the hydroxyl radical attacked the electron rich centers in the structure of acetaminophen leading to the production of essentially carbon (iv) oxide through the amide and carboxylic acid intermediates. The optimum amount of both hydrogen peroxide and green nano zero valent iron were thus successfully applied in the jet loop hydrodynamic cavitation system to achieve a high degradation of acetaminophen solution into its constituent mineral forms. Besides, a significant reduction in the amount of iron content in the treated acetaminophen wastewater was also reported for the first time by the application of green nano zero valent iron in place of iron sulfate as a Fenton catalyst. The residual iron can be easily removed with the aid of a bar magnet.

CHAPTER 7

Sequential Coagulation or Fenton oxidation followed by jet loop hydrodynamic cavitation as an alternative for industrial textile wastewater treatment

7.1 Overview

Complex textile wastewater effluents are opaque liquids with poor bio-degradability, high chemical stability and persistence. Conventional treatment of this wastewater is expensive and may lead to the generation of a large amount of unaccounted intermediate products and a heavily contaminated solid sludge. In the current studies, raw textile wastewater obtained from an industrial source was treated either by using Fenton oxidation or alum coagulation method. These primary treatments were followed by treatment in the jet loop hydrodynamic cavitation. The percentage COD removal during the alum coagulation or Fenton oxidation treatments were 94.8% or 97% respectively at their optimum conditions. The quantity of microbes in the alum coagulation treated wastewater effluent was reduced by 96% while that of Fenton oxidation was reduced by 98%. Likewise, the quality of sludge generated during alum coagulation was 37% of the treated wastewater effluent while that of Fenton oxidation was 22%. Meanwhile, Fenton oxidation treated textile wastewater became biodegradable because the BOD/ COD increased from 0.13 to 0.43 during the treatment while the increased BOD/ COD for alum coagulation (from 0.086 to 0.14) was insignificant in effecting the biodegradability of the textile wastewater effluent. On the further treatment (secondary) of alum coagulation treated textile wastewater in the jet loop hydrodynamic cavitation, the BOD/ COD increased to 0.32. The further treatment step using jet loop hydrodynamic cavitation showed the capacity for further improving the biodegradability of alum treated textile wastewater. Therefore, the Fenton oxidation has been demonstrated as an efficient primary treatment for textile wastewater effluent while the combination of jet loop hydrodynamic cavitation with either the alum treated or Fenton treated wastewater can deliver efficient treatment outcome.

7.2 Introduction

Textile products such as fibers, fabrics, yarns and thread are next only to food in term of human basic needs. The ever expanding textile industries have employed millions of people, enhanced gross domestic product (GDP) and generated foreign exchange in many countries (Keane and Willem, 2008). Besides, the textile manufacturing companies offer tremendous opportunities in term of economic development in low income countries because of their capability to offer a less costly labour advantage. Based on its global demand which currently stands above $18 trillion, the textile industry is an "investor's heaven" with a propensity for excellent returns on investment (Samonikov and Samonikov, 2013). The processes of manufacturing textiles such as scouring, bleaching, dyeing, washing and steaming involve expenditure of large volumes of water (Vajnhandl and Valh, 2014). About 200 L of water is used in the production of a kilogram (kg) of textiles with the consumption of a substantial amount of complex chemicals (Table 7.1).

Table 7.1: Water consumptions in textile manufacturing industries

Process	Water consumption (L/ 1000 kg of product)	Constituent	Wastewater characterization
Bleaching	2500- 25000	H_2O_2, NaOCl, Organic compound	High pH, TDS
Mercerisation	17000-32000	NaOH	High pH, BOD, soluble solid
Dyeing	10000-300000	Colour, Metal, Sulfide, Salts, Acidity/ Alkalinity, Form-aldehyde	Toxicity, COD, BOD, pH, TDS, colour
Printing	8000-16000	Urea, metal, solvents and colour	COD, BOD, pH, TDS, strong colour
Sizing	500-8200	Yarn waste, unused starch-base size,	COD and BOD
Desizing	2500-21000	Enzymes, starch, waxes and ammonia	COD, BOD and high temperature
Scouring	20000-45000	Disinfectants, insecticide residue, NaOH, surfactants, soap	Oily fats, BOD, high Ph
Finishing	4000-12000	Chlorinated compounds, resins, softeners	Dark colour, high temperature (70-80^{0}C)

Consequently, a large volume of wastewater is generated during textile manufacturing, with a corresponding high content of complex and toxic chemicals as well as bacterial load which causes a detrimental environmental impact (Pang and Abdullah, 2013; UNEP/AMAP, 2011; UNESCO, 2012; United Nation Water Analytical, 2009). The effect of these toxic chemicals include ulceration of skin, nausea, hemorrhage, reduction in dissolved oxygen, increase chemical oxygen demand (COD) as well as high biochemical oxygen demand (BOD) and excessive nitrate, phosphate and sulfate in effluents (Pang and Abdullah, 2013).

7.3 Treatment of textile wastewater

The major environmental concerns in textile wastewater effluent are the colour content (50-2500), BOD (100-4000 mg/ L) microbes and COD (150-10,000 mg/ L). It is very important to remove these contaminants to a large extent before discharging the wastewater effluent into the environment (Multani et al., 2014). The conventional treatment of wastewater which includes physical, chemical and biological methods of wastewater treatment have served as the bedrocks of clean water for municipalities for many years. However, the current advancement in analytical technologies has led to the detection of many toxic chemicals and pathogens in the treated water. Apparently, a single process (chemical, physical or biological) by itself is not effective for the removal of all dyes and chemicals used in the textile industry (Ghaly et al., 2013).

7.3.1 Conventional Treatment of Textile Wastewater

The application of chemical oxidation for the removal of environmental toxicants in textile wastewater is considered inefficient and very expensive due to the formation of unquantifiable intermediate products (Arslan et al., 2016). Besides, it has been observed that the intermediate products formed during various oxidation methods are often more toxic than the parent compounds and resistant to chemical decomposition (Liu et al., 2017). The conversion of these intermediate products into harmless inorganic compounds requires more energy, long reaction times and use of expensive chemical oxidants. Meanwhile, the physico-chemical methods such as coagulation and flocculation have been used for a long time because of their relative capital low cost and propensity for significant pathogen reduction (Angel, 2017). They are commonly applied prior to biological treatment for the removal of contaminants in textile wastewater, in a

well designed conventional treatment system. Coagulants such as aluminum sulfate, calcium hydroxide, ferric chloride and ferric sulfate are commonly applied in the primary treatment of wastewater. The increasing complexity of wastewater calls for stringent discharge policies and development of more efficient treatment technologies. The appropriate conventional method must be able to meet the recommended microbiological and chemical standards set by the regulatory authority at an inexpensive operational and maintenance cost (Pescod, 2004). Besides, it should be capable of removing heavy metals, colloidal/ suspended particles and degrade organic as well as remove inorganic components. The generation of large quantities and poor quality of sludge as well as frequent ineffectiveness are the greatest demerits of most of the conventional methods (Garcia-Segura et al., 2016; Hou et al., 2016). Besides, the options for low energy and cost effectiveness as well as short treatment times must be considered in the choice of a suitable treatment technology for highly persistent chemical compounds in textile wastewater (Mahamuni and Adewuyi, 2010). The iron salts are known for their use in coagulation and form heavier flocs at a relatively low toxicity and wider pH compared to aluminum salts (Sena et al., 2008). Consequently, application of iron salts as catalyst in Fenton oxidation for the treatment of toxic and biologically refractory organic contaminants in textile wastewater has effective treatment potential (Ghaly et al., 2013; Olalla, 2007).

7.4 Fenton oxidation for textile wastewater

The Fenton process involves the generation of active oxygen species from the reaction of peroxides (usually hydrogen peroxide) and iron II oxide. The hydroxyl radical (HO•) which is formed during Fenton oxidation is a powerful oxidant (2.7 V) which reacts non-specifically in acidic medium and/ or in neutral solutions (1.8 V). The oxidative properties of the hydroxyl radical have been utilised in the treatment of several persistent organic compounds among many other applications (Bagal and Gogate, 2014a; Benitez et al., 2011; Blanco et al., 2014). The activity of the OH radical in the Fenton process increases as the pH decreases until a certain optimum level of pH between 2 to 3.5 (Rahmani et al. 2015) . Therefore, appropriate pH control is essential for efficient degradation of persistent organic pollutants using Fenton oxidation (Benitez et al., 2001). Besides, the amount of iron (II) and hydrogen peroxide needed for the degradation of pollutants in Fenton process must be carefully optimised in a laboratory based

experiment to prevent their toxicity to aquatic organisms and negative impacts on secondary biological treatment stages (Babuponnusami and Muthukumar, 2014).

7.5 Experimental method

This chapter investigates an efficient and cost effective strategy for the treatment of textile wastewater effluent collected from a branch of a textile manufacturing company (Freudenberg Nonwovens (Pty Ltd), Cape Town, South Africa). Coagulation (Alum) and Fenton oxidation were comparatively studied as primary methods of wastewater treatment in terms of quantity and quality of sludge generated as well as efficiency of the entire procedure. Further treatment with hydrodynamic cavitation is also executed and the results are compared.

7.5.1 Primary treatment using alum coagulation of textile wastewater

A 20 L sample of the textile wastewater effluent (pH 5.76) was treated with a quantity (20 -1000 mg) of $Al_2(SO_4)_3$ (Alum) to establish the optimum amount of alum needed for the primary treatment of the collected textile wastewater effluent. The experimental condition for the primary treatment of textile wastewater using alum coagulation is presented in Table 7.2.

Table 7.2: Treatment of textile wastewater using alum coagulation (2 hours, 20 ^{o}C, 20 L)

Experimental code	Concentration of alum (mg/ L)	pH
AL2	20	6
AL4	40	6
AL8	80	6
AL10	100	6
AL20	200	6
AL30	300	6
AL40	400	6
AL50	500	6
AL100	1000	6
CPH2	100	2
CPH4	100	4
CPH6	100	6
CPH8	100	8
CPH10	100	10

The mixture was mechanically agitated for 10 minute in a calibrated plastic container and allowed to stand for the remaining part of the 2 hours reaction time. The distinct top clear layer was tapped off and the dark semi-solid sludge that settled out was also collected at the end of the reaction time for further treatment. Another experiment was set-up at the derived optimum amount of ($Al_2(SO_4)_3$) using the same condition (20 L) while the solution pH (2-10) was varied by using a 20% hydrochloric acid or 50% sodium hydroxide. Experimental condition for primary treatment of textile wastewater at varied pH is presented in Table 7.2. The mixture was mechanically agitated for 10 minute in a calibrated plastic container and allowed to stand for the remaining part of the 2 hours reaction time. The distinct top clear layer was tapped off and the dark semi-solid sludge was also collected at the end of the reaction time for further investigation. At the end of the two procedures (alum coagulation and pH variation), the amount of the treated textile wastewater and the residual sludge were gently tapped off from the container and measured using the industrial balance described in Section 3.7.16. Further quantification of the treated wastewater was done using COD, BOD and turbidity meter as described in Section 3.7.12, 3.7.13 and 3.8.4 respectively. Thereafter, the treated wastewater was collected and subjected to further treatment using the jet loop hydrodynamic cavitation system (pH 2, 400 kPa, 4 mm orifice plate hole size, 1 hour, n = 3) as described in Section 3.6.

7.5.2 Primary treatment of textile wastewater using Fenton oxidation

Samples of textile wastewater (20 L) from Freudenberg nonwovens (Pty ltd) were treated using Fenton oxidation (H_2O_2 / Fe^{2+}). The optimum pH as well as the concentration of hydrogen peroxide and iron (II) sulfate required to achieve efficient COD reduction during the treatment of textile wastewater have been reported to be dependent on the nature of the specific pollutant content treated wastewater (Angel, 2017; Garcia-Segura et al., 2016; Kos et al., 2010). In the current study, the optimum pH for the Fenton treatment of textile wastewater was detected by varying the initial pH of the collected wastewater from 2 to 4 when the H_2O_2 concentration was 40 mg/ L and that of $FeSO_4.7H_2O$ was 800 mg/ L. The experimental conditions for Fenton treatment of the textile wastewater in the current investigation is presented in Table 7.3.

Table 7.3: Experimental conditions for Fenton oxidation treatment of textile wastewater (2 hours, 20 ^{o}C, n = 3)

Experimental code	Ph	Hydrogen peroxide (mg/ L)	$Fe(SO_4)_2$ (mg/ L)
FPH20	2.0	40	800
FPH25	2.5	40	800
FPH30	3.0	40	800
FPH35	3.5	40	800
FPH40	4.0	40	800
1HPE	2.5	10	800
2HPE	2.5	20	800
3HPE	2.5	30	800
4HPE	2.5	40	800
5HPE	2.5	50	800
10HPE	2.5	100	800
1FE	2.5	40	100
2FE	2.5	40	200
4FE	2.5	40	400
8FE	2.5	40	800
10FE	2.5	40	1000
20FE	2.5	40	2000

The concentrations of hydrogen peroxide were also varied between 10 to 100 mg/ L, at 800 g $FeSO_4.7H_2O$ and pH 2.5. Thereafter, the $FeSO_4.7H_2O$ concentration was varied while maintainning constant concentration of H_2O_2 at 40 mg/ L and wastewater pH at 2.5. The mixture was mechanically stirred with the aid of glass rod for 10 minute and allowed to stand for the remaining part of the 2 hours to allow complete reaction and formation of distinct layers. The textile wastewater formed two distinct layers with a clearer top layer which was decanted off. The amount of the treated textile wastewater and the residual sludge were measured using a balance. Further evaluation of the treated wastewater quality was done by measuring the turbidity, COD and BOD. Thereafter, the treated wastewater was subjected to further treatment using jet loop hydrodynamic cavitation system as described in the next section (Section 7.4.3).

7.5.3 Secondary treatment of textile wastewater using jet loop hydrodynamic cavitation

The treated real textile wastewater effluents collected from Freudenberg Nonwovens (Pty ltd), which were recovered from the preceding primary treatments (alum coagulation and Fenton oxidation) were separately subjected to further treatment in the jet-loop hydrodynamic cavitation system (pH 2, 400 kPa, 4 mm orifice plate hole size, 1 hour). The samples were subsequently analysed for chemical oxygen demand (Section 3.7.12), biochemical oxygen demand (Section 3.7.13), pH, turbidity and microbiology testing with a dilution plate counting method (Section 3.7.14).

7.6 Results and Discussion

The treatment of real textile wastewater effluent is usually performed in phases, starting from primary through secondary to tertiary stages and sometime final pH adjustment. The treatment method chosen should produce a low quantity of non-toxic sludge and the treated wastewater should be non-toxic to micro organisms so as to allow further treatment using biological organisms, followed by safe discharge as well as biodegradability. An effective method for primary treatment of persistent chemicals content of textile wastewater effluent should have the capacity for removal of inherent high turbidity, TDS, COD and BOD at minimum application of energy. In the current studies, the investigation was conducted to compare alum coagulation with Fenton oxidation as primary treatment method for the reduction of COD and BOD as well as for the removal of persistent organic contaminants in textile wastewater effluent. Table 7.4., gives the characteristics of the untreated real textile wastewater collected from the Freudenberg Nonwovens (Pty. Ltd).

Table 7.4: Characterisation of the untreated textile wastewater effluent (n = 3)

Analytical Test	Values
Turbidity (mg/ L)	4250
pH	5.65
Conductivity (µS/cm)	45
Bacterial count (CFU)	75 000
Biological Oxygen Demand (BOD) (mg/ L)	380
Chemical Oxygen Demand (COD) (mg/ L)	3222 - 4556

7.6.1 Primary Treatment using Alum Coagulant

Alum ($Al_2(SO_4)_3$) is a traditional coagulant with efficient turbidity and COD removal. However, excessive application may be a deterrent to the cost effectiveness of its application in industrial wastewater treatment. Therefore, the determination of the optimum amount of alum is very important to prevent expensive or excessive chemical application in order to achieve a suitable wastewater treatment outcome. In the current investigation, a varied amount of alum (20 -1000 mg) was applied for the primary treatment of textile wastewater effluent in order to determine the optimum amount of alum that is required for the reduction of COD in the sample of textile wastewater effluent (pH 6). After adding the alum (20 ^{o}C), the wastewater effluent was stirred manually for 10 minutes with a long glass rod and allowed to stand for 2 hours. The clear uppermost layer of the treated wastewater was gently tapped off and subjected to COD analysis as described in Section 3.7.12. The bar chart of the % COD removal achieved for different alum dosages is presented in Figure 7.1.

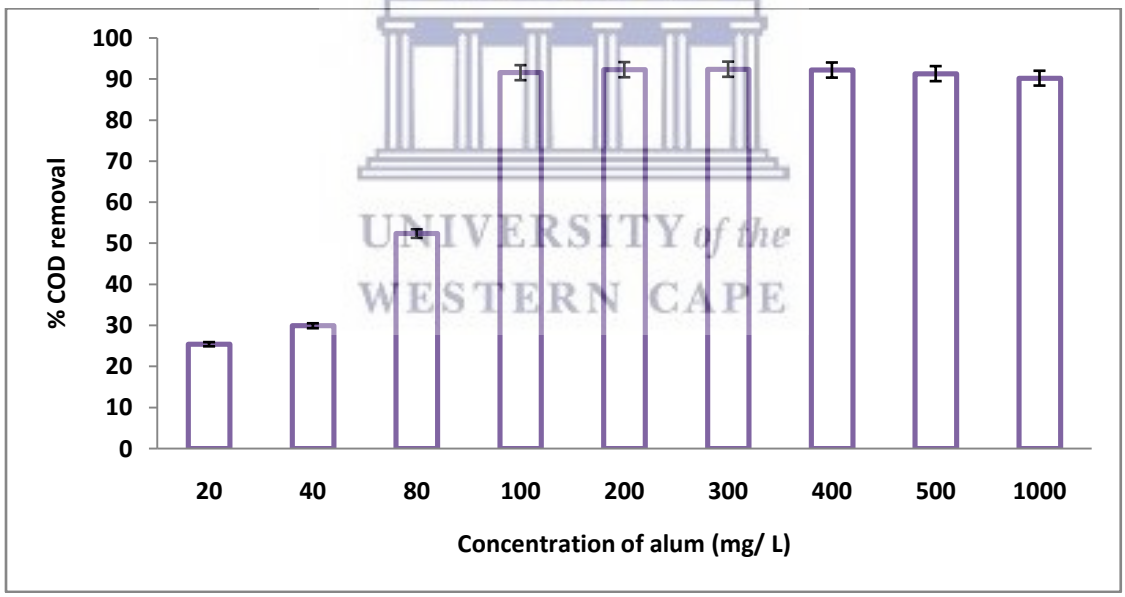

Figure 7.1: Optimisation of the amount of alum salt ($Al_2(SO_4)_3$) used for coagulation primary treatment of textile wastewater (pH 6, 20 ^{o}C, 20 L, 2 hours, n = 3)

The increased amount of positively charged species derived from the alum dosage favoured the precipitation of aluminum hydroxide and the consequential alteration or destabilisation or transformation of the negatively charged particulate, soluble salt and/or colloidal contaminants

which invariably resulted to settleable flocculants. It was observed that the addition of alum caused marginal but continuous increases in the % COD removal until the optimum concentration of alum (300 mg/ L) when the % COD removal was at its maximum. Thereafter, no further COD removal was obtained despite the increased alum dosage. The efficiency of this method is very high and likewise, the possibility of treating wastewater at an optimum dosage. The continuous addition of alum above 300 mg/ L caused the reduction in efficiency of the process and resulted in an unwanted effect on the electrical conductivity of the textile wastewater effluent. The effect of alum addition on the electrical conductivity of the treated wastewater is presented in Table 7.5.

Table 7.5: Effect of the amount of alum salt ($Al_2(SO_4)_3$) on COD, electrical conductivity

CODE	Amount of alum (mg/ L)	COD (mg/ L)	% COD removal	Conductivity (µS/cm)
AL0	0	4556	0.00	45
AL2	20	3397	25.45	200
AL4	40	3192	29.94	108
AL8	80	2170	52.37	82
AL10	100	385	91.55	62
AL20	200	352	92.27	74
AL30	300	347	92.38	84
AL40	400	356	92.19	92
AL50	500	396	91.31	106
AL100	1000	446	90.21	144

A 92.38% COD reduction was achieved when an amount of $Al_2(SO_4)_3$ equal to 300 mg/ L was applied for the treatment of 20 L textile wastewater effluent at the initial COD of 4556 mg/ L. There was decreased electrical conductivity (EC) in the treated wastewater as the concentration of applied $Al_2(SO_4)_3$ increased. The lowest value of EC was recorded when an amount of $Al_2(SO_4)_3$ equal to 100 mg/ L was applied to the textile wastewater effluent. At this point, the percentage COD removal was optimum (52.37% to 91.55%). And a further addition of $Al_2(SO_4)_3$ leads to a slight increase in COD and EC. The increased EC was expected because a significant amount of the applied alum coagulant went into solution and subsequently

contributed to EC. The high EC has a direct proportionality with the total dissolvable solid (TDS) and may impact negatively on the efficiency of the treatment method (Wang et al., 2013). Therefore, it is imperative to optimise the amount of coagulant used in order to limit the EC, TDS increases and prevent unnecessary investment in the chemical coagulant as well as improve the economic efficiency of the process. The effectiveness of COD removal in treated water is dependent on the amount of the applied coagulant and as well as pH (Klimiuk et al., 1999). The pH of wastewater effluent is an important parameter with a strong influence on the performance of a coagulant (alum). Consequently, the specific optimum pH was investigated further in the current study.

7.6.2 Effect of pH on the coagulation of textile wastewater using Alum

Acidity or alkalinity of a wastewater is a determinant of the effectiveness of the treatment process. The pH influences the effectiveness of the coagulation process through the control of speciation of both the coagulant and contaminants as well as their solubility in the wastewater effluent (Wang et al., 2013). According to the current investigation, a 20 L of textile wastewater was treated using 100 mg/ L of alum as described in Table 7.3. The effect of pH (100 mg/L, $Al_2(SO_4)_3$, 20 ^oC, 20 L, 2 hours, n = 3) on the COD removal during the alum coagulation treatment of textile wastewater is presented in Figure 7.2.

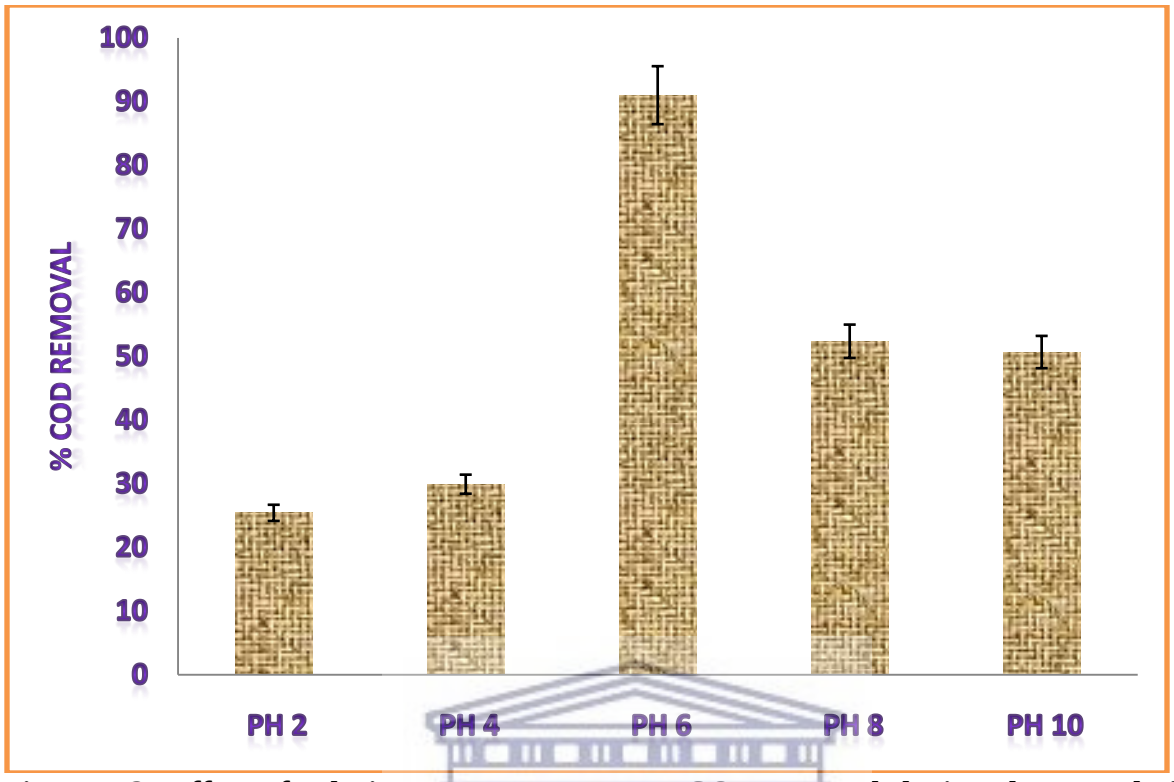

Figure 7.2: Effect of solution pH on percentage COD removal during the coagulation of textile wastewater using alum salt (100 mg/ L Al2(SO4)3, 20 oC, 20 L, 2 hours, n = 3).

The pH 6 was the optimum for the removal of COD in textile wastewater using alum ($Al_2(SO_4)_3$) coagulation. There was an increase in the % COD removal from 25.44% to 29.94% when the pH of the wastewater was increased from 2 to 4 respectively. The optimum COD removal of 91.00% was achieved when 100 mg/ L alum was added to 20 L of textile wastewater at pH 6. Meanwhile, the % COD removal decreased to 52.3% and 50.68% when the pH was increased to 8 and 10 respectively. The application of alum coagulation in wastewater treatment is limited because its efficiency depends on a very narrow pH range (Dalvand et al., 2016). The solution pH was reported to have significant role in the determination of floc strength and recovery factors during wastewater treatment (Ma et al., 2012). The floc strength for alum coagulation can be said to be strongest at pH 6. Furthermore, since the floc strength is closely related to the balance of attraction and repulsion between the particles, the near charge neutrality at pH 6 is therefore favourable to the coagulation mechanism and consequently high % COD removal was achieved. Despite the success of alum coagulation as a primary treatment method for the removal of COD, the alum coagulation is inefficient for the treatment of heavily polluted wastewater

because of the generation of a large volume of heavily contaminated sludge during the treatment procedure (Frederick, 2016; Keeley et al., 2014). A primary treatment method for textile wastewater effluent must be capable of removing the turbidity, COD and BOD efficiently and it must also generate a low quantity of nontoxic and biodegradable sludge.

7.7 Application of Fenton oxidation for the primary treatment of textile wastewater

A very strong oxidant such as the hydroxyl radical which is used in the advanced oxidation processes (AOPs) is required in the primary treatment of textile wastewater. The hydroxyl radical is formed through a chain of reaction processes which is initiated by the decomposition of hydrogen peroxide in the presence of bivalent iron salts (Angel, 2017). The Fenton oxidation is one of the AOPs which can serve the dual role of oxidation and coagulation during its application in the treatment of textile wastewater (Badawy and Ali, 2006). The influence of factors such as pH, amount of iron and hydrogen peroxide in the removal of COD during the primary treatment of textile wastewater using Fenton oxidation is investigated in this section.

7.7.1 Effect of initial pH of the textile wastewater effluent on the COD removal

The degree of acidity or alkalinity of wastewater (pH) plays a very important role in the efficiency of COD removal during the treatment of textile wastewater using Fenton oxidation. The determination of the optimum pH for a specific Fenton oxidation treatment is a very essential aspect of the treatment procedure. It is known that the Fenton oxidation is pH sensitive and the optimum pH is always between 2 and 4 (Li et al., 2016; Singh and Tang, 2013; Taha and Ibrahim, 2014). Therefore, the optimum pH for the treatment of textile wastewater was determined during the Fenton oxidation (800 mg/ L $FeSO_4.7H_2O$, 40 mg/ L H_2O_2, 20 L, 2 hour) of textile wastewater effluent collected from Freudenberg Nonwovens (Pty Ltd.) as presented in Table 7.4. The codes FPH20, FPH25, FPH30, FPH35 and FPH4 represent the treatment at pH 2, pH 2.5, pH 3.0, pH 3.5 and pH 4 respectively. The value of COD at varied pH during the treatment of textile wastewater effluent is presented in Table 7.7.

Table 7.6: Effect of initial pH on the COD removal during the Fenton oxidation treatment of textile wastewater (100 mg/ L $FeSO_4.7H_2O$, 40 mg/ L H_2O_2, and 20 L textile wastewater, 2 hour, n = 3)

CODE	Ph	COD (mg/ L)	% COD removal
FPH0	5.5	3397	00.00
FPH20	2	573	83.12
FPH25	2.5	422	87.58
FPH30	3	544	83.99
FPH35	3.5	588	82.69
FPH40	4	634	81.34

The highest % removal of COD was attained when the initial pH of the wastewater effluent was 2.5. Further increase in the pH resulted in a lower percentage COD removal. The % COD across the varied pH of the treated textile wastewater after 2 hours treatment is presented in Figure 7.3.

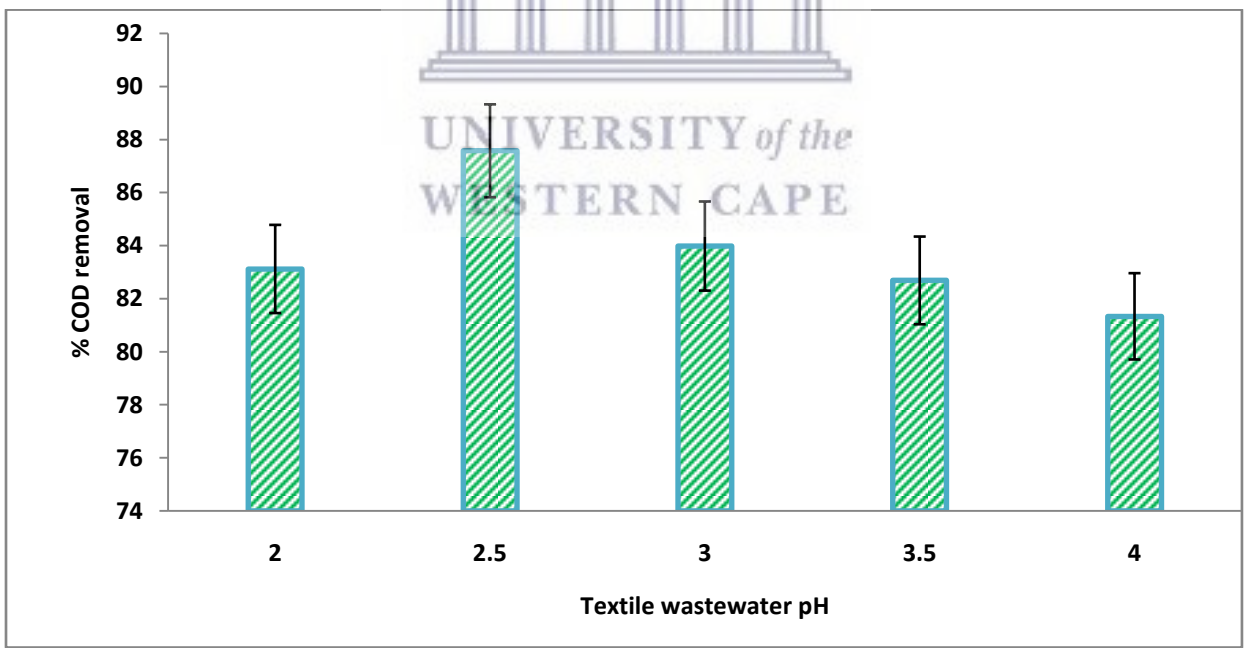

Figure 7.3: Effect of initial pH on the % COD removal during the Fenton oxidation treatment of textile wastewater (800 mg/ L $FeSO_4.7H_2O$, 40 mg/ L H_2O_2, and 20 L textile wastewater, 2 hour, n = 3)

It can be obsereved from Figure 7.3 that the pH of wastewater has a strong influence on the COD removal. The optimum percentage COD removal was ontained when textile wastewater was treated using the Fenton process (800 mg/ L $FeSO_4.7H_2O$, 40 mg/ L H_2O_2, 20 L, 2 hours, 3397 mg/ L initial COD, n = 3) at pH 2.5. The relatively high % COD removal (81.34% to 87.58%) which was observed across the investigated pH range (2-4) is a demonstration of the fact that the Fenton oxidation was possible at a relatively broad acidic pH range. The current investigation also revealed the effectiveness of Fenton oxidation in the primary treatment of acidic textile wastewater and as a better choice for primary treatment of textile wastewater compared to the alum coagulation (pH 6). Conversely, an excessive amount of hydrogen peroxide is capable of scavenging the produced hydroxyl radicals and therefore, lead to ineffective result (Andreozzi et al., 1999; Badawy and Ali, 2006). The optimum amount of hydrogen peroxide should be determined to prevent the demerit of its excessive application.

7.7.2 Effect of hydrogen peroxide concentration during the treatment of wastewater using Fenton oxidation

There is a need for determination of the exact the amount of hydrogen peroxide for effective treatment of a specific textile wastewater effluent. The pH of the freshly collected textile wastewater effluent was adjusted to 2.5 using 40% hydrochloric acid. Thereafter, the amount of hydrogen peroxide needed for the primary treatment of textile wastewater using Fenton oxidation was optimised by varying the concentration of the hydrogen peroxide from 10 mg/ L to 100 mg/ L at 800 mg/ L $FeSO_4.7H_2O$ for 2 hours as presented in Table 7.4. The codes 1HPE, 2HPE, 3HPE, 4HPE, 5HPE and 10HPE represent the application of 10 mg/ L, 20 mg/ L, 30 mg/ L, 40 mg/ L, 50 mg/ L and 100 mg/ L hydrogen peroxide respectively to the textile wastewater effluent collected from Freudenberg Nonwovens (Pty Ltd). The treated wastewater samples were collected and the COD analysis was done as described in Section 3.7.12. The effect of hydrogen peroxide concentration on the extent of COD removal over 2 hours treatment of textile wastewater effluent using Fenton oxidation is presented in Table 7.8.

Table 7.7: Effect of hydrogen peroxide concentration on the extent of COD removal in Fenton oxidation treatment of textile wastewater (20 L, pH 2.5, 800 mg/ L $FeSO_4.7H_2O$, initial COD 3222 mg/ L, n = 3)

CODE	Hydrogen peroxide (mg/ L)	COD (mg/ L)	% COD removal
0HPE	0	3222	0
1HPE	10	471	85.38
2HPE	20	479	85.13
3HPE	30	462	85.66
4HPE	40	439	86.37
5HPE	50	567	82.40
10HPE	100	678	78.96

The textile wastewater COD decreased as the amount of applied hydrogen peroxide increased until the optimum amount of hydrogen peroxide (40 mg/ L) when COD was 439 mg/ L. There was a decline in the COD after the optimum amount of hydrogen peroxide. A plot of the % COD reduction against the varied amount of hydrogen peroxide for the treated wastewater samples (pH 2.5, 20 L, initial COD 3222 mg/ L, n = 3) is presented in Figure 7.4.

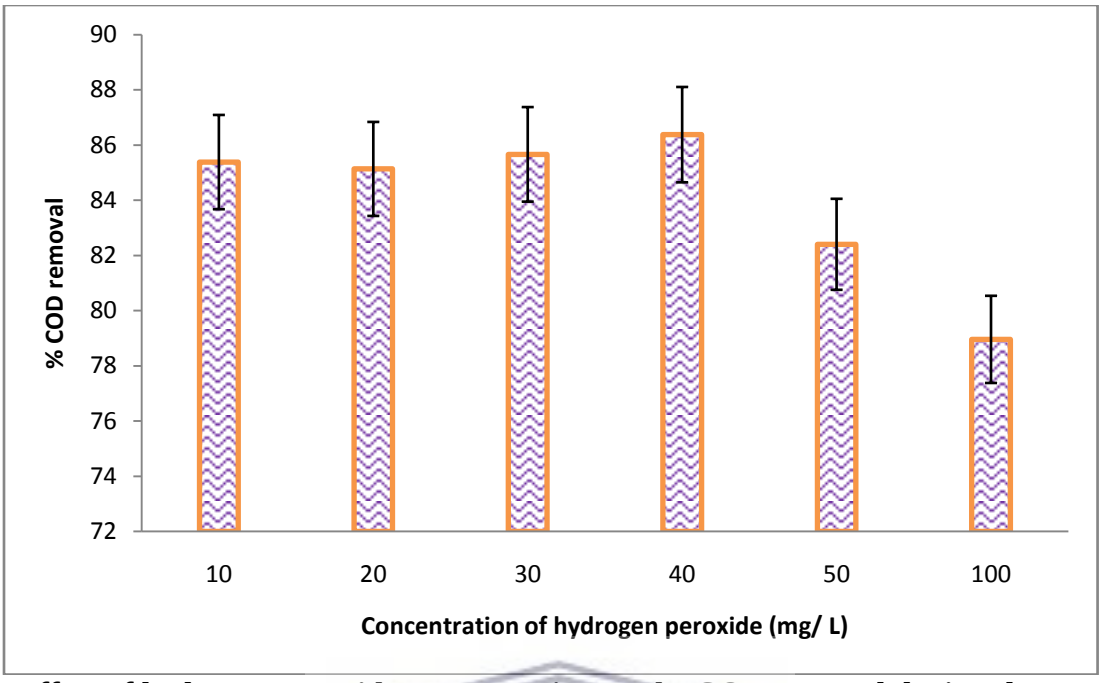

7.4: Effect of hydrogen peroxide concentration on the COD removal during the Fenton oxidation treatment of textile wastewater (20 L, pH 2.5, 100 mg/ L FeSO4.7H2O, n = 3)

It was observed that after 2 hours treatment of textile wastewater effluent using Fenton oxidation, that as the amount of hydrogen peroxide increased the % COD removal increased marginally until the optimum amount of hydrogen peroxide was achieved at 40 mg/ L when the COD removal was 86.37%. A further application of hydrogen peroxide (50 and 100 mg / L) above the optimum, leads to the reduction in the % COD removal (82.4 and 78.96%). The excessive application of hydrogen peroxide can lead to scavenging of the produced hydroxyl and consequently caused reduction of the COD removal in the textile wastewater (Babuponnusami and Muthukumar, 2014). The excessive application of elemental iron can also scavenge the hydroxyl radicals formed during the hydrolysis of the hydrogen peroxide. Therefore applying optimum amount of ferric iron is also necessary to prevent the reduction in the % COD and inefficient treatment outcome.

7.7.3 Influence of iron II sulfate concentration on the Fenton oxidation treatment of textile wastewater

The optimum amount of the ferric iron needed for the Fenton oxidation treatment of the textile wastewater (pH 2.5) was investigated by varying the concentration of iron ($FeSO_4.7H_2O$) from

100 mg/ L to 2000 mg/ L at a constant concentration of hydrogen peroxide (40 mg/ L). The effect of iron sulfate application on the COD removal during the treatment of textile wastewater is presented in Table 7.9.

Table 7.8: Effect of iron II sulfate application on COD removal during the Fenton oxidation treatment of textile wastewater (20L, pH 2.5, 40 mg/ L H_2O_2, n = 3)

CODE	Concentration of iron sulfate (mg/ L)	COD (mg/ L)	% COD removal
OFE	0	3397	0
1FE	100	471	85.38
2FE	200	479	85.13
4FE	400	462	85.66
8FE	800	439	86.37
10FE	1000	567	82.40
20FE	2000	678	78.96

1FE, 2FE, 4FE, 8FE, 10FE and 20FE stand for the application of 100 mg/ L, 200 mg/ L, 400 mg/ L, 800 mg/ L, 1000 mg/ L and 2000 mg/ L respectively in the treatment of textile wastewater effluent using Fenton oxidation. The COD decreased as the amount of applied iron sulfate increased until an optimum amount of iron sulfate (800 mg/ L) was applied to the textile wastewater. The bar chart representing the percentage COD reduction obtained during the current investigation is presented in Figure 7.5.

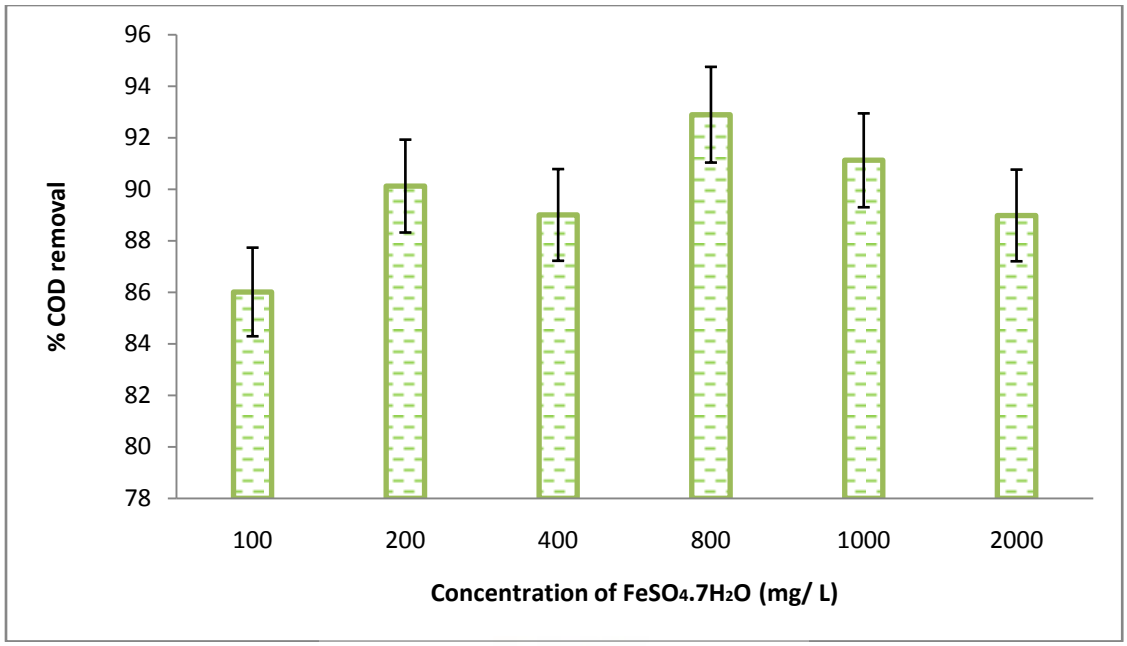

Figure 7.5: Effect of iron II sulphate on Fenton oxidation treatment of textile wastewater (20 L, pH 2.5, 40 mg/ L H2O2, 20 oC, 2 hours, n = 3).

In Figure 7.5 the percentage (%) COD values show that 800 mg/ L iron sulfate ($FeSO_4.7H_2O$) was the optimum dosage required for high COD removal in the textile wastewater at a fixed value of hydrogen peroxide and pH which were 40 mg/L and 2.5 respectively for 2 hours. However, a good COD removal was obtained at a lower concentration of the iron sulfate such as 100 mg/ L (85.38%). A low concentration of iron sulfate must be used in order to prevent the scavenging role of the iron II sulfate on the generated OH radicals during the Fenton oxidation treatment and also to prevent the excessive concentration of iron in the sludge. Apart from promoting the production of hydroxyl radicals for the oxidation of contaminants in the textile waste water, the iron content of the Fenton reagent also promotes coagulation. This is possible because the ferrous iron reacts in the aqueous phase to generate ferric hydroxide particles which form a readily adsorbed macroscopic flocs with capability for charge neutralisation and coagulation (Bustamante et al., 2001).

7.8 Quantity and quality of sludge in alum coagulation and Fenton oxidation treated textile wastewater effluent

Wastewater sludge contains microbes (such as viruses, bacteria and parasites) which can be responsible for diseases and severe environmental contamination. The quantity of microbes in sludge depends to a large extent on the applied wastewater treatment method. Many of the physico-chemical methods such as alum coagulation cause phase separation of solids and liquids in wastewater effluents while the advanced oxidation treatment methods like Fenton oxidation generates a very strong oxidant (hydroxyl radical) with capability for broad antimicrobial treatment through oxidation and consequent killing of pathogenic organisms as well as coagulating pollutants. The quantity of sludge generated after the respective optimum alum coagulation (300 mg / L alum, pH 6) and Fenton oxidation treatment (800 mg/ L $FeSO_4.7H_2O$, 40 mg/L H_2O_2, pH 2.5) was measured after treating 20 L of a separate, freshly collected, textile wastewater effluent. The sludge was measured using an industrial weighing balance described in Section 3.7.15. The microbial content of the textile wastewater effluent and that of the treated samples were determined using the dilution plate counting method as described in Section 3.8.14. The dilution plate count result for the triplicate investigation in the two processes is presented in Table 7.10.

Table 7.9: Weight and bacterial content of the treated textile wastewater and produced sludge (Kg)

Process	Slurry weight (Kg)	Number of colony forming unit (cfu) per Litre
Textile effluent	20.5 ± 0.4	75000 ± 55
Treated wastewater (coagulation)	12.9 ± 0.2	0
Treated wastewater (Fenton oxidation)	16.05 ± 0.2	0
Sludge weight (coagulation) / %	7.60 ± 0.4/ 37%	2800 ± 06
Sludge weight(Fenton)/ %	4.45 ± 0.3/ 22%	1410 ± 04
Cavitation (after coagulation)	0	0
Cavitation (after Fenton)	0	0

There was no microbial count in the treated wastewater after the alum coagulation or after the Fenton oxidation. There was equally no microbial count in the treated wastewater after the treatment in jet loop hydrodynamic cavitation (pH 2, orifice plate hole = 4 mm and inlet pressure

= 400 kPa). Thus, the amount of sludge generated during the alum coagulation primary treatment method was 37% of the treated wastewater while the amount of sludge generated during the Fenton oxidation process was only 22% of the treated wastewater. The microbial content of the sludge generated in the alum coagulation primary treatment method was 2800 ± 06 cfu/ L while that of the Fenton was 1410 ± 04 cfu/ L. It can be seen that there was a higher microbial count left in the alum coagulation treated sludge compared to that of the Fenton oxidation treated sludge. This is probably because the hydrogen peroxide in Fenton oxidation produces hydroxyl radicals which oxidised and consequently killed the microorganisms. Despite the potential of COD removal by both alum coagulation and Fenton oxidation from textile wastewater treatment, a secondary phase of treatment using hydrodynamic cavitation was applied to enhance the treatment outcome.

7.9 Secondary Treatment of Textile Wastewater with Hydrodynamic cavitation

A further analysis was done to investigate how the treatment in the jet loop hydrodynamic cavitation (pH 2, 4 mm orifice plate hole, 400 kPa inlet pressure, 1 hour, n = 3) has impacted on the treated wastewater. A freshly collected wastewater effluent (20 L) was subjected to either alum coagulation (100 mg / L alum, 2 hours, pH 6, n = 3) or to Fenton oxidation (800 mg/ L $FeSO_4.7H_2O$, 40 mg/ L H_2O_2, pH 2.5, 2 hours n = 3) at their separate optimum conditions (Section 7.4.1 and 7.4.2). The alum coagulated treated wastewater or Fenton oxidation treated wastewater were separately subjected to further degradation in the jet loop hydrodynamic cavitation system (pH 2, 4 mm orifice plate hole size, 400 kPa inlet pressure, 1 hour, n = 3) as described in Section 7.4.3.

7.9.1 Biodegradability of treated textile wastewater effluent

The raw textile wastewater effluent cannot be discharged in its untreated condition because of the low value of BOD/ COD ratio (0.083) as presented in Table 7.11.

Table 7.10: BOD/ COD of treated textile wastewater for the determination of biodegradability

Analysis	Raw wastewater	Primary treatment by alum coagulation	Primary treatment by Fenton oxidation	Secondary treatment (Alum coagulation + Cavitation)	Secondary treatment (Fenton oxidation + Cavitation)
COD (mg/ L)	4556	237	138	293	138
BOD (mg/ L)	380	32.4	60	94.4	46.7
BOD/COD	0.083	0.14	0.43	0.32	0.34
Biodegradation	No	No	Yes	Yes	Yes

A low BOD/ COD value (less than 0.3) of wastewater effluent render it non biodegradable and consequently unfit for discharge because of its high toxicity on aquatic organisms. The relationship between BOD/ COD, biodegradability and discharge is presented in Section 3.7.15. During the coagulation treatment, the BOD/ COD increased from 0.083 to 0.14. This increase was insufficient for the discharge approval of the treated textile wastewater effluent. Further treatment of the wastewater in the jet loop hydrodynamic cavitation (pH 2, 4 mm orifice plate hole size, 1 hour, 400 kPa inlet pressure) after primary alum coagulation treatment was able to increase the BOD/ COD ratio to 0.32. At this value the treated wastewater can be approved for discharge into streams. It can also be subjected to further treatment using microorganisms because it (wastewater effluent) is no longer toxic at BOD/ COD ratio of 0.32. Meanwhile, the Fenton oxidation treated wastewater was able to increase the BOD/ COD to 0.43 from 0.083. The wastewater effluent became suitable for biological treatment and discharge when it was treated using Fenton oxidation. This is another justification of Fenton oxidation superiority over alum coagulation as a primary method for textile wastewater effluent.

However, further treatment (of Fenton oxidation wastewater effluent) in the jet loop hydrodynamic cavitation system (pH 2, 4 mm orifice plate hole size, 400 kPa inlet pressure, 1 hour, n = 3) led to a slight decrease in the BOD/ COD (0.34). It can generally be stated that the

advanced oxidation process using Fenton oxidation (primary treatment) followed by jet loop hydrodynamic cavitation (secondary treatment) ensured biodegradability of the textile wastewater effluent.

7.10 Chapter summary

Alum coagulation or Fenton oxidation was applied for the treatment of heavily polluted textile wastewater. The two procedures are simple and effective primary treatment methods for the removal of insoluble matter, turbidity and COD in textile wastewater. The COD was reduced from 4556 mg/ L to 237 mg/ L (94.8%) when an amount of alum equal 100 mg / L was applied in the coagulation treatment of textile wastewater at pH 6 for 2 hours. Meanwhile, with Fenton oxidation, the COD was reduced from 4556 mg /L to 138 (97%) using 800 mg/ L $FeSO_4.7H_2O$, 40 mg/ L H_2O_2, pH 2.5 and 2 hours treatment time. The BOD/ COD ratio of 0.14 was obtained for wastewater effluent generated during the alum coagulation process. The value of BOD/ COD (0.14) shows thar alum coagulation treated wastewater has a poor biodegradability status. Therefore, the alum coagulation process is ineffective in the removal of soluble and persistent organic substances. Consequently, the effluent generated during the alum coagulation treatment method cannot be further treated in biological media or discharged into the environment because of its high toxicity. Additionally, the primary treatment method using alum coagulation generated 37% of microbial contaminated sludge. Fenton oxidation was presented as an alternative to alum coagulation as a primary treatment method for the textile wastewater effluent. At the end of the Fenton treatment, the BOD/ COD ratio of wastewater effluent generated was 0.43. This implies that the effluent generated in Fenton oxidation treatment is biodegradable. Meanwhile, the secondary treatment of either alum coagulation or Fenton oxidation in the jet loop hydrodynamic cavitation system yielded BOD/ COD values of 0.32 and 0.34 respectively. Thus, a novel combination of primary treatment using alum coagulation or Fenton oxidation with jet loop hydrodynamic cavitation system resulted in the efficient treatment of textile wastewater effluent.

CHAPTER 8

8.1 Introduction

The major findings and achievements of the study were summarized in this chapter. It also gives an overview of the previous chapters and the extent at which the research objectives outlined in the introductory chapter were accomplished. This was followed by contributions of the research to knowledge and recommendations for the future investigations relative to the treatment of persistent organic pollutants in wastewater using combined advance oxidation.

8.2 Overview

The specific objectives achieved by this study are: (i) Synthesis and characterisation of green nano zero valent iron (gnZVI) as a stable and efficient alternative to the conventional nano zero valent iron (nZVI) for use as a catalyst in the treatment of persistent organic pollutants (POPs) in wastewater. (ii) The determination of the optimum conditions for degradation of POPs as represented by orange II sodium salt solution in the jet loop hydrodynamic cavitation system. (iii) Investigation of the efficiency of the synthesised gnZVI as a Fenton catalyst for the degradation of orange II sodium salt in the jet-loop hydrodynamic cavitation system. (iv) Determination of the optimum conditions for degradation of POPs as represented by acetaminophen solution in jet loop hydrodynamic cavitation system. (v) Investigation of the effect of applying the synthesised gnZVI as a Fenton catalyst for the degradation of acetaminophen solution in the jet-loop hydrodynamic cavitation system. (vi) Determination the optimum amount of Fenton agent (iron II sulfate and hydrogen peroxide) required for the primary treatment of real textile wastewater effluent. (vii) Determination of the optimum amount of aluminium sulfate required for the primary treatment of real textile wastewater effluent. (viii) Investigation of the synergistic effect of a combination of Fenton oxidation and jet-loop hydrodynamic cavitation for the secondary treatment of real textile wastewater effluent.

To accomplish the set objectives, different experimental procedures were employed. Based on this, results were obtained as presented in the previous chapters. The research questions were summarily answered as follows:

- How can a stable and efficient nano zero valent iron be synthesised using aqueous extract of *H. caffrum*?

The synthesis of an efficient and stable novel green nano zero valent iron (gnZVI) was achieved through the simultaneous addition of the leaf extracts of *H. caffrum* (4 g/ L) and $NaBH_4$ (0.1 M) to the $FeCl_3.6H_2O$ (0.4 M) in a nitrogen inert environment. The high antioxidant activity and polyphenolic content of *H. caffrum* leaf extract enable capping, reducing and ensures the stability of the synthesised gnZVI in air and moisture. The synthesised gnZVI (**N**) possessed a higher surface area in comparison with the conventionally synthesised nZVI (**C**) obtained through $NaBH_4$ (0.1 M) solely reduction of $FeCl_3.6H_2O$ (0.4 M). The leaf extract of *H. caffrum* formed a metal-organic complex which protects the nano zero valent iron against oxidation in moist air and thereby enhances stability. The use of locally sourced environmentally benign and renewable material as described in this study will enhance efficiency and sustainability in the production of nano zero valent iron.

- What are the optimum conditions for decolouration of orange II sodium salt in jet loop hydrodynamic cavitation equipment?

Alone, the jet-loop hydrodynamic cavitation at 400 kPa inlet pressure and the orifice plates hole sizes of 2 mm was able to achieve 68.69 ± 1.2% decolouration of OR2 solution (10 L of 10 mg/ L, pH 2) during an hour treatment. Further investigations were performed on how jet loop hydrodynamic cavitation factors such as orifice sizes, inlet pressure, OR2 solution pH as well as its concentration influences the decolouration of OR2 dye solution.

The percentage decolouration were 68.69 ± 1.2%, 69.92 ± 1.5% and 69.59 ± 0.7% when the orifice plates hole sizes were 2 mm, 3 mm and 4 mm respectively. Therefore, approximately 70% decolouration was achieved with all the different orifice plates hole sizes. Consequently, the extent of decolouration of OR2 solution in the jet loop hydrodynamic cavitation in the current design is not affected by the hole sizes (2, 3 or 4 mm) in the orifice plates. The half-life for OR2 decolouration in the jet loop hydrodynamic cavitation equipment was 37.66, 36.67 and 36.47 minutes for orifice hole sizes 2, 3 and 4 respectively. The lowest time magnitude (decolouration half-life, $t_{1/2}$ = 36.47 minutes) was obtained during the decolouration of OR2 solution in the jet

loop hydrodynamic cavitation when the orifice hole sizes were 4 mm. Therefore, the optimum orifice hole sizes in the current design of jet loop hydrodynamic cavitation was 4 mm.

Besides, the extent of decolouration of OR2 solution (10 mg/ L, pH 2) during an hour treatment in the jet loop hydrodynamic cavitation equipment at inlet pressure 200 kPa, 300kPa, 400 kPa and 500 kPa was 12.8, 64.01, 69.37 and 9.3% respectively. Therefore, the optimum inlet pressure was observed at 400 kPa when the extent of OR2 decolouration was 69.37% within an hour treatment in the jet loop hydrodynamic cavitation equipment.

According to the current investigation, the percentage decolouration of OR2 solution (10 L of 10 mg/ L) over an hour treatment time in the jet loop hydrodynamic cavitation equipment (400 kPa, 4 mm orifice hole sizes) was 69.70, 32.06, 26.81, 17.89 and 8.9% when the solution pH was 2, 4, 6, 8 and 10 respectively. Consequently, the optimum decolouration of OR2 solution in the jet loop hydrodynamic cavitation was obtained at pH 2. Likewise, the influence of OR2 concentration on its decolouration in the jet loop hydrodynamic cavitation was also investigated. The extent of OR2 decolouration in the jet loop hydrodynamic cavitation (pH 2, 400 kPa, 4 mm orifice hole size, 1 hour, n = 3, 10 L) was 80.92%, 69.56% or 48.50% for OR2 concentration of 5 mg/ L, 10 mg/ L or 20 mg/ L respectively. Therefore, it can be reported that the decolouration of OR2 solution increases as its concentration decreases during the treatment in the jet loop hydrodynamic cavitation.

- What is the optimum amount of hydrogen peroxide that was needed for the degradation of orange II sodium salt in jet loop hydrodynamic cavitation equipment?

A quantities of hydrogen peroxide equal to 0.5 mg/ L, 1 mg/ L, 2 mg/ L, 5 mg/L or 10 mg/ L was applied for the treatment of OR2 solution (10 mg/ L) in the jet loop hydrodynamic cavitation (pH 2, 400 kPa, 4 mm orifice hole size, 1 hour, n = 3, 10 L). The decolouration of OR2 increased as the concentration of the hydrogen peroxide increased until the optimum decolouration (92.92%) was observed when the concentration of hydrogen peroxide was 1 mg/ L. Beyond the optimum concentration of hydrogen peroxide (2 mg/ L, 5 mg/ L and 10 mg/ L) a reduction in the extent of decolouration of OR2 was observed during an hour treatment in the jet loop hydrodynamic cavitation system.

- Does applying the synthesised green nano zero valent iron/ hydrogen peroxide in jet-loop hydrodynamic cavitation offer a greater efficiency compared to the iron (II) sulfate/ hydrogen peroxide combination during on the decolouration of OR2 solution?

The combination of hydrogen peroxide/ iron II sulfate during the decolouration of OR2 solution in the jet loop hydrodynamic cavitation system gave 97.05% decolouration and 12.38 minutes decolouration half-life ($t_{1/2}$) while hydrogen peroxide/ gnZVI combination gave 98.59% decolouration and 10.25 minutes decolouration half-life ($t_{1/2}$) during an hour treatment in the jet loop hydrodynamic cavitation. Therefore, it can be reported that the gnZVI/ hydrogen peroxide is a more efficient Fenton reagent in comparison to iron (II) sulfate/ hydrogen peroxide combination during the decolouration of OR2 solution in the jet loop hydrodynamic cavitation.

After the establishment of the influence of factors such as orifice hole sizes, pH of OR2 solution, solution pH, hydrogen peroxide/ iron II sulfate combination as well as hydrogen peroxide/ gnZVI combination on the treatment of OR2 in the jet loop hydrodynamic cavitation, a further research question was asked based on the treatment of acetaminophen in the jet loop hydrodynamic cavitation. According to the objectives of the current research, the influence of factors such as solution pH, application hydrogen peroxide to the treatment of acetaminophen in the jet loop hydrodynamic cavitation was investigated by asking the following questions.

- What is the optimum pH for the transformation of acetaminophen solution in jet loop hydrodynamic cavitation equipment?

The % increase in the UV absorbance intensity was used to estimate the extent of transformation of acetaminophen solution during the treatment in the jet loop hydrodynamic cavitation system. The % change in absorption was 35.17%, 30.08% and 9.58% for the acetaminophen solution at pH 2, 3 and 4 respectively. The largest amount of acetaminophen solution was transformed when the solution pH was 2. The optimum transformation of acetaminophen can be achieved in the jet-loop hydrodynamic cavitation (pH 2, 400 kPa, 10 L of 10 mg/ L ACE, 4 mm orifice plate hole size, 60 minutes, n = 3) at pH 2.

- Does applying hydrogen peroxide during the degradation of acetaminophen solution influence the extent of degradation in jet-loop hydrodynamic cavitation?

Hydrogen peroxide was applied to aid the degradation of acetaminophen during its treatment in the jet loop hydrodynamic cavitation (pH 2, 400 kPa, 10 L of 10 mg/ L ACE, 4 mm orifice plate hole size, 60 minutes, n = 3). 0.5 mg/ L, 1 mg/ L, 2 mg/ L, 5 mg/ L or 10 mg/ L of hydrogen peroxide was respectively for the degradation of acetaminophen in the jet loop hydrodynamic cavitation. According to the current finding, 5 mg/ L hydrogen peroxide was needed to achieve the optimum degradation of acetaminophen (49.25%) in the jet loop hydrodynamic cavitation. A substantial degradation of acetaminophen was achieved rather than transformation into intermediate products.

- Does the application gnZVI as a substitute to iron (II) sulfate lead to the reduction of the elemental iron in the acetaminophen solution during their treatment in the jet loop hydrodynamic cavitation?

10 mg/ L iron (II) sulfate or gnZVI were separately applied during the treatment of acetaminophen in the jet loop hydrodynamic cavitation (pH 2, 400 kPa, 10 L of 10 mg/ L ACE, 4 mm orifice plate hole size, 60 minutes, n = 3) and the magnet A magnetic bar (Science Wiz, 7/8" wide, 17/8" long and 3/8" thick) was used to filter off the iron before the elemental analysis (ICP-OES). The concentration of recovered elemental iron was 73.81 ± 11.06 or 49.76 ± 10.26 mg/ L for iron (II) sulfate or gnZVI respectively. According to the current investigation, it can be reported that there is a significant reduction in the elemental iron content of the sludge when the iron (II) sulfate was replaced with gnZVI during their application in the jet loop hydrodynamic cavitation.

Furthermore, the jet loop hydrodynamic cavitation was applied in combination with coagulation or Fenton oxidation for the treatment of raw textile wastewater and the following research question was applied.

- What are the optimum conditions for the primary treatment of raw real textile wastewater effluent using aluminum sulfate that is needed?

The amount of aluminum sulfate as well as the wastewater pH required for optimum treatment of raw textile wastewater was investigated. The concentration of alum sulfate was varied from 20 to 1000 mg/ L and the pH 2 to 10 was applied at a different time. The wastewater COD was reduced from 4556 to 347 mg/ L at the optimum when 300 mg/ L aluminum sulfate was applied to raw textile wastewater at pH 6.

- What is the optimum amount of Fenton reagent (iron sulfate and hydrogen peroxide) that is needed for the primary treatment of real textile wastewater effluent?

The raw textile wastewater pH (2 to 4), hydrogen peroxide (10 to 100 mg/ L) as well as iron (II) sulfate (100 to 1000 mg/ L) concentration was investigated to achieve the optimum condition for the treatment of textile wastewater using Fenton oxidation. The optimum Fenton oxidation treatment of textile wastewater was achieved when the COD removal was 87.57% at pH 2 or 86.37% at 40 mg/ L, hydrogen peroxide and 800 mg/ L iron (II) sulfate.

8.3 General Conclusion

The synthesis of an efficient and stable novel green nano zero valent iron (gnZVI) was achieved through the simultaneous addition of the leaf extracts of *H. caffrum* (4 g/ L) and $NaBH_4$ (0.1 M) to the $FeCl_3.6H_2O$ (0.4 M) in a nitrogen inert environment. The high antioxidant activity and polyphenolic content of *H. caffrum* leaf extract enable capping, reducing and ensures the stability of the synthesised gnZVI in air and moisture. The synthesised gnZVI (**N**) possessed a significant higher surface area in comparison with the conventionally synthesised nZVI (**C**) obtained through $NaBH_4$ (0.1 M) solely reduction of $FeCl_3.6H_2O$ (0.4 M). The leaf extract of *H. caffrum* formed a metal-organic complex which protects the nano zero valent iron against oxidation in moist air and thereby enhances stability. The use of locally sourced environmentally benign and renewable material as described in this study will enhance economic competiveness and sustainability in the production of nano zero valent iron.

The achievement of 98% decolouration and 74% mineralisation of orange II sodium salt in a jet loop hydrodynamic cavitation system (pH 2, 4 mm orifice hole sizes, 400 kPa, n = 3) in

combination with 1 mg/ L and 10 mg/ L hydrogen peroxide and gnZVI respectively was reported for the first. The mineralisation of orange II sodium salt solution in the current study causes significant reduction its total organic content of the orange II sodium salt through the generation of inorganic nitrate anions.

The gnZVI was also applied as a novel Fenton catalyst in the degradation of acetaminophen solutions in a jet loop hydrodynamic cavitation system. 49% degradation acetaminophen solution was achieved when 5 mg/ L hydrogen peroxide was applied to the solution in its jet loop hydrodynamic cavitation system (pH 2, 400 kPa, 10 L of 10mg/ L ACE, 4 mm orifice plate hole size, 60 minutes, n = 3). Meanwhile, the enhancement of hydrogen (5 mg/ L) with 10 mg/ L iron (II) sulfate or 10 mg/ L gnZVI during the degradation in the jet loop hydrodynamic cavitation resulted in 57.8% and 57.6% respectively. The treatment of acetaminophen in the jet loop hydrodynamic cavitations system also resulted into 53% and 50% mineralisation during the combine application of 5 mg/ L hydrogen peroxide with 10 mg/ L iron (II) sulfate or 10 mg/ L gnZVI respectively. 41% of the residual iron content in the treated effluent was removed with the aid of a magnetic bar.

The mineralisation of persistent organic pollutants as measured by the increased biodegradability in a heavily contaminated raw textile industry wastewater was achieved in a jet loop hydrodynamic cavitation reactor after their primary treatment using alum coagulation or Fenton oxidation. The primary treatment using alum coagulation produced 37% of the treated effluent as microbial contaminated (2800 cfu/ L) sludge while Fenton oxidation treated textile wastewater effluent produced 22% of the treated effluent sludge with about 50% reduction in microbial contamination (1410 cfu/ L). At the end of the alum coagulation and Fenton treatment, the BOD/ COD ratio of wastewater effluent generated were 0.14 and 0.43. This implies that the effluent generated in alum coagulation is very toxic and non biodegradable while the Fenton oxidation treated effluent is less toxic and biodegradable. Meanwhile, the secondary treatment of either alum coagulation or Fenton oxidation in the jet loop hydrodynamic cavitation system produced biodegradable effluent with BOD/ COD values of 0.32 and 0.34 respectively. The jet loop hydrodynamic cavitation equipment is very suitable for the secondary or tertiary treatment of persistent organic pollutants in the wastewater effluent. Thus, this method offers a low energy

and less chemical form of advanced oxidation process for the secondary and tertiary phase of wastewater treatment.

REFERENCES

Adeleye, A.S., Conway, J.R., Garner, K., Huang, Y., Su, Y., Keller, A.A., 2016. Engineered nanomaterials for water treatment and remediation: Costs, benefits, and applicability. Chem. Eng. J. 286, 640–662.

Adewuyi, Y.G., Khan, N.E., 2012. Modeling the Ultrasonic Cavitation-Enhanced Removal of Nitrogen Oxide in a Bubble Column Reactor. React. Kinet. Catalyis 58, 2397–2411.

Akbari, S., Ghanbari, F., Moradi, M., 2016. Bisphenol A degradation in aqueous solutions by electrogenerated ferrous ion activated ozone , hydrogen peroxide and persulfate : Applying low current density for oxidation mechanism. Chem. Eng. J. 294, 298–307.

Akhtar, M.F., Ashraf, M., Javeed, A., Anjum, A.A., Sharif, A., Saleem, A., Akhtar, B., Khan, A.M., Altaf, I., 2016. Toxicity Appraisal of Untreated Dyeing Industry Wastewater Based on Chemical Characterization and Short Term Bioassays. Bull. Environ. Contam. Toxicol. 96, 502–507.

Aksglaede, L., Juul, A., Leffers, H., Skakkebæk, N.E., Andersson, A.M., 2006. The sensitivity of the child to sex steroids: Possible impact of exogenous estrogens. Eur. Soc. Hum. Reprod. Embryol. 12, 341–349.

Ali, H., 2010. Biodegradation of synthetic dyes - A review. Water. Air. Soil Pollut. 213, 251–273.

Ali, M.G., Bastami, T.R., Ahmadpour, A., Eshaghi, Z., 2008. Environmental Application of Nanotechnology. Annu. Rev. Nano Res. 2, 439–493.

Altmann, J., Ruhl, A.S., Zietzschmann, F., Jekel, M., 2014. Direct comparison of ozonation and adsorption onto powdered activated carbon for micropollutant removal in advanced wastewater treatment. Water Res. 55, 185–193.

Andrade, C.H., de Freitas, L.M., de Oliveira, V., 2011. Twenty-six years of HIV science: An overview of anti-HIV drugs metabolism. Brazilian J. Pharm. Sci. 47, 209–230.

Andreozzi, R., Caprio, V., Insola, A., Marotta, R., 1999. Advanced oxidation processes (AOP) for water purification and recovery 53, 51–59.

Angel, M., 2017. Coagulation- flocculation sequential with Fenton or Photo-Fenton processes as an alternative for the industrial textile wastewater treatment. J. Environ. Manage. 191, 189–197.

Araujo, F.V.F., Yokoyama, L., Teixeira, L.A.C., Campos, J.C., 2011. Heterogeneous Fenton process using the mineral hematite for the discolouration of a reactive dye solution. Brazilian J. Chem. Eng. 28, 605–616.

Arslan, S., Eyvaz, M., Gürbulak, E., Yüksel, E., 2016. Review of State-of-the-Art Technologies in Dye- Containing Wastewater Treatment – The Textile Industry Case. INTECH.

Asahina, S., Uno, S., Suga, M., Stevens, S.M., Klingstedt, M., Okano, Y., Kudo, M., Schüth, F., Anderson, M.W., Adschiri, T., Terasaki, O., 2011. A new HRSEM approach to observe fine structures of novel nanostructured materials. Microporous Mesoporous Mater. 146, 11–17.

Asghar, A., Raman, A.A.A., Daud, W.M.A.W., 2015. Advanced oxidation processes for in-situ production of hydrogen peroxide/hydroxyl radical for textile wastewater treatment: A review. J. Clean. Prod. 87, 826–838.

Ashokkumar, R., Ramaswamy, M., 2014. Original Research Article Phytochemical screening by FTIR spectroscopic analysis of leaf extracts of selected Indian Medicinal plants. Int. J. Microbiol. Appl. Sci. 3, 395–406.

Ashton, L., Buxton, G. V, Stuart, C.R., 1995. Temperature dependence of the rate of reaction of OH with some aromatic compounds in aqueous solution. Evidence for the formation of a π-complex intermediate? J. Chem. Soc. Faraday Trans. 91, 1631–1633.

Babuponnusami, A., Muthukumar, K., 2014. A review on Fenton and improvements to the Fenton process for wastewater treatment. J. Environ. Chem. Eng. 2, 557–572.

Badawy, M.I., Ali, M.E.M., 2006. Fenton's peroxidation and coagulation processes for the treatment of combined industrial and domestic wastewater. J. Hazard. Mater. 136, 961–966.

Badmus, K.O., Coetsee-Hugo, E., Swart, H., Petrik, L., 2018a. Synthesis and characterisation of stable and efficient nano zero valent iron. Environ. Sci. Pollut. Res.

Badmus, K.O., Tijani, J.O., Eze, C.P., Fatoba, O.O., Petrik, L.F., 2016a. CHEMISTRY Quantification of Radicals Generated in a Sonicator.

Badmus, K.O., Tijani, J.O., Eze, C.P., Fatoba, O.O., Petrik, L.F., 2016b. Quantification of Radicals Generated in a Sonicator. Anal. Bioanal. Chem. Res. 3, 139–147.

Badmus, K.O., Tijani, J.O., Massima, E., Petrik, L., 2018b. Treatment of persistent organic pollutants in wastewater using hydrodynamic cavitation in synergy with advanced oxidation process. Environ. Sci. Pollut. Res. 25, 7299–7314.

Bae, S., Gim, S., Kim, H., Hanna, K., 2016. Effect of NaBH4 on properties of nanoscale zero-valent iron and its catalytic activity for reduction of p-nitrophenol. Appl. Catal. B Environ. 182, 541–549.

Bagal, M. V., Gogate, P.R., 2014a. Degradation of diclofenac sodium using combined processes based on hydrodynamic cavitation and heterogeneous photocatalysis. Ultrason. Sonochem. 21, 1035–1043.

Bagal, M. V., Gogate, P.R., 2014b. Wastewater treatment using hybrid treatment schemes based on cavitation and Fenton chemistry: A review. Ultrason. Sonochem. 21, 1–14.

Bahmani, P., Kalantary, R.R., Esrafili, A., Gholami, M., Jafari, A.J., 2013. ENVIRONMENTAL HEALTH Evaluation of Fenton oxidation process coupled with biological treatment for the removal of reactive black 5 from aqueous solution. J. Environ. Heal. Sci. Eng. 11, 1.

Baloul, Y., Aubry, O., Colas, C., Colas, C., 2016. Degradation of paracetamol in aqueous solution by non termal plasm.

Barati, A.H., Mokhtari-dizaji, M., Mozdarani, H., Bathaie, Z., 2007. Effect of exposure parameters on cavitation induced by low-level dual-frequency ultrasound. Ultrason. Sonochem. 14, 783–789.

Barik, A.J., Gogate, P.R., 2016. Degradation of 4-chloro 2-aminophenol using a novel combined process based on hydrodynamic cavitation, UV photolysis and ozone. Ultrason. Sonochem. 30, 70–78.

Barik, A.J., Gogate, P.R., 2018. Ultrasonics - Sonochemistry Hybrid treatment strategies for 2 , 4 , 6-trichlorophenol degradation based on combination of hydrodynamic cavitation and AOPs. Ultrason. - Sonochemistry 40, 383–394.

Barkhudarov, E.M., Kossyi, I. a, Kozlov, Y.N., Temchin, S.M., Taktakishvili, M.I., Christofi, N., 2013. Multispark discharge in water as a method of environmental sustainability problems solution. J. At. Mol. Phys. 2013, 6–7.

Benitez, F.J., Acero, J.L., Real, F.J., Roldan, G., Casas, F., 2011. A Comparison Study of the Removal of Selected Pharmaceuticals in Waters by Chemical Oxidation Treatments. World Acad. Sci. Eng. Technol. 78, 257–260.

Benitez, F.J., Acero, J.L., Real, F.J., Rubio, F.J., Leal, a I., 2001. The Role of Hydroxyl Radicals for the Decomposition of p-hydroxy Phenylacetic Acid in Aqueous Solutions. Water Res.

35, 1338–1343.
Benito, Y., Arrojo, S., Hauke, G., Vidal, P., 2005. Hydrodynamic Cavitation as a low-cost AOP for wastewater treatment : preliminary results and a new design approach. WIT Trans. Ecol. Environ. 80, 495–503.
Benzie, I.F.F., Strain, J.J., 1996. The Ferric Reducing Ability of Plasma (FRAP) as a Measure of ‘“ Antioxidant Power ”’: The FRAP Assay. Anal. Biochem. 239, 70–76.
Berger, C.M., Geiger, C.L., Clausen, C.A., Billow, A.M., Quinn, J.W., Brooks, K.B., 2006. International Conference on Remediation of Chlorinated and Recalcitrant Compounds, 5th. In: Evaluating Trichloroethylene Degradation Using Differing Nano- and Micro-Scale Iron Particles. p. c 23 ppr/1-c 23 ppr/8.
Bethi, B., Sonawane, S.H., Rohit, G.S., Holkar, C.R., Pinjari, D. V., Bhanvase, B.A., Pandit, A.B., 2016. Investigation of TiO2 photocatalyst performance for decolorization in the presence of hydrodynamic cavitation as hybrid AOP. Ultrason. Sonochem. 28, 150–160.
Bishop, E.J., Fowler, D.E., Skluzacek, J.M., Seibel, E., Mallouk, T.E., 2010. Anionic homopolymers efficiently target zerovalent iron particles to hydrophobic contaminants in sand columns. Environ. Sci. Technol. 44, 9069–9074.
Blanco, J., Torrades, F., Morón, M., Brouta-agnésa, M., García-montaño, J., 2014. Photo-Fenton and sequencing batch reactor coupled to photo-Fenton processes for textile wastewater reclamation : Feasibility of reuse in dyeing processes 240, 469–475.
Bother, C.J., 1993. Acoustic and Hydrodynamic 2.pdf. University of Natal.
Boxall, A.B.A., Rudd, M.A., Brooks, B.W., Caldwell, D.J., Choi, K., Hickmann, S., Innes, E., Ostapyk, K., Staveley, J.P., Verslycke, T., Ankley, G.T., Beazley, K.F., 2012. Review Pharmaceuticals and Personal Care Products in the Environment : What Are the Big Questions ? Environ. Health Perspect. 120, 1221–1229.
Braeutigam, P., Franke, M., Schneider, R.J., Lehmann, A., Stolle, A., Ondruschka, B., 2012. Degradation of carbamazepine in environmentally relevant concentrations in water by Hydrodynamic-Acoustic- Cavitation (HAC) 6, 2–10.
Brand-Williams, W., Cuvelier, M.E., Berset, C., 1995. Use of a free radical method to evaluate antioxidant activity. LWT - Food Sci. Technol. 28, 25–30.
Bustamante, H.A., Shanker, S.R.A.J., Pashley, R.M., Karaman, M.E., 2001. Interraction between cryptosporidium oocysts and water treatment coagulants. Pergamon 35, 3179–3189.
Cai, M., Su, J., Zhu, Y., Wei, X., Jin, M., Zhang, H., Dong, C., Wei, Z., 2015. Decolorization of azo dyes Orange G using hydrodynamic cavitation coupled with heterogeneous Fenton process. Ultrason. Sonochem. 28, 302–310.
Cao, D., Niu, K.Y., Yu, F., 2011. Economic Analysis on Pollution Control for Textile Industry. Adv. Mater. Res. 332–334, 1087–1092.
Cao, J., Clasen, P., Zhang, W., 2005. J. Mater. Res. J. Mater. Res. 20, 3238–3243.
Capocellia, M., Prisciandarob, M., Lanciac, A., 2014. Comparison between hydrodynamic and acoustic cavitation in microbial cell disruption. Chem. … 38, 13–18.
Carocci, A., Rovito, N., Sinicropi, M.S., Genchi, G., 2014. Reviews of Environmental Contamination and Toxicology, Reviews of environmental contamination and toxicology.
Cayuela, A., Ben??tez-Mart??nez, S., Soriano, M.L., 2016. Carbon nanotools as sorbents and sensors of nanosized objects: The third way of analytical nanoscience and nanotechnology. TrAC - Trends Anal. Chem. 84, 172–180.
Chakinala, A.G., Gogate, P.R., Burgess, A.E., Bremner, D.H., 2008. Treatment of industrial wastewater effluents using hydrodynamic cavitation and the advanced Fenton process.

Ultrason. Sonochem. 15, 49–54.
Chakinala, A.G., Gogate, P.R., Burgess, A.E., Bremner, D.H., 2009. Industrial wastewater treatment using hydrodynamic cavitation and heterogeneous advanced Fenton processing. Chem. Eng. J. 152, 498–502.
Charlier, C., Desaive, C.L., Plomteux, G., 2002. Human exposure to endocrine disrupters: consequences of gastroplasty on plasma concentration of toxic pollutants. Int. J. Obes. Relat. Metab. Disord. 26, 1465–1468.
Chhillar, N., Singh, N.K., Banerjee, B.D., Bala, K., Sharma, D., Chhillar, M., 2013. Organochlorine Pesticide Levels and Risk of Parkinson ' s Disease in North Indian Population. Neurology 2013, 6.
Chin, A., Bérubé, P.R., 2005. Removal of disinfection by-product precursors with ozone-UV advanced oxidation process. Water Res. 39, 2136–2144.
Chiou, C.T., Freed, V.H., Schmedding, D.W., Kohnert, R.L., 1977. Partition coefficient and bioaccumulation of selected organic chemicals. Environ. Sci. Technol. 11, 475–478.
Chiron, S., Minero, C., 2007. Occurrence of 2 , 4-Dichlorophenol and of 2 , 4-Dichloro-6-Nitrophenol in the Rhone River Delta (Southern France). Environ. Sci. Technol. 41, 3127–3133.
Chong, M.N., Sharma, A.K., Burn, S., Saint, C.P., 2012. Feasibility study on the application of advanced oxidation technologies for decentralised wastewater treatment. J. Clean. Prod. 35, 230–238.
Chu, L., He, S., Han, B., Pillai, S., 2011. Radiation Treatment of Wastewater for Reuse with Particular Focus on Wastewaters Containing Organic Pollutants.
Clara, M., Kreuzinger, N., Strenn, B., Gans, O., Kroiss, H., 2005. The solids retention time - A suitable design parameter to evaluate the capacity of wastewater treatment plants to remove micropollutants. Water Res. 39, 97–106.
Clark, R., Fisher, J.E., Sketris, I.S., Johnston, G.M., 2012. Population prevalence of high dose paracetamol in dispensed paracetamol/opioid prescription combinations: An observational study. BMC Clin. Pharmacol. 12, 1.
Colt, J.S., Rothman, N., Severson, R.K., Hartge, P., Cerhan, J.R., Chatterjee, N., Cozen, W., Morton, L.M., De Roos, A.J., Davis, S., Chanock, S., Wang, S.S., 2009. Organochlorine exposure, immune gene variation, and risk of non-Hodgkin lymphoma. Blood 113, 1899–1906.
Concerns, E., 2013. The Environmental, Health and Economic Impacts of Textile Azo Dyes, House of Parliament-Parliament of Science and Technology.
Corcoran, E., Nellemann, C., Baker, E., Bos, R., Osborn, D., Savelli, H., 2010. Sick Water? The central role of waste- water management in sustainable development. A Rapid Re- sponse Assessment., United Nations Environment Pro- gramme, UN-HABITAT.
Côté, S., Ayotte, P., Dodin, S., Blanchet, C., Mulvad, G., Petersen, H.S., Gingras, S., Dewailly, E., 2006. Plasma organochlorine concentrations and bone ultrasound measurements: a cross-sectional study in peri-and postmenopausal Inuit women from Greenland. Environ. Health 5, 33.
Counts, E.W., 2013. Every Woman Counts.
Cripps, C., Bumpus, J.A., Aust, S.D., 1990. Biodegradation of azo and heterocyclic dyes by Phanerochaete chrysosporium. Appl. Environ. Microbiol. 56, 1114–1118.
Cui, K., Yi, H., Zhou, Z.-J., Zhuo, Q.-F., Bing, Y.-X., Guo, Q.-W., Xu, Z.-C., 2014. Fenton Oxidation Kinetics and Intermediates of Nonylphenol Ethoxylates. Environ. Eng. Sci. 31,

217–224.
Dağdelen, S., Acemioğlu, B., Baran, E., Koçer, O., 2014. Removal of remazol brilliant blue R from aqueous solution by pirina pretreated with nitric acid and commercial activated carbon. Water. Air. Soil Pollut. 225.
Dalvand, A., Gholibegloo, E., Ganjali, M.R., 2016. Comparison of Moringa stenopetala seed extract as a clean coagulant with Alum and Moringa stenopetala -Alum hybrid coagulant to remove direct dye from Textile Wastewater. Environ. Sci. Pollut. Res. 16396–16405.
Daniel, E.F., 2010. Synthesis of mannetite-derived zero valent nano iron and targentin of zero valent iron for application in environmental remediation.
de Vidales, M.J.M., Sáez, C., Pérez, J.F., Cotillas, S., Llanos, J., Cañizares, P., Rodrigo, M.A., 2015. Irradiation-assisted electrochemical processes for the removal of persistent organic pollutants from wastewater. J. Appl. Electrochem.
DEFRA, 2012. Waste water treatment in the United Kingdom, Implication of the European Union Urban Waste Water Treatment Directive-91/271/EEC.
Demir, A., Topkaya, R., Baykal, A., 2013. Green synthesis of superparamagnetic Fe 3 O 4 nanoparticles with maltose : Its magnetic investigation. Polyhedron 65, 282–287.
Dianyi, Y.M., 2016. Case studies in environmental medicine polychlorinated biphenyls (PCBs) toxicity.
Diem, Q., Elisa, A., Tran-nguyen, P.L., 2013. ScienceDirect Effect of extraction solvent on total phenol content , total flavonoid content , and antioxidant activity of Limnophila aromatica. J. Food Drug Anal. 22, 296–302.
Dimitrakopoulou, D., Rethemiotaki, I., Frontistis, Z., Xekoukoulotakis, N.P., Venieri, D., Mantzavinos, D., 2012. Degradation, mineralization and antibiotic inactivation of amoxicillin by UV-A/TiO 2 photocatalysis. J. Environ. Manage. 98, 168–174.
Dong, H., Ahmad, K., Zeng, G., Li, Z., Chen, G., He, Q., Xie, Y., Wu, Y., Zhao, F., Zeng, Y., 2016. Influence of fulvic acid on the colloidal stability and reactivity of nanoscale zero-valent iron. Environ. Pollut. 211, 363–369.
Dular, M., Griessler-Bulc, T., Gutierrez-Aguirre, I., Heath, E., Kosjek, T., Krivograd Klemenčič, A., Oder, M., Petkovšek, M., Rački, N., Ravnikar, M., Šarc, A., Širok, B., Zupanc, M., Žitnik, M., Kompare, B., 2016. Use of hydrodynamic cavitation in (waste)water treatment. Ultrason. Sonochem. 29, 577–588.
EEA, 2011. Annual report 2010 and Environmental statement 2011.
Fazlzadeh, M., Rahmani, K., Zarei, A., Abdoallahzadeh, H., Nasiri, F., Khosravi, R., 2016. A novel green synthesis of zero valent iron nanoparticles (NZVI) using three plant extracts and their efficient application for removal of Cr(VI) from aqueous solutions. Adv. Powder Technol. 28, 122–130.
Fram, M.S., Belitz, K., 2011. Occurrence and concentrations of pharmaceutical compounds in groundwater used for public drinking-water supply in California. Sci. Total Environ. 409, 3409–3417.
Fratianni, F., Pepe, R., Nazzaro, F., 2014. Polyphenol Composition , Antioxidant , Antimicrobial and Quorum Quenching Activity of the " Carciofo di Montoro " (Cynara cardunculus var . scolymus) Global Artichoke of the Campania Region , Southern Italy. Food Nutr. Sci. 5, 2053–2062.
Frederick, P., 2016. Chitosan as a Drinking Water Treatment Coagulant. Am. J. Civ. Eng. 4, 205.
Frenken, K., Gillet, V., 2012. Irrigation water requirement and water withdrawal by country. Rome, Italy.

Gadipelly, C., Rathod, V.K., Marathe, K. V, 2014. Pharmaceutical Industry Wastewater: Review of the Technologies for Water Treatment and Reuse. Ind. Eng. Chem. Res. 53, 11571–11592.

Ganiyat, A.M., 2008. The Toxicological Evaluation of Sewage Effluents and Pharmaceuticals with the use of Zebrafish as a Model Organism. Anim. Sci.

Garcia-Segura, S., Bellotindos, L.M., Huang, Y.H., Brillas, E., Lu, M.C., 2016. Fluidized-bed Fenton process as alternative wastewater treatment technology, A review. J. Taiwan Inst. Chem. Eng. 67, 211–225.

Geng, B., Jin, Z., Li, T., Qi, X., 2009. Kinetics of hexavalent chromium removal from water by chitosan-Fe0 nanoparticles. Chemosphere 75, 825–830.

Ghaly, A.., Ananthashankar, R., Alhattab, M., Ramakrishnan, V.., 2013. Production, Characterization and Treatment of Textile Effluents: A Critical Review. J. Chem. Eng. Process Technol. 05, 1–19.

Ghosh, G.C., Nakada, N., Yamashita, N., Tanaka, H., 2010. Oseltamivir carboxylate, the active metabolite of oseltamivir phosphate (tamiflu), detected in sewage discharge and river water in Japan. Environ. Health Perspect. 118, 103–107.

Giannakis, S., Liu, S., Carratalà, A., Rtimi, S., Bensimon, M., Pulgarin, C., 2017. Effect of Fe(II)/Fe(III) species, pH, irradiance and bacterial presence on viral inactivation in wastewater by the photo-Fenton process: Kinetic modeling and mechanistic interpretation. Appl. Catal. B Environ. 204, 156–166.

Giersig, M.G.B.K., 2008. Nanomaterials for Application in Medicine and Biology NATO Science for Peace and Security Series.

Giri, R.R., Ozaki, H. et al, 2010. Degradation of common pharmaceuticals and personal care products in mixed solutions by advanced oxidation techniques[J]. Int. J. Environ. Sci. {&} Technol. 7, 251–260.

Goel, M., Hongqiang, H., Mujumdar, A.S., Ray, M.B., 2004. Sonochemical decomposition of volatile and non-volatile organic compounds - A comparative study. Water Res. 38, 4247–4261.

Gogate, P.R., Patil, P.N., 2015. Combined treatment technology based on synergism between hydrodynamic cavitation and advanced oxidation processes. Ultrason. Sonochem. 25, 60–69.

Gome, A., Upadhyay, K., 2013. Biodegradability Assessment of Pharmaceutical Wastewater Treated by Ozone. Int. Res. J. Environ. Sci. 2, 21–25.

Gomes, H.I., Dias-ferreira, C., Ottosen, L.M., Ribeiro, A.B., 2014. Journal of Colloid and Interface Science Electrodialytic remediation of polychlorinated biphenyls contaminated soil with iron nanoparticles and two different surfactants. J. Colloid Interface Sci. 433, 189–195.

Gong, C., Hart, D.P., 1998. Ultrasound Induced Cavitation and Sonochemical Yields. J. Acoust. Soc. Am. 104.

Gore, M.M., Chavan, P. V, 2013. Hydrodynamic Cavitation Using Degradation of Reactive Orange 4 Dye. Int. J. Chem. Sci. 11, 1314–1320.

Gore, M.M., Saharan, V.K., Pinjari, D. V., Chavan, P. V., Pandit, A.B., 2014. Degradation of reactive orange 4 dye using hydrodynamic cavitation based hybrid techniques. Ultrason. Sonochem. 21, 1075–1082.

Grande, G.A., 2015. Treatment of wastewater from textile dyeing by ozonization. POLITECNICO DI TORINO.

Greenlee, L.F., Torrey, J.D., Amaro, R.L., Shaw, J.M., 2012. Kinetics of zero valent iron nanoparticle oxidation in oxygenated water. Environ. Sci. Technol. 46, 12913–12920.

Haber, F. and Weiss, J., 1934. The Catalytic Decomposition of Hydrogen Peroxide by Iron Salts [WWW Document]. http://rspa.royalsocietypublishing.org/.

Hai-Jiao, L., Jing-Kang, W., Steven, F., Ting, W., Ying, B., Hong-xun, H., 2016. Nanoscale. Nanoscale 1, 1–13.

Hamamoto, S., Kishimoto, N., 2017. Characteristics of Fluoride Adsorption onto Aluminum (III) and Iron (III) Hydroxide Flocs Shinya. Sep. Sci. Technol. 52 (1), 42–50.

Hannah G. Bulovsky, 2016. The Stability, Toxicity, and Reactivity of Zero Valent Iron Nanoparticles. Oregon State University Honors College.

He, C., Han, L., Zhang, R.Q., 2016. More than 500 million Chinese urban residents (14 % of the global urban population) are imperiled by fi ne particulate hazard *. Environ. Pollut. 218, 558–562.

He, F., Zhao, D., 2005. Preparation and Characterization of a New Class of Starch-Stabilized Bimetallic Nanoparticles for Degradation of Chlorinated Hydrocarbons in Water. Environ. Sci. Technol 39, 3314–3320.

He, F., Zhao, D., Liu, J., Roberts, C.B., 2007. Stabilization of Fe - Pd nanoparticles with sodium carboxymethyl cellulose for enhanced transport and dechlorination of trichloroethylene in soil and groundwater. Ind. Eng. Chem. Res. 46, 29–34.

Hoag, G.E., Collins, J.B., Holcomb, J.L., Hoag, J.R., Nadagouda, M.N., Varma, R.S., 2009. Degradation of bromothymol blue by 'greener' nano-scale zero-valent iron synthesized using tea polyphenols. J. Mater. Chem. 19, 8671.

Hossain, M.M., Islam, K.M.N., Rahman, I.M.M., 2012. An Overview of the Persistent Organic Pollutants in the Freshwater System. In: Ecological Water Quality - Water Treatment and Reuse Edited. p. 496.

Hou, X., Huang, X., Ai, Z., Zhao, J., Zhang, L., 2016. Ascorbic acid/Fe@Fe2O3: A highly efficient combined Fenton reagent to remove organic contaminants. J. Hazard. Mater. 310, 170–178.

Huang, L., Weng, X., Chen, Z., Megharaj, M., Naidu, R., 2014. Green synthesis of iron nanoparticles by various tea extracts: Comparative study of the reactivity. Spectrochim. Acta - Part A Mol. Biomol. Spectrosc. 130, 295–301.

Jamei, M.R., Khosravi, M.R., 2013. DEGRADATION OF OIL FROM SOILUSING NANO ZERO VALENT. Sci. Int. 25, 863–867.

Jamei, M.R., Khosravi, M.R., Anvaripour, B., 2014. A novel ultrasound assisted method in synthesis of NZVI particles. Ultrason. Sonochem. 21, 226–233.

Jelonek, P., Neczaj, E., 2012. The use of Advanced Oxidation Processes (AOP) for the treatment of landfill leachate. Inżynieria i Ochr. Środowiska 15, 203–217.

Jewell, K.P., Wilson, J.T., 2011. Water level monitoring pressure transducers : a need for industry-wide standards. Ground Water Monit. Remediat. 31, 82–94.

K. M. Sirk, Saleh, N.B., Phenrat, T., Kim, H., Dufour, B., Ok, J., Golas, P.L., Matyjaszewski, K., Llwry, G. V., Tilton., R.D., 2009. Effect of adsorbed Ppolyelectrolytes on nanoscale zero valent Iron particle attachment to soil surface models. Environ. Sci. Technol. 43, 3803–3808.

Kapalka, A., 2008. Reactivity of Electrogenerated Free Hydroxyl Radicals and Activation of Dioxygen on Boron-Doped Diamond Electrodes. ÉCOLE Polytech. FÉDÉRALE LAUSANNE.

Kasprzyk-Hordern, B., Dinsdale, R.M., Guwy, A.J., 2009. The removal of pharmaceuticals, personal care products, endocrine disruptors and illicit drugs during wastewater treatment and its impact on the quality of receiving waters. Water Res. 43, 363–380.
Kataoka, R., Takagi, K., Kamei, I., Kiyota, H., Sato, Y., 2010. Biodegradation of dieldrin by a soil fungus isolated from a soil with annual endosulfan applications. Environ. Sci. Technol. 44, 6343–6349.
Kaur, S., Singh, V., 2007. Visible light induced sonophotocatalytic degradation of Reactive Red dye 198 using dye sensitized TiO2. Ultrason. Sonochem. 14, 531–537.
Kavitha, S.K., Palanisamy, P.N., 2011. Photocatalytic and Sonophotocatalytic Degradation of Reactive Red 120 using Dye Sensitized TiO 2 under Visible Light. Eng. Technol. 5, 1–6.
Keane, J., Willem, D., 2008. The role of textile and clothing industries in growth and development strategies.
Keeley, J., Jarvis, P., Judd, S.J., 2014. Coagulant recovery from water treatment residuals: A review of applicable technologies. Crit. Rev. Environ. Sci. Technol. 44, 2675–2719.
Khan, M.A.N., Siddique, M., Wahid, F., Khan, R., 2015. Removal of reactive blue 19 dye by sono, photo and sonophotocatalytic oxidation using visible light. Ultrason. Sonochem. 26, 370–377.
Khan, M.M., Adil, S.F., Al-Mayouf, A., 2015. Metal oxides as photocatalysts. J. Saudi Chem. Soc. 19, 462–464.
Kharisov, B.I., Dias, H.V.R., Kharissova, O. V, Jime, M., Kharisov, B.I., 2012. Iron-containing nanomaterials : synthesis , properties , and environmental applications. Advances 2, 9325–9358.
Kiparissis, Y., Balch, G.C., Metcalfe, T.L., Metcalfe, C.D., 2003. Effects of the isoflavones genistein and equol on the gonadal development of Japanese medaka (Oryzias latipes). Environ. Health Perspect. 111, 1158–1163.
Klimiuk, E., Filipkowska, U., Korzeniowska, A., 1999. Effects of pH and Coagulant Dosage on Effectiveness of Coagulation of Reactive Dyes from Model Wastewater by Polyaluminium Chloride (PAC) 8, 73–79.
Korniluk, M., Ozonek, J., 2013. Investigation on Landfill Leachate Biodegradability Improvement by Use of Hydrodynamic Cavitation and Ozone.
Kos, L., Michalska, K., Perkowski, J., 2010. Textile wastewater treatment by the fenton method. Fibres Text. East. Eur. 81, 105–109.
Koutahzadeh, N., Esfahani, M.R., Arce, P.E., 2016. Removal of Acid Black 1 from water by the pulsed corona discharge advanced oxidation method. J. Water Process Eng. 10, 1–8.
Kozma, G., Rónavári, A., Kónya, Z., Kukovecz, Á., 2016. Environmentally Benign Synthesis Methods of Zero-Valent Iron Nanoparticles. ACS Sustain. Chem. Eng. 4, 291–297.
Kürschner, M., Nielsen, K., Andersen, C., Sukhorukov, V.L., Schenk, W. a., Benz, R., Zimmermann, U., 1998. Interaction of Lipophilic Ions with the Plasma Membrane of Mammalian Cells Studied by Electrorotation. Biophys. J. 74, 3031–3043.
Kwan, W.P., Voelker, B.M., 2003. Rates of hydroxyl radical generation and organic compound oxidation in mineral-catalyzed fenton-like systems. Environ. Sci. Technol. 37, 1150–1158.
Lester, Y., Avisar, D., Gozlan, I., Mamane, H., 2011. Removal of pharmaceuticals using combination of UV/H2O2/O3 advanced oxidation process. Water Sci. Technol. 2, 1–10.
Li, H., Yanhua, G., Qianqian, H., Hui, Z., 2016. Degradation of Orange II by UV-Assisted Advanced Fenton Process : Response Surface Approach , Degradation Pathway , and Biodegradability Degradation of Orange II by UV-Assisted Advanced Fenton Process :

Response Surface Approach , Degradation Pathway , an. Ind. Eng. Chem. Res.
Li, P., Song, Y., Wang, S., Tao, Z., Yu, S., Liu, Y., 2015. Enhanced decolorization of methyl orange using zero-valent copper nanoparticles under assistance of hydrodynamic cavitation. Ultrason. Sonochem. 22, 132–138.
Li, S., Yan, W., Zhang, W., 2009. Solvent-free production of nanoscale zero-valent iron (nZVI) with precision milling. Green Chem. 11, 1618.
Liang, J., Komarov, S., Hayashi, N., Kasai, E., 2007. Improvement in sonochemical degradation of 4-chlorophenol by combined use of Fenton-like reagents. Ultrason. Sonochem. 14, 201–207.
Lin, C., Tanangteerpong, D., Neramittagapong, A., 2017. Improvement of As (III) removal with diatomite overlay nanoscale zero-valent iron (nZVI-D): adsorption isotherm and adsorption kinetic studies Nusavadee Pojananukij , Kitirote Wantala , Sutasinee Neramittagapong ,. Water Sci. Technol. Water Supply 212–220.
Liu, A., Zhang, W., 2014. Fine structural features of nanoscale zero-valent iron characterized by spherical aberration corrected scanning transmission electron microscopy (Cs-STEM). Analyst 139, 4512–4518.
Liu, J., Lewis, G., 2014. Environmental toxicity and poor cognitive outcomes in children and adults. J. Environ. Health 76, 130–8.
Liu, J., Ye, J., Chen, Y., Li, C., Ou, H., 2017. UV-driven hydroxyl radical oxidation of tris(2-chloroethyl) phosphate: Intermediate products and residual toxicity. ECSN.
Lopez-Telleza, G., Barrera-Diaza, C.E., Balderas-Hernandeza, P., Bilyeub., 2011. Removal of hexavalent chromium in aquatic solutions by iron nanoparticles embedded in orange peel pith. Chem. Eng. J. 173, 480–485.
López, Z.M., Eunice, E.E., 2016. Degradation of Acetaminophen and Its Transformation Products in Aqueous Solutions by Using an Electrochemical Oxidation Cell with Stainless Steel Electrodes. Water 8, 1–12.
Louisnard, O., González-garcía, J., 2011. Acoustic cavitation. In Ultrasound technologies for food and bioprocessing. Springer New York.
Lu, W., Shen, Y., Xie, A., Zhang, W., 2010. Journal of Magnetism and Magnetic Materials Green synthesis and characterization of superparamagnetic Fe 3 O 4 nanoparticles. J. Magn. Magn. Mater. 322, 1828–1833.
Ma, Y., 2012. Short review : Current trends and future challenges in the application of sono-Fenton oxidation for wastewater treatment. Sustain. Environ. Res 22, 271–278.
Ma, Z., Qin, J.-J., Liou, C.-X., Zhang, L., Valiyaveettil, S., 2012. Effects of Coagulation, pH and Mixing Conditions on Characteristics of Flocs in Surface Water Treatment. In: World Congress on Advances in Civil, Environmental and Material Research. pp. 26–30.
Mahamuni, N.N., Adewuyi, Y.G., 2010. Advanced oxidation processes (AOPs) involving ultrasound for waste water treatment: A review with emphasis on cost estimation. Ultrason. Sonochem. 17, 990–1003.
Mahdad, F., Younesi, H., Bahramifar, N., Hadavifar, M., 2015. Optimization of fenton and photo-fenton-based advanced oxidation processes for post-treatment of composting leachate of municipal solid waste by an activated sludge process. KSCE J. Civ. Eng. 00, 1–12.
Mahmoud, M.E., Saad, E.A., Soliman, M.A., Abdelwahab, M.S., 2016. Synthesis and surface protection of nano zerovalent iron (NZVI) with 3-aminopropyltrimethoxysilane for water remediation of cobalt and zinc and their radioactive isotopes. RSC Adv. 6, 66242–66251.
Malik, M.A., Hughes, D., Heller, R., Schoenbach, K.H., 2015. Surface Plasmas Versus Volume

Plasma: Energy Deposition and Ozone Generation in Air and Oxygen. Plasma Chem. Plasma Process. 35, 697–704.
Markova, Z., Novak, P., Kaslik, J., Plachtova, P., Brazdova, M., Jancula, D., Siskova, K.M., Machala, L., Marsalek, B., Zboril, R., Varma, R., 2014. Iron(II,III)-polyphenol complex nanoparticles derived from green tea with remarkable ecotoxicological impact. ACS Sustain. Chem. Eng. 2, 1674–1680.
Marshall, S., 2011. The Water Crisis in Kenya : Causes , Effects and Solutions. Glob. Major. E-Journal 2, 31–45.
Mehrvar, M., Anderson, W.A., Moo-young, M., 2001. Photocatalytic degradation of aqueous organic solvents in the presence of hydroxyl radical scavengers. Int. J. Photoenergy 3, 187–191.
Meral, T., Simsek, U.B., 2017. Effect of synthesis parameters on the particle size of the zero valent iron particles. Inorg. Nano-Metal Chem. 47, 1033–1043.
Miller, C.J., Rose, A.L., Waite, T.D., 2016. Importance of Iron Complexation for Fenton-Mediated Hydroxyl Radical Production at Circumneutral pH. Front. Mar. Sci. 3, 1–13.
Minakata, D., Song, W., Mezyk, S.P., Cooper, W.J., 2015. Experimental and theoretical studies on aqueous-phase reactivity of hydroxyl radicals with multiple carboxylated and hydroxylated benzene compounds. Phys. Chem. Chem. Phys. 17, 11796–11812.
Miniero, R., L'lamiceli, A., 2008. Persistent Organic Pollutants, Encyclopedia of Ecology.
Mishra, K.P., Gogate, P.R., 2010. Intensification of degradation of Rhodamine B using hydrodynamic cavitation in the presence of additives. Sep. Purif. Technol. 75, 385–391.
Molden, D., 2007. Summary A Comprehensive Assessment of Water Management in Agriculture.
Mu, Y., Jia, F., Ai, Z., Zhang, L., 2017. Environmental Science Nano remediation properties of nano zero-valent iron. Environ. Sci. Nano 4, 27–45.
Mukherjee, R., Kumar, R., Sinha, A., Lama, Y., Saha, A.K., 2016. A review on synthesis, characterization, and applications of nano zero valent iron (nZVI) for environmental remediation. Crit. Rev. Environ. Sci. Technol. 46, 443–466.
Multani, M.Y., Shah, M.J., Student, P.G., 2014. Removal of Colour and COD from Reactive Green – 19 Dyeing Wastewater using Ozone *1. Int. J. Eng. Sci. Res. Technol. 3.
Multigner, L., Kadhel, P., Rouget, F., Blanchet, P., Cordier, S., 2016. Chlordecone exposure and adverse effects in French West Indies populations. Environ. Sci. Pollut. Res. 23, 3–8.
Muruganandham, M., Suri, R.P.S., Jafari, S., Sillanpää, M., Lee, G., Wu, J.J., Swaminathan, M., 2014. Recent Developments in Homogeneous Advanced Oxidation Processes for Water and Wastewater Treatment. Int. J. Photoenergy 2014.
Mystrioti, C., Xenidis, A., Papassiopi, N., 2014. Application of Iron Nanoparticles Synthesized by Green Tea for the Removal of Hexavalent Chromium in Column Tests. J. Geosci. Environ. Prot. 2, 28–36.
Natalija, K., Iva, S.H., Hrvoje, K. ´, 2006. Fe-exchanged zeolite as the effective heterogeneous Fenton-type catalyst for the organic pollutant minimization: UV irradiation assistance. Chemosphere 65, 65–73.
Nawwar, M., Hussein, S., Ayoub, N., Hashim, A., El-Sharawy, R., Lindequist, U., Harms, M., Wende, K., 2011. Constitutive phenolics of Harpephyllum caffrum (Anacardiaceae) and their biological effects on human keratinocytes. Fitoterapia 82, 1265–1271.
Oakes, J.S., 2013. Investigation of Iron Reduction by Green Tea Polyphenols for Application in Soil Remediation. University of Connecticut.

OECD, 2011. OECD environmental outlook to 2050: The Consequences of inaction, OECD environmental outlook to 2050.
Olalla, M.J.F., 2007. Combination of Advanced Oxidation Processes with biological treatment for the remediation of water polluted with herbicides.
Olivier, D.K., 2012. The ethnobotany and chemistry of South African traditional tonic plants by submitted in fulfillment of the requirements for the degree PHILOSOPHIAE DOCTOR. University of Johanessburg.
ONU, 2009. International Migration Report 2009 : A Global Assessment.
Ozonek, J., 2012. Application of Hydrodynamic Cavitation in Environmental Engineering. Taylor & Francis Group, LLC., 6000 Broken Sound Parkway NW, Suite 300 Boca Raton, FL 33487-2742.
Ozonek, J., Lenik, K., 2011. Effect of different design features of the reactor on hydrodynamic cavitation process. Arch. Mater. Sci. Eng. 52, 112–117.
Pandey, P.K., Kass, P.H., Soupir, M.L., Biswas, S., Singh, V.P., 2014. Contamination of water resources by pathogenic bacteria. AMB Express 4, 51.
Pang, Y.L., Abdullah, A.Z., 2013. Current status of textile industry wastewater management and research progress in malaysia: A review. Clean - Soil, Air, Water 41, 751–764.
Pankaj, S.K., Bueno-Ferrer, C., Misra, N.N., Milosavljević, V., O'Donnell, C.P., Bourke, P., Keener, K.M., Cullen, P.J., 2014. Applications of cold plasma technology in food packaging. Trends Food Sci. Technol. 35, 5–17.
Panorel, I.C., 2013. Pulsed Corona Discharge As an Advanced Oxidation Process for the Degradation of Organic. Lappeenranta University of Technology, Lappeenranta, Finland).
Patil, P.N., Bote, S.D., Gogate, P.R., 2014. Degradation of imidacloprid using combined advanced oxidation processes based on hydrodynamic cavitation. Ultrason. Sonochem. 21, 1770–1777.
Pattanayak, M., Nayak, P.L., 2013. ECOFRIENDLY GREEN SYNTHESIS OF IRON NANOPARTICLES FROM VARIOUS PLANTS AND SPICES EXTRACT. Int. J. Plant, Anim. Environ. Sci. 3, 68–78.
Perron, N.R., Brumaghim, J.L., 2009. A review of the antioxidant mechanisms of polyphenol compounds related to iron binding. Cell Biochem. Biophys. 53, 75–100.
Pescod, M.., 2004. Wastewater treatment and use in agriculture - FAO irrigation and drainage paper 47 Food and agriculture organization of United Nations.
Pitt, J.J., 2009. Principles and applications of liquid chromatography-mass spectrometry in clinical biochemistry. Clin. Biochem. Rev. 30, 19–34.
Pokethitiyook, P., Poolpak, T., 2012. Heptachlor and Its Metabolite : Accumulation and Degradation in Sediment. In: Pesticides - Recent Trends in Pesticide. pp. 217–252.
Polar, J.A., 2007. After Wastewater Treatment. FLORIDA WATER Resour. J. 26–31.
Pradhan, A.A., Gogate, P.R., 2010. Removal of p-nitrophenol using hydrodynamic cavitation and Fenton chemistry at pilot scale operation. Chem. Eng. J. 156, 77–82.
Proestos, C., Boziaris, I.S., Kapsokefalou, M., Komaitis, M., 2008. Natural antioxidant constituents from selected aromatic plants and their antimicrobial activity against selected pathogenic microorganisms. Food Technol. Biotechnol. 46, 151–156.
Pullin, H., Springell, R., Parry, S., Scott, T., 2017. The effect of aqueous corrosion on the structure and reactivity of zero-valent iron nanoparticles. Chem. Eng. J. 308, 568–577.
Radjenovic, J., Petrovic, M., Barceló, D., 2007. Analysis of pharmaceuticals in wastewater and removal using a membrane bioreactor. Anal. Bioanalitical Chem. 387, 1365–1377.

Rahmani, A.R., Shabanloo, A., Mehralipou, J., Fazlzadeh, M., Poureshgh, Y., 2015. Degradation of Phenol in Aqueous Solutions Using Electro-Fenton Process. Res. J. Environ. Sci. 9, 332–341.

Rajan, C.S., 2011. Nanotechnology in Groundwater Remediation. Int. J. Environ. Sci. Dev. 2, 182–187.

Rajoriya, S., Bargole, S., Saharan, V.K., 2017. Degradation of a cationic dye (Rhodamine 6G) using hydrodynamic cavitation coupled with other oxidative agents: Reaction mechanism and pathway. Ultrason. Sonochem. 34, 183–194.

Raut-jadhav, S., Saini, D., Sonawane, S., Pandit, A., 2016. Ultrasonics Sonochemistry Effect of process intensifying parameters on the hydrodynamic cavitation based degradation of commercial pesticide (methomyl) in the aqueous solution. Ultrason. Sonochem. 28, 283–293.

Rawat, D., Mishra, V., Sharma, R.S., 2016. Detoxification of azo dyes in the context of environmental processes. Renew. Energy, 99, 118-126. 155, 591–605.

Rehman, S., Ullah, R., Butt, A.M., Gohar, N.D., 2009. Strategies of making TiO2 and ZnO visible light active. J. Hazard. Mater. 170, 560–569.

Reis, R.M., Beati, A.A.G.F., Rocha, R.S., Assumpção, M.H.M.T., Santos, M.C., Bertazzoli, R., Lanza, M.R. V, 2012. Use of gas diffusion electrode for the in situ generation of hydrogen peroxide in an electrochemical flow-by reactor. Ind. Eng. Chem. Res. 51, 649–654.

Rosas-Casarez, C.A., Arredondo-Rea, S.P., 2014. Experimental study of XRD, FTIR and TGA techniques in geopolymeric materials. Proc. 4, 25–30.

Saif, S., Tahir, A., Chen, Y., 2016. Green Synthesis of Iron Nanoparticles and Their Environmental Applications and Implications. Nanomaterials 6, 209.

Samaei, M.R., Maleknia, H., Azhdarpoor, A., 2015. Effects of pH on the Kinetics of Methyl Tertiary Butyl Ether Degradation by Oxidation Process (H 2 O 2 / Nano Zero-Valent Iron / Ultrasonic) 7, 4–9.

Samonikov, E.V., Samonikov, and M.G., 2013. The role and importanc of the textile in the national economy of the republic of Macedonia: Share of GDP, exports and employment. J. Process Manag. – New Technol. 1, 1–7.

Santos, D.C., Silva, L., Albuquerque, A., Simões, R., Gomes, A.C., 2013. Biodegradability enhancement and detoxification of cork processing wastewater molecular size fractions by ozone. Bioresour. Technol. 147, 143–151.

Santos, H.M., Capelo, J.L., 2007. Trends in ultrasonic-based equipment for analytical sample treatment. Talanta 73, 795–802.

Santos, H.M., Lodeiro, C., Capelo-Mart, J. e-L., Nez, R., 2008. The Power of Ultrasound.

Saranraj, P., 2013. Bacterial biodegradation and decolourization of toxic textile azo dyes. African J. Microbiol. Res. 7, 3885–3890.

Šarc, A., Stepišnik-Perdih, T., Petkovšek, M., Dular, M., 2017. The issue of cavitation number value in studies of water treatment by hydrodynamic cavitation. Ultrason. Sonochem. 34, 51–59.

Sena, R.F. De, Moreira, R.F.P.M., José, H.J., 2008. Bioresource Technology Comparison of coagulants and coagulation aids for treatment of meat processing wastewater by column flotation. Bioresour. Technol. 99, 8221–8225.

Shah, A.D., Dai, N., Mitch, W.A., 2013. Application of ultraviolet, ozone, and advanced oxidation treatments to washwaters to destroy nitrosamines, nitramines, amines, and aldehydes formed during amine-based carbon capture. Environ. Sci. Technol. 47, 2799–

2808.
Shah, M., 2014. Effective Treatment Systems for Azo Dye Degradation : A Joint Venture between Physico-Chemical & Microbiological Process. Int. J. Environ. Bioremediation Biodegrad. 2, 231–242.
Shahwan, T., Abu Sirriah, S., Nairat, M., Boyaci, E., Ero??lu, A.E., Scott, T.B., Hallam, K.R., 2011. Green synthesis of iron nanoparticles and their application as a Fenton-like catalyst for the degradation of aqueous cationic and anionic dyes. Chem. Eng. J. 172, 258–266.
Sharma, A., Gogate, P.R., Mahulkar, A., Pandit, A.B., 2008. Modeling of hydrodynamic cavitation reactors based on orifice plates considering hydrodynamics and chemical reactions occurring in bubble. Chem. Eng. J. 143, 201–209.
Sharma, R., Lall, N., 2014. Antibacterial, antioxidant activities and cytotoxicity of plants against Propionibacterium acnes. S. Afr. J. Sci. 110, 1–8.
Sharma, S., Ruparelia, J., Patel, M., 2011. A general review on advanced oxidation processes for waste water treatment, International conference on current …. Ahmedabad, Gujarat.
Sillanpää, M., Shrestha, R.A., Pham, and T.-D., 2011. Ultrasound Technology in Green Chemistry. In: Green Chemistry for Sustainability. pp. 1–21.
Silverstone, A.E., Rosenbaum, P.F., Weinstock, R.S., Bartell, S.M., Foushee, H.R., Shelton, C., Pavuk, M., 2012. Polychlorinated biphenyl (PCB) exposure and diabetes: Results from the Anniston community health survey. Environ. Health Perspect. 120, 727–732.
Singh, R., Misra, V., 2015. Stabilization of Zero-Valent Iron Nanoparticles : Role of Polymers and Surfactants. Handb. Nanoparticles 1–19.
Singh, S.K., Tang, W.Z., 2013. Statistical analysis of optimum Fenton oxidation conditions for landfill leachate treatment. Waste Manag. 33, 81–88.
Snyder, S., Westerhoff, P., Yoon, Y., Sedlak, D., 2003. Disruptors in Water : Implications for the Water Industry. Environ. Eng. Sci. 20, 449–469.
Stefaniuk, M., Oleszczuk, P., Ok, Y.S., 2016. Review on nano zerovalent iron (nZVI): From synthesis to environmental applications. Chem. Eng. J. 287, 618–632.
Stocking, A., Rodriguez, R., Browne, T., 2011. 3.0 Advanced Oxidation Processes, Evaluation.
Su, L., Liu, C., Liang, K., Chen, Y., Zhang, L., 2018. Performance evaluation of zero-valent iron nanoparticles (NZVI) for high-concentration H 2 S. R. Soc. Chem. Adv. 8, 13798–13805.
Suárez, S., Carballa, M., Omil, F., Lema, J.M., 2008. How are pharmaceutical and personal care products (PPCPs) removed from urban wastewaters? Rev. Environ. Sci. Biotechnol. 7, 125–138.
Sun, J., Xie, X., Bi, H., Jia, H., Zhu, C., Wan, N., Huang, J., Nie, M., Li, D., Sun, L., 2017. Solution-assisted ultrafast transfer of graphene-based thin films for solar cells and humidity sensors. Nanotechnology 28, 1–7.
Suponik, T., Lemanowicz, M., Wrona, P., 2016. Stability of green tea nanoscale zero-valent iron 8.
Svetla, K., 2006. Basic Characteristics of Persistent Organic Polutants (P O P S). 67, W.Gladstone Str. Sofia, 1000.
Swartz, C., Petrik, L., Tijani, J., Adeleye, A., Coomans, C., Ohlin, A., Falk, D., And, J.M., B Genthe, 2016. Emerging contaminants in wastewater treated for direct potable re-use: The human health risk priorities in South Africa.
Sychev, A., Isak, V., 1995. Iron compounds and the mechanisms of the homogeneous catalysis of the activation of O2 and H2O2 and of the oxidaiton of organic substrates. Russ. Chem. Rev. 65, 1105–1129.

Taha, M.R., Ibrahim, A.H., 2014. Characterization of nano zero-valent iron (nZVI) and its application in sono-Fenton process to remove COD in palm oil mill effluent. J. Environ. Chem. Eng. 2, 1–8.
Tao, Y., Cai, J., Huai, X., Liu, B., Guo, Z., 2016. Application of Hydrodynamic Cavitation to Wastewater Treatment. Chem. Eng. Technol. 39, 1363–1376.
Tartu, S., Bourgeon, S., Aars, J., Andersen, M., Polder, A., Thiemann, G.W., Welker, J.M., Routti, H., 2017. Science of the Total Environment Sea ice-associated decline in body condition leads to increased concentrations of lipophilic pollutants in polar bears (Ursus maritimus) from Svalbard , Norway. Sci. Total Environ. 576, 409–419.
Texas, H.K., 2016. Metal Chelation of Polyphenols 6879.
Thakur, S., Chauhan, M.S., 2016. Removal of Malachite Green Dye from aqueous solution by Fenton Oxidation. Int. Res. J. Eng. Technol. 03, 254–259.
Thekkae, V., Vinod, P., Senan, C., Somashekarappa, H.M., Cern, M., 2017. Gum karaya (Sterculia urens) stabilized zero-valent iron nanoparticles: characterization and applications for the removal of chromium and volatile organic pollutants from water. RSC Adv. 13997–14009.
Thomé, A., Reddy, K.R., Reginatto, C., Cecchin, I., 2015. Review of nanotechnology for soil and groundwater remediation: Brazilian perspectives. Water. Air. Soil Pollut. 226, 1–20.
Thuy, T.T., 2015. Effects of ddt on environment and human health. J. Educ. Soc. Sci. 2, 108–114.
Tian, L., Shi, X., Yu, L., Zhu, J., Yang, X., 2012. Chemical Composition and Hepatoprotective E ff ects of Polyphenol- Rich Extract from Houttuynia cordata Tea. J. Agric. Food Chem. 60, 4641–4648.
Tinne, N., Kaune, B., Kruger, A., Ripken, T., 2014. Interaction mechanisms of cavitation bubbles induced by spatially and temporally separated fs-laser pulses. PLoS One 9, 1–26.
Toft, G., Hagmar, L., Giwercman, A., Bonde, J.P., 2004. Epidemiological evidence on reproductive effects of persistent organochlorines in humans. Reprod. Toxicol. 19, 5–26.
Torun, M., Gültekin, Ö., Şolpan, D., Güven, O., 2015. Mineralization of paracetamol in aqueous solution with advanced oxidation processes. Environ. Technol. 36, 970–982.
Trzcinski, A.P., Stuckey, D.C., 2016. Inorganic fouling of an anaerobic membrane bioreactor treating leachate from the organic fraction of municipal solid waste (OFMSW) and a polishing aerobic membrane bioreactor. Bioresour. Technol. 204, 17–25.
U.S. EPA., 1999. Wastewater Technology Fact Sheet Ozone Disinfection, Office of Water Washington, D.C.
UN-Habitate, 2006. Annual Report.
UNEP/AMAP, 2011. Climate change and pops: Predicting the Impacts, Annals of Physics.
Üner, O., Geçgel, Ü., Bayrak, Y., 2016. Adsorption of Methylene Blue by an Efficient Activated Carbon Prepared from Citrullus lanatus Rind: Kinetic, Isotherm, Thermodynamic, and Mechanism Analysis. Water, Air, Soil Pollut. 227, 247.
UNESCO, 2012. Managing Water under Uncertainty and Risk.
United Nation Water Analytical, 2009. Wastewater management.
UNW-DPC, 2012. Water and the Green Economy.
Vajnhandl, S., Valh, J.V., 2014. The status of water reuse in European textile sector. J. Environ. Manage. 141, 29–35.
Wang, C., Klamerth, N., Messele, S.A., Singh, A., Belosevic, M., Gamal El-Din, M., 2016. Comparison of UV/hydrogen peroxide, potassium ferrate(VI), and ozone in oxidizing the

organic fraction of oil sands process-affected water (OSPW). Water Res. 100, 476–485.
Wang, Q., Qian, H., Yang, Y., Zhang, Z., Naman, C., Xu, X., 2010. Reduction of hexavalent chromium by carboxymethyl cellulose-stabilized zero-valent iron nanoparticles. J. Contam. Hydrol. 114, 35–42.
Wang, X., Wang, A., Ma, J., Fu, M., 2017. Facile green synthesis of functional nanoscale zero-valent iron and studies of its activity toward ultrasound-enhanced decolorization of cationic dyes. Chemosphere 166, 80–88.
Wang, X.P., Zhang, X.W., Lei, L.C., 2013. High Conductivity Water Treatment Using Water Surface Discharge with Nonmetallic Electrodes. Plasma Sci. Technol. 15, 528–534.
Wang, Z., 2013. Iron Complex Nanoparticles Synthesized by Eucalyptus Leaves. Sustain. Chem. Eng. 1551–1554.
Webb, I.R., Payne, S.J., Coussios, C., 2011. The effect of temperature and viscoelasticity on cavitation dynamics during ultrasonic ablation. Acoust. Soc. Am. 130, 3458–3466.
WHO, 2008. Persistent organic pollutants (POPs) children 's health and the environment, UN Environment.
Wilén, B.M., Lumley, D., Mattsson, A., Mino, T., 2008. Relationship between floc composition and flocculation and settling properties studied at a full scale activated sludge plant. Water Res. 42, 4404–4418.
Wolff, M.S., Landrigan, P.J., 1994. Environmental estrogens. Am. Sci. Vol. 266, 526–527.
Wong, K.T., Yoon, Y., Snyder, S.A., Jang, M., 2016. Phenyl-functionalized magnetic palm-based powdered activated carbon for the effective removal of selected pharmaceutical and endocrine-disruptive compounds. Chemosphere 152, 71–80.
World Health Organization, 2004. Endrin in Drinking Water, Endrin in Drinking-water, Background document for development of WHO Guidelines for Drinking-water Quality.
Wu, T., Shi, M., 2010. pH-affecting Sonochemical Formation of Hydroxyl Radicals Under 20 KHz Ultrasonic Irradiation. Sustain. Environ. Res., 20, 245–250.
Wu, T.Y., Guo, N., Teh, C.Y., Hay, J.X.W., 2013. Advances in Ultrasound Technology for Environmental Remediation. Adv. Ultrasound Technol. Environ. Remediat. 5–12.
Xiao, G., Xu, W., Wu, R., Ni, M., Du, C., Gao, X., Luo, Z., Cen, K., 2014. Non-thermal plasmas for VOCs abatement, Plasma Chemistry and Plasma Processing.
Xiu, Z. ming, Jin, Z. hui, Li, T. long, Mahendra, S., Lowry, G. V., Alvarez, P.J.J., 2010. Effects of nano-scale zero-valent iron particles on a mixed culture dechlorinating trichloroethylene. Bioresour. Technol. 101, 1141–1146.
Yaacob, W.Z.W., Kamaruzaman, N., Samsudin, A.R., 2012. Development of nano-zero valent iron for the remediation of contaminated water. Chem. Eng. Trans. 28, 25–30.
Yan, W., 2011. Iron-based nanoparticles : Investigating the microstructure , surface chemistry , and reactions with environmental contaminants.
Yew, Y.P., Shameli, K., Miyake, M., Kuwano, N., Bt Ahmad Khairudin, N.B., Bt Mohamad, S.E., Lee, K.X., 2016. Green Synthesis of Magnetite (Fe3O4) Nanoparticles Using Seaweed (Kappaphycus alvarezii) Extract. Nanoscale Res. Lett. 11, 276.
Yoo, B.Y., Hernandez, S.C., Koo, B., Rheem, Y., Myung, N. V., 2007. Electrochemically fabricated zero-valent iron, iron-nickel, and iron-palladium nanowires for environmental remediation applications. Water Sci. Technol. 55, 149–156.
Yoo, H.C., Cho, S.H., Ko, S.O., 2001. Modification of coagulation and Fenton oxidation processes for cost-effective leachate treatment. J. Environ. Sci. Heal. - Part A Toxic/Hazardous Subst. Environ. Eng. 36, 39–48.

Yuvakkumar, R., Elango, V., Rajendran, V., Kannan, N., 2011. Preparation and Characterization of Zero Valent Iron. Dig. J. Nanomater. Biostructures 6, 1771–1776.
Zaleska-Medynska, A., Marchelek, M., Diak, M., Grabowska, E., 2016. Noble metal-based bimetallic nanoparticles: The effect of the structure on the optical, catalytic and photocatalytic properties. Adv. Colloid Interface Sci. 229, 80–107.
Zangeneh, H., Zinatizadeh, A.A.L., Habibi, M., Akia, M., Hasnain Isa, M., 2015. Photocatalytic oxidation of organic dyes and pollutants in wastewater using different modified titanium dioxides: A comparative review. J. Ind. Eng. Chem. 26, 1–36.
Zhang, D., Yang, M., Gao, H., Dong, S., 2017. Translating XPS Measurement Procedure for Band Alignment into Reliable Ab-initio Calculation Method.
Zhang, J., Li, J., Thring, R., Liu, L., 2013. Application of Ultrasound and Fenton's Reaction Process for the Treatment of Oily Sludge. Procedia Environ. Sci. 18, 686–693.
Zhu, L. inda Z. and D.B.Z., 2006. Oxidation Processes For Degradation Of Organic Pollutant in Water.
Zupanc, M., Kosjek, T., Petkovšek, M., Dular, M., Kompare, B., Širok, B., Blažeka, Ž., Heath, E., 2013. Removal of pharmaceuticals from wastewater by biological processes, hydrodynamic cavitation and UV treatment. Ultrason. Sonochem. 20, 1104–1112.

APPENDIX

Appendix 1

Calibration curve for the intensity (CPS) against known concentration of 2-hydroxyl terephthslic acid as determined using optical fibre spectrometer (NanoLog® i-HR 320, USA)

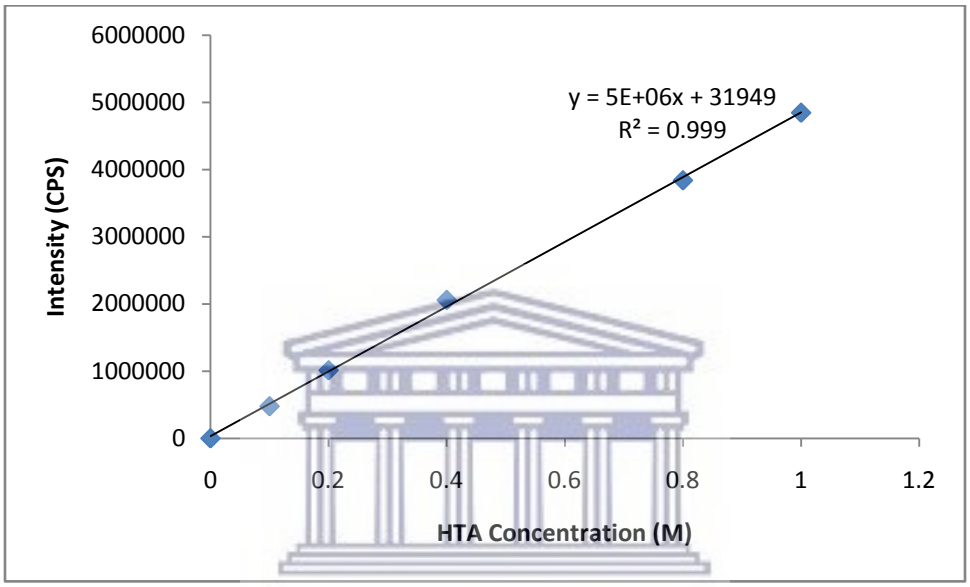

Appendix 2

GC-MS spectra of the identified intermediates during the decolouration of OR2 solution in jet-loop hydrodynamic cavitation system (20 mg/ L, pH 2, 400 KPa) at optimised conditions of gnZVI catalyst.

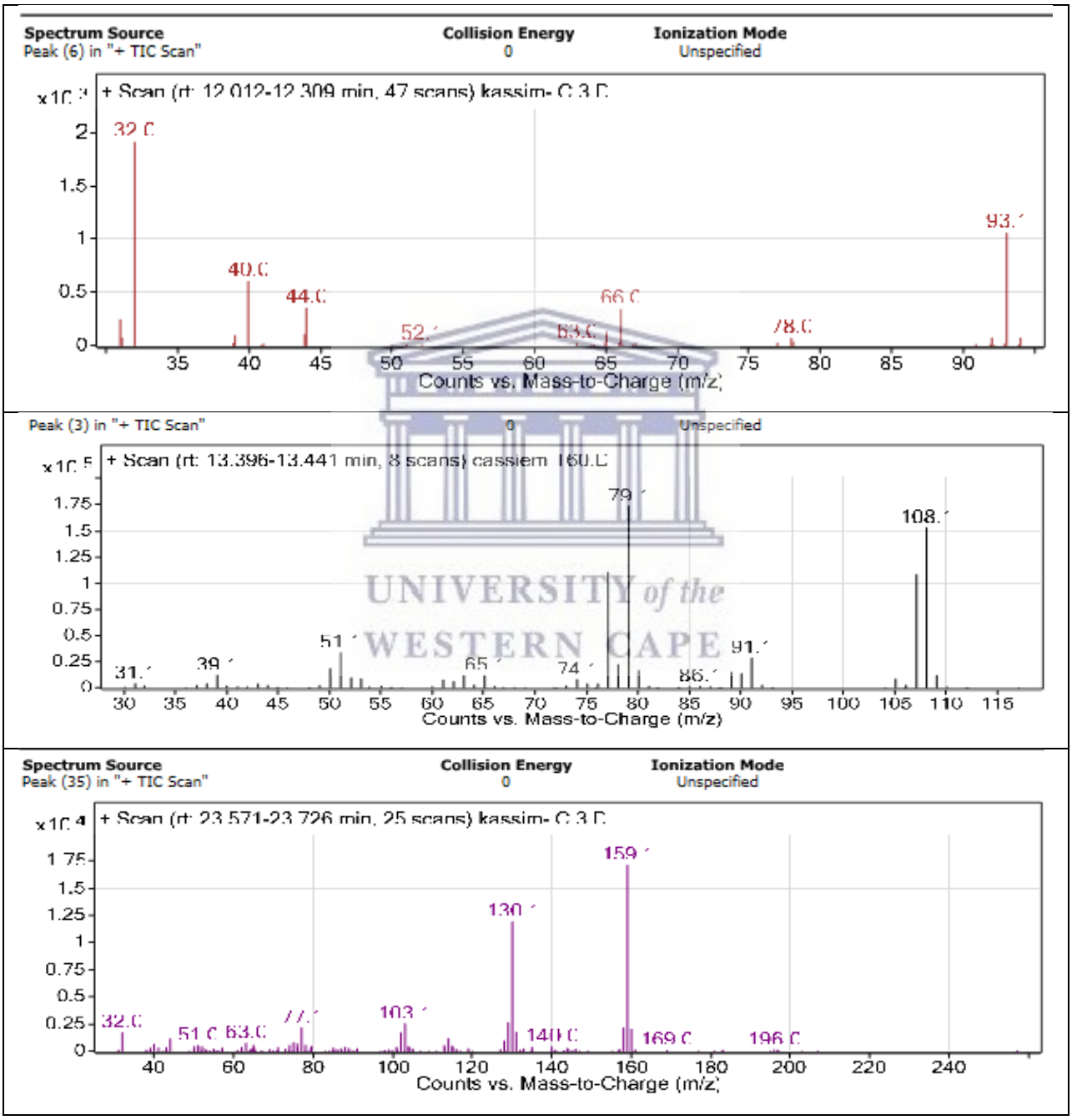

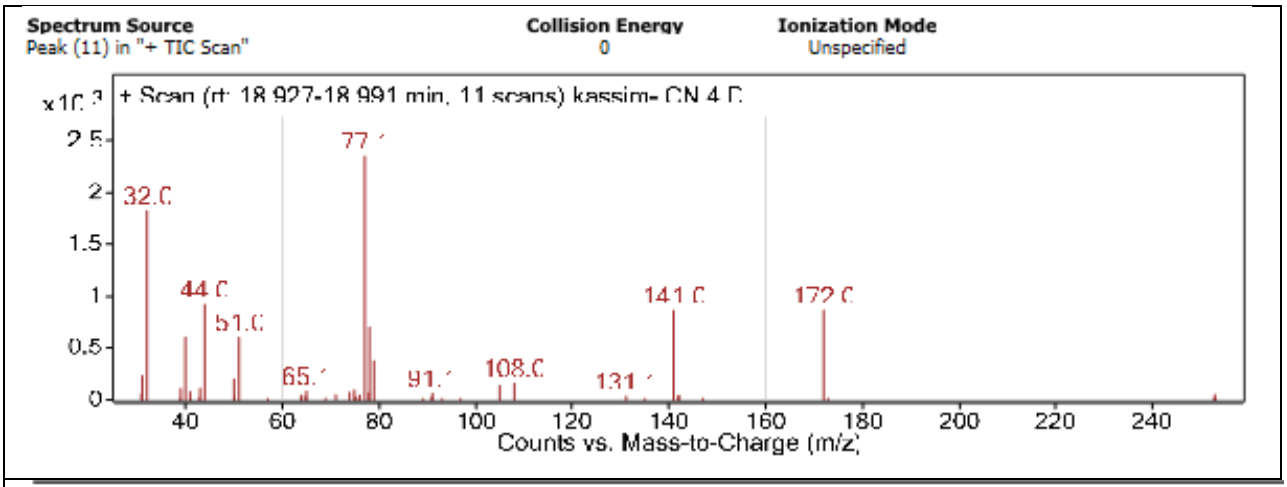

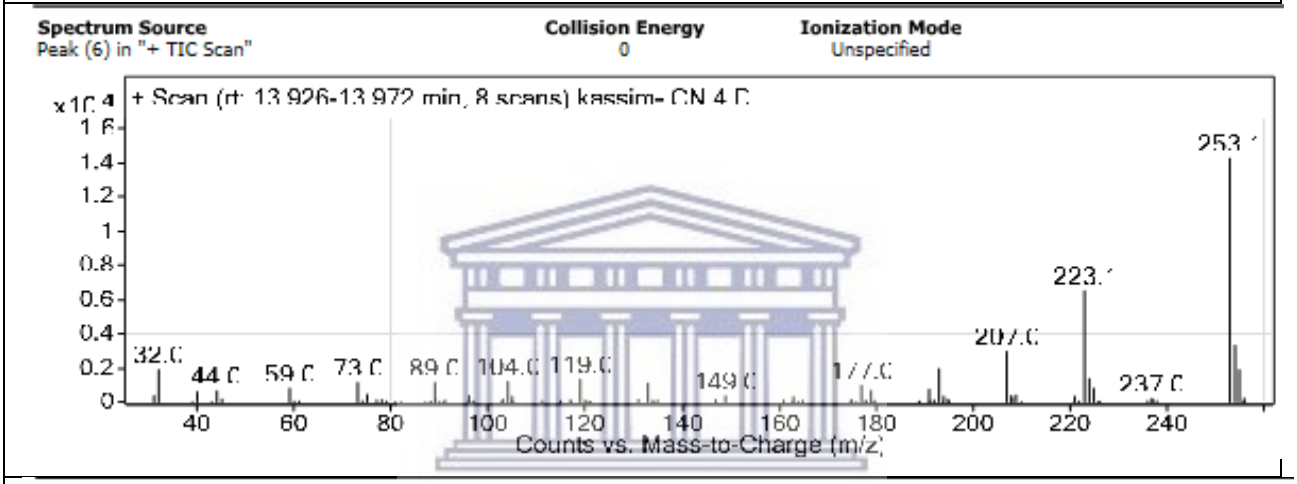

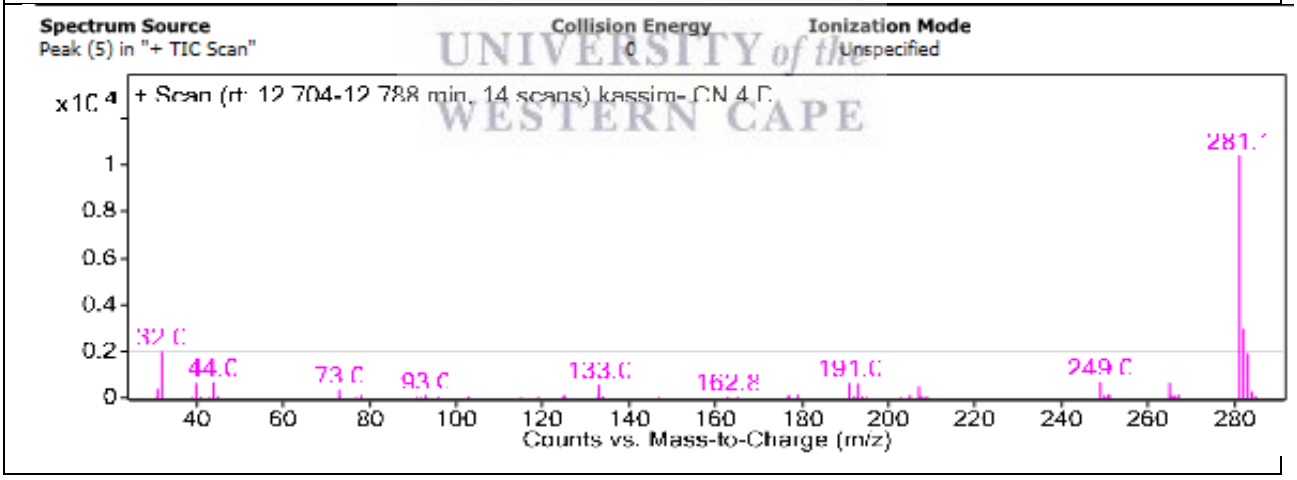

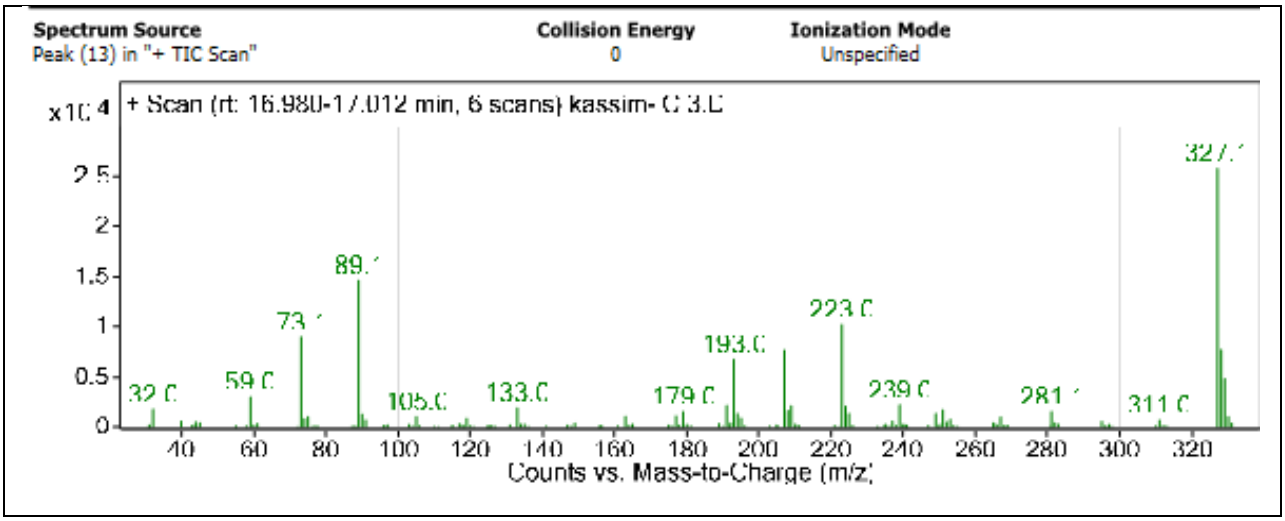

Appendix 3

UV specra showing the effect of H_2O_2 (0, 0.5 or 1 mg/ L) application during the transformation of acetaminophen in the jet loop hydrodynamic cavitation system (pH 2, 400 kPa, 10 L of 10 mg/ L ACE, 4 mm orifice plate hole size, n = 3)

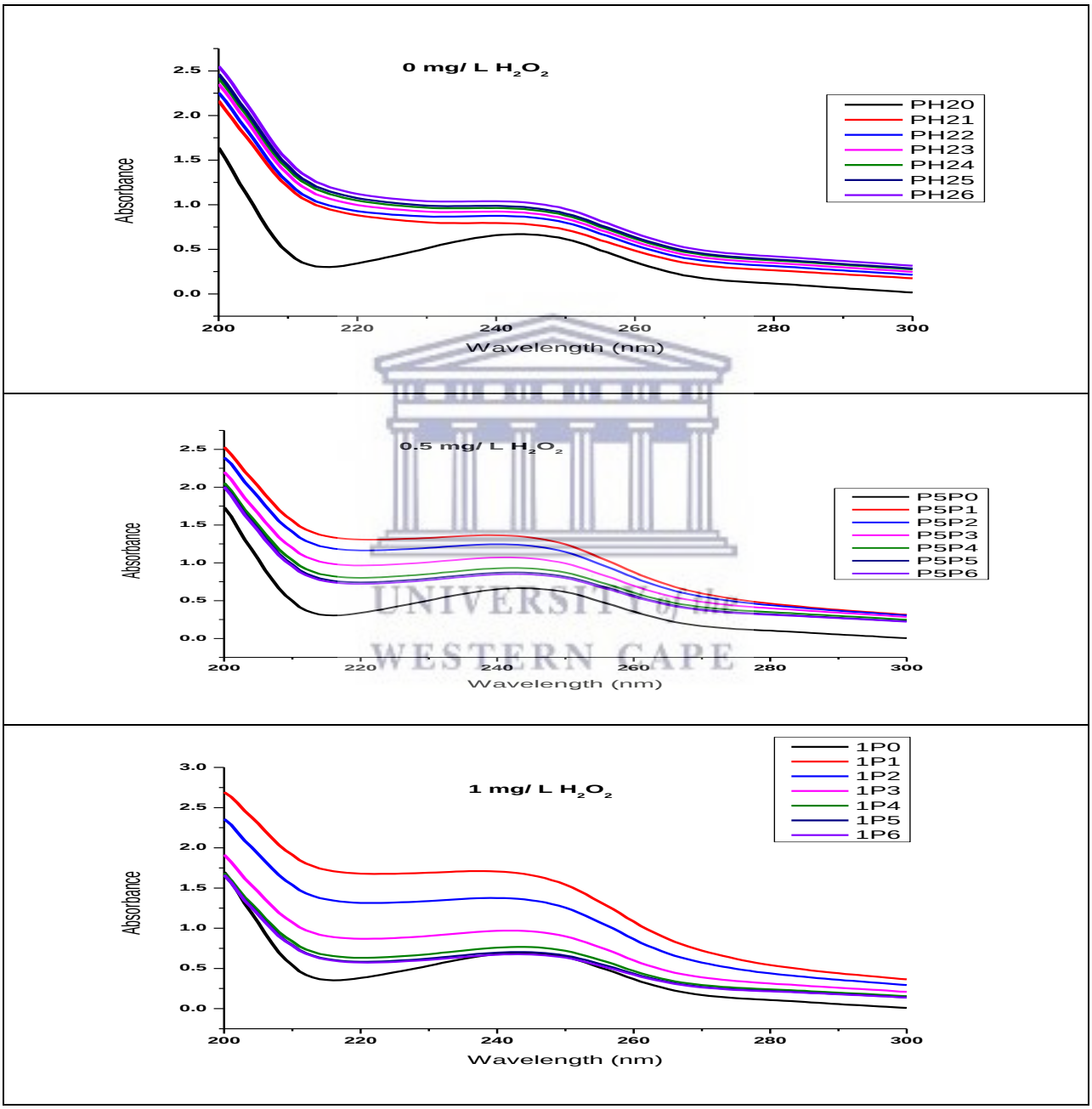

Appendix 4

UV specra showing the effect of H_2O_2 (2.0, 5.0 or 10 mg/ L) application during the transformation of acetaminophen in the jet loop hydrodynamic cavitation system (pH 2, 400 kPa, 10 L of 10 mg/ L ACE, 4 mm orifice plate hole size, n = 3)

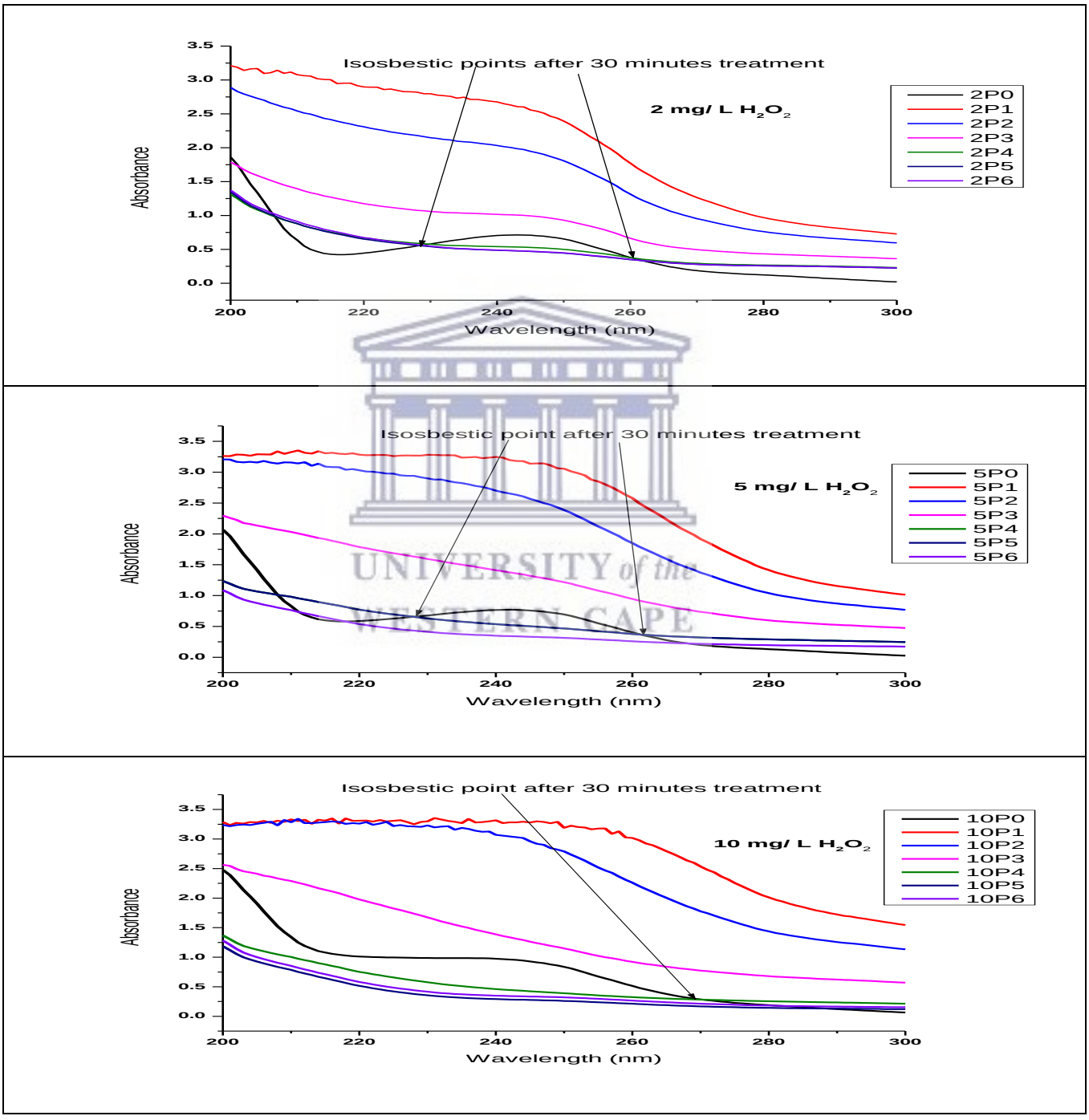

Appendix 5

The UV spectrograph of degradation of acetaminophen in the jet loop hydrodynamic cavitation system, showing the isosbestic point (pH 2, 400 kPa, 10 L of 10 mg/ L ACE, 4 mm orifice plate hole size, 5 mg/ L hydrogen peroxide, 10 mg/ L iron (II) sulfate, 60 minutes, n = 3)

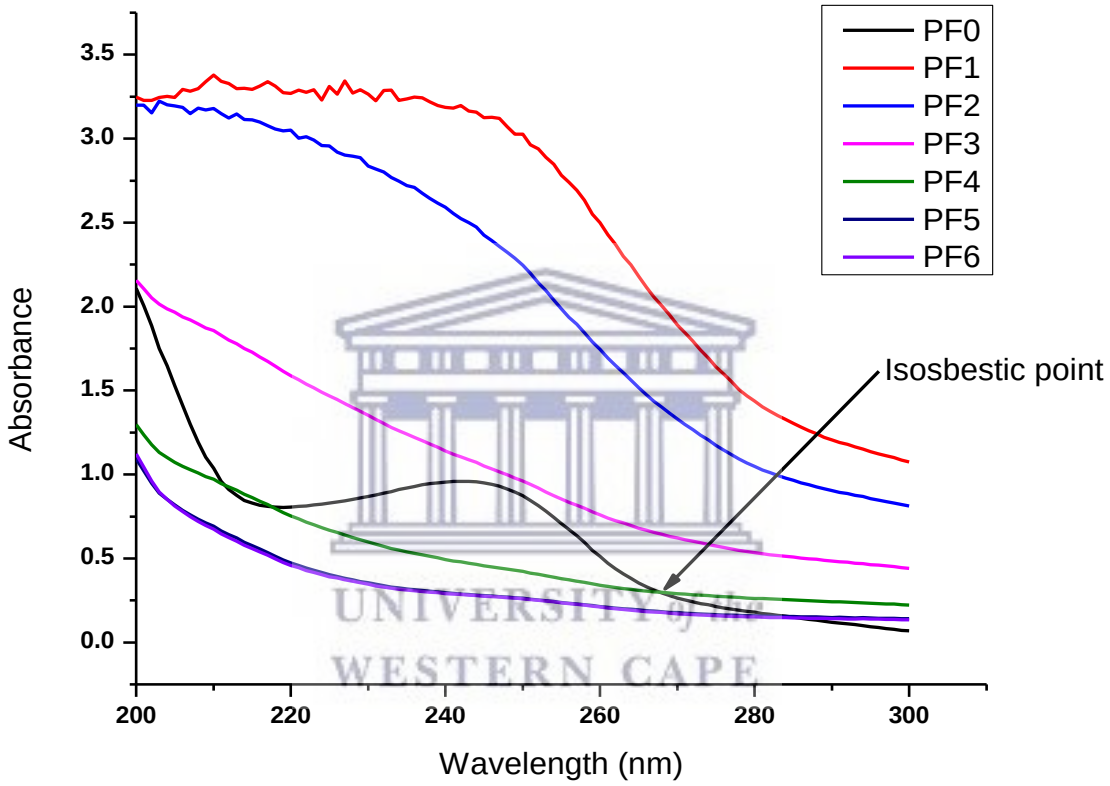

Appendix 6

UV spectrograph of degradation of acetaminophen in the jet loop hydrodynamic cavitation system, showing the isosbestic point (pH 2, 400 kPa, 10 L of 10 mg/ L ACE, 4 mm orifice plate hole size, 5 mg/ L hydrogen peroxide, 10 mg/ L gnZVI, 60 minutes, n = 3)

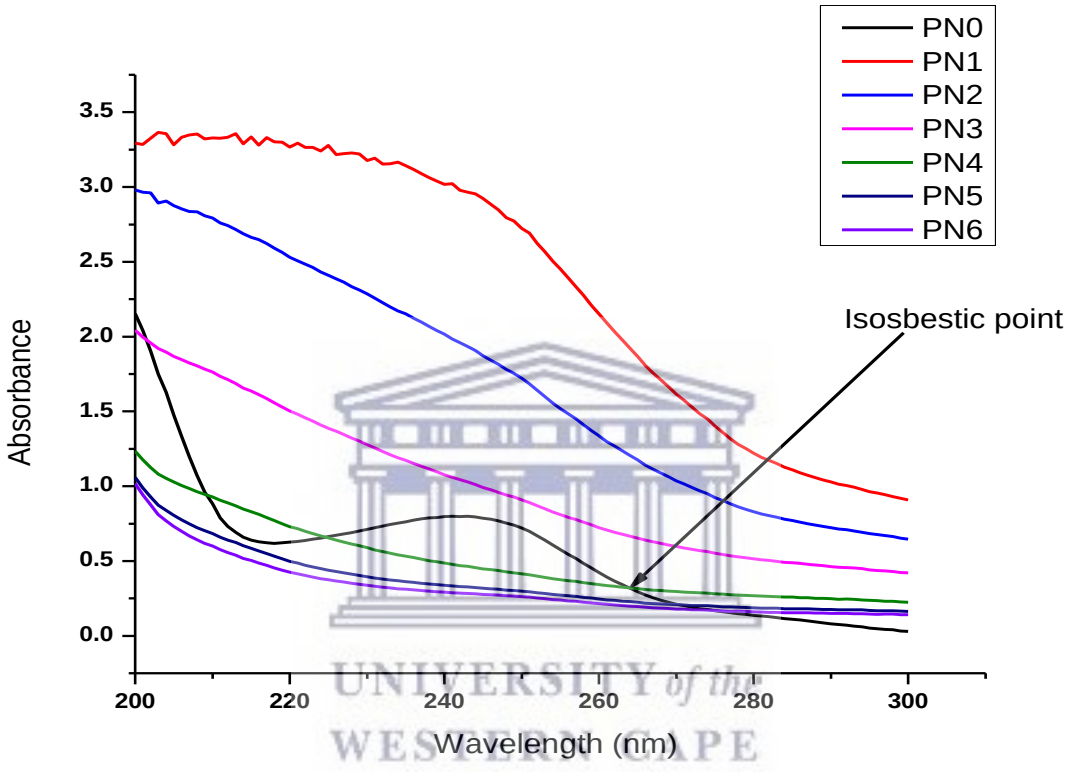

Appendix 7

TOC of acetaminophen during its treatment in the jet loop hydrodynamic cavitation system with the application of 10 mg/ L iron sulfate [F] or gnZVI [N] (pH 2, 400 kPa, 10 mg/ L ACE, 10 L ACE, 4 mm orifice plate hole size, 5 mg/ L hydrogen peroxide, 60 minutes, n = 3)

CSIR
our future through science
Tel: (+27) 21 888 2400/2433
Fax: (+27) 21 888 2630

CSIR Implementation Unit
Jan Celliers Street
Stellenbosch, 7600
P O Box 320
Stellenbosch, 7599
Chemistry Laboratory - Stellenbosch

Certificate of Analysis

Report NO: SAL-2017-11549
Customer: UWC Environmental & Nanoscience
Address: New Chemical Science Building
Bellville
Contact: Kassim Badmus
Phone: Fax:
Email: 3481395@myuwc.ac.za

Sample Description: Water samples in 15ml vails with blue caps
No of Samples 14
Sample Condition: Room Temperature
Date Received: 05-Oct-2017
Date Completed: 20-Nov-17
Order No:

Sample Disposal: a) Liquid Sample One Month - After issuing of final Certificate of Analysis; b) Solid Sample Three Months - After issuing of final Certificate of Analysis

Sample Identification	Analysis / Sample Date / Unit	Total Organic Carbon mg/l
1711549-79071EF F00		15
1711549-79072EF F10		7.8
1711549-79073EF F20		7.9
1711549-79074EF F30		7.0
1711549-79075EF F40		7.7
1711549-79076EF F50		8.2
1711549-79077EF F60		7.1
1711549-79078EF N00		16
1711549-79079EF N10		7.8
1711549-79080EF N20		9.5
1711549-79081EF N30		10
1711549-79082EF N40		8.0
1711549-79083EF N50		12
1711549-79084EF N60		8.3

Appendix 8

FT-IR of acetaminophen standard showing the functional groups

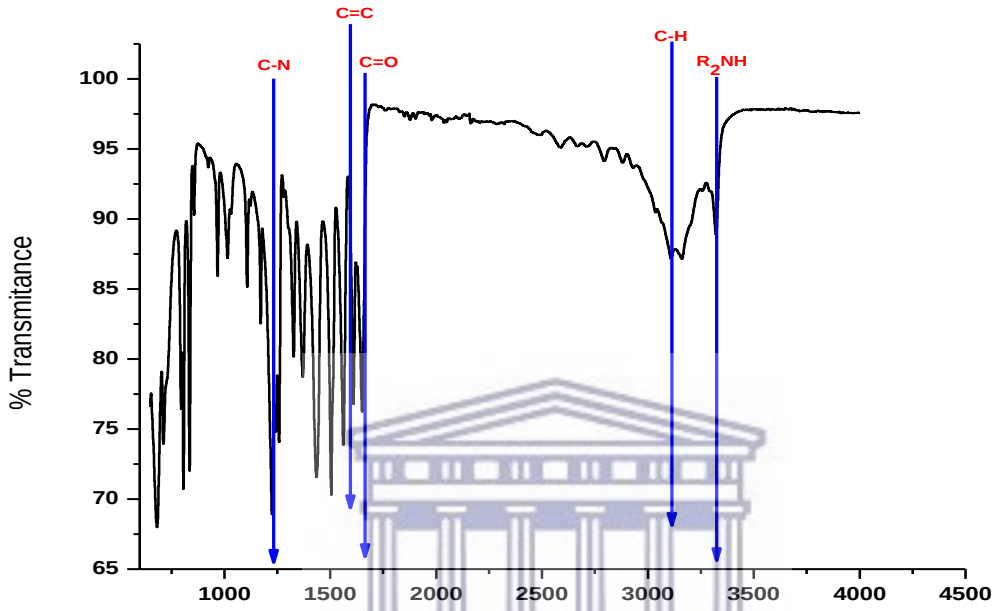

Appendix 9

FT-IR of acetaminophen duing the treatment in the jet loop hydrodynamic cavitation system (pH 2, 400 kPa, 10 L of 10 mg/ L ACE, 4 mm orifice plate hole size, 5 mg/ L hydrogen peroxide, 10 mg/ L iron (II) sulfate, 60 minutes, n = 3)

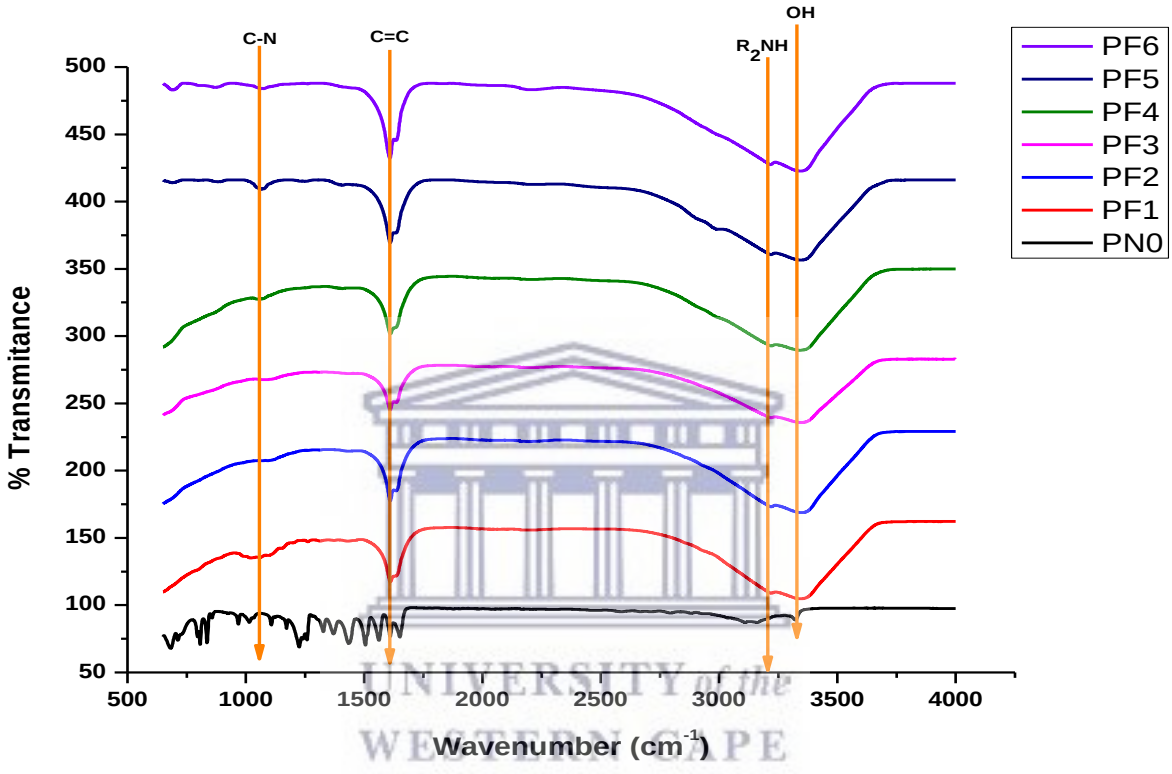

Appendix 10

FT-IR of acetaminophen duing the treatment in the jet loop hydrodynamic cavitation system, showing the functional groups (pH 2, 400 kPa, 10 L of 10 mg/ L ACE, 4 mm orifice plate hole size, 5 mg/ L hydrogen peroxide, 10 mg/ L gnZVI, 60 minutes, n = 3)

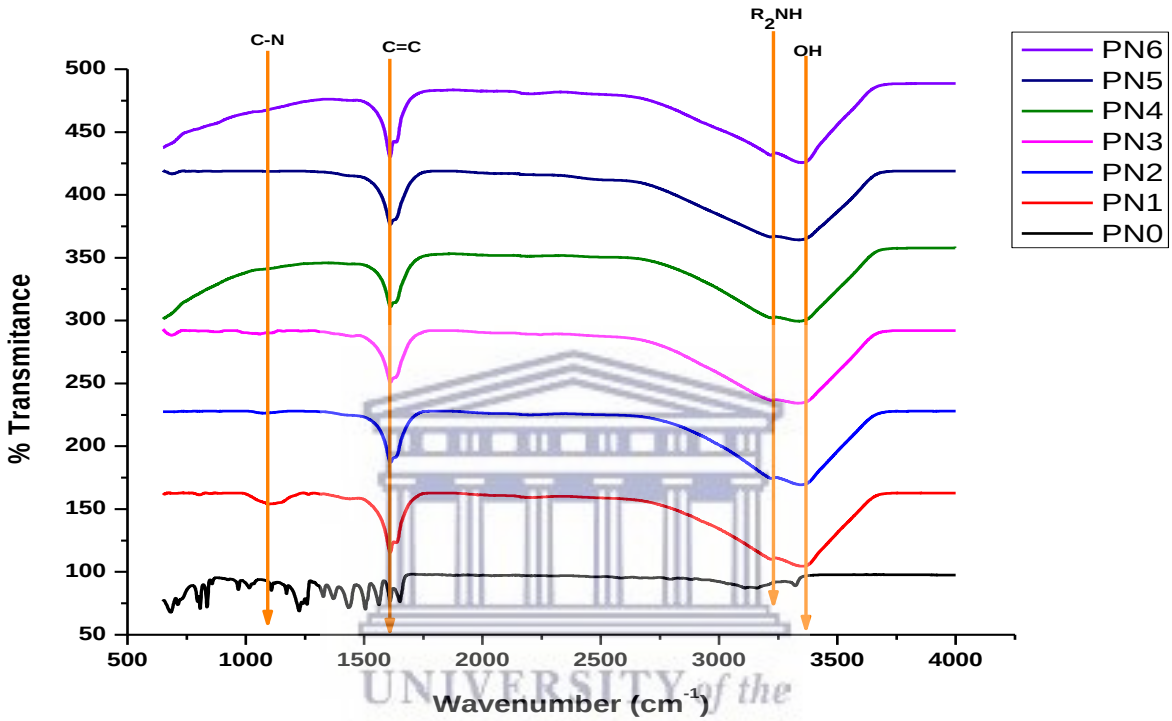

Appendix 11

GC-MS of the acetaminophen and intermediate products during the degradation in the jet loop hydrodynamic cavitation system (pH 2, 400 kPa, 10 mg/ L ACE, 10 L ACE, 4 mm orifice plate hole size, 5 mg/ L hydrogen peroxide, 10 mg/ L iron (II) sulfate, 60 minutes, n = 3)